Error Correction of Loudspeakers:

A study of Loudspeaker Design supported by Digital Signal Processing

Aalborg University
Bo Rohde Pedersen
PhD thesis, May 2008

Published by: The department of Software, Medialogy, and Electronics. Esbjerg Tekniske Institut. Aalborg University, DK6700 Esbjerg, Denmark, 2008. ISBN: 987-87-7606-024-4

Preface

From my experience in the sales and support of digital amplifiers in Japan, 2001, I learned about the marketplace and the drivers for home audio applications. In the marketplace of music sound systems there is a considerable technical and marketing advantage to be gained by focusing on improving the efficiency and thereby achieving smaller designs. Currently, overheating tends to be the primary cause of loudspeaker breakdowns, a factor that constrains both design freedom and innovation in music system technology. From a marketing perspective, it makes good sense to work towards increasing the efficiency of loudspeakers, as this would inevitably lead to the need for smaller power amplifiers, making music systems more compact overall and less expensive to manufacture. The size of audio equipment is a main market driver today.

In 2002, through Jens Arnspang, Aalborg Univeristy Esbjerg, I met Knud Bank Christensen who had a proposal for a PhD project in loudspeaker modelling. This led to 5 years employment by Aalborg University of ½ lecturing position and ½ PhD position, and this is the final Thesis.

Finn T. Agerkvist from Ørsted, Acoustic Technology, Technical University of Denmark (DTU) was included in the supervisory committee at the beginning of 2003. He has, throughout the project, been very supportive with comments, ideas and has always been a helpful reviewer. Many of the experiments in this project have been carried out at the acoustic lab at DTU. In 2005, Per Rubak, from Aalborg University, became a member of the supervisory committee. Per has been very inspiring and has been very helpful with digital signal processing.

At the end of the project, I visited John Mourjopoulos and his Audio Group at the University of Patras in Greece. During my three month stay, there was studied digital loudspeakers, which has been a great supplement to the objective of this project; namely, loudspeaker design supported by digital signal processing.

_____

Bo Rohde Pedersen

Summary

Throughout this thesis, the topic of electrodynamic loudspeaker unit design and modelling are reviewed. The research behind this project has been to study loudspeaker design, based on new possibilities introduced by including digital signal processing, and thereby achieving more freedom in loudspeaker unit design.

This freedom can be used for efficiency improvements where different loudspeaker design cases show design opportunities. Optimization by size and efficiency, instead of flat frequency response and linearity, is the basis of the loudspeaker efficiency designs studied.

In the project, a nonlinear loudspeaker model has been used for both power consumption and distortion simulations. The nonlinear model has been improved by adding time varying suspension behaviour. The basic improvement is a heating phenomenon of the suspension. The addition to the model improves the loudspeaker model performance at low frequencies.

A model based controller has been constructed, where a simulation study including a measurement series of parameter drift in the loudspeaker units has been included. This led to the conclusion that a parameter update of the loudspeaker parameters is needed during operation of a nonlinear feed forward controller.

System identification is used for tracking the loudspeaker parameters. Different system identification methods are reviewed, and the investigations ends with a simple FIR based algorithm. Finally, the parameter tracking system is tested with music signals on a 6½ inch bass-mid range loudspeaker unit.

The knowledge of loudspeaker construction and efficiency is used for the analysis of Digital Loudspeaker Arrays (DLA). This work is made in cooperation with the University of Patras, where DLA is a focus area. This project focuses on efficiency and transducer limitations of the DLA. Performance analysis of DLA is the name of the joint research project. Parts from this project are presented in this thesis.

Table of Contents:

0.1 Reading Guide

The thesis is divided into 8 chapters followed by 5 appendixes. Each chapter begins with a short introduction that explains the connection of the chapter to the thesis and a short introduction of the contents of the chapter. Each chapter ends with a partial conclusion; the final conclusion and discussion can be found in chapter 8.

Figures, tables, and equations are numbered with the chapter number followed by an index number; Figure 2.5 is the fifth figure in chapter two.

On page 8 and 9 a list of notations and abbreviations can be found. On page 157-162 the literature is listed. The literature reference consists of the initial of the surname of the main author followed by a number.

As a supplement to this report, four AES convention papers were published: one at each convention from the 120th to 123rd [P20, P21, P22, P24]. One paper was also published for the AES "DSP for Loudspeaker" conference [P23], and one has been submitted to the AES Journal [P25].

The new results from the PhD study are presented in the following sections:

Chapter 2:	- Time varying behaviour of the suspension.
	- Simulation and measurement of the diaphragm velocity.
Chapter 3:	- Measurement series of loudspeaker parameter drift.
Chapter 4:	- Nonlinear efficiency design.
Chapter 5:	- Simulation of feed forward controller.
Chapter 6:	- Musical system identification.
Chapter 7:	- Efficiency and transducer properties for digital loudspeaker arrays.

0.2 Notations and Abbreviations

Notations:

a_n	the filer coefficients (IIR)
a(t)	diaphragm acceleration [m/s^2]
A(z)	Z-transform of IIR filer
Bl	the force factor [N/A] or [Vs/m]
b_n	the filer coefficients (FIR)
B(z)	Z-transform of FIR filer
c	speed of sound [m/s]
c_m	suspension compliance [m/N]
$e_{in}(t)$	the loudspeaker input voltage [V]
e(n)	error signal, defined as: e(n) = d(n) – y(n)
E{}	expected value (mean)
f_o	the mechanical resonance frequency [Hz]
$F_{in}(t)$	the force applied to the diaphragm [N]
L_e	the voice coil inductance [H]
k	amplification constant
K	1,57 ρ/c
ς	the mechanical damping factor
ξ	the total loudspeaker damping factor
i(t)	the loudspeaker current [A]
J()	cost function
ρ	density of air [kg/m^3]
m_m	moving mass [kg]
N	number of bits
r	radius of the diaphragm [m]
r_m	acoustic resistance of a loudspeaker, mechanical units [Ns/m]
R_e	the voice coil resistance [Ω]
U(z)	Z-transform of input signal
μ	step size parameter
v(t)	diaphragm velocity [m/s]
ŵ	a vector containing the model parameters, b_n
W_e	electrical power [W]
W_a	acoustic power [W]
ω	frequency [rad/s]
ω_o	the mechanical resonance frequency [rad/s]
x(t)	diaphragm displacement [m]
x(s)	Laplace transformed diaphragm displacement [m]
Y(z)	Z-transform of estimated signal

Abbreviations:

AES	Audio Engineering Society
ARMA	Auto Regressive Moving Average
DAC	Digital to Analogue Converter
dBFs	Decibel full scale
dB SPL	Decibel sound pressure level
DLA	Digital loudspeaker array
DSP	Digital Signal Processing
EMF	Electro Motive Force, in electrodynamic loudspeaker also Back EMF
FIR	Finite Impulse Response
Hz	Hertz
LMS	Least Mean Square
LSB	Least Significant Bit
IIR	Infinite Impulse Response
MA	Moving Average
MSB	Most Significant Bit
NLMS	Normalized Least Mean Square
PCM	Pulse Code modulation
SPL	Sound Pressure Level
THD+N	Total Harmonic Distortion plus Noise

0.3 Introduction

The development of the electrodynamic loudspeaker started with the telephone and can be dated back to 1874. This is described by Siemens [S40], who did not use his device for audible transmission. Alexander G. Bell did, and in 1876 he patented the telephone [B40]. The first transducers were inspired by electrical motors that are rotation and the loudspeaker makes translation movements. Figure 0.1 shows the transducer principle used by Bell in the telephones where an electromagnet moved the magnetic diaphragm. A DC bias was needed for reproducing the sound field. In Figure 0.1 the DC field is applied by a permanent magnet.

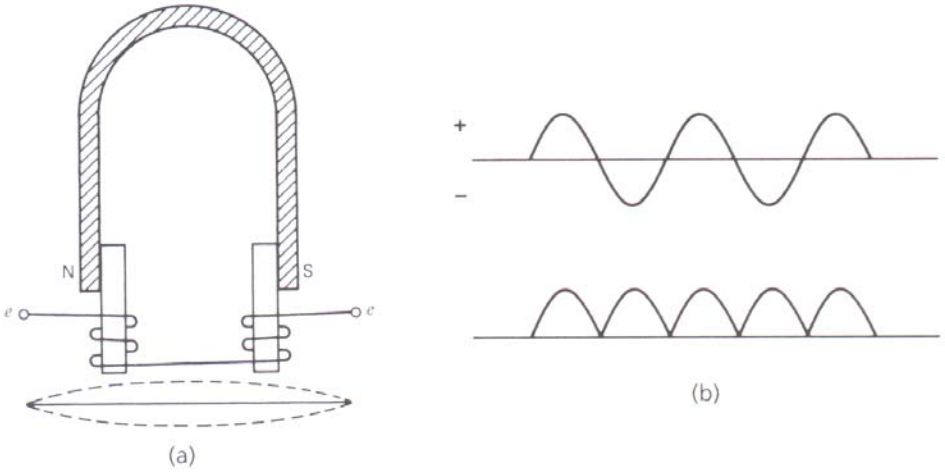

Figure 0.1: (a) Moving iron diaphragm loudspeaker as used in Bells telephone. (b) Without bias magnet input will be rectified. Figure from [B1]

The moving-coil motor used in loudspeakers today was patented by Oliver Lodge in 1898 [L1]. However, the transducer was not used until the vacuum tube was developed and wireless communication was invented (the radio).

Around 1925, Rice and Kellog [R10] developed the loudspeaker that we know today, the electrodynamic loudspeaker. This type of loudspeaker became a part of the entertainment products known today: movies, home audio music, television, games. Since Rice and Kellog's work in the 1920s the loudspeaker has been essentially left unchanged [B1].

The electrodynamic loudspeaker has been improved by small steps through material development and the capability of computer simulations. Permanent magnets have been made stronger while diaphragm materials have been made lighter and stiffer. Computer based simulations have brought improvements; for example, the diaphragm behaviour can be studied with finite element methods [S20].

In the early days of loudspeakers it was necessary to make them very efficient for playing in theatres driven with the limited output power of the power amplifiers. Over the years, the power amplifier has developed much better output capability. The loudspeaker development focus has now changed from high efficiency to obtaining better sound reproduction. Portable

devices with high quality audio capabilities and the decreasing size of home audio systems create the need for small size loudspeakers with high sound qualities. In home audio, the size of the musical systems has been decreasing in recent years with highly efficient power amplifiers [C20] and integrated digital signal processing. In portable systems, the mobile phone is a major product where size and efficiency are very important. In short, the size and efficiency of the loudspeaker is of major importance today.

Loudspeaker efficiency has recently been studied by several authors. A study of the possibilities provided by strong magnets has been made by Vanderkooy, Boers, and Aarts 2002 [V2, V3] who showed significant efficiency improvements, but the loudspeaker frequency response does not remain flat and a prefilter is necessary. Klippel and Bright 2001 [B10, B13] have proposed to improve efficiency by decreasing the moving mass through shortening of the voice coil. The drawback is loss of linearity, which must be re-established by digital signal processing. Active loudspeakers and digital signal processing opens up new opportunities in relation to efficiency improvements, which are investigated and summed up in chapter 4.

For the engineering of loudspeakers modelling is very important. Studies of loudspeaker behaviour and computer models are essential, not only for improving the loudspeaker, but also for development of digital signal processing for distortion cancellation. Many publications are available and some of the important studies from the last 20 years are presented here. The LoDist project results were presented in 1995 [O1, O2, O3, C1]. This project studied loudspeaker unit errors and presented an improved loudspeaker model. The model included creep that was analysed by Knudsen and Jensen in 1995 [K15]. The loudspeaker model was able to estimate the distortion pattern and behaviour of the first two harmonics in of 10dB. The same year Aldoshina, Voishvillo, and Mazin showed further improvements of the loudspeaker model by including flux modulation [A10]. Modelling is reviewed and studied in detail in chapter 2.

The author believes loudspeaker distortion cancellation to be the next big step for loudspeakers. For many years, power amplifiers have used feedback to decrease distortion. This solution is not very useful for a loudspeaker, because it is difficult to obtain the output signal, and use it as feedback signal. In 1997, Schurer made a study of a model based on feed forward distortion cancellation [S2]. Schurer implemented a sensor-less feed forward controller that decreased the distortion level. Bright found the feed forward compensator inefficient due to loudspeaker parameter drift. Bright has made an estimation of loudspeaker parameter drift from voltage and current, with system identification [B10].

System identification, applied to loudspeakers, was shown by Knudsen in 1996 [K12], where it was used for measuring linear loudspeaker parameters based on a voltage, current, and displacement measurement. This system was extended by Klippel, in 2001 [K4], who introduced a measurement system that became commercially available. Klippel added nonlinear system identification of the loudspeaker motor nonlinearities: force factor, suspension compliance and voice coil induction as function of position, estimated from the loudspeaker current and voltage. Bright investigated system identification for mobile phones, where low power calculation is available [B10]. The system is able to find the loudspeaker resonance frequency and damping factor, but with music or speech signal the conversion time

is very long. In chapter 6, a musical system identification method for loudspeaker parameter tracking is developed and system identification methods are reviewed.

The basic idea of this project is to develop a loudspeaker based on the possibilities that digital signal processing provides. This will be used to improve the loudspeaker efficiency and lead to smaller size requirements. Different methods are proposed, but the overall objective is to move towards the system structure shown in Figure 0.2.

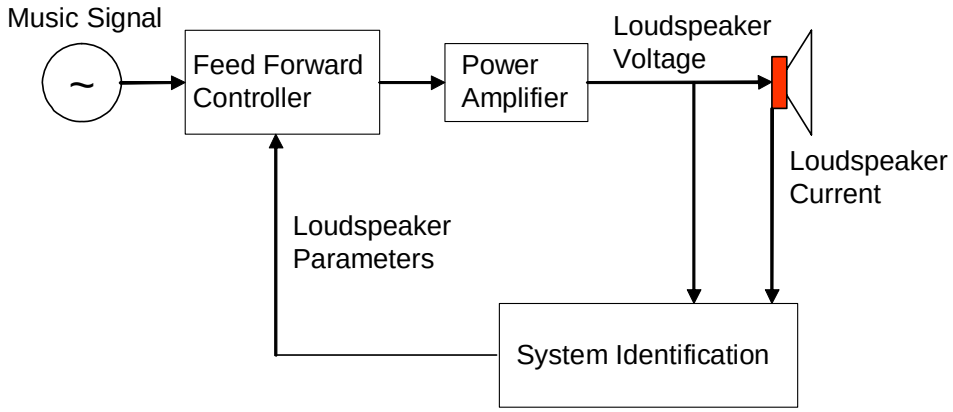

Figure 0.2: System structure of the investigated loudspeaker system of this project.

All stages of Figure 0.2 are investigated, except for the power amplifier. The influence of the loudspeaker parameter drift on the feed forward controller is investigated, in chapter 3 and 5. The feed forward controller is model based; therefore, the loudspeaker model is investigated and improved in chapter 2. The parameter tracking system is studied in relation to a typical music audio system in chapter 6.

Digitized amplification and signal processing leads to improved design possibilities in the coming years of loudspeakers development: Will the next step be to make the loudspeaker digital? This question can definitely only be answered in the future, but some investigations made in this thesis are applied to digital loudspeaker arrays for reviewing the driver properties, in chapter 7.

0.4 Research Objectives

The main objective is to develop a loudspeaker that is based on the possibilities that digital signal processing provides. Instead of using an existing loudspeaker unit and applying digital signal processing, a loudspeaker can be designed that requires digital signal processing. This procedure removes some of the design criteria that usually limit the design: flat frequency response and linear behaviour. The emphasis can then be moved to efficiency that is important in all devices today due to environment. Marketing-wise, an interesting parameter is the possibility of making small size, high performance loudspeakers.

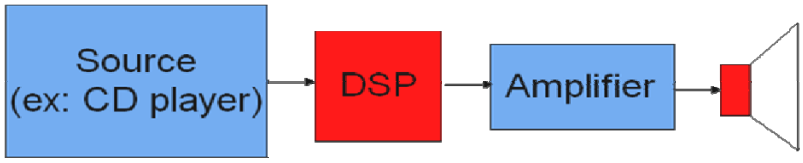

Figure 0.3: A typical audio chain. The red parts; digital signal processing and the loudspeaker are part of the project investigated.

The state of the art signal processing for loudspeakers is reviewed and used in the loudspeaker design based on digital signal processing. In looking at today's loudspeaker market, there are loudspeakers that implement linear signal processing to adjust the frequency response and compensate for the placement in the room; Beolab 5 from Bang and Olufsen provides a good example. So far, the market has not seen any products that implement nonlinear distortion cancellation even though research projects have shown positive indications [S2, B10]. From previous studies, it is known that one of the problems with digital signal processing for loudspeakers is the drift of the loudspeaker parameters [B10, S2]. The problem with loudspeaker parameter drift is investigated, and a useful method for tracking the parameter drift is found for end product music playing by the consumer.

In relation to this project, where signal processing for loudspeakers is needed, a study of the loudspeaker behaviour is made. For testing the loudspeaker parameter drifts influence of the distortion reduction with a feed forward compensator is a controller implemented.

A brief investigation and introduction of digital loudspeaker arrays are made for looking at an alternative loudspeaker technology that can enable multi dimensional signal processing. Digital loudspeakers are reviewed as a possible future loudspeaker solution in terms of efficiency and driver properties.

Summary of the objectives:

- Can digital signal processing enable efficiency improvements of loudspeakers?
- Can a digital controller compensate for the introduced distortion coming from the loudspeaker efficiency design?
- Is it possible to track the loudspeaker parameters while playing music?
- Will loudspeakers of the future become digital?

Chapter 1

1. The Linear Loudspeaker

This chapter describes the basics of electrodynamic loudspeaker drivers. The basic linear lumped model is presented and the block diagram is derived. The block diagram is used in the simulations made in the project. The classical electrical equivalent circuit is also shown. Finally, the important transfer functions are derived and examples of bode plots are shown.

1.1. The Electrodynamic Loudspeaker

A loudspeaker converts electrical signals to acoustic waves. The conversion is made by first converting the electrical signals to mechanical movements, and then the mechanical movements to acoustic waves. The loudspeaker acts as a piston for the mechanical-acoustic conversion. The electro-mechanical conversion can be implemented according to different principles. This research will study the most common loudspeaker type; the electrodynamic loudspeaker, which uses an electromagnetic energy conversion.

Figure 1.1 shows a cross section of a bass mid-range loudspeaker unit. The functionality and implementation of the individual parts are explained below.

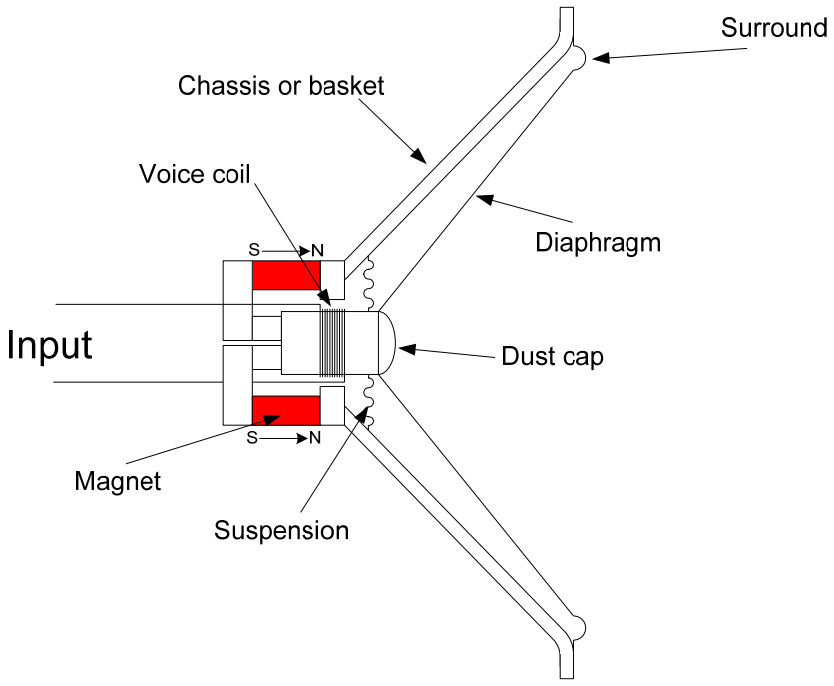

Figure 1.1: Cross-section of loudspeaker, principle.

Diaphragm:	The diaphragm or cone converts the mechanical movement produced by the loudspeaker to sound waves. The diaphragm mass is a part of the model parameter moving mass, m_m.
Suspension:	The suspension fixes the diaphragm to a defined rest position. c_m, is the suspension compliance of the spinner and the edge suspension, (see spinner Figure 1.2).
Surround:	The surround, or the edge suspension, fixes the edge of the diaphragm to the chassis. It makes the movement of the diaphragm unidirectional and stops rappelling. The surround also stops the air flow from the back of the diaphragm to the front.
Dust Cap:	The dust cap makes it impossible for dust and metal parts from the outside to come into the magnet gap. It is also included in the moving mass.
Chassis:	The chassis holds the surround in the front and the spider is mounded in the middle. The magnet system is fixed on the back (Figure 1.4).
Magnet:	This is a permanent magnet in a soft iron structure, with the soft iron leading the magnetic flux to the magnet gap, where it is concentrated.
Voice Coil:	The voice coil is mounted onto the diaphragm and the coil is placed in the magnet gap. Due to the B-field from the magnet, the voice coil current is converted to a force. The magnet field, B and the length, l of the wire in the field generates the force factor Bl. The voice coil also has two electrical parameters; the voice coil resistance, R_e, and the voice coil induction, L_e.

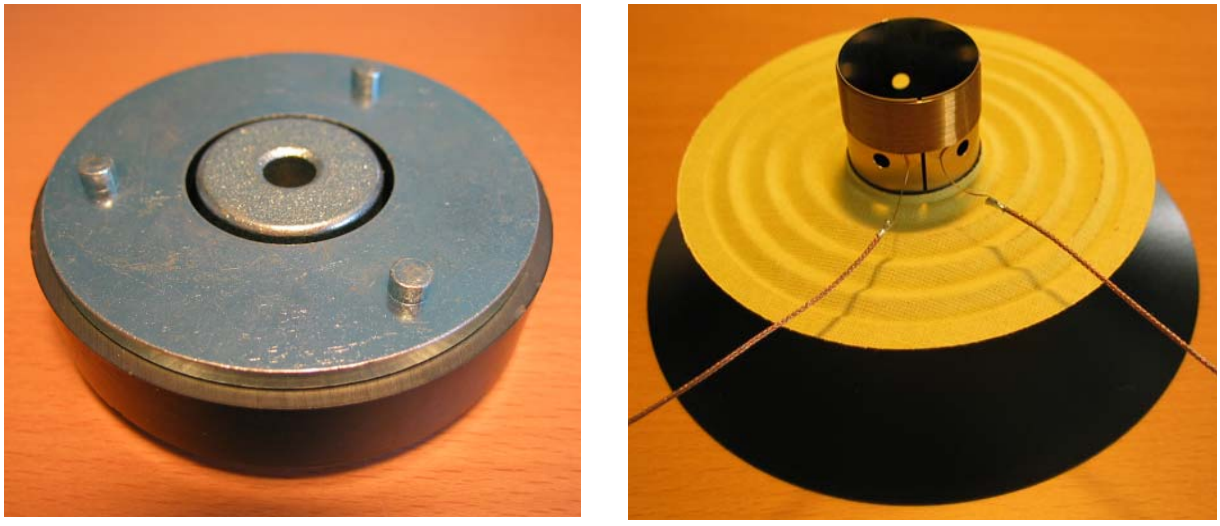

Figure 1.2: Left picture is of a magnet system. Right picture is from the bottom of the diaphragm, suspension (the spider) and the voice coil.

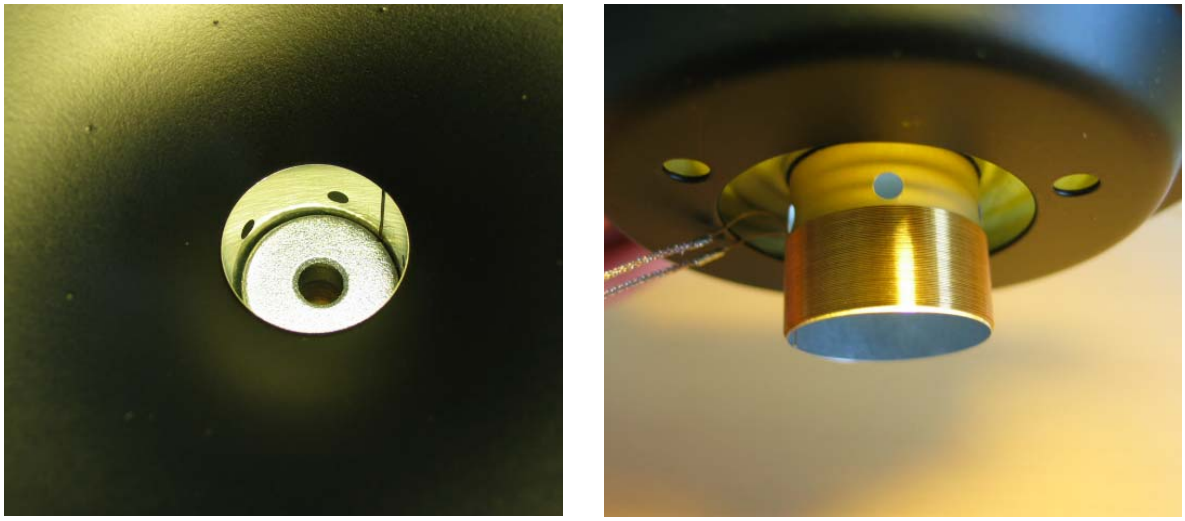

Figure 1.3: Left picture is the diaphragm and voice coil in the magnet system.
Right picture is the voice coil and spider in the chassis.

Figure 1.4: Left picture shows the voice coil and spider in the magnet system.
Right picture shows the chassis and the edge suspension.

1.2. Different types of Electrodynamic Loudspeaker

Electrodynamic loudspeakers are used in many different applications, from very small devices such as hearing aids and mobile phones to very large applications such as public performance systems (PA-audio). The loudspeaker, shown in the last section, used in this report is a mitt-sized loudspeaker unit and this section will highlight some of the differences that must be taken into account. However, in general, the same technology can be used for all sizes loudspeaker units as the basic mechanisms of all electrodynamic loudspeaker units are the same.

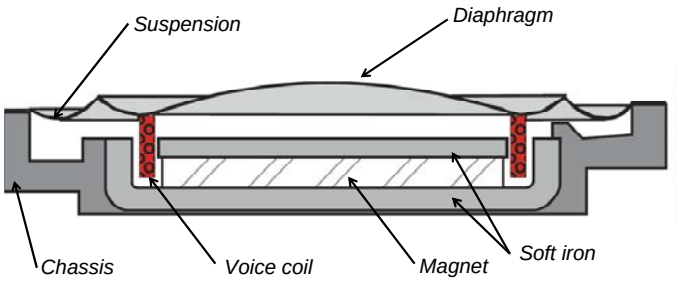

Figure 1.5: Micro-loudspeaker as typically used in mobile phones. Figure from Bright [B10].

One important application where the results from this thesis might be used is in mobile phones. Figure 1.5 shows a typical micro-loudspeaker structure used in mobile phones. The principle is the same as for the loudspeaker unit presented previously. However, it is important to note that the suspension is not made with spider and edge suspension. Instead, there is only the edge suspension, which is typically made of the same material as the diaphragm. This is in contrast to the typical mitt-range loudspeaker studied in this thesis. The suspension for the micro-loudspeaker exhibits different behaviour and suspension data have to be studied separately.

The large low-frequency drivers emphasize the large magnetic structure and the need for a more detailed model of the magnetic structure than used in this thesis [K6]. Acoustic properties that are important for horn loudspeakers are not included in the thesis.

1.3. Modeling of Loudspeaker

The loudspeaker is separated into three parts; the mechanical, the electrical, and the electro-mechanical conversion. The basic law of physics for the different parts are given in the next section; furthermore, simulation blocks and electrical equivalent diagrams are depicted.

1.3.1. The Linear Lumped Model

Mechanical Part

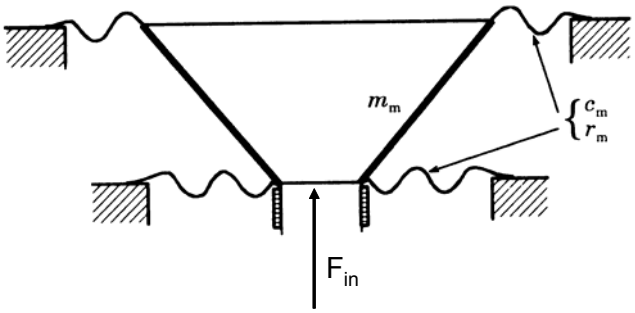

Figure 1.6: Free body diagram of mechanical system. Figure is taken from [R1].

The mechanical part is described by Newton's second law:

$$F_{in}(t) = m_m \cdot a(t) + r_m \cdot v(t) + \frac{1}{c_m} \cdot x(t) \qquad \textit{Equation 1.1}$$

$F_{in}(t)$	the force applied to the diaphragm
a(t)	diaphragm acceleration
v(t)	diaphragm velocity
x(t)	diaphragm displacement
m_m	moving mass
r_m	mechanical losses
c_m	suspension compliance

Equation 1.1 can also be depicted with a block diagram, shown in Figure 1.7.

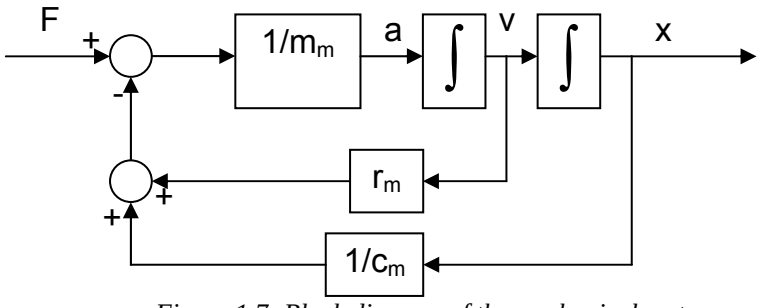

Figure 1.7: Block diagram of the mechanical system.

Electrical Part

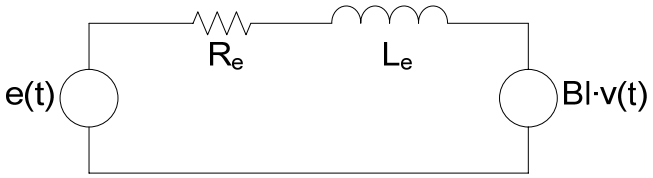

Figure 1.8: Electrical diagram of a loudspeaker.

The electrical part is described with Kirchhoff's voltage law:

$$e(t) = L_e \cdot \frac{di}{dt} + R_e \cdot i(t) + Bl \cdot v(t) \qquad \textit{Equation 1.2}$$

e(t)	the loudspeaker input voltage
i(t)	the loudspeaker current
L_e	the voice coil inductance
R_e	the voice coil resistance
Bl	the force factor

Equation 1.2 includes the back electrical motor force (EMF) from the movement of the voice coil in a magnetic field. Figure 1.9 illustrates the block diagram of the electrical part, including the EMF, where the diaphragm velocity is the input.

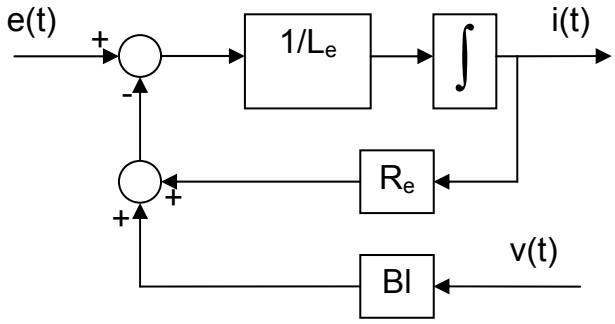

Figure 1.9: Block diagram of the electrical system.

Electro-Mechanical Conversion

The electro-mechanical conversion is the conversion between current and force. This conversion is dependent on the force factor Bl which, as previously described, also occurs in the back EMF when the voice coil is moving.

$$F_{in}(t) = Bl \cdot i(t) \qquad \textit{Equation 1.3}$$

Figure 1.10 has, with Equation 1.3, connected the two previous block diagrams to one diagram for the loudspeaker.

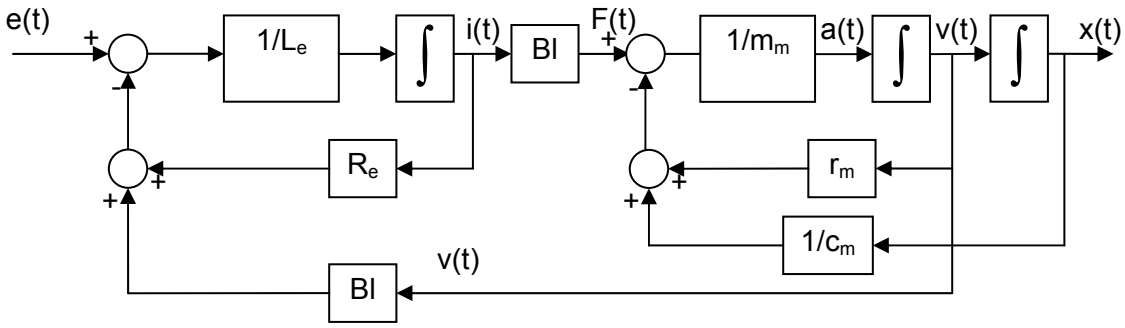

Figure 1.10: Block diagram of the linear loudspeaker.

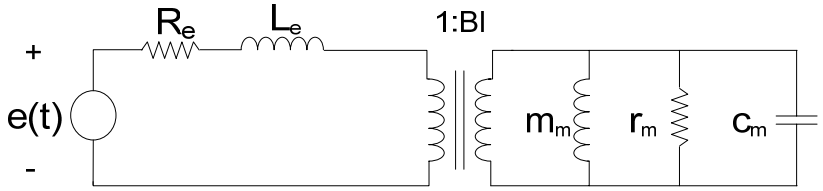

Figure 1.11: Electrical equivalent circuit diagram of the linear loudspeaker.

The electrical equivalent diagram is a classic way of showing the electro-mechanical system, Figure 1.11. It can improve understanding of the loudspeaker and act as a supplement to the block diagrams in the next section.

Acoustic Load

Acoustic load, which refers to the air on the back and front of the diaphragm, has to be taken into account in order to present a complete model. Under normal conditions, a loudspeaker unit is mounted in a box, known as the rear cabinet. In relation to modelling the diaphragms movements, the acoustic load can be simplified into two elements; on the front of the loudspeaker, the moving air mass can be added to the moving mass, m_m, and on the back side of the rear cabinet, where the air inside acts like a compliance, it can be included in the suspension compliance, c_m [R1].
The moving air mass is recalculated to mechanical parameters, but it can also be included as an acoustic parameter by applying the mechanical acoustic transformation of the effective diaphragm area, S (Figure 1.12). The acoustic load is shown as a complex resistor on the acoustic side.

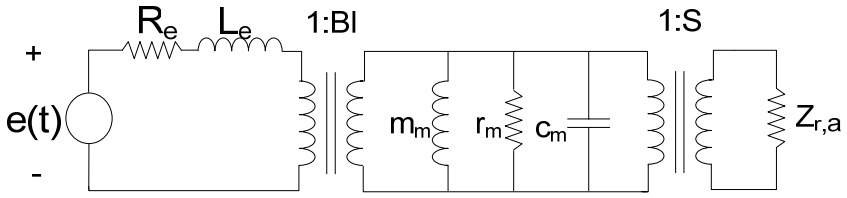

Figure 1.12: Electrical equivalent circuit diagram of the linear loudspeaker.

1.3.2. Frequency Response

One reason for using a linear model is that it gives a simple overview of loudspeaker characteristics. The found linear model is Laplace-transformed in Equations 1.4 to 1.6. These equations can be rewritten to the transfer function (Equation 1.7). Typically, the output of interest is the diaphragm acceleration, due to its proportionality to the sound pressure in the far field [T1]. However, in relation to loudspeaker design, the displacement of the diaphragm is of interest (Equation 1.7). A bode plot from input voltage to diaphragm acceleration is shown in Figure 1.13; the loudspeaker from Appendix 2 is used.

Laplace transformation equation:

$$e(s) = L_e \cdot s \cdot i(s) + R_e \cdot i(s) + Bl \cdot s \cdot x(s) \qquad \textit{Equation 1.4}$$

$$F_{in}(s) = m_m \cdot s^2 \cdot x(s) + r_m \cdot s \cdot x(s) + \frac{1}{c_m} \cdot x(s) \qquad \textit{Equation 1.5}$$

$$F_{in}(s) = Bl \cdot i(s) \qquad \textit{Equation 1.6}$$

Transfer function input voltage to diaphragm displacement:

$$H(s) = \frac{x(s)}{e(s)} = \frac{\dfrac{Bl}{m_m\left(L_e s + R_e\right)}}{s^2 + \left(\dfrac{Bl^2}{m_m(L_e \cdot s + R_e)} + \dfrac{r_m}{m_m}\right)s + \dfrac{1}{c_m \cdot m_m}} \qquad \textit{Equation 1.7}$$

Transfer function input voltage to diaphragm acceleration:

$$H(s) = \frac{x(s)}{e(s)} = \frac{\dfrac{Bl}{m_m\left(L_e s + R_e\right)} \cdot s^2}{s^2 + \left(\dfrac{Bl^2}{m_m(L_e \cdot s + R_e)} + \dfrac{r_m}{m_m}\right)s + \dfrac{1}{c_m \cdot m_m}} \qquad \textit{Equation 1.8}$$

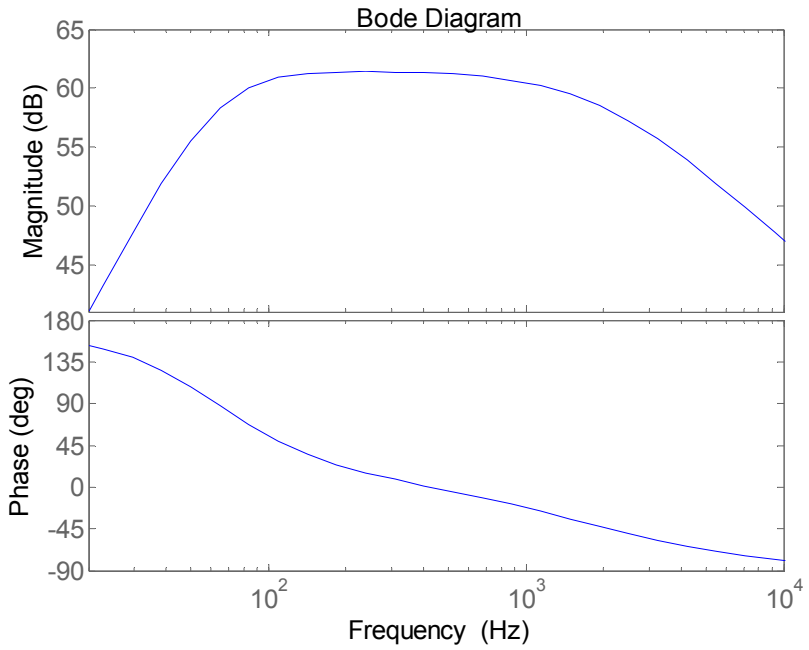

Figure 1.13: Bode plot of the loudspeaker from Appendix 1. Input voltage to diaphragm acceleration.

The transfer function can be simplified by excluding the voice coil inductance, L_e=0. In the case shown in Figure 1.13, the voice coil inductance introduced a pole at 1 kHz. The simplified transfer function, Equation 1.9, is a second-order low-pass function. The general second-order low-pass transfer function is shown in Equation 1.10.

$$H(s) = \frac{x(s)}{e(s)} = \frac{\frac{Bl}{R_e \cdot m_m}}{s^2 + \left(\frac{Bl^2}{R_e \cdot m_m} + \frac{r_m}{m_m}\right)s + \frac{1}{c_m \cdot m_m}} \qquad \textit{Equation 1.9}$$

$$H(s) = \frac{x(s)}{e(s)} = K \cdot \frac{\omega_n^2}{s^2 + 2 \cdot \xi \cdot \omega_n \cdot s + \omega_n^2} \qquad \textit{Equation 1.10}$$

ω_o	the mechanical resource frequency
ξ	the electro-mechanical damping factor
K	amplification constant

From Equation 1.9 and 1.10, the resonance frequency, damping, and amplification constant can be found.

Resonance frequency:

$$f_0 = \frac{1}{2\pi\sqrt{m_m \cdot c_m}} \qquad \textit{Equation 1.11}$$

f_o the mechanical resource frequency

Damping factor:

$$\xi = \frac{Bl^2\sqrt{c_m}}{2 \cdot R_e\sqrt{m_m}} + \frac{r_m\sqrt{c_m}}{2\sqrt{m_m}} \qquad \textit{Equation 1.12}$$

Amplification constant:

$$K = \frac{Bl}{\mathrm{R_e} \cdot m_m} \qquad \textit{Equation 1.13}$$

1.3.3. Impedance of Loudspeaker

The impedance of the loudspeaker is interesting in constructing the driver to match the power amplifier. The loudspeaker impedance is often modelled as a resistor. This assumption is far from sufficient. The impedance function can be calculated from Equation 1.14 to 1.17, which gives the impedance or the transfer function from voltage to current.

Loudspeaker impedance:

$$H(s) = \frac{e(s)}{i(s)} = \frac{s^2 + \frac{Bl^2 + (R_e + sL_e) \cdot r_m}{m_m \cdot (R_e + sL_e)} \cdot s + \frac{1}{c_m \cdot m_m}}{\frac{1}{\mathrm{R_e} + sL_e} \cdot \left(s^2 + \frac{r_m}{m_m} \cdot s + \frac{1}{c_m \cdot m_m} \right)} \qquad \textit{Equation 1.14}$$

As example is the impedance of the previous used loudspeaker shown on Figure 1.14.

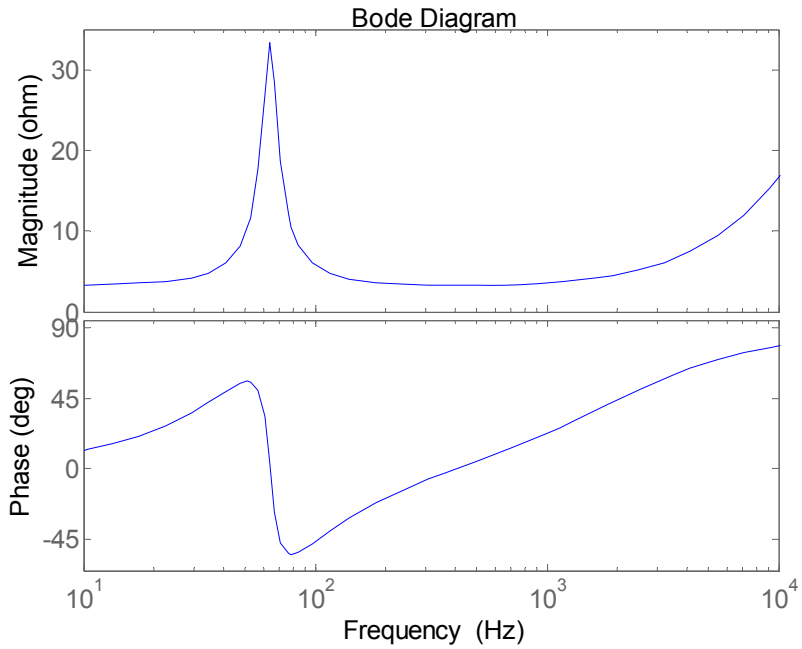

Figure 1.14: Impedance of the loudspeaker described in Appendix 2 and used in many examples throughout this thesis, modelled by Equation 1.11

The voice coil inductance is often neglected and the simplified impedance with the low-frequency impedance model lead to Equation 1.13.

Loudspeaker impedance, $L_e \equiv 0$:

$$H(s) = \frac{e(s)}{i(s)} = \frac{s^2 + \frac{Bl^2 + R_e \cdot r_m}{m_m \cdot R_e} \cdot s + \frac{1}{c_m \cdot m_m}}{\frac{1}{R_e}\left(s^2 + \frac{r_m}{m_m} \cdot s + \frac{1}{c_m \cdot m_m}\right)} \qquad \textit{Equation 1.13}$$

With or without the voice coil inductor, the dynamic of the high-frequencies of a loudspeaker are not well-represented. The voice coil inductors core, the loudspeaker magnet, has high losses in the structure as eddy currents [V1]. Vanderkooy (1988) found that a half inductor model had a good structure for the voice coil inductor (Equation 1.14).

$$e_{L_e}(s) = L_e \cdot i_{L_e}(s) \cdot s^{1/2} \qquad \textit{Equation 1.14}$$

Thorborg, 2007 [T10] has made an extended loudspeaker model where the eddy currents are modelled with two LC circuits. The four extra components, as presented at the AES Convention, are related to physical aspects of the loudspeaker magnet, and not a black box model as presented by Vanderkooy.

1.4. Conclusion of the Linear Loudspeaker

In many end product loudspeaker designs, the linear loudspeaker equations are sufficient. For designing loudspeaker units it is necessary to understand the non-linearities that occur in the loudspeaker unit. The linear loudspeaker equations are very helpful in obtaining this knowledge.

For more detailed investigations of loudspeaker unit design with linear equations see Section 4.2.2, Loudspeaker Efficiency; Design of Loudspeaker Units.

Chapter 2

2. Nonlinearities in Loudspeakers

The following description is a review of sources for nonlinear distortion in electrodynamic loudspeaker units. Nonlinear loudspeaker modelling is crucial for understanding loudspeaker unit design and is the basis for implementing a feed forward compensator.

This chapter reviews the nonlinearities in an electrodynamic loudspeaker, based on various experiments of a typical 6½ inch loudspeaker unit. The chapter begins with the nonlinearities in the electromagnetic conversion, including some magnet designs. This is followed by the section, the Suspension, where a part of the project studies are added, Time Varying Behaviour of the suspension. Finally, the voice coil induction nonlinearity and the diaphragm mass and area nonlinearities are reviewed. The chapter ends with a simulation case that is compared with the measurements of a loudspeaker unit.

2.1. One Dimensional Nonlinearities

All of the described nonlinearities in this chapter are one-dimensional, which is one of the most important aspects of the project: Error Correction of Loudspeakers. Multi dimensional nonlinearities are not possible to pre-distort and cannot be eliminated with the one-dimensional input of the loudspeaker; examples of this are the break-up and oscillations on the diaphragm. However, the break-up of the diaphragm will not be described here, although this is a very important issue regarding creating a successful loudspeaker unit design.

A multi-input speaker system is studied at the end of the thesis as an alternative to the conventional loudspeaker system. This can open opportunities for controlling the sound field and possibilities of cancelling more then one dimensional errors.

2.2. Force Factor

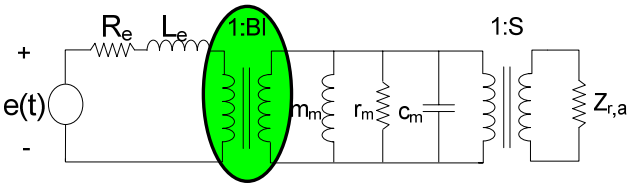

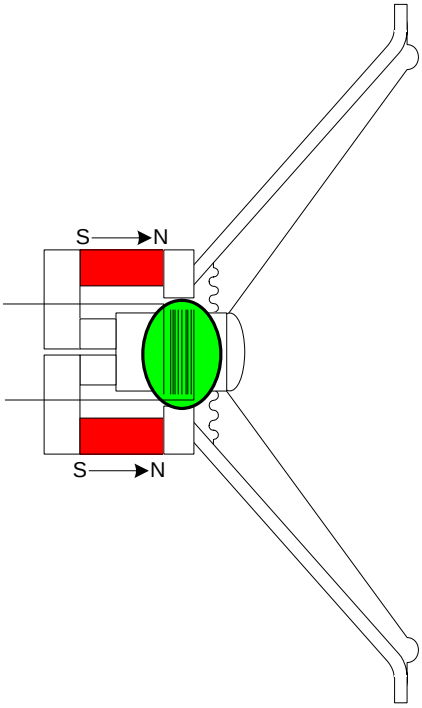

Figure 2.1 The force factor is marked on the electrical equivalent diagram. This is the transformation from current to force. The area is marked where the magnet gap and voice are on the loudspeaker cross section.

The electromagnetic conversion of current to force has additional characteristics then described in the linear loudspeaker model. In the linear loudspeaker model, the force factor is modeled as a constant dependent of the B-field and the effective length of the wire in the field. When the wire is moved away from the field the force factor Bl decreases, resulting in the displacement dependency of the force factor [W10], which is one of the main nonlinearities [S1]. The geometry of the loudspeaker's magnet and voice coil is an important design parameter [B1], as illustrated through examples.

The magnetic field in the magnet gap is disturbance from the field made by the current through the voice coil, this is a nonlinearity that applies hysteresis loop behaviour, flux modulation [M1, A10, B20, V10].

A more detailed description is found in the following three sections:

1. The Displacement Dependency Force Factor
2. Magnet and Voice Coil Design
3. Flux Modulation

2.2.1. The Displacement Dependency Force Factor

A good starting point is to look at the loudspeaker magnet, as the purpose is to have a gap with a constant flux. A typical magnet design is shown in Figure 2.2. Soft iron transports the flux from the permanent magnet to the gap.

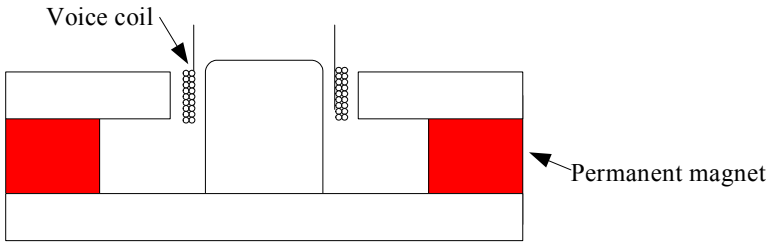

Figure 2.2: Cross-section of a loudspeaker magnet and the voice coil.

The displacement nonlinearity of the force factor is primarily dependent on the geometry of the magnetic system and the voice coil. The force factor decreases when the voice coil moves away from the central position of the magnet gap. Figure 2.3 shows an example of a displacement depending force factor function. This can be

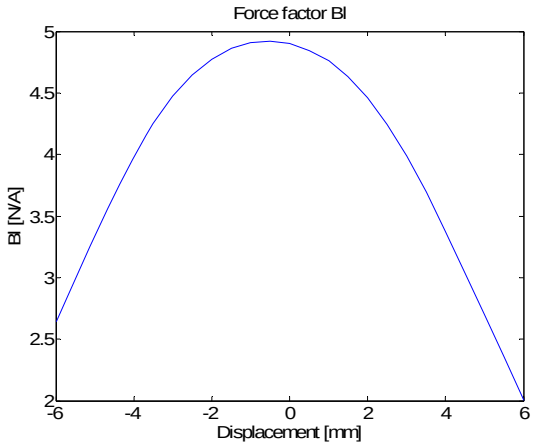

Figure 2.3: Electromechanical conversion current to force. The Bl force factor.

modelled with a polynomial fit, Equation 2.1, or a Gaussian curve, Equation 2.2 [S2, K10, K11].

$$Bl(x) = Bl_0 + Bl_1 \cdot x + Bl_2 \cdot x^2 + Bl_3 \cdot x^3 + ... \qquad \textit{Equation 2.1}$$

$$Bl(x) = Bl_0 \cdot e^{-\mu(x-x_0)^2} \qquad \textit{Equation 2.2}$$

Where Bl_0 is the static force factor at the rest position(x_0), Bl_1, Bl_2 and μ are nonlinear parameters.

2.2.2. Magnet and Voice Coil Design

The magnet shall provide a homogeneous and strong B-field in the magnetic gap. The field or the spread of the field depends on the geometry of the magnet. In this section, three different magnet structures will be shown together with the corresponding displacement dependent force factor function. For more detailed magnetic field analysis the Finite Element Methods can be used [D1].

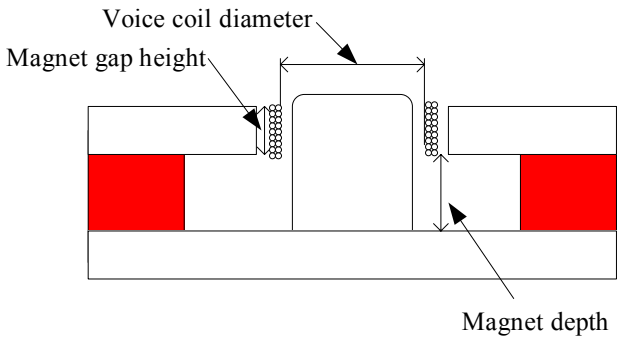

Figure 2.4 Cross section of the used magnet with voice coil.

For the examples shown here, the force factor is measured with a small two-layered voice coil with 6 windings (see Appendix 4 for the measurement setup). The simple magnet structure shown in Figure 2.5 has a non-symmetric design. The negative x-axes of the force factor functions correspond to the voice coil moving into the magnet. The flux flow of the magnet inwards compared with the flux flow outwards corresponds to the principle flux flow as seen in Figure 2.5 (The flux is spread out in an inward fashion due to the metal of the central pole). On top of the magnet gap, the flux creeps around to the top of the central pole piece.

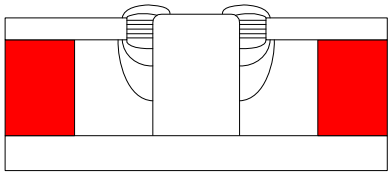

Figure 2.5 Illustration of the magnetic flux in a non-symmetric magnet, asymmetrical flux. To the right is the electro mechanical conversion, the Bl factor.

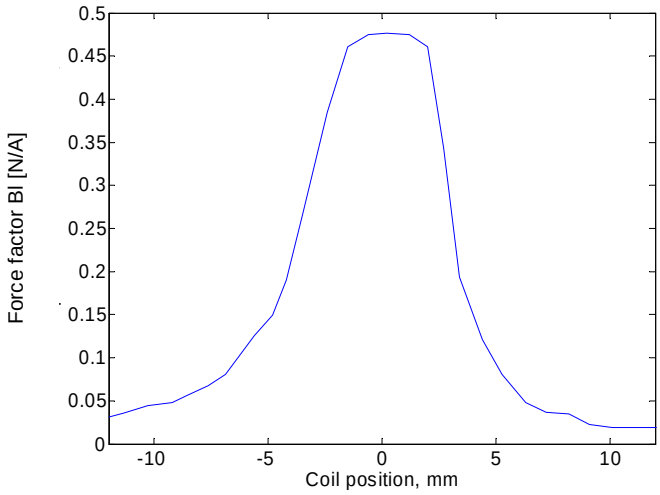

A symmetric design can be achieved by extending the central pole piece, Figure 2.6, or by adding an extra piece of metal to the central pole to obtain symmetry, Figure 2.7.

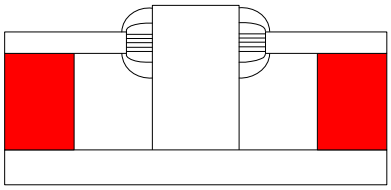

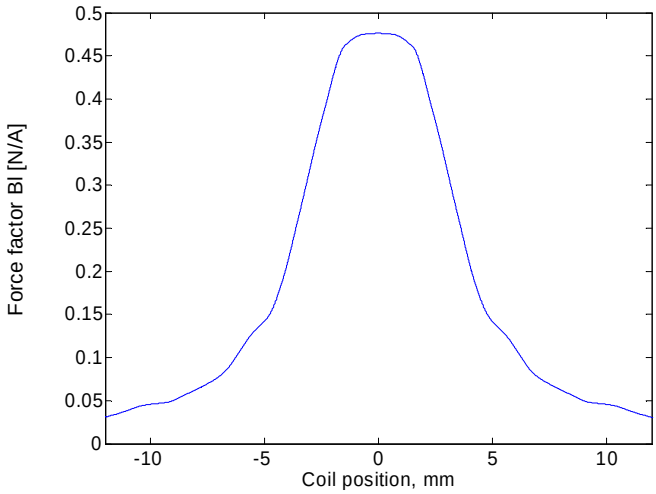

Figure 2.6 Magnetic design with symmetry flux: magnetic system with overhang. To the right is the electro mechanical conversion, the Bl factor.

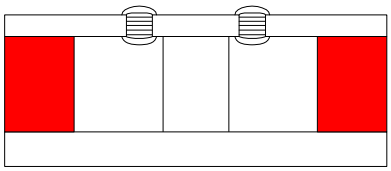

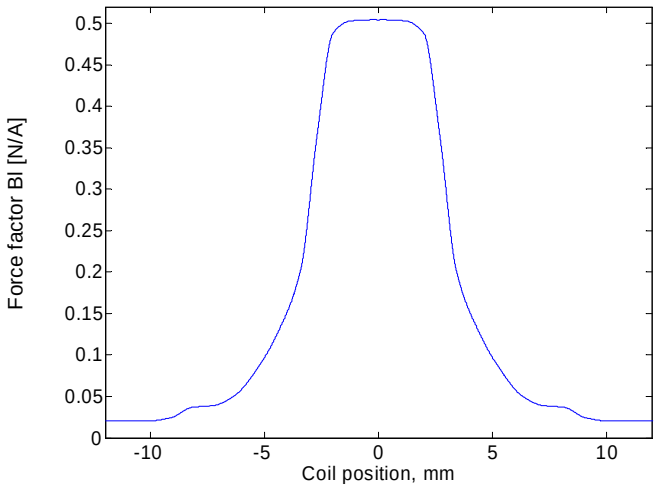

Figure 2.7 Magnetic design with concentrated symmetry flux: Magnetic system with extension metal. To the right is the electro mechanical conversion, the Bl factor.

Comparing the two symmetric designs illustrates the different behaviours in the nonlinear force factor. The magnet system with extension metal is nearly linear at small displacements but more nonlinear at large displacements.

The second parameter in the force factor is the length of wire in the magnetic field, the voice coil. From the basic equation F=Bli it is simple to see that a longer wire provides a stronger force, but other design parameters limit the design resulting in the thermal limitations of the maximum power loss in the voice coil. This leads to a maximum voice coil resistance, and in order to fulfil the voice coil resistance requirement, the wire needs to be thicker if it is made longer. Indeed, as the wire diameter increases, the number of windings inside the magnetic gap decreases. This relationship then leads to a direct comparison between a short voice coil and a long voice coil. For the purpose of this comparison, the voice coil resistance will be held constant. Table 2.1 shows the data

from the short and long voice coil. The magnet from Figure 2.6 is used and the magnet gap height is 4 mm.

	Short voice coil designs	Full voice coil
Resistance	2.34Ω	2.34Ω
Voice coil length	6.5mm	13.5mm
Number of windings	48	78
Wire diameter	0.27mm	0.35mm
Wire length	8.0m	13.1m
Voice coil weight	4.1g	11.0g
Diaphragm diameter	124mm	124mm
Diaphragm mass	7.9g	7.9g
Moving mass (m_m)	12.0g	18.9g

Table 2.1 Voice coil designs, specifications.

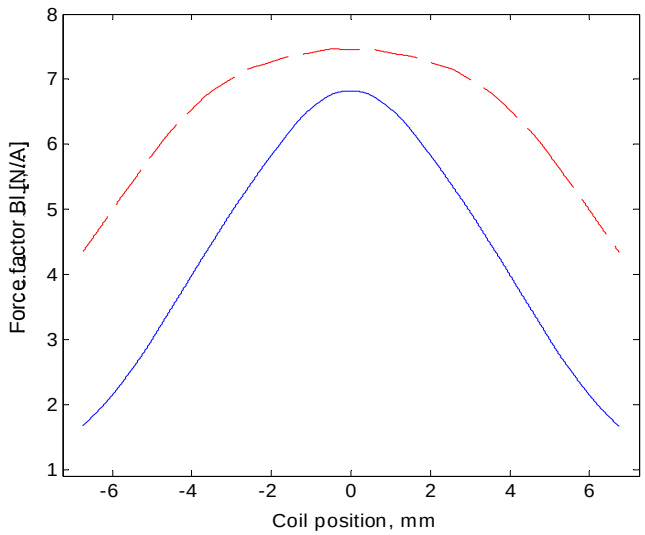

Figure 2.8 Red dashed; fully-winded voice coil. Blue, full line; Short voice coil

The force factor from the two voice coil designs are presented in Figure 2.8. As illustrated, the long voice coil improves linearity; thus, explaining its popularity in long voice coil designs. However, the comparison does not take into account that the thicker wire needs a larger magnet gap which will decrease the overall force factor level of the long voice coil; in the above case it is estimated to 4%. A second drawback is that the longer wire is heavier and will decrease the sensitivity (see Chapter 4).

2.2.3. Flux Modulation

An external field on a static magnetic field causes the static field to be deformed. This deformity is a part of 'flux modulation', and will change the flux in the magnetic gap.

Figure 2.9 illustrates the principles of a wire with a current through a magnetic field. If the magnetic field is stronger, the disturbance of the field is less. Simulation of the magnetic systems can be done with Finite Element Methods, [D1] and flux modulation included. Figure 2.10 shows two examples of the same magnet systems force factor as a function of position. The figure is taken from an Irina Aldoshina paper, 1995 [A10]. The first force factor function has a positive current and the second has a negative current. Similar results are obtained by David Bird in 1990 [B20].

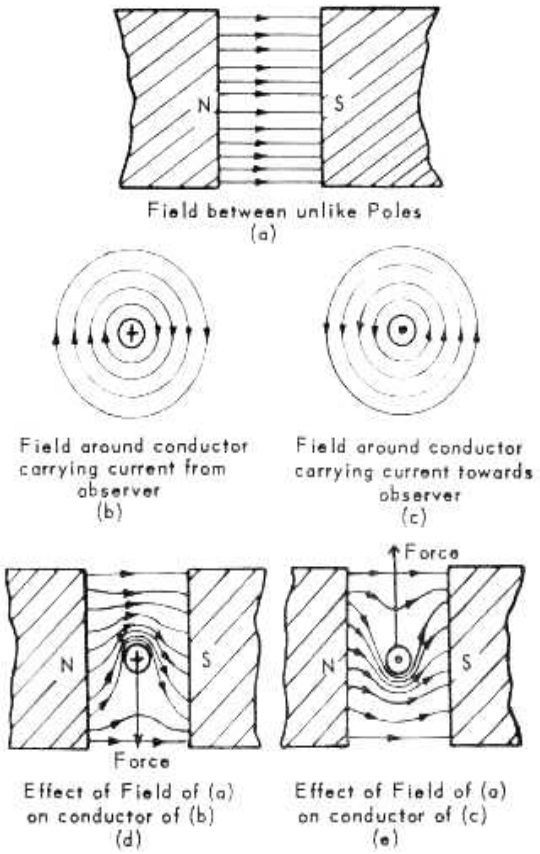

Figure 2.9 Principle of flux modulation. Taken from [N1]

Voishvillo obtained significantly better simulation results of the diaphragm movements by including flux modulation [V10]. The significant difference is in frequencies above the resonance frequency where Voishvillos simulations show an improvement of more than 10dB in distortion level.

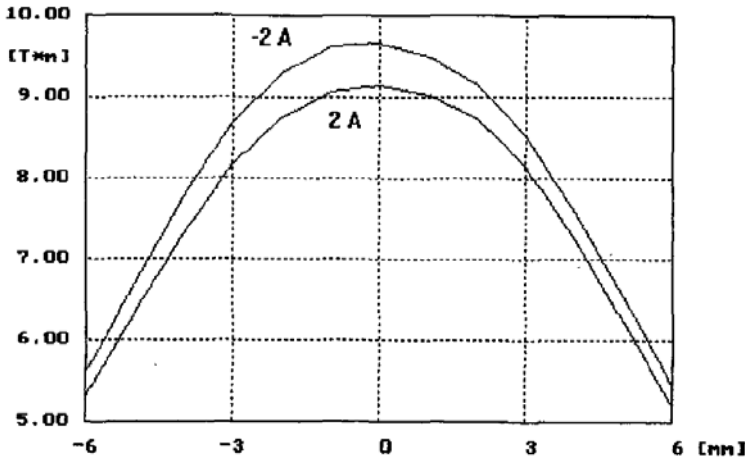

Figure 2.10: Force factor as function of position. Taken from [A10]

2.3. Suspension

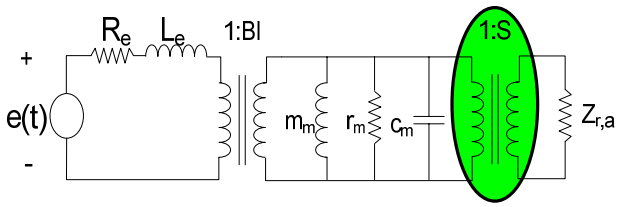

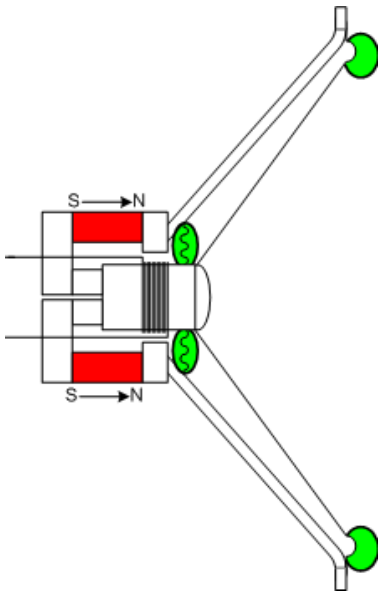

Figure 2.11 The suspension is marked on the electrical equivalent diagram. The spider and edge suspension are marked on the cross section of the loudspeaker unit.

The suspension of an electrodynamic loudspeaker serves the purpose of fixing the voice coil in a well defined resting position. In the simple linear lumped parameter model the suspension is modeled as a linear spring with a simple viscous damping in parallel. Together with the moving mass of the loudspeaker the compliance of the suspension defines the resonance frequency of the system. A more detailed analysis of the suspension has shown that the suspension behaves nonlinearly at higher displacement levels [K3][C1]; this is one of the causes of distortion in the loudspeaker. The suspension cannot be modeled as a simple spring due to a viscous relaxation effect in the materials, commonly known as creep, which causes the compliance of the suspension to appear softer as frequency is decreased [K15]. Other experiments have shown that the suspension is time-varying as the resonance frequency of the loudspeaker often drops significantly during and shortly after high level excitation. This can be a major problem when tuning box design, especially for the vented systems. If all of these properties of the suspension not are fully understood and properly modeled it will be very difficult to successfully implement the nonlinear compensation techniques [K2][B10], which rely on an inverted model of the loudspeaker in order to calculate the input voltage signal that generates the distortion canceling effect of the loudspeaker.

The nonlinear suspension section consists of the following three categories:

1. The Displacement Dependency Suspension
2. Suspension Creep
3. Time Varying Behaviour of the Suspension

2.3.1. The Displacement Dependency Suspension

Suspension stiffness depends of the diaphragm position, [O3] as increasing displacement increases suspension stiffness. The compliance of the loudspeaker is made by the following two components: the spider typically consists of polymer (left picture in Figure 2.12) and on top of the chassis is the edge suspension which is made of rubber (Right picture in Figure 2.12).

Figure 2.12 Left picture of the spider mounded between the diaphragm and the voice coil. Right picture shows the edge suspension on top of the basket.

The suspension compliance of a 6½ inch loudspeaker unit, Appendix 1, has been tested with the Klippel Analyzer, [K1], and then measured as a function of position. First, the entire loudspeaker unit was tested. This was followed by additional testing without the edge suspension, which was physically removed. The spider has the main stiffness, the edge suspension in this case about 3 times softer, see Figure 2.13.

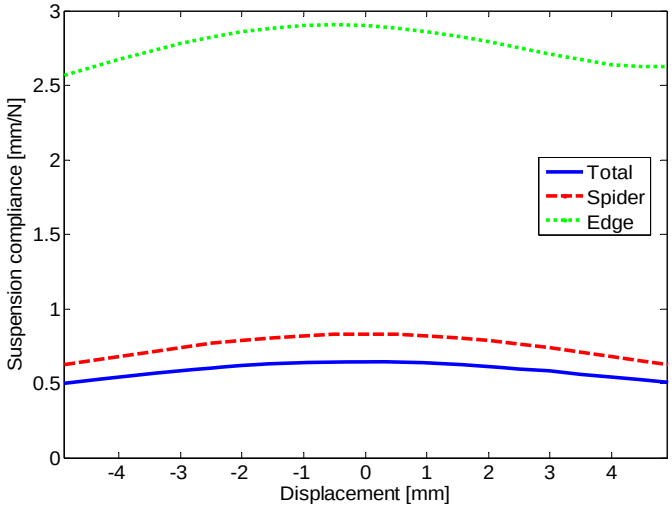

Figure 2.13 Suspension compliance as a function of the position. Total suspension (___), the Spider (---), and the edge suspension (...).

2.3.2. Suspension Creep

Creep was described by Knudsen and Jensen (1992) [K13] as "continued slow displacement under sustained force." They tested a linear creep model, an exponential model, and a logarithmic model. The logarithmic model was found useful for modelling the creep, Equation 2.3 [K13].

$$c_l(s) = c_l \cdot (1 - \lambda \cdot \log(s)) \qquad \textit{Equation 2.3}$$

$c_l(s)$	Suspension compliance of the logarithmic creep model [m/N]
c_l	Stay stated suspension compliance [m/N]
λ	Relative magnitude slope per decade.

Knudsen and Jensen's logarithmic creep model improves the coherence of the diaphragm movements by frequencies under and around the resonance frequency.

Figure 2.14 shows the displacement of the diaphragm when a constant force is applied. The constant force is implemented by adding mass to a horizontally placed loudspeaker unit. The figure illustrates the creep effect as the diaphragm moves slowly for a long time after the mass was added. When removing the mass, the diaphragm does not go straight back to the rest position, but rather creeps back.

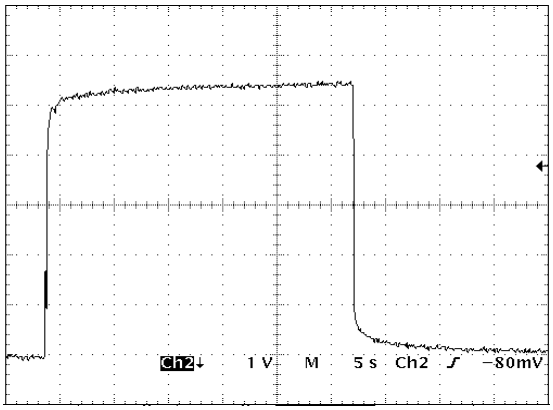

Figure 2.14 Displacement of the diaphragm by adding mass. x axis 5 s/div. y axis 1mm/div. Positive displacement is defined as movement into the unit.

Diaphragm displacement	Before excitation	After excitation	Change
6.6mm	0.541mm/N	0.566mm/N	4.6%

Table 2.2 Suspension data at the rest position before and after creep.

Table 2.2 compares the small signal compliance after 10 minutes displaced at approximately 6.6mm with the compliance before the excitation. The resonance frequency is measured with the multi-tone signal, described in section 2.3.3. The compliance change corresponds to the change introduced by the displacement nonlinearity of the suspension compliance, due to the offset of the diaphragm generated by creep.

2.3.3. Time Varying Behaviour of the Suspension

The suspension has a time-varying behaviour dependent on the input power [A1] and the diaphragm displacement. Investigations into this topic have been made during the project period, and are published at AES [P24] and documented in this section.

A thermal model of the loudspeaker suspension is made and the heating causes are investigated. Heating of the suspension can come from heat transfer from the voice coil or from mechanical work. Mechanical work is produced by movement of the loudspeaker diaphragm. Testing shall characterize the influence of displacement and the velocity of the diaphragm.

The investigations are limited to investigating the small signal parameter and the compliance at the rest position. Loudspeaker distortion simulations of the found results are displayed at the end of the chapter based on the thermal model of the suspension.

Thermal model of the Suspension

The physical cause of time-varying behaviour of the suspension is believed to be the heating of the suspension. Agerkvist has tested a suspension model based on the power dissipation in the loudspeaker [A1] that relates to heat. Heating of a material increases the movement of molecules and leads to a weaker interconnection between the molecules, which results in a softer material [M30].

Figure 2.15 shows the tested thermal model, and the corresponding equations are given by Equation 2.3 and 2.4.

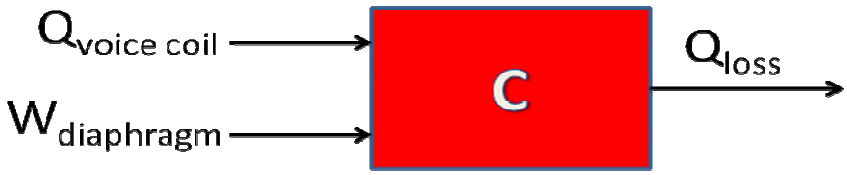

Figure 2.15 Thermal loudspeaker suspension model

C	Heat capacity of the suspension [J/K]
$Q_{voice\ coil}$	Heat transfer from the voice coil [J]
$W_{diaphragm}$	Mechanical work applied from the diaphragm [J]
Q_{loss}	General cooling, heat loss of the suspension [J]

$$C = c \cdot m_{suspension}$$ *Equation 2.3*

c	Specific heat capacity of the suspension [J/K kg]
$m_{suspension}$	Mass of the suspension [kg]

$$C\frac{dT}{dt} = Q_{voice\_coil} + W_{diaphragm} - Q_{loss}$$ *Equation 2.4*

T	Temperature [K]

The model consists of the heat capacity of the suspension and energy to and from suspension. This results in logarithmic behaviour as long as the 'in' and 'output' functions are linear equations.

The loss is the cooling of the suspension. A precise thermal model is difficult to obtain and so a simplified model is used. A general cooling model of the suspension has to take static cooling into account as heat transfers to the various loudspeaker parts and to ambient. Thus, when the diaphragm is moving, a ventilation effect will occur and generate a major change. The cooling principle of the voice coil in many loudspeaker units is made with an airflow generate around the voice coil when the diaphragm is moving. The heated air from the voice coil will pass by the spider and transmit heat to the suspension depending of the diaphragm movements, see Figure 1.2. When there has been a large long term power dissipation in the loudspeaker the magnet structure heats up and conducts a heat wave to the spider, see Figure 1.4. Inferred heat wave energy transferred is a function of the temperature difference of the objects, the magnet structure and the spider, to the power of four: not a linear function. The thermal model of the loudspeaker suspension needs a very precise investigation and this project does not have the necessary equipment. However, one solution is to make a final element model and validate the model with thermal scans. In a case when the diaphragm is not moving and the temperature difference is small, the thermal losses can be estimated as a constant [D10].

The mechanical work is the energy that heats up the suspension by the movements the suspension is making: a function of diaphragm velocity. It can also be a displacement level dependent function.

Experiment

The experiment was designed to investigate and support the thermal model. A test series was made to investigate the influence of diaphragm displacement, velocity, and dissipated power in the voice coil. The measurement setup is shown in Appendix 5, where the loudspeaker voltage, current, and displacement are measured.

The objective was to obtain the suspension compliance at the rest position and afterwards to apply a test signal, a loudspeaker stimulus. The loudspeaker stimulus was represented in three stimulus sets. The first investigated the influence of diaphragm displacement level by applying a sinus signal with different voltage levels. The second set tested the velocity dependency by using two different frequencies sinus signals under the loudspeaker resonance frequency. The third added extra power in the voice coil by applying a 1 kHz sinus signal at the same voltage level. The details of the stimulus signals are displayed in Tables 2.3 and 2.4.

Sinusoidal stimulus signal	Diaphragm displacement
40Hz, 0.99V_{rms}	0.9mm peak
40Hz, 1.98V_{rms}	1.9mm peak
40Hz, 3.97V_{rms}	3.8mm peak
40Hz, 7.84V_{rms}	6.6mm peak

Table 2.3 Stimulus set 1

Sinusoidal stimulus signal	Diaphragm displacement
40Hz, 7.84V_{rms}	6.6mm peak
20Hz, 7.84V_{rms}	6.1mm peak
40Hz, 7.84V_{rms}+1kHz, 7.84V_{rms}	7.3mm peak

Table 2.4 Stimulus set 2 and 3

The small signal resonance frequency was measured with a multi-tone signal centred at the resonance frequency. In order to drive the loudspeaker at high levels and still measure the small signal resonance frequency, the test signal was 2 seconds of a 100mV_{rms} multi-tone signal, followed by 4 seconds of the high level stimulus signal (see Figure 2.15 and 2.16). This sequence was repeated for 10 minutes, and afterwards the low level measurement was repeated for 20 minutes. The stimulus was made in three sets. The resonance frequency was found by the minimum of the loudspeaker current. The moving mass was assumed to be constant; therefore, the suspension compliance can be found from the resonance frequency.

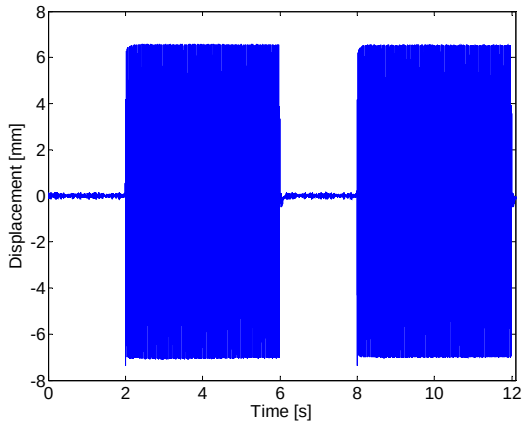

Figure 2.15 Displacement of the cone in the measurement. Stimulus with 40Hz sinusoidal.

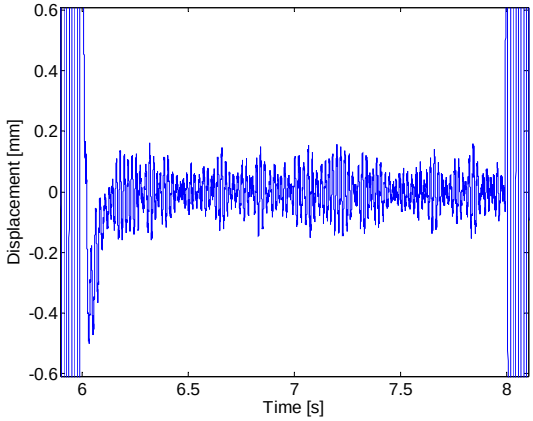

Figure 2.16 Zoom of figure 2.15. Displacement of the cone in the measurement. Stimulus with 40Hz sinusoidal.

Figures 2.15 and 2.16 are measurements from Data Set 1 showing the diaphragm displacement. Figure 2.16 is a zoom of the multi-tone measurement signal after a stimulus. Approximately 200ms after the onset of the measurement signal the diaphragm has reached the stationary movement. The resonance frequency estimate is based on the data from 500ms after the stimulus with a 1s time span of data used.

Figure 2.17 shows the frequency contained in the loudspeaker current signal, obtained by doing a measurement. There are used 20 sinusoidal signals, from 44Hz to 63Hz, with a 1Hz interval. The figure below shows the resonance frequency, in this case to be approximately 56Hz.

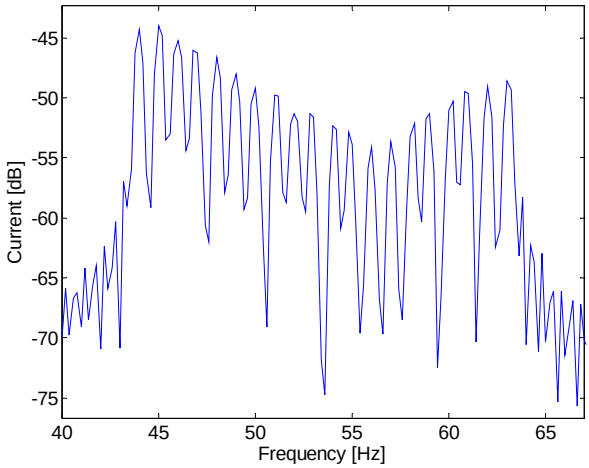

Figure 2.17 FFT of the loudspeaker current of the used multi-tone measurement signal from the experiment.

The measured multi-tone current is fitted with a second order polynomial. The loudspeaker is assumed to be a second order system around the resonance frequency, ±10Hz. In the frequency domain, or the Laplace transformed transfer function, (Equation 1.8) is a second order polynomial in the denominator, L_e=0; therefore, the second order fit is a good choice for frequencies around the resonance frequency.

Measurement Results

Figure 2.18-2.21 shows the compliance at the rest position as a function of time. There are two figures of one measuring set. For example, stimulus set 1 starts in Figure 2.18 and continues uninterrupted in time, in Figure 2.19 where the stimulus is turned off. Figures 2.18 and figure 2.19 show stimulus set 1, the displacement dependency of the suspension compliance. Figures 2.20 and 2.21 both include stimulus set 2 and 3, the velocity and power consumption test.

Displacement depending suspension compliance:

The displacement depending suspension test was made with a standard loudspeaker unit and the suspension was not tested separately, which caused a non-independent test. The major error source was that the heat from the voice coil heated the suspension, as did by the displacement level which was being tested. Equation 2.4 shows that the heat transferred from the voice coil added to the temperature of the suspension and the heat flow from the suspension cooled the suspension.

Heat from the voice coil:
Under the displacement test, the heat transferred has to be negligible in comparison to the energy from the mechanical work, or the heat flow from the voice coil has to be subtracted. By the largest displacement level, approximately 4W is dissipated, which is primarily lost in the voice coil.

Cooling of the voice coil:
The cooling is modelled as a linear function in Equation 2.4, which is not the case. The linear cooling function was valid when the diaphragm was not moving significantly and was not generating an air flow around the suspension. In doing the displacement test, a cooling effect must be taken into account as it will decrease the change of suspension stiffness.

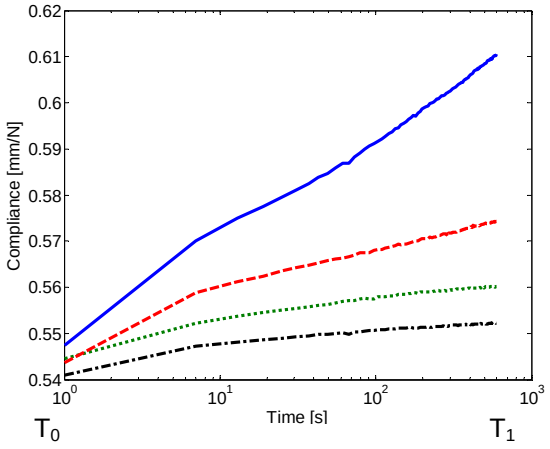

Figure 2.18 Suspension compliance as a function of time, before and during stimulus. Four different levels of stimulus with 40Hz sinusoidal. 6.6mm displacement (___), 3.8mm displacement (---), 1.9mm displacement (....), and 0.9mm displacement (.-.-.).

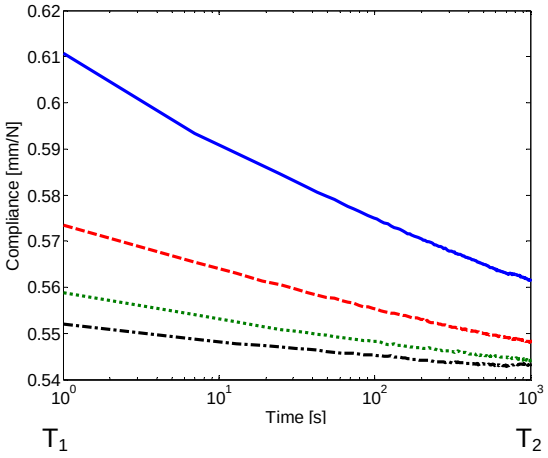

Figure 2.19: Suspension compliance as function of time, after stimulus. Four different levels of stimulus with 40Hz sinusoidal. 6.6mm displacement (___), 3.8mm displacement (---), 0.9mm displacement (....), and 1.9mm displacement (.-.-.).

The result showed the assumption that the effect is mainly due to the mechanical movements and that the stiffness change has a correlation with the displacement level. In Figure 2.18, the four displacement tests did not have the same compliance at the beginning because the tests were made using too short a time interval in between so the suspension did not recovered.

Velocity depending on suspension compliance:

The velocity test was made at half the frequency of the displacement tests, 20Hz with the same voltage level as the largest displacement test, and resulted in approximately the same displacement level. At 20Hz, the loudspeaker's impedance is 4.6Ω in contradiction to the 14Ω at 40Hz, which leads to a power consumption of 4W by 40Hz and 13W by 20Hz. Figure 2.20 illustrates that the 20Hz and 40Hz tone almost results in the same compliance change. After 100 seconds at the 20Hz test, the compliance level was raised, which is the opposite what would be expected if the diaphragm velocity were to influence the suspension stiffness. The reason is believed to be found in the loudspeaker impedance, which is smaller by 20Hz, thus leading to a higher power loss in the voice coil heating the suspension.

Power loss depending on suspension compliance:

The loudspeaker impedance by 40Hz is 14Ω and 3.4Ω at 1kHz. By the 40Hz 7.8V sinusoidal signal, 4W is dissipated in the loudspeaker, and under the power test, there is an additional 17W from a 1kHz sinusoidal which adds up to 21W total power consumption, more than 5 times as much as the 40Hz test. This result shows that, after

approximately 40 seconds, the slope of the measured suspension compliance raises (see the red line in Figure 2.20). This rapid increase is believed, by the author, to be the heat conductance from the voice coil and the magnet structure, which warmed up significantly in the extra power test after some time. It could be this same effect that, to a lesser extent, raises the compliance by the velocity test, 40Hz compared with 20Hz.

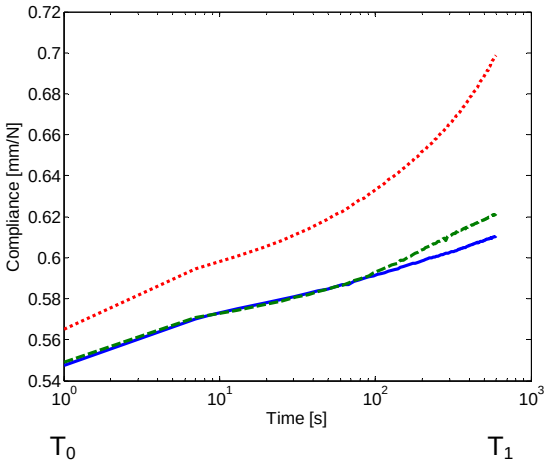

Figure 2.20: Suspension compliance as function of time, before and during stimulus. Stimulus with 40Hz sinusoidal (___), and stimulus with 40Hz, 1kHz sinusoidal (---), and stimulus with 20Hz sinusoidal (....).

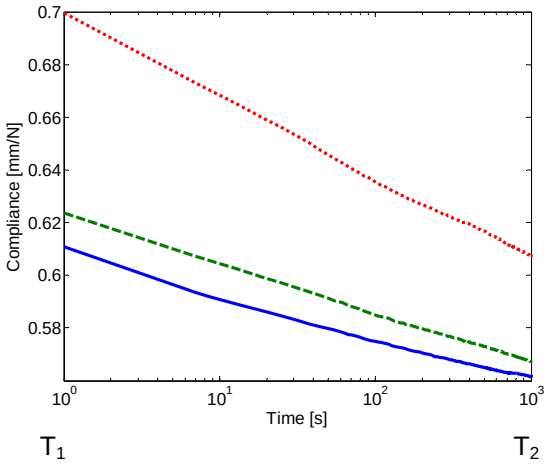

Figure 2.21: Suspension compliance as a function of time after stimulus. Stimulus with 40Hz sinusoidal (___), stimulus with 40Hz and 1kHz sinusoidal (---), and stimulus with 20Hz sinusoidal (....).

Table 2.5 sums up the conditions for the three stimulus in Figures 2.20 and 2.21.

Sinusoidal stimulus signal	Diaphragm displacement	Loudspeaker impedance	Power participation
40Hz, 7.84V_{rms}	6.6mm peak	14Ω @40Hz	4W
20Hz, 7.84V_{rms}	6.1mm peak	4.6Ω @20Hz	13W
40Hz, 7.84V_{rms}+ 1kHz, 7.84V_{rms}	7.3mm peak	3.4Ω @1kHz	21W

Table 2.5 Displacement levels, impedance and power participation

It is from material behaviour known that staging of rubber produces heat inside the material, producing the viscoelasticity effect [M30]. The suspension shall be tested with a generator that applies mechanical force to the suspension, separating the internal material heating from the voice coil heating. It is believed that the internal material heating has a significant effect. When the voice coil and the magnet structure become hot, large power dissipation levels create a heat flow to the spider comparable or larger than the internal heating in the spider material due to the displacement of the diaphragm. This is based on stimulus with 40Hz sinusoidal, where extra energy is applied using a 1 kHz sinusoidal, seen in stimulus 3.

From the suspension tests, it is concluded that the displacement level of the diaphragm is a good parameter for modelling the change of the suspension compliance. In addition, the power loss in the voice coil has to be taken into account. The assumption that the heat from the voice coil spreads to the spider and makes the spider softer is assumed to be correct. Agerkvist [A1] also illustrates these findings, which correspond to the suggested thermal model, Equation 2.4.

Model based on Experiment

The data was investigated based on the model shown in Figure 2.15. According to a first order differential equation, seen in Equation 2.4 and repeated in Equation 2.6, the data should have a logarithmic characteristic.

From the test, it was observed that the displacement level of the diaphragm is an important relationship for heating of the suspension. Figure 2.22 shows the result of a brief, four data points of the four displacement tests after 10 minutes, as the suspension compliance is plotted as a function of the displacement. At larger displacements the slope increased, which could be due to the heat transfer from the voice coil to the suspension.

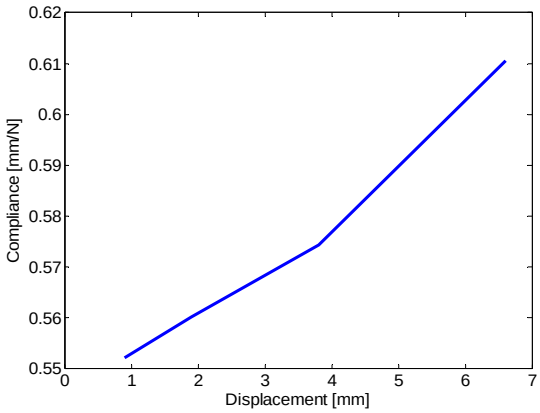

Figure 2.22 Suspension compliance as a function of displacement after the applied stimulus of data set 1. 6.6mm displacement with a 40Hz sinusoidal.

Equation 2.6 models the temperature change of the suspension from the power loss in the voice coil, the mechanical work, and the thermal loss to ambient areas. The thermal loss to ambient areas depends on the suspension temperature and is rewritten in Equation 2.6.

$$C\frac{dT_{Suspension}}{dt} = Q_{voice\_coil} + W_{diaphragm} - Q_{loss} \qquad \textit{Equation 2.6}$$

$$C\frac{dT_{Suspension}}{dt} = Q_{voice\_coil} + W_{diaphragm} - \theta_{Suspension}\cdot(T_{Suspension} - T_{Ambient})\cdot t$$

$T_{Ambient}$	The temperature of the surroundings that cools the suspension
$\theta_{Suspension}$	The thermal resistance of the suspension

The temperature of the suspension is very difficult to monitor, and so, has not been monitored in the experiment. Additionally, the thermal mass of the suspension was not calculated. The temperature of the suspension can be used for calculating the stiffness of the suspension, as shown in Equation 2.7.

$$c_m = \beta_{c_m}\cdot T_{Suspension} \qquad \textit{Equation 2.7}$$

c_m	Suspension compliance at the central position, the small signal value at rest position
β_{cm}	Suspension viscosity temperature constant

In the tests presented here, the suspension compliance found leading to the temperature of the suspension not has to be used. Instead of using the temperature of the suspension, the temperature was replaced by the suspension compliance; Equation 2.6 is rewritten with Equation 2.7.

$$C\frac{dT_{Suspension}}{dt} = \qquad \textit{Equation 2.8}$$

$$C\cdot\frac{1}{\beta_{c_m}}\frac{dc_m(t)}{dt} = Q_{voice\_coil} + W_{diaphragm} - K_{Suspension}\cdot(T_{Suspension} - T_{Ambient})\cdot t$$

The thermal suspension model is a first order-differential equation where the energy can be stored in the thermal mass of the suspension and cooling to the ambient is lost, as inputs are the heat transference from the voice coil and the mechanical work. Equation 2.9 is the time domain solution of the first order differential equation (2.8). This equation includes the mechanical work, the thermal loss, and heat from the voice coil in a combined constant in the logarithmic function. All physical material constants from equation 2.8 are rewritten to the normalized magnitude slope constant per decade, α_{cm}.

Under the displacement test, it is believed that the heat transferred from the voice coil to the suspension has only a minor influence and can, thus, be neglected.

$$c_m(t) = c_{m(t_0)} + x_{peak}(t) \cdot \alpha_{c_m} \cdot \log(t) \qquad \textit{Equation 2.9}$$

x_{peak} diaphragm displacement
$c_m(t_0)$ starting suspension compliance
α_{cm} normalized magnitude slope constant per decade

The normalized magnitude slop per decade is calculated from Figure 2.22 and is shown in Table 2.6. The slope was found using the beginning time until the stimulus was finished. The normalized magnitude slop per decade was relatively constant, except from the 0.9mm displacement test, which was the first measurement done in the test series. Based on the first test, a long-term suspension change can appear, which is not included in the model. Therefore, the 0.9mm displacement tests inequalities that are not believed to be significantly inconsistent with a displacement depending model. The displacement model is suggested as a useful model, and the average slope value was used in the simulations in section 2.7.3. The slop difference between the 1.9mm and 3.8mm measurement was 1.6% and is in the spread that can be expected for this measurement. The difference from 3.8 to 6.6mm is 18,3% which is believed to be caused by significant heating from the power loss in the voice coil.

Stimulus level, displacement	Before and during stimulus, α_{cm}
0.9 mm	$4.78 \cdot 10^{-3}$ N^{-1}
1.9 mm	$3.16 \cdot 10^{-3}$ N^{-1}
3.8 mm	$3.11 \cdot 10^{-3}$ N^{-1}
6.6 mm	$3.68 \cdot 10^{-3}$ N^{-1}

Table 2.6 Displacement level; normalized suspension compliance slope

The power transferred from the voice coil is very imported to model, as shown by the power test; however, a further investigation for a more precise thermal model is needed. Agerkvist [A1] obtained coherent results with a simple first order model, depending on the power loss in the loudspeaker unit. The cooling by small diaphragm movements shows a linear behaviour observed both in Figures 2.19 and 2.21. Depending on the temperature or the suspension compliance level the cooling decay is different. An improved cooling model is recommended, but the model used in the simulation used the displacement magnitude slope per decade.

Stimulus level, displacement	After stimulus, Cooling slope α_{cm}
0.9 mm	$-3.33 \cdot 10^{-3}$ N^{-1}
1.9 mm	$-2.60 \cdot 10^{-3}$ N^{-1}
3.8 mm	$-2.22 \cdot 10^{-3}$ N^{-1}
6.6 mm	$-2.54 \cdot 10^{-3}$ N^{-1}

Table 2.7 Normalized cooling suspension compliance slope

Displacement Time Varying Behaviour of the Suspension

After analysing the small signal suspension compliance, a small investigation of the time varying behaviour of the diaphragm displacement nonlinearity is presented. The nonlinearity was measured with the Klippel Analyzer, shown in Figure 2.23. As this measurement is performed with a noise signal, the stimulus is different from the one used in the test, and the results are compared in Table 2.8. The measurements are performed by limiting the dissipated power to ¼W, 1W, 4W, and 16W in 10 minutes.

Suspension compliance at x=0, measured with Klippel analyzer	Suspension compliance at x=0, measured with 40Hz stimulus.
0.623mm/N @1.5mm	0.546mm/N @0.9mm
0.665mm/N @3.0mm	0.554mm/N @1.9mm
0.732mm/N @6.0mm	0.568mm/N @3.8mm
0.835mm/N @11.0mm	0.604mm/N @6.6mm

Table 2.8 Suspension data obtained from the Klippel analyser and test set 1 from this work.

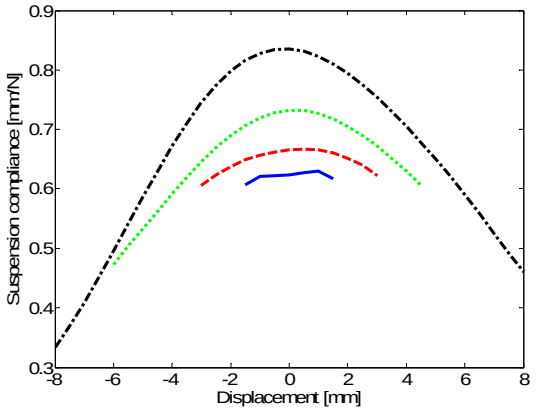

Figure 2.23 Measurement of the suspension as a function of the position measured with the Klippel analyzer. 0.25W (___), 1W (---), 4W (....), and 16W (.-.-.).

The compliance obtained by the Klippel analyzer is softer than what has been fount in the previous tests, which can be due to the larger power dissipation than in Test Series 1. The compliance from test set 3 is 0.698mm/N closer to the compliance obtained by the Klippel analyzer. The sequence from data set 3 only has the stimulus applied 2/3 of the time due to the small multi-tone signal in between, and the stimulus has only been applied in 6 2/3 minutes, compared to the 10 minutes applied in the Klippel analyzer. After 10 minutes of the test signal the compliance is still increasing, see Figure 2.20.

Conclusion of Time Varying Behaviour of the Suspension

The loudspeaker suspension is highly nonlinear with time varying behaviour. A signal depending on the time varying function of small signal suspension compliance has been developed from a measurement series of a loudspeaker unit related to a simple thermal model. Suggested inputs are the power dissipated in the voice coil and the displacement of the diaphragm. This finding is based on measurements and the suggested physical cause.

The measurements show a diaphragm displacement dependent upon change of the suspension compliance. This is approximately proportional to the displacement and has a time-logarithmic slope. The recovery slope of the suspension is about 29-45% steeper than the change under excitation. The recovery is due to cooling of the suspension, and a model for the cooling is not made due to complexity and lack of equipment. Finally, the study of the suspension has been the last part of this project and there are open questions and further investigated in relation to the suspension behaviour are required.

2.4. Voice Coil Induction

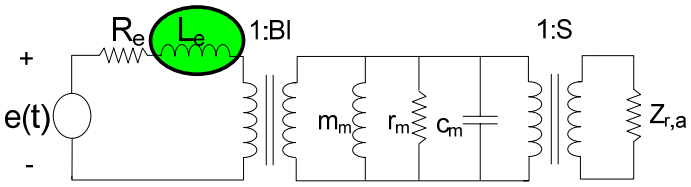

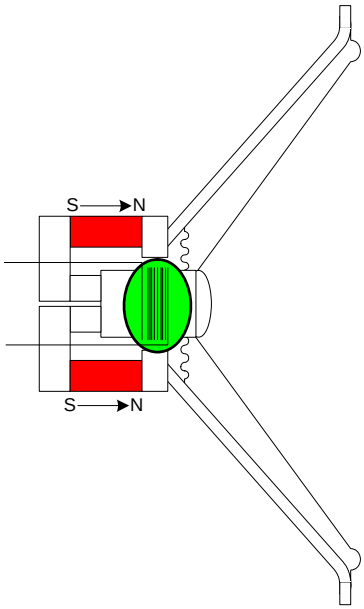

Figure 2.24 The voice coil inductance is marked on the electrical equivalent diagram and on the cross section of the marked voice coil.

The voice coil is placed in the loudspeaker unit surrounded by metal from the magnetic system. The inductance changes when the voice coil moves in the magnetic system, "the inductor core". This section only describes the nonlinear voice coil inductor and it is applied in the distortion simulation, section 2.7.

2.4.1. The Voice Coil Inductions Displacement Dependency

The voice coil inductance increases when the voice coil moves into the magnet and decreases when it moves away. This position dependency is measured with the Klippel analyzer, shown in Figure 2.25, loudspeaker from Appendix 1.

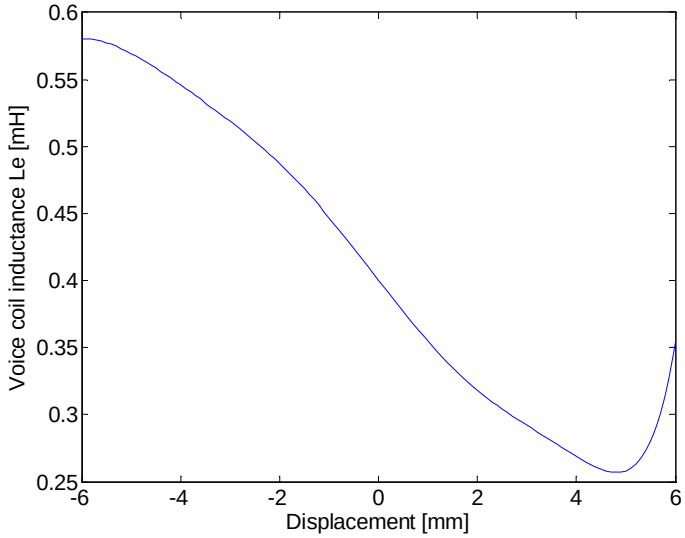

Figure 2.25 Voice coil induction as function of displacement

The change in voice coil inductance has two nonlinear phenomena. By looking at the energy stored in an inductor, Equation 2.7, one sees that the energy is proportional with the current squared. The energy stored in the magnet structure cannot suddenly change and will remain constant. When the inductance decreases and the current is constant, the excess energy provides a force trying to pull the voice coil back to the previous position. Equation 2.8 shows the conversion of the energy stored in the magnet structure to force the voice coil either back or forth.

$$W(t) = \int_0^{i(t)} i(t) \cdot L_e(x) di(t) = \frac{1}{2} \cdot L_e(x) \cdot i(t)^2 \qquad \textit{Equation 2.7}$$

$$F_r(x(t), i(t)) = \frac{\partial W_{L_e}}{\partial x(t)} = \frac{1}{2} \cdot i(t)^2 \cdot \frac{dL_e(x)}{dx(t)} \qquad \textit{Equation 2.8}$$

For a constant inductance, Equation 2.9 is used, while 2.10 is used if the inductance is not constant and the inductance has to be differentiated.

$$U_L(t) = L_e \frac{di(t)}{dt} \qquad \textit{Equation 2.9}$$

$$U_{L_e}(t, x(t)) = \frac{di(t) \cdot L_e(x(t))}{dt} = L_e(x(t)) \frac{di(t)}{dt} + i(t) \frac{dL_e(x(t))}{dx(t)} \frac{dx(t)}{dt} \qquad \textit{Equation 2.10}$$

The right side of Equation 2.10 consists of two parts the first is the linear inductance with the constant inductance replaced by the position dependence, like equation 2.9; the second part applies an extra voltage generator, U_r.

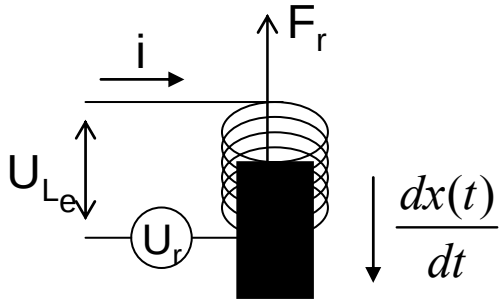

Figure 2.26 A fixed coil with a moving metal core.

Figure 2.26 shows a coil with a moving metal core, in principle this is the same phenomenon as a loudspeaker:

- U_{Le} The coil voltage
- U_r Relative voltage source, Equation 2.10
- F_r Relative force, Equation 2.8

2.5. Diaphragm Area and Mass

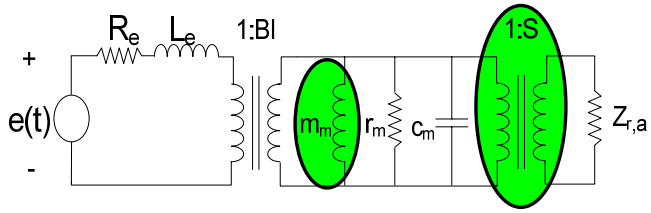

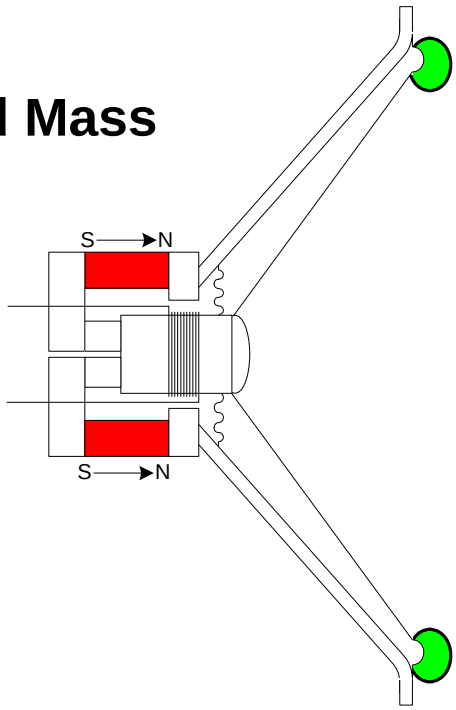

Figure 2.27 The transformation factor S, effective diaphragm area, and the moving mass is marked on the electrical equivalent diagram. The cause for these nonlinearities is the edge suspension marked on the loudspeaker cross section.

Changes in the diaphragm area and moving-mass changes have been combined in one section due to their physical cause being the same: the displacement dependency of the movement along of the edge suspension. The edge suspension has a kind of rolling effect that changes the part of the edge suspension moving along; this changes the diaphragm area and the moving mass. The edge suspension described here is a single roll; the rolling effect changes the position where the edge suspension bends. The bend is not a sharp corner but more of a small circle. The markers in Figure 2.28 indicate the bending point for the three diaphragm positions shown.

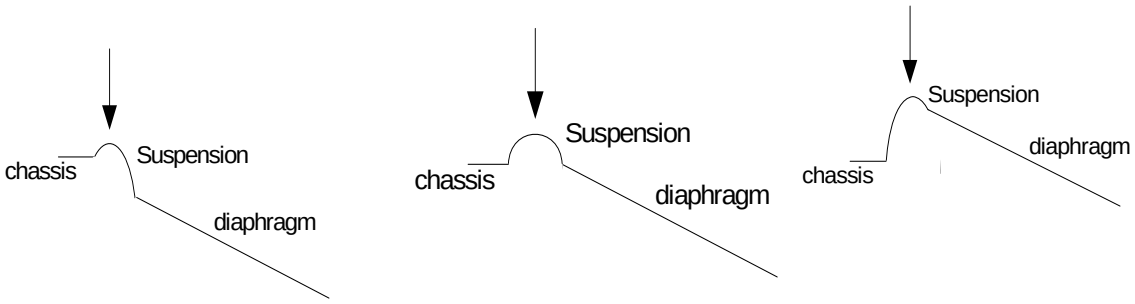

Figure 2.28 Single-roll edge suspension, the marker indicates the "rolling point". From Left; diaphragm moved back, diaphragm at the rest position, and diaphragm moved to the front.

The effective diaphragm area increases when the diaphragm moves to the back where more of the edge suspension is moving along. When the diaphragm moves to the front, less of the edge suspension is swinging. This has also been shown by Olsen and Thorborg in 1995, [O3]. According to their paper, the two nonlinearities cancel each other out to some extent. When frequencies move beyond the resonance frequency, the sound pressure is proportional to the ratio between the diaphragm area and the moving mass.

2.6. Air in the Loudspeaker Enclosure

The air in the loudspeaker enclosure gives adiabatic distortions which raise the nonlinear compliance [S2]. The air in the box is not an ideal acoustical compliance; the linear assumption is based on Equation 2.11 where *kst* is assumed to be a constant, but it is more like the adiabatic gas law.

$$\frac{dp}{dV} = -\frac{1}{C_{a,cabinet}} = kst \qquad \textit{Equation 2.11}$$

The nonlinear relation, the adiabatic gas law, Equation 2.12

$$p \cdot V^{\gamma} = kst \qquad \textit{Equation 2.12}$$

$$\frac{dp}{dV} = -kst \cdot \gamma \cdot V^{-\gamma-1} \text{ for air is } \gamma=1.4 \qquad \textit{Equation 2.13}$$

Equation 2.13 shows that dp/dV is not a constant but a function of volume. This nonlinearity may create distortions in small boxes with large volume changes. According to Schurer [S2], the loudspeaker enclosure air nonlinearity is of importance if diaphragm movement produces a change in volume of more than ½% of the net effective enclosure volume, resulting in a produced distortion of 1%.

The change of ½% of the net effective enclosure volume is usually not the case accept from very small enclosures. Not only is the enclosure of interest, but other small air volumes in the loudspeaker where air can be trapped are as well. With an efficient design, and in relation to the typical bass-mitt range, the loudspeaker investigated in this study has no significance on the loudspeaker enclosure air nonlinearity.

For horn loudspeakers, the adiabatic behaviour of air can be of interest. A more detailed study of this has been conducted by Voishvillo, [V11].

2.7. Simulation study of major Nonlinearities

A simulation series is made for comparison with a measurement series of harmonic distortion. The measurements are based on a Polytec Doppler laser velocity measurement of the diaphragm. The simulations are based on the nonlinear measurements of the force factor, suspension compliance and voice coil induction as a function of diaphragm position obtained by the Klippel analyzer [K4]. The loudspeaker unit used in this simulation is described in Appendix 2. The simulation model was a Matlab/Simulink-based system, which is described in Appendix 1. This section starts with a simulation study of the individual nonlinearities.

2.7.1. Distortion Simulation Study

The simulations were made with the nonlinearities listed in Table 2.9 and the nonlinear functions shown in Figures 2.29-2.31. The time varying suspension behavior is important mostly in regards to the short time measurements for adjusting the displacement suspension nonlinearity to the correct level, see Figure 2.23 and section 2.3.3.

Nonlinearities	Described in section
Bl(x) Force factor displacement dependency	2.2.1
$c_m(x)$ Suspension compliance displacement dependency	2.3.1
Time varying suspension behavior	2.3.3
$L_e(x)$ Voice coil induction displacement dependency	2.4.1

Table 2.9 Nonlinearities included in the simulation study

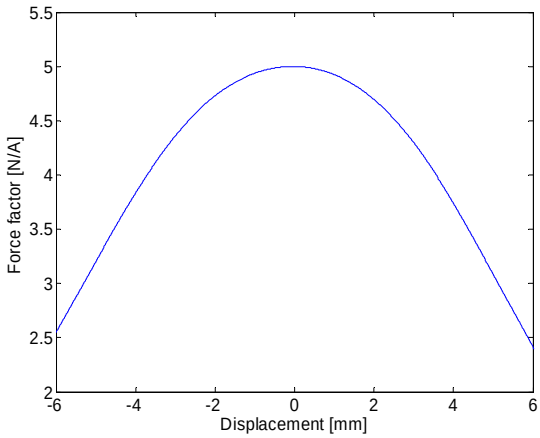

Figure 2.29 Force factor nonlinearity used in the simulation

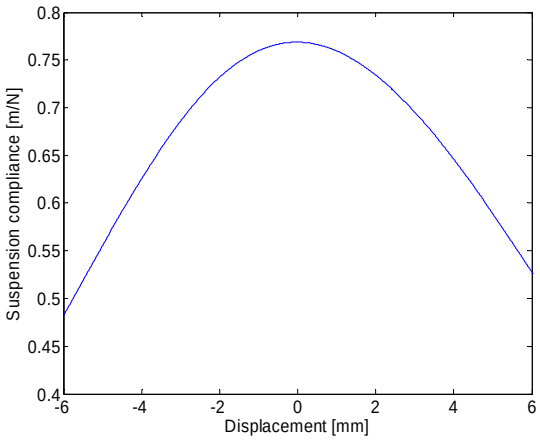

Figure 2.30 Suspension compliance on linearity used in the simulation

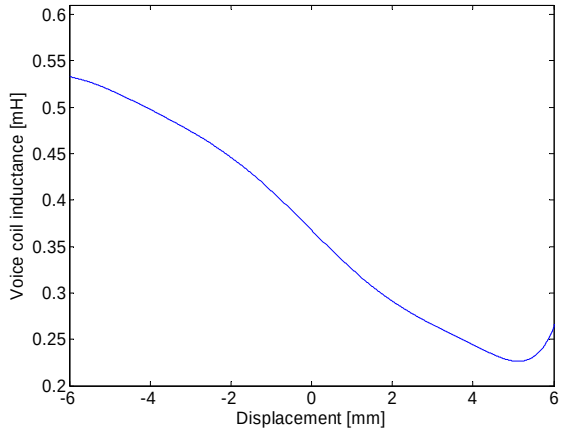

Figure 2.31 Voice coil inductance nonlinearity used in the simulation

2.7.2. Harmonic Distortion Analysis

THD simulations were performed with a sinusoidal signal at frequencies half the resonance frequency, at the resonance frequency, and at twice the resonance frequency. The simulation was repeated three times by applying nonlinearities one at a time: either force factor, suspension compliance, or the voice coil inductance. The results are presented with FFT plots of the diaphragm velocity. The simulation tool is shown in Appendix 1. After Figures 2.32-2.40, the simulation results are revealed where all nonlinearities are applied. The measurement results are shown on the same plots, Figures 2.41-2.43. The measurement setup is described in Appendix 5.

The nonlinear force factor will introduce distortion by large displacements, which is the case by the simulation at and under the resonance frequency. Thus, by the resonance frequency is the distortion smaller caused by the force factor due to the decaying diaphragm velocity with a first order slope above the resonance frequency that suppresses the distortion level.

The suspension nonlinearity applied also causes distortion by large displacement, primarily under the resonance frequency where the loudspeaker is compliance controlled, [K6].

The voice coil induction position nonlinearity introduces small distortion by the three simulated frequencies, but by higher frequencies where the other nonlinear distortion sources decay becomes the voice coil induction distortion important.

The distortion patron shown in Figures 2.32-2.40 can change significantly by a DC offset of the diaphragm, as an offset changes the distribution between the odd and even harmonics, [C1].

Half the resonance frequency (28Hz):

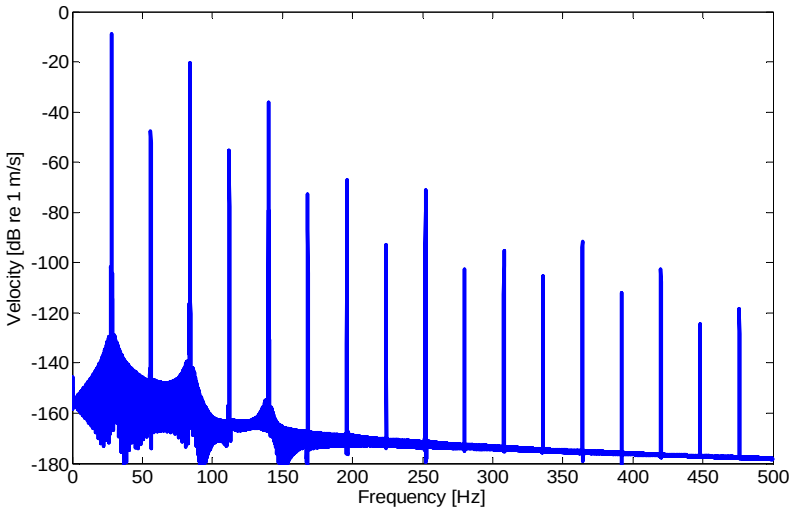

Force factor
THD+N: 27.8%

Figure 2.32

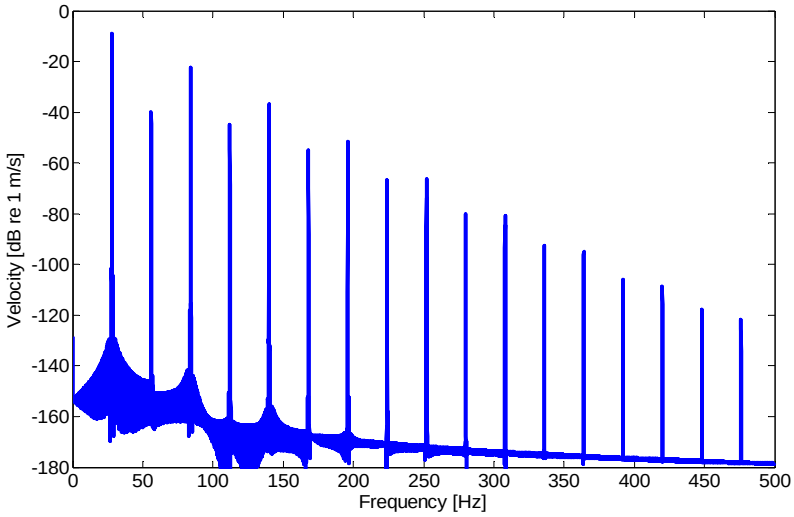

Suspension compliance
THD+N: 22.7%

Figure 2.33

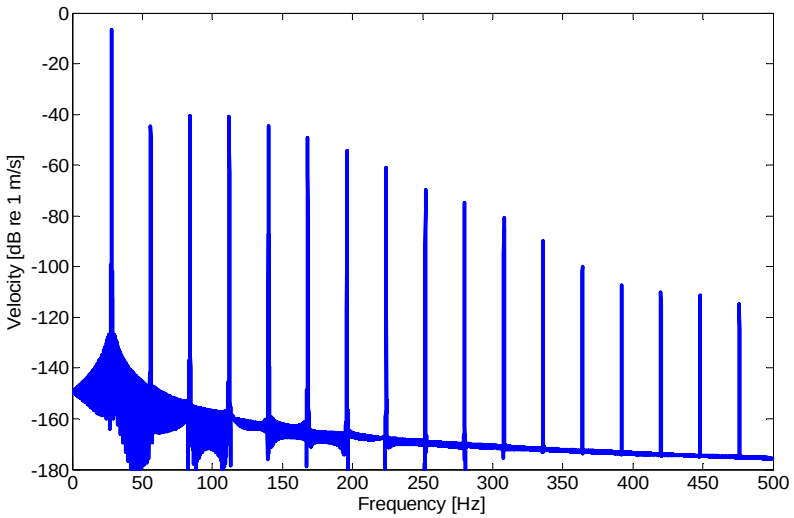

Voice coil induction
THD+N: 3.4%

Figure 2.34

At the resonance frequency (55Hz):

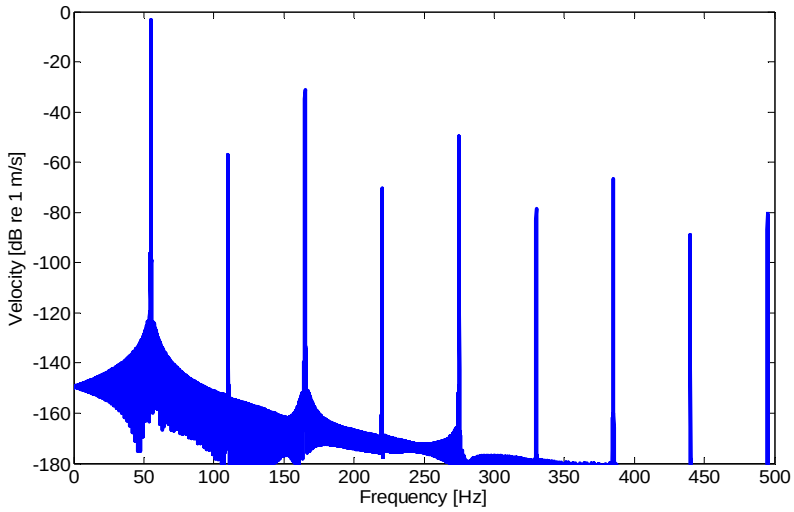

Force factor
THD+N: 4.1%

Figure 2.35

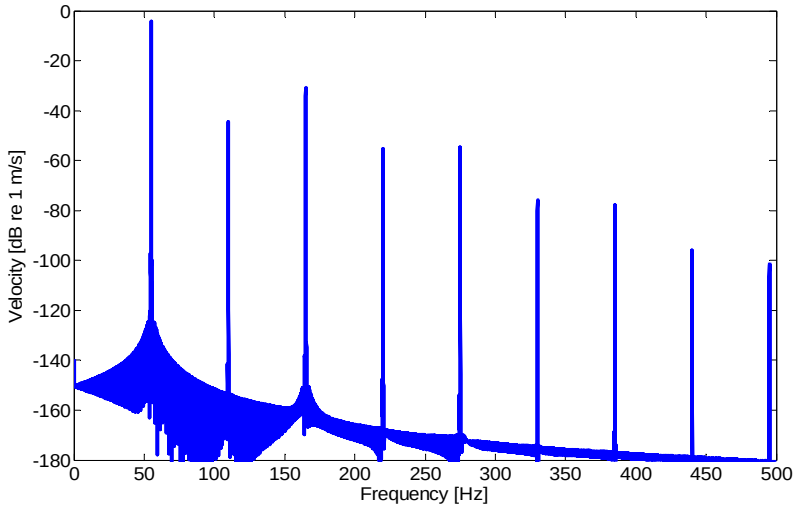

Suspension compliance
THD+N: 5.3%

Figure 2.36

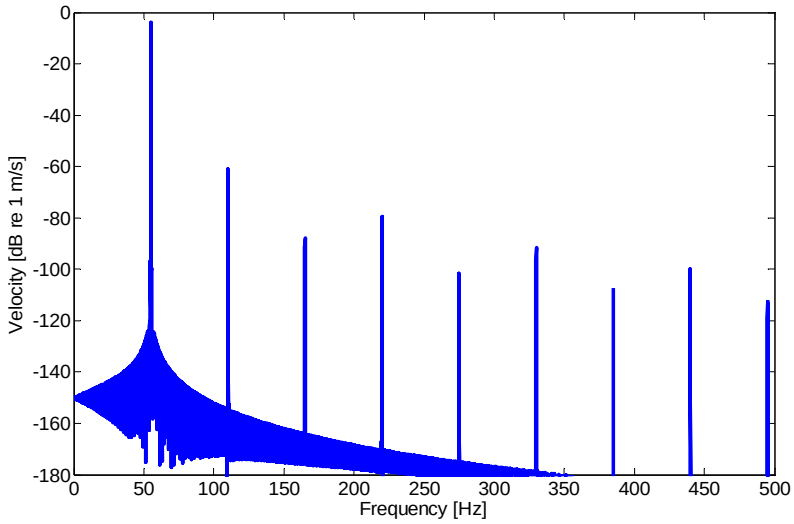

Voice coil induction
THD+N: 0.2%

Figure 2.37

Twice the resonance frequency (110Hz):

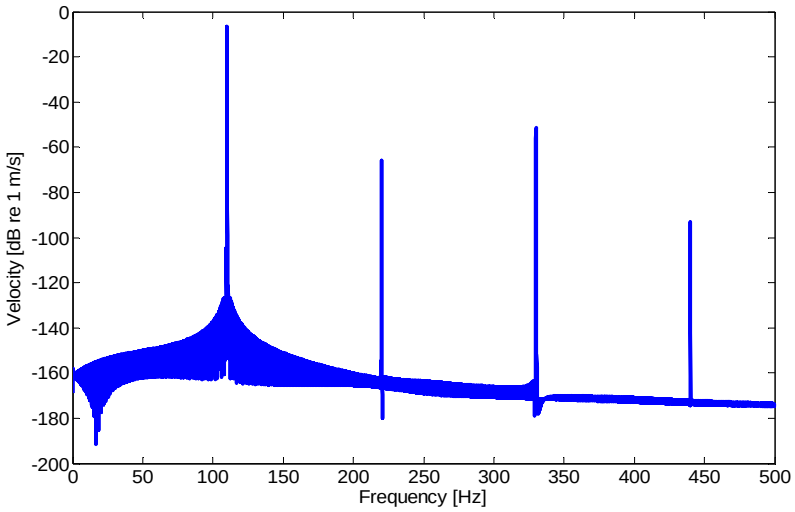

Force factor
THD+N: 0.6%

Figure 2.38

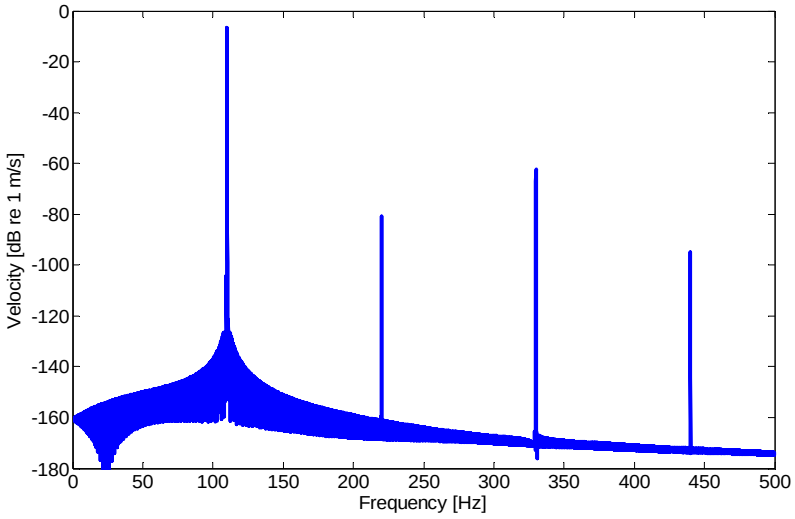

Suspension compliance
THD+N: 0.2%

Figure 2.39

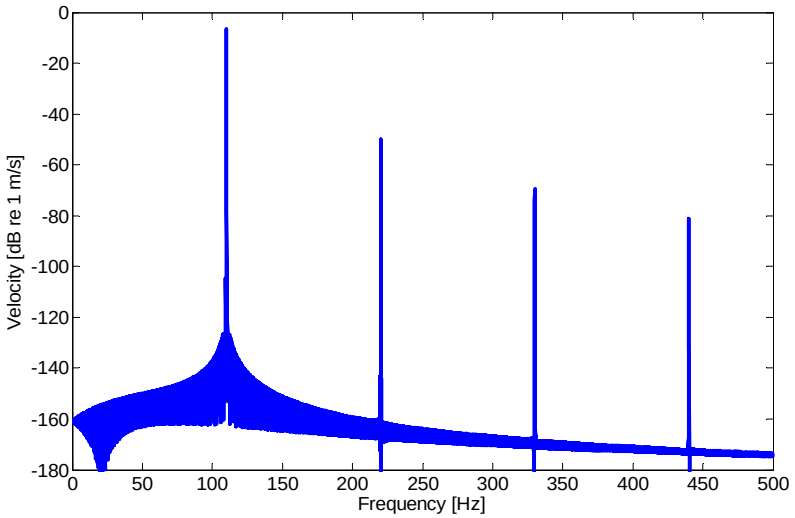

Voice coil induction
THD+N: 0.6%

Figure 2.40

2.7.3. Diaphragm Velocity Measurement

The simulation and measurement results are described and compared in this section. Connections can be related to the simulations shown in Figures 2.32-2.40.

Generally, the small displacement levels show less agreement between the simulations and the measurements. At increasing displacements there are generally correspondences in the distortion patterns, even though the distortion level not is correct. Based on this fact, this section will only show the results from the large amplitude measurements. The total measurement series is shown in Appendix 3.

Half the resonance frequency (28Hz):

Both the force factor and the compliance produce large harmonic distortions due to the large diaphragm displacement level, 5.4 mm peak. The overall simulation result has 45.8% distortion versus the measured result of 65.9%. The even harmonics are more than 10dB too low; however the odd harmonics are better modelled. A DC-offset could be the source to generate the even harmonic distortion. The simulation was performed with a laser velocity measurement and therefore a DC offset can not be monitored. There could be more causes for the modelling errors; some of these are listed below:

- There can be a displacement offset between the measured nonlinear functions and the rest position of the diaphragm in the test.
- At frequencies lower than the resonance frequency, where the suspension has high influence, it is believed that the time/heat variation of the suspension nonlinearity might be a cause.
- The large displacement level and power handling cause most of the loudspeaker parameters to drift, causing amplitude and phase difference [P22].

At the resonance frequency (55Hz):

Both the force factor and the compliance still produce large harmonic distortion due to the diaphragm displacement level, and at the resonance frequency the peak remains 5.4 mm. The diaphragm velocity reaches its maximum at the resonance frequency and decays 20dB/dec under the resonance frequency, see *Figure 2.41*. By comparing the third harmonic of the 28Hz and 55Hz simulations, the diaphragm velocity will change approximately 9dB. According to a linear assumption, *Figure 2.41*, the velocity changes approximately 7dB.

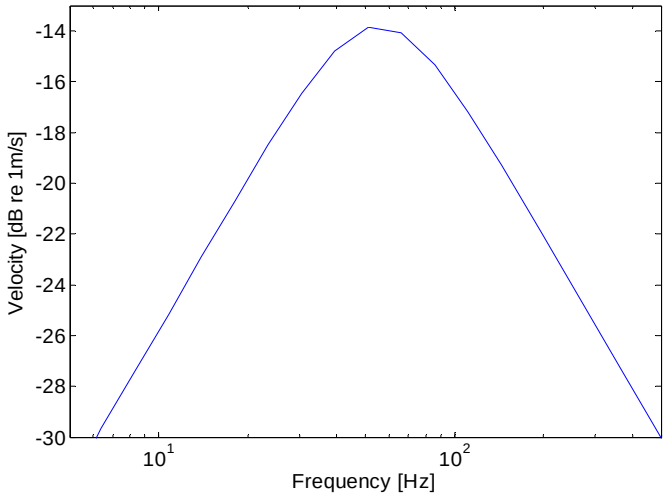

Figure 2.41 Magnitude plot of the linear transfer function voltage to velocity

Comparing the simulation and measurements in Figure 2.43 show the differences in distortion are comparable with Figure 2.42. The even harmonics are under-modelled while the third harmonics have good coherence. The even harmonics disagreement can be due to flux modulation, which is a non-symmetric distortion source.

Twice the resonance frequency (110Hz):

The simulated THD from the three nonlinearities are relatively small, all ending up with a result of less than 1% with a diaphragm displacement of 2.0 mm peak. The measurement provides a distortion level of 2.2% more than twice that simulated, and the fundament is simulated 1.1dB too high. Again, it is the even harmonics that are under modeled. Possible causes are listed below:

- Flux modulation has an impact near the resonance frequency and should be included [V10]. The flux modulation is mentioned in some of Klippel's papers and is included as a major nonlinearity [K6].
- There could be a displacement offset between the measured nonlinear functions and the rest position of the diaphragm in the test.

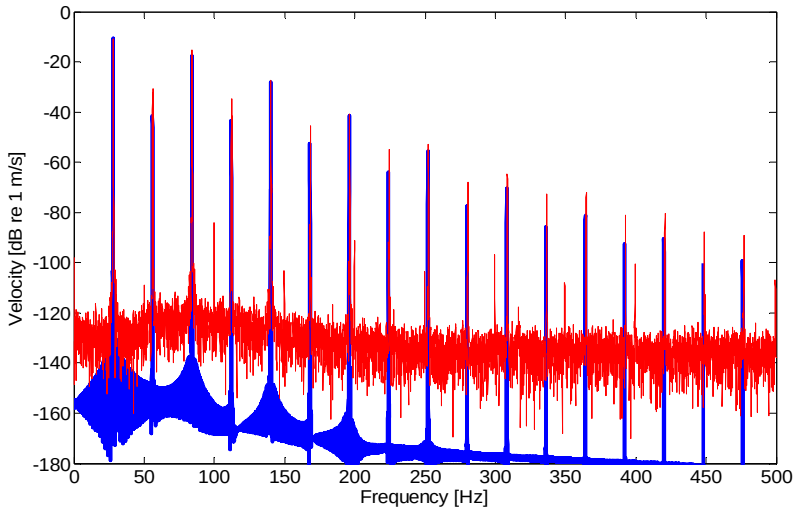

Half the resonance frequency (28Hz):

Simulation, blue:
THD+N: 45.8%

Measurement, red:
THD+N: 65.9%

Difference in fundamental simulated, minus measured 0.6 dB

Figure 2.42

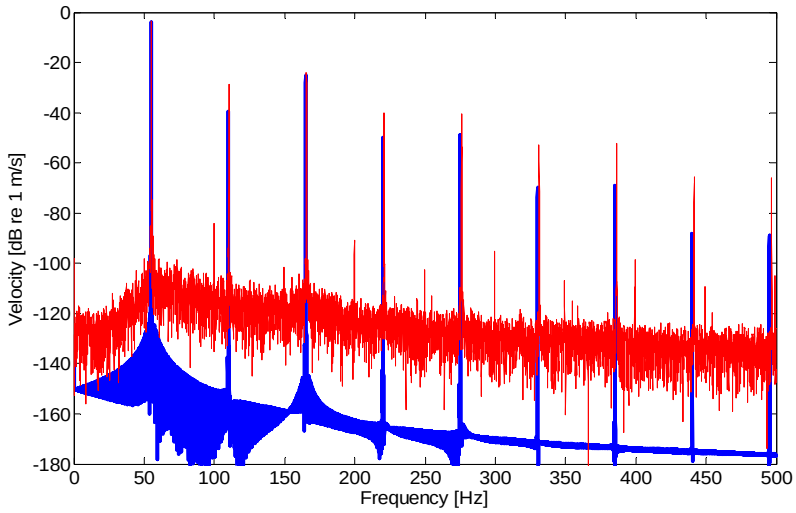

At the resonance frequency (55Hz):

Simulation, blue:
THD+N: 9.7%

Measurement, red:
THD+N: 11.2%

Difference in fundamental simulated minus measured -0.3 dB

Figure 2.43

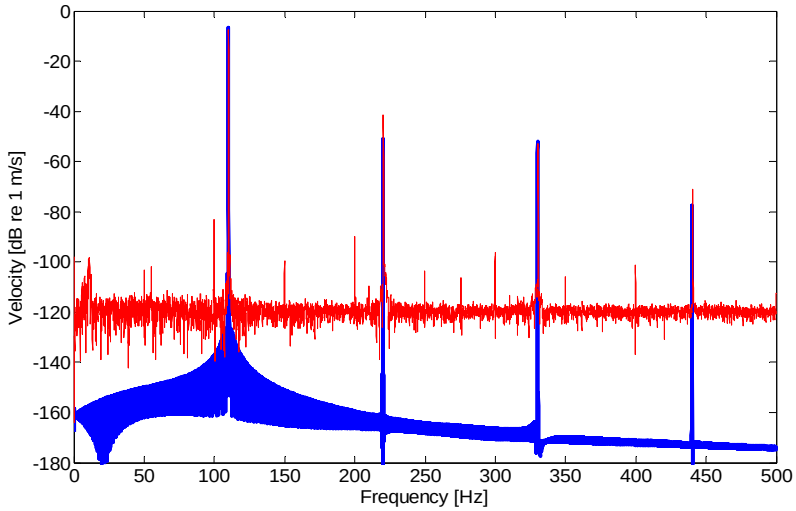

Twice the resonance frequency (110Hz):

Simulation, blue:
THD+N: 0.8%

Measurement, red:
THD+N: 2.2%

Difference in fundamental simulated minus measured 1.1 dB

Figure 2.44

2.7.4. Simulation Study Conclusions

The comparison of the simulation results and the measurements show that not all the dynamics of the loudspeaker are taken into consideration. For example, at large displacements, there is a fairly good coherence but less by small displacement levels. The suspension compliance adjustment at the rest position improves the results in terms of the fundamental level, phase, and distortion level. Other simulation studies have shown that adding the flux modulation can improve the results of the resonance frequency.

For the small displacements, either the nonlinearities were not correctly obtained or other nonlinearities may have a high influence. This chapter shows that the suspension nonlinearity is signal-dependent and that the test signal used in the Klippel analyzer has more energy than any of the signals used in this simulation study and more energy than the typical music application will apply.

2.8. Discussion of Modelling Nonlinearities in Loudspeakers

The loudspeaker model with displacement depending nonlinearities was able to model the distortion pattern with a difference of approximately 10dB from large displacements, while the even harmonics had the main difference of 10dB; the odd harmonics were simulated better. Past literature shows that by including flux modulation, the voice coil current dependency will improve the model [V10, K6]. The flux modulation inclusion is expected to improve the even distortion level.

Part of this project has been to expand the model of suspension with time varying behaviour [P24]. This inclusion improves the loudspeaker model, but further studies of suspension nonlinear time-varying behaviour could provide further improvements. Indeed, Christensen and Olsen [C1] improved their simulation results significantly by adjusting the suspension compliance, which can be related to the time varying behaviour.

Further, the coherence is smaller by small displacement. According to Christensen and Olsen [C1], the non-rigidness of the diaphragm becomes important, and the magnetic nonlinearities become a dominant source of distortion by higher frequencies. However, the model used in this project is only valid for low frequencies. In the simulations, low frequencies with small displacement levels have less coherence, a finding which was also discovered by Christensen and Olsen [C1] in their simulations. None of the magnetic nonlinearities were modeled in this study and they should be investigated; however, it should be noted that small displacement offsets from diaphragm equilibrium positions can change the distortion pattern.

The model errors could have additional causes. To begin, it is important to decipher if the loudspeaker's parameter drift was neglected. Also, was the model too simple or wrong? The model was based on measured physical causes and non of the parameters were adjusted without physical evidence. It is important to note that the model is too simple and inadequate for modelling the behaviour by small displacement levels, which is a good start for improvements before increasing the frequency range of the model.

Precise loudspeaker modelling is becoming more and more interesting with digital signal processing. A model-based compensator of distortion in the loudspeaker can be made as a feed forward compensator, but the model presented in this chapter is not sufficient for this, even though it will make some improvements by large displacement levels.

Precise nonlinear loudspeaker modelling can be used for more than feed forward error correction: knowledge can be used for improving designs of loudspeakers, and in this context, it is important to discern the different behaviours and understand how these relate to sound quality. In relation to sound quality, both small and large displacements

have to be studied. The study of loudspeakers has primarily focused on investigating the nonlinearities at large displacements, but human hearing is much more sensitive to distortion at small sound pressures [P1]. The simulation and measurement series are very inconsistent at small displacement levels and the model is assumed to have the best fit for large displacements. A study of the transducer behaviour at small displacement levels is therefore recommended. The author recommends a continued study to focus improvements of the loudspeaker model from this prospective.

The loudspeaker model used in this chapter has been used for the study of the loudspeakers power consumption where this model has a sufficient coherence with a real loudspeaker.

2.9. Conclusion of Modelling Nonlinearities in Loudspeakers

The loudspeaker model with major nonlinearities is not sufficient for modelling distortion. Including the time varying suspension behaviour improves the loudspeaker model by low frequencies up to the mechanical resonance frequency. The 3rd harmonic is simulated within a level of 2 dB, but the even harmonic distortion is approximately 10dB off. The reviewed literature shows that flux modulation shall be included before a very detailed conclusion of the model can be made. The flux modulation is a non-symmetrical distortion source and can introduce the missing even distortion in the simulation. A small displacement offset from diaphragm equilibrium position can also generate the under-modeled even harmonics.

The tested model with the major nonlinearities is entirely displacement dependent and generates distortion by large displacements where the model has coherence. It is believed that the model, with minor modifications, could simulate the distortion by large displacements levels accurately within 2dB. In small displacements the coherence is less. The distortion level is in the simulation 10-20dB to small at the 1V simulation (measurement shown in Appendix 3).

Further research is recommended to focus on the modelling of small displacement and connection to sound quality.

Chapter 3

3. Loudspeaker Parameter Drift

After obtaining a loudspeaker model, the stability of the loudspeaker parameters need to be analyzed. The difference between parameter drift and nonlinear functions are that, in parameter drift it is external non-signal dependent changes are altering the parameters. This may be humidity or temperature change in the room, and it may also be partially caused by aging. Some of the drift is a mixture of signal dependence and external conditions. For example, temperature has an influence because the signal is heating both the loudspeaker unit and the air around it; however, room temperature can offset this.

In this chapter, measurement data from a temperature test and production spread of four batches of loudspeaker units will be presented. Linear parameters and the major nonlinear parameters will be discussed.

3.1. Bases of Investigation

These investigations were conducted using a 6½ inch bass-mid range loudspeaker unit (see Table 3.1 and Figure 3.1). The loudspeaker units were measured with the Klippel analyzer, [K2]. Measurements of the linear parameters were based on position, voltage and current measurements. This specific loudspeaker unit was chosen primarily because it has been possible to get these units, used and unused, from different production batches and different years. The loudspeaker unit was assumed to be of typical loudspeaker unit construction. This chapter analyzes this unit, and this specific model shall therefore be taken as representative. The author has discussed loudspeaker unit parameter drift with other loudspeaker engineers, and has also presented these data at the 122nd AES convention in Vienna. The results found for this loudspeaker corresponded to the observations made by other engineers.

Parameter	Size
Voice coil resistance, R_e	3.36 Ω
Voice coil inductor, L_e	0.274 mH
Voice coil inductor LR circuit, L2	0.396 mH
Voice coil inductor LR circuit, R2	1.27 Ω
Force factor, Bl	4.90 N/A
Moving mass, m_m	14.7 g
Suspension compliance, c_m	0.56 mm/N
Mechanical resistance, r_m	0.784 kg/s

Table 3.1: Linear data of the DALI 311541 6½" unit.

Figure 3.1:The used DALI 6½ loudspeaker unit.

3.2. Temperature Drift of Parameters

Temperature drift has been investigated on one loudspeaker unit for a range from 20 to 50°C. The loudspeaker was placed in a conditioning cabinet and measured with the Klippel analyser.

3.2.1. Temperature Drift of Linear Parameters

The results are displayed in Table 3.2 alongside results obtained by Krump [K20]. Krump tested the change in linear parameters of a car loudspeaker.

Parameter	Change 20°C to 80°C	Change 20°C to 50°C
Voice coil resistance, R_e	20 %	11 %
Force factor, Bl	-13 %	-6 %
Moving mass, m_m	-10 %	-3 %
Suspension compliance, c_m	9 %	21 %
Mechanical resistance, r_m	-42 %	-20 %

Table 3.2: Temperature drifts of linear parameters. Second column shows Krump's results for a car loudspeaker [K20], third column shows measurements on DALI loudspeakers.

The two tests used different loudspeakers but the coherence of the tests is reasonable. The change in voice coil resistance can be calculated from the temperature coefficient of the material, in this case copper. For the tested loudspeaker, the theoretical change is an increase of 10.8% and the measured value was 10.7%.

The force factor decreases with increasing temperature. This is the expected behaviour of a permanent magnet. Surprisingly, the moving mass was also found to change. This change was evident in both measurements. It is postulated that the edge suspension changes rolling behaviour because it is getting softer (see section 2.5 for the edge suspension rolling behaviour). The temperature change of the edge suspension influences the mass and area nonlinearity.

3.2.2. Temperature Drift of Displacement Nonlinearities

The three major non-linearities were measured; force factor, compliance and voice coil induction as a function of position. It was expected that the curve shape of the force factor would remain the same, but that the magnet strength would decrease with an increase in temperature. To eliminating the drift of the linear parameters, the nonlinear functions were normalized at zero displacement.

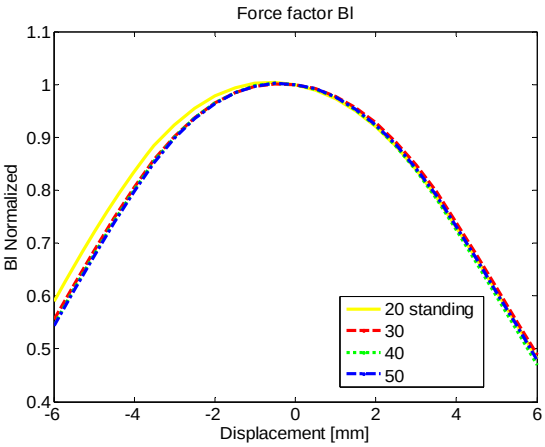

Figure 3.2: The normalized force factor function, Bl(x).

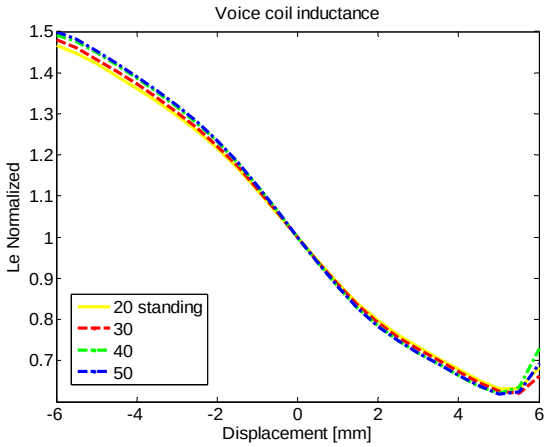

Figure 3.3: The normalized voice coil induction function, $L_e(x)$.

The measurement taken at 20°C was made outside the conditioning cabinet with the loudspeaker standing vertical; in the conditioning cabinet it had been placed horizontally. This explains the small offset in the force factor (Figure 3.2). In general, the change in the nonlinearities was very small for the force factor. The same behaviour was expected for the voice coil inductance. The estimate from the measurement system of the voice coil inductance shows a small spread at the maximum displacement point which is been assumed to be caused by the measurement system (Figure 3.3).

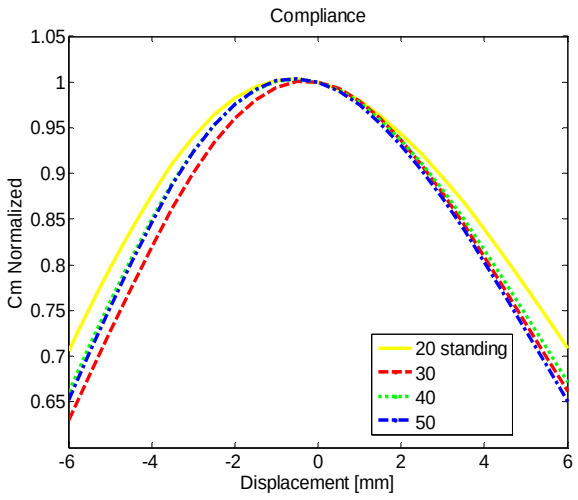

Figure 3.4: The normalized compliance function $c_m(x)$.

The compliance had a more complicated temperature relation, as shown in section 2.3.3.

The compliance function showed changes but these were not consistent, from top, 20°C, 40°C, 50°C and then 30°C. The compliance measurement is too uncertain to draw any conclusions. From the investigation of "the time varying suspension behaviour", it is known that the measuring signal of the Klippel analyzer heats up the suspension and therefore, the suspension measurement is invalid.

3.3. Production Spread of Parameters

To measure the production spread, a small investigation was performed on four lots of the loudspeaker units (see table 3.2). The loudspeaker units from 2002 were used while all other units were unused.

Year	Lot	Quant
2002	2T92A	3
2003	3TD4A	2
2005	5H1132A	4
2006	6H734B	4

Table 3.2: Year, production lot, and quantity of the loudspeaker unit DALI 311541.

All units were measured with the Klippel analyser. From the linear parameters, the mean value and the spread were calculated, and the minimum subtracted from the maximum value (table 3.3).

	Bl	R_e	L_e	m_m	c_m	r_m
Mean value	4.97A/N	3.31Ω	0.27mH	14.5g	0.54N/m	0.81kg/s
Min to max	7.24 %	4.83%	5.6%	8.7%	12.9%	20.9%
Spread	0.54 %	0.42%	0.49%	0.78%	1.10%	1.69%

Table 3.3: Parameter variations of the 13 Dali loudspeakers units.

The gaps between the lowest and the highest values were relatively large for the mechanical parameters and must be taken into account in sensitive designs. The total dataset can be seen in Appendix 2.

Figures 3.5-3.7 show the force factor, compliance, and voice coil induction as a function of displacement. They are normalized at zero displacement. The force factor shows an offset in displacement, while the curve form is identical. The spread of the nonlinear force factor is assumed to be small, because it is dependent on the magnet geometry, and because the production spread of the metal size should be very small. The strain of the magnet varies and this changes the overall level, including the linear loudspeaker parameter, as shown in Table 3.3. The force factors central position was shifted due to a displacement offset of the voice coil in magnetic gap (see Figure 3.5).

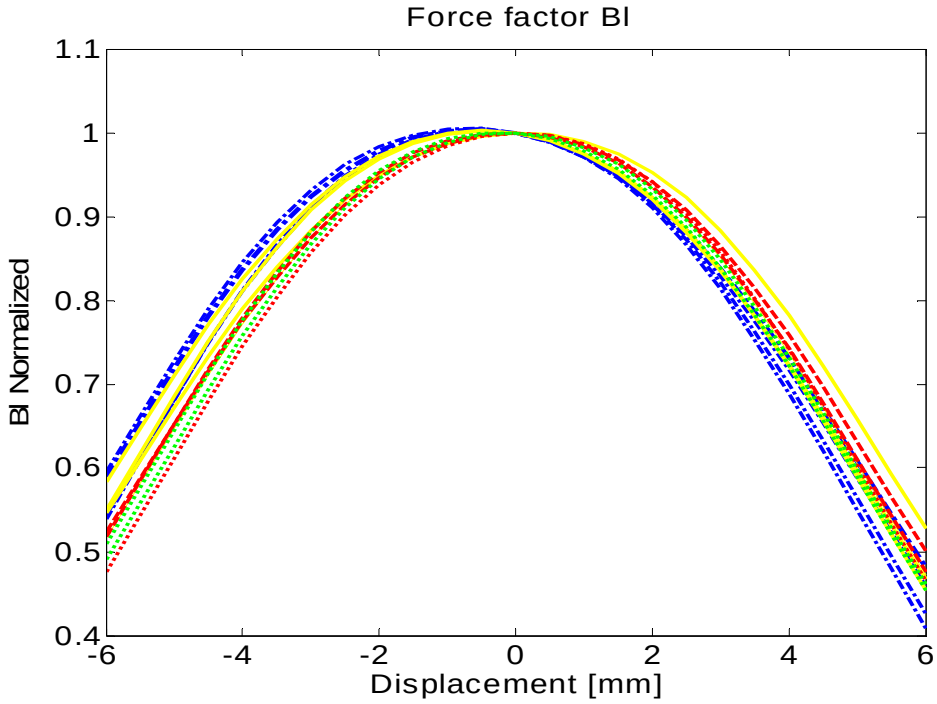

Figure 3.5: The normalized force factor function, Bl(x)

The compliance also has an offset in displacement, but the shape varies as well (Figure 3.6).

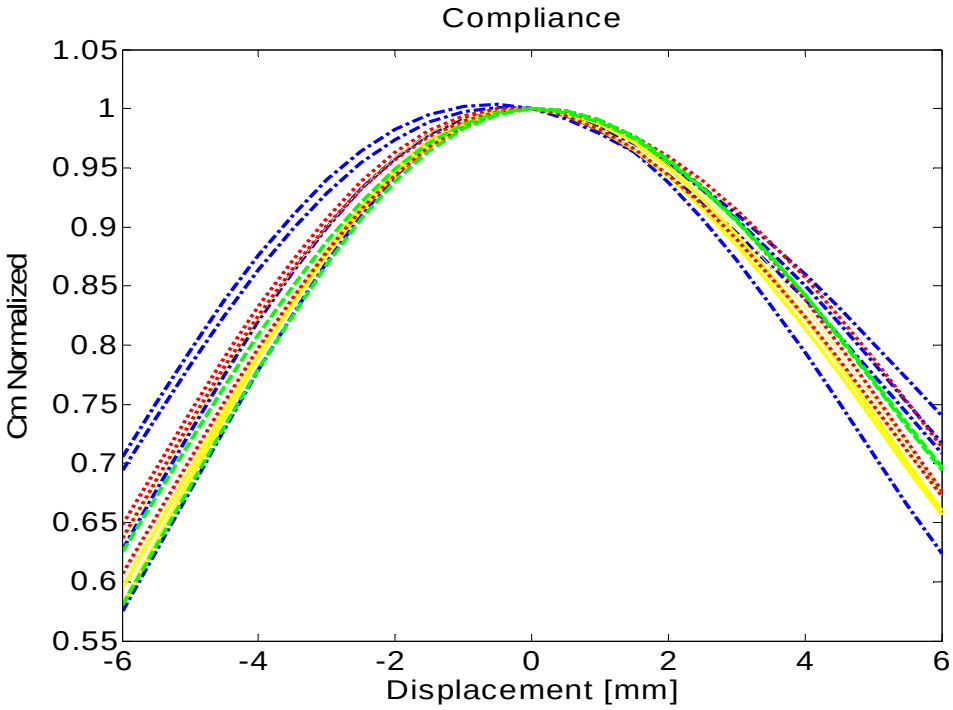

Figure 3.6: The normalized compliance function, $C_m(x)$

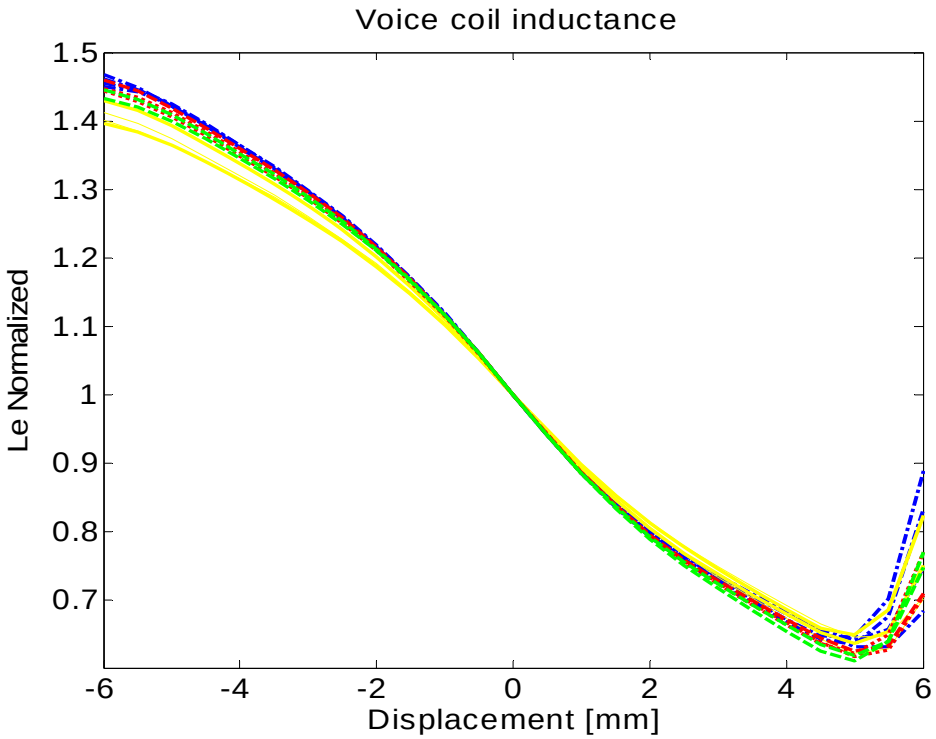

Figure 3.7: The normalized voice coil induction function, $L_e(x)$

The voice coil inductances were very similar, but it is worth noting that the polynomial fit used deviates at large displacements due to the curve form of the voice coil induction. Agerkvist proposes using fitting functions other than the polynomial fit to reducing these deviations [A1]

3.4. Summary of Loudspeaker Parameter Drift

The linear parameters have a relative large drift where temperature change is concerned and similar behaviour was observed by Krump [K20]. In addition to the temperature, there are other non-analysed factors such as humidity and aging that are known to cause parameter drift. The small production spread analysis shows changes comparable to a 30^{o}C temperature change.

In the analysis of the three position-dependent nonlinearities, the voice coil inductance and force factor nonlinearity were relative stable and only small changes were found. A production spread analysis of the force factor showed a displacement offset of ±0.5mm. The compliance was more complex; in addition to a displacement offset, there was a difference in the decay of the suspension compliance with regard to the displacement also found. This was the case for both the production spread and temperature change.

3.5. Conclusion of Loudspeaker Parameter Drift

The drift of the linear parameters typically ranged from 5% to 20%, but this can easily add up to more. The displacement-dependent force factor and voice coil inductance showed relatively good stability. The nonlinear displacement compliance changed its decay during the test and it is also known that the suspension is signal-dependent (see section 2.3.3).

Chapter 4

4. Loudspeaker Efficiency

After reviewing and studying the modelling, an important parameter has been superseded: efficiency. Efficiency is an important parameter, but often, it is a second priority in linear loudspeaker design as loudspeaker efficiency interferes with sound quality.

This chapter defines loudspeaker efficiency and power consumption. The possibilities for improving the efficiency with a non-flat frequency response are reviewed using a simulation case study. Finally, a concept of nonlinear efficiency improvement from this project is presented.

4.1. Definition of Loudspeaker Efficiency

Loudspeakers typically have a very low efficiency. The low efficiency is caused by the acoustic load on the diaphragm, which is relatively low compared to the mechanical load. In addition, the electro-mechanical conversion is quite inefficient. [B1]

According to the Loudspeaker Handbook [B1], efficiency can be calculated as the acoustic power divided by the power consumed. The consumed power in a loudspeaker is equal to sum of the resistive heating of the coil, the loss in the mechanical damping, the absorption in the enclosure, eddy currents, and the radiated acoustic power. The low efficiency of a loudspeaker leads to the acoustical power being much lower than the consumed power. The resistance loss in the voice coil is much greater than the mechanical loss, the loss inside the enclosure and the eddy currents. At the mechanical resonance frequency, this is not valued (see section 4.3).

The resistive loss can be approximated from the power consumption of the loudspeaker, i.e.:

$$W_e = I_{rms}^{\ 2} \cdot R_e \qquad \textit{Equation 4.1}$$

The acoustic power output is determined by the real part of the acoustic impedance multiplied by the square of the diaphragm velocity; the acoustic version of the electrical power law.

At low frequencies, the real part of the acoustic radiation impedance is:

$$r_m = 1{,}57 \frac{\rho}{c} \omega^2 r^4 \qquad \textit{Equation 4.2}$$

r_m is the acoustic resistance of a loudspeaker, mechanical units [Ns/m]
ρ is the density of air [kg/m^3]
c is the speed of sound [m/s]
ω is the frequency [rad/s]
r is the radius of the diaphragm [m]

The diaphragm velocity above resonance frequency is:

$$v_{rms} = \frac{BlI_{rms}}{\omega m_m} \qquad \textit{Equation 4.3}$$

The radiated acoustic power is then given by

$$W_a = v_{rms}^2 R_m = \left(\frac{BlI_{rms}}{\omega m_m} \right)^2 K\omega^2 r^4 = Kr^4 \left(\frac{BlI_{rms}}{m_m} \right)^2 \qquad \textit{Equation 4.4}$$

Where K is a constant consisting of three constants; K=1,57 ρ/c

The efficiency is acoustic power divided by the electrical power, $W_e = I_{rms}^2 R$

$$Eff = \frac{Kr^4 B^2 l^2 I_{rms}^{\ 2}}{m_m^2 I_{rms}^{\ 2} R_e} = Kr^4 \cdot \frac{Bl^2}{m_m^2} \cdot \frac{1}{R_e} \qquad \textit{Equation 4.5}$$

Equation 4.5 is the definition of the electrodynamic loudspeaker efficiency. This relationship will be used for investigating efficiency together with nonlinear simulations.

4.2. Improving Efficiency

The basic possibilities of electrodynamic loudspeakers regarding efficiency will be reviewed with a study of the linear relations based on the linear lumped model.
According to Equation 4.5, the force factor and the moving mass are the most important for obtaining high efficiency, followed by a low electrical resistance. A list of possible solutions to low efficiency is considered below;

- The first option is to use an enlarged magnet; this option will be discussed in section 4.2.1. Magnets have developed to become more powerful and less expensive, making this an interesting option.

- The second option is to decrease the weight of the moving system: the moving mass m_m. The moving system consists of three parts;

1. The diaphragm: There are many different diaphragm materials and structures. The diaphragm has to be as stiff as possible to prevent resonance and breaking up. Generally, a stiffer diaphragm is heavier and will improve sound quality. The breaking up of the diaphragm can be simulated with finite element methods [S20]. The diaphragm break up, materials and structure are not investigated in this project.

2. The voice coil: More windings and a longer voice coil increase loudspeaker linearity, leading to better sound quality; the trade-off is an increase in weight (see section 2.2.2). When electrical impedance is decreased, the radius of the wire must be increased correspondingly which increases weight and reduces the gain in efficiency. The force factor also decreases due to fewer wires in the magnetic gap.

3. The suspension: The spider is typically a small part of the moving mass. The edge suspension is heavier and has an impact on the moving mass. The thickness of the suspension has issues of lifetime. The geometry of the suspension has an influence on the sound quality (see section 2.5).

The diaphragm and suspension qualities are recognised but not considered for this project. Figure 4.1 shows the parts of the loudspeaker unit that relate to the moving mass; the air mass is not included. The example, used for this chapter, is a 6½ inch loudspeaker unit. The weights of the individual parts are shown and the total moving mass, according to the manufacturer, is 11.2g. The linear loudspeaker data for the used loudspeaker unit are shown in Table 4.1. The mass of the suspensions are only partly included as they are only partly moving along. The edge suspension is very heavy due to the thick edge part that is glued to the chassis.

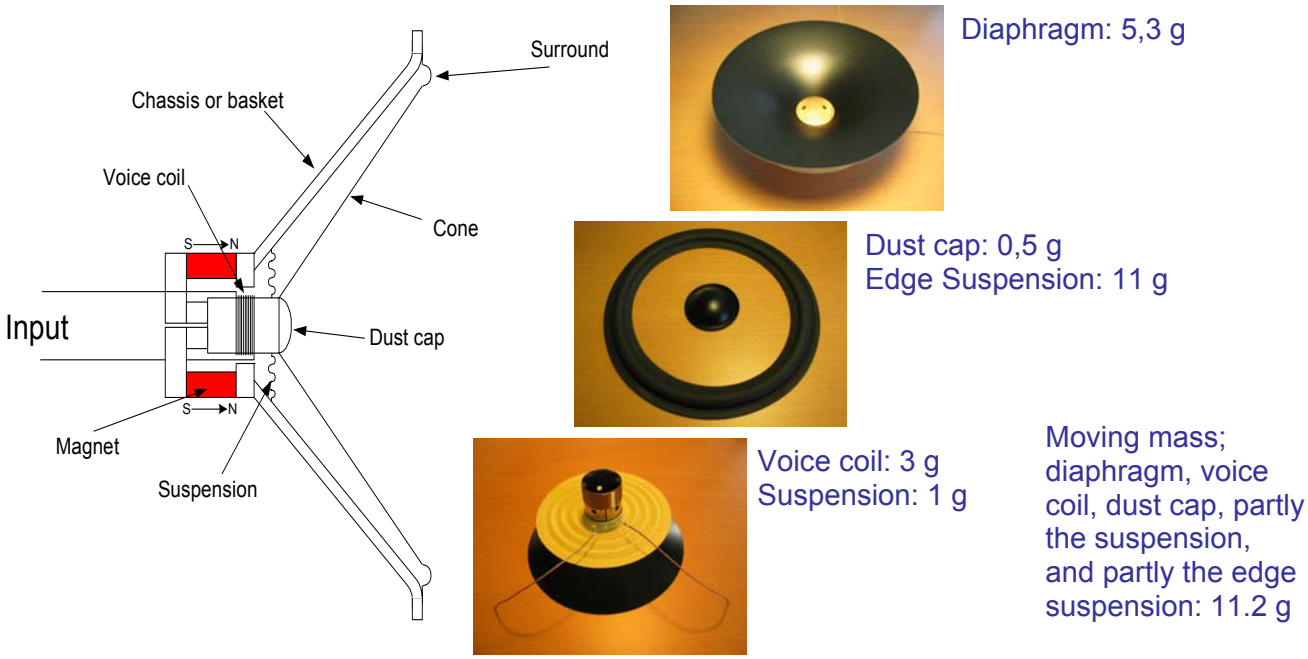

Figure 4.1: Moving mass divided into subparts of a 6½ inch loudspeaker unit. The moving mass according to the manufacturer is 11.2 g.

Parameter	Size
Voice coil resistance, R_e	2.30 Ω
Voice coil inductor, L_e	0.6 mH
Force factor, Bl	4.0 N/A
Moving mass, m_m	11.2 g
Suspension compliance, c_m	1.32 mm/N
Mechanical resistance, r_m	1.73 kg/s

Table 4.1: Linear data of the loudspeaker unit used in the efficiency simulations.

To obtain more detailed information about the design limitations of the loudspeaker in relation to improving efficiency, the next two sections consider two efficiency improvement options: a stronger magnet (Section 4.2.1), and a decrease in the moving mass (Section 4.2.2).

4.2.1. Increasing Force Factor: High Bl

The High Bl strong force factor, with stronger magnets was investigated by Vanderkooy, Boers, and Arts in 2002 [V2, V3, A20]. The increased force factor improves efficiency, but it is also a design parameter for obtaining a flat-frequency response. In Chapter 1, the damping of the mechanical system was derived in Equation 1.11 and is repeated in Equation 4.6.

Definition of the damping factor:

$$\xi = \frac{Bl^2\sqrt{c_m}}{2 \cdot R_e\sqrt{m_m}} + \frac{r_m\sqrt{c_m}}{2\sqrt{m_m}} \qquad \textit{Equation 4.6}$$

The damping is usually designed to include the rear cabinet compliance to achieve a flat-frequency response. By increasing the force factor the damping factor, ξ will be too high: an over-damped system. In Figure 4.2 is an example of the frequency response of a loudspeaker unit with four different force factors. The weakest was 2N/A, second is the originally flat-frequency response design, 4,5N/A followed by 9 and 15N/A. A force factor of 2 and 4,5N/A result in a second order complex pole pair. 9 and 15 N/A split the pole pair into two real poles at individual positions. The one pole moves to lower frequencies and the other to higher frequencies. To obtain a linear frequency response with a high Bl, it is necessary to increase the amplifier voltage at low frequencies. John Vanderkooy, Paul Boers and Ronald Aarts have shown useful equalisation [V3].

$$Poles = 2\pi \cdot f_o \cdot \xi \pm 2\pi \cdot f_o \cdot \sqrt{\xi^2 - 1} \qquad \textit{Equation 4.7}$$

Equation 4.7 describes the pole placement either for real poles or a complex pole pair.

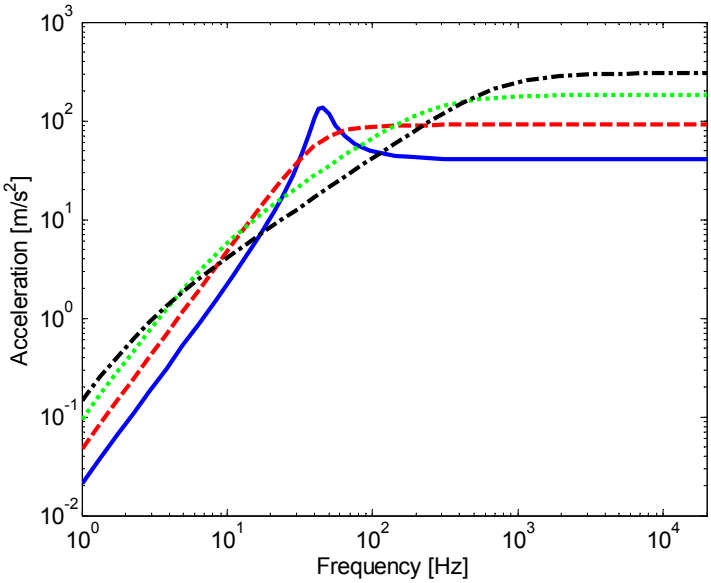

Figure 4.2: Magnitude of loudspeaker with different magnets. Bl=2 (___), Bl=4.5 (---), Bl=9 (....), and Bl=15 (.-.-.).

An alternative graphical representation of the linear system shows the resonance frequency/pole placement and damping factor as functions of the force factor (Figure 4.3).

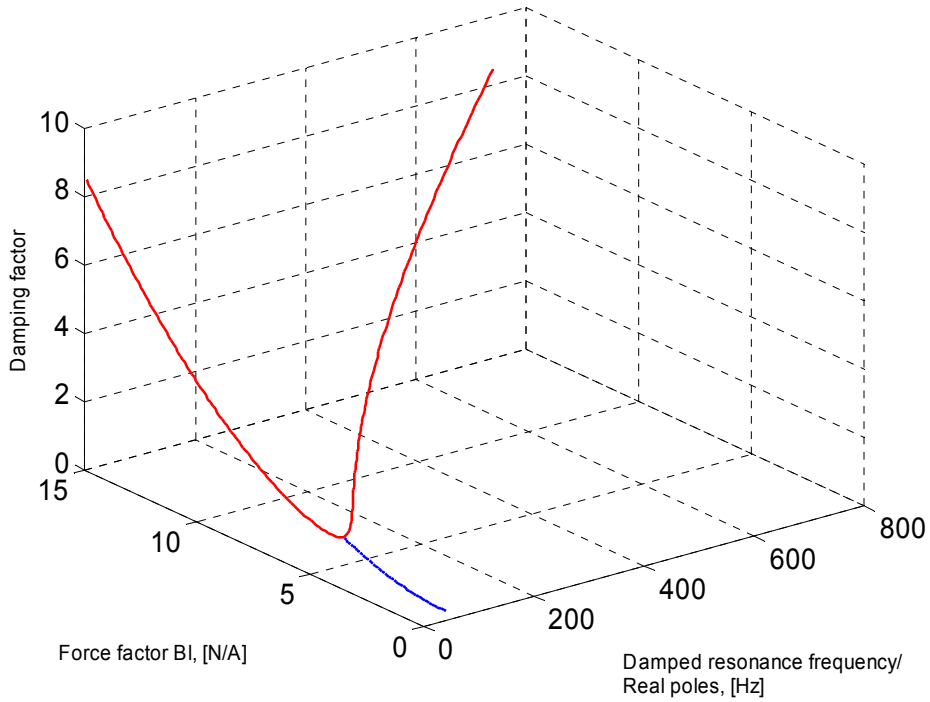

Figure 4.3: Damped resonance frequency, real pole frequencies and damping factor as functions of force factor Bl, modelled by Equation 1.8. Default Bl= 4.5N/A.

Figure 4.3 shows the pole behaviour of the loudspeakers modelled as a second-order system with the poles that cause the resonance frequency. All loudspeaker parameters remain constant and the force factor is swept. The first axis depicts the frequency at the poles locations, the second axis is the force factor and the third axis is the damping factor of the second-order system. In the first part, from 0 to 5N/A, the loudspeaker has a complex pole pair. The resonance frequency and the damping factor increase when the force factor is increased. The complex pole pair change to two real poles when the damping factor exceeds 1 (Equation 4.6). The real poles have individual frequency placement and this is indicated on the plots with a colour change: there is a “pole split”. The pole-damping plot is a tool to supplement the frequency response plot and can be helpful in the study or design phase of a loudspeaker unit.

Figure 4.3 illustrates through the increasing force factor that one pole is moving towards a low frequency, where it will not disturb the loudspeaker design. The other pole moves to a relatively high frequency and introduces a first-order roll-off in the frequency response. Overall the pole-damping plot shows the sensitivity of the force factor in relation to the frequency response. A comparison of the frequency responses in Figure 4.2 and the pole-damping plot in Figure 4.3 will clarify the use of the pole-damping plot that will be used for further investigations.

Neither of the two figures representing the frequency response or pole/damping of the loudspeaker shows the power consumption. A 6½ inch sub-woofer has been redesigned with an enlarged magnet in a student project. The project resulted in a comparison of a normal flat

frequency response design with a high Bl loudspeaker unit that has been linearised by motional feedback, [H10]. Figure 4.4 shows the power consumption for the two loudspeaker designs with a constant diaphragm acceleration level. The high force factor has significantly lower power consumption. At the resonance frequency, the power consumption of the two units is identical due to the smaller damping factor of the flat-frequency response loudspeaker unit. In Figure 4.5 the frequency responses of the two loudspeaker units are compared. Table 4.1 shows the parameters of the loudspeaker used in the student project.

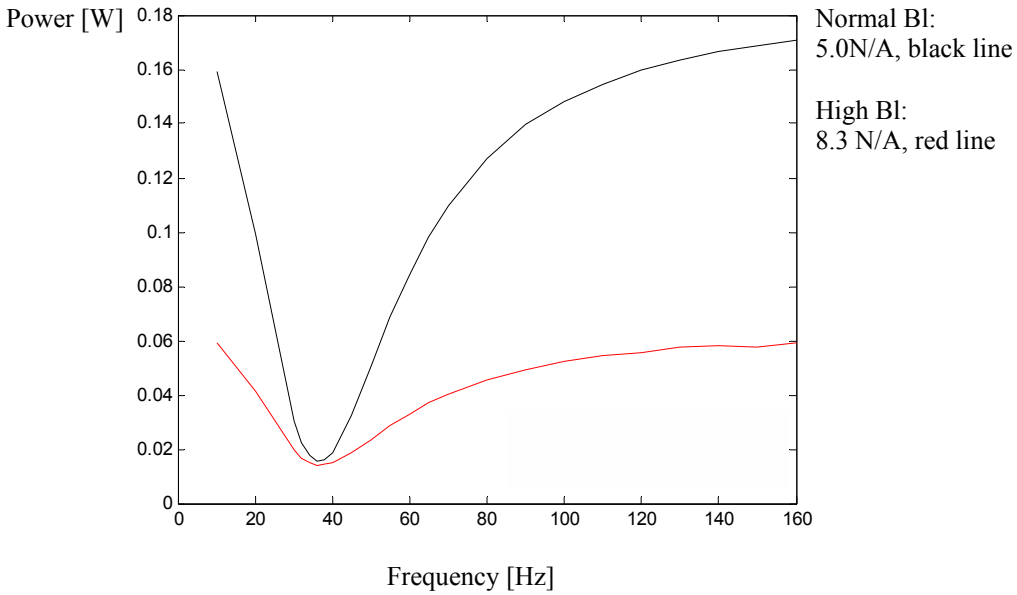

Figure 4.4: Power consumption as a function of frequency, Upper black line is the normal flat frequency response, lower red line is the high force factor design. Figure taken from a student project [H10].

Moving mass	35.2 g
Suspension compliance	0.55 mm/N
Mechanical loss	1.29 kg/s
Force factor Normal/high	5.0/8.3 N/A
Voice coil resistance	2.8 Ω

Table 4.2: Linear loudspeaker data from the loudspeaker used in the example (figures 4.4 and 4.5).

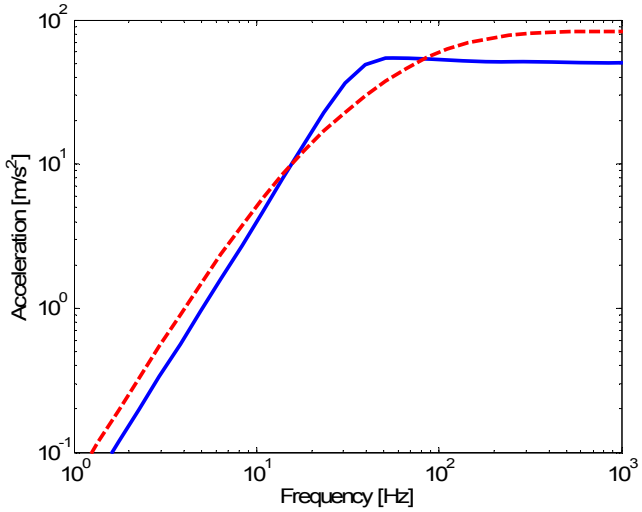

Figure 4.5: Frequency response of the loudspeaker units from figure 4.4, non-equalized frequency response. Bl=5N/A (___), Bl=8.3N/A (---)

Increasing the force factor (Bl) can be done by increasing the strength of the permanent magnet or increasing the length of the wire in the field. If only the magnet level is increased, the power loss in the loudspeaker decreases, as shown in Figure 4.4 leading to less heat in the voice coil. This presents an opportunity to decrease the thickness of the voice coil wire leading to more winding in the magnetic gap; an extra increase of Bl. The thinner voice coil wire increases the voice coil resistance, decreasing the efficiency but also decreasing moving mass, which could be more important with regard to loudspeaker efficiency. On a system level, the power requirements of the power supply and the power amplifier are less, which to some extent can cancel the extra cost of the loudspeaker magnet.

Summary of high force factor, Bl

Improving loudspeaker efficiency by increasing the force factor changes the frequency response of the loudspeaker. However, the efficiency will also be increased in a wide-frequency range. The other linear loudspeaker parameters influencing the frequency response need to be investigated.

4.2.2. Design of Loudspeaker Units

The objective when designing a bass mid-range loudspeaker unit is to achieve a flat-frequency response in the final application. The physical parameters change both the damping factor and the resonance frequency (Equations 1.10 and 1.11). In today's designs, the flat-frequency is a response achieved by tuning the loudspeaker parameters. In addition, it is usual to use a ventilated enclosure design that changes the required damping of the loudspeaker unit; however, the design procedure is basically the same. If the loudspeaker design does not achieve a flat-frequency response, it is possible to re-establish this with digital signal processing.

This section gives an overview of the possibilities for improving efficiency in loudspeaker unit design. The moving mass and voice coil resistance can improve efficiency. The suspension and the mechanical losses are also investigated to review the design possibilities in relation to frequency response.

All of the mechanical parameters will be investigated by fixing all parameters and then sweeping the investigated parameter in a range around normal use. The normal tuning consists of two complex poles critically damped. The output of these functions are shown in a three dimensional graph, where the swept parameter is a function of the real pole frequencies, the resonance frequency and the damping factor for the force factor sweep. See also, figures 4.2 and 4.3, the force factor, Bl.

Moving mass

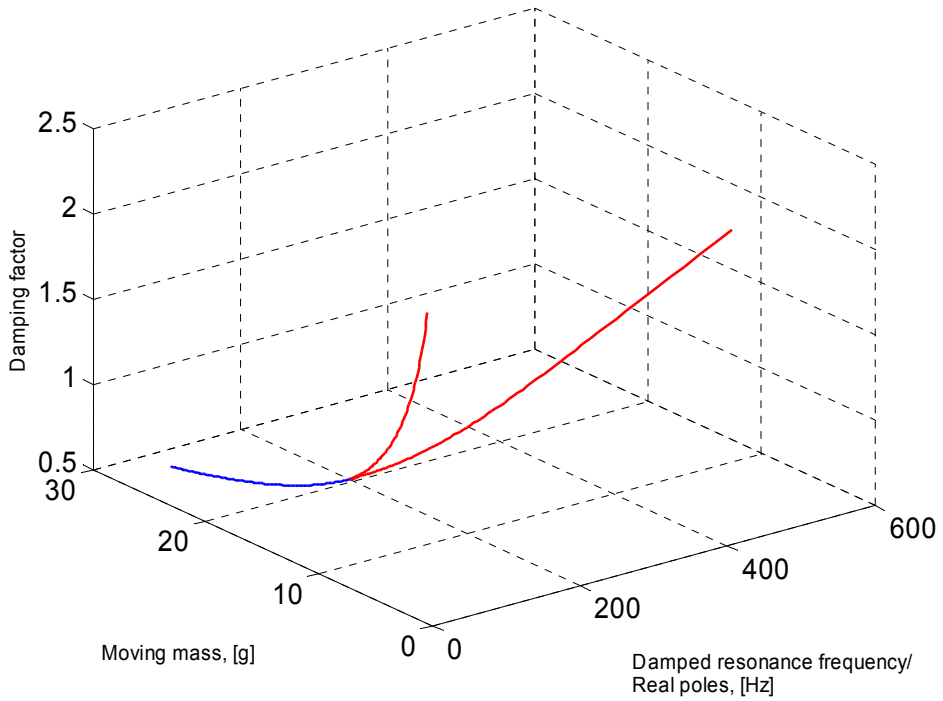

Figure 4.6: Resonance frequency, blue; real poles, red; and damping factor as function of moving mass m_m, modelled by equation 1.8. Default m_m= 11.2g.

The decrease of moving mass has a similar effect in increasing the force factor. It is possible to double the force factor, but very difficult to halve the moving mass. The influence of the reduction of moving mass in terms of efficiency is described in Section 4.1.

Suspension compliance

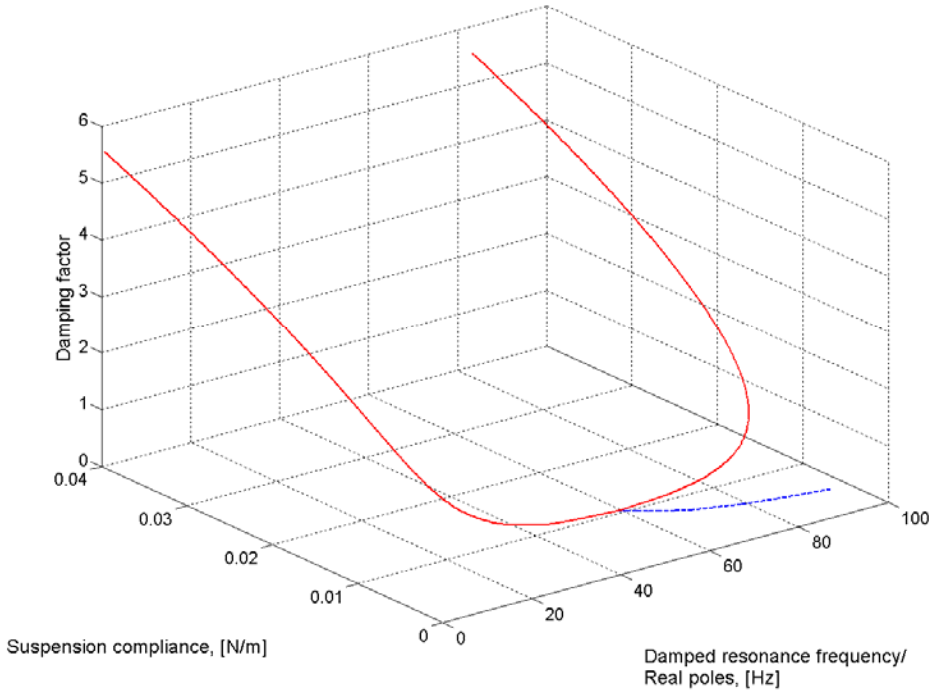

Figure 4.7: Resonance frequency, blue; real poles, red; and damping factor as function of suspension complaisance c_m, modelled by equation 1.8. Default c_m= 1.2mm/N.

A softer suspension decreases the resonance frequency due to the suspension compliance sets the resonance frequency together with the moving mass. The suspension compliance also influences the damping, which changes the complex pole pair into two real poles by increasing compliance. The purpose of the suspension is to fix the diaphragm at a well-defined rest position and this gives an upper limit of softness.

Mechanical resistance

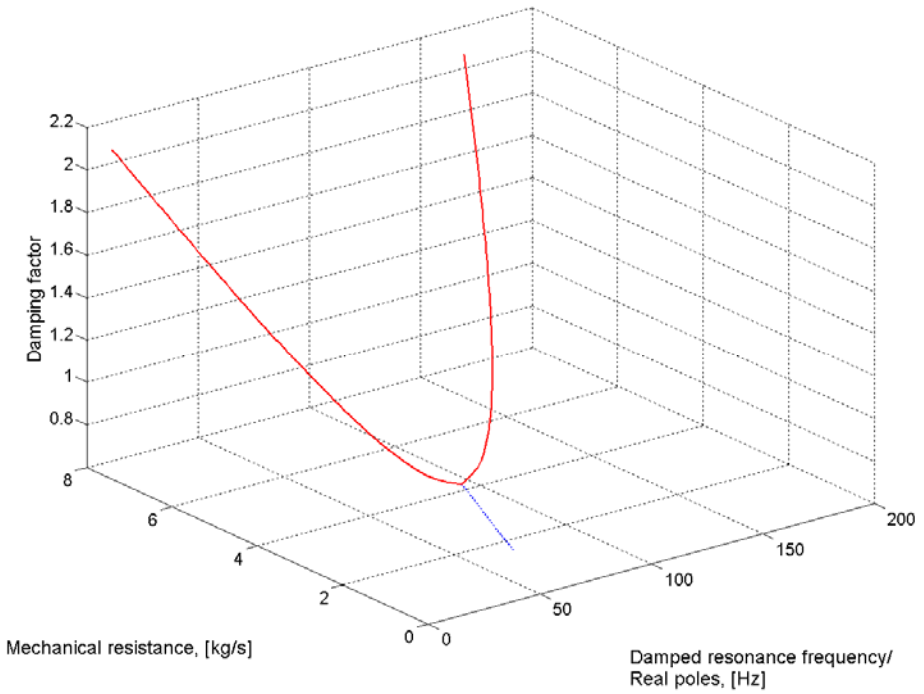

Figure 4.8: Resonance frequency, blue; real poles, red; and damping factor as function of mechanical losses r_m, modelled by equation 1.8. Default r_m=1.3kg/s

The mechanical loss is directly controlled by the damping factor. The resonance frequency changes slightly as it is the damped resonance frequency and not the natural frequency there is shown on the plots. Again, the system changes here from a complex second-order system into a second-order system with two real poles when the damping factor exceeds 1.

Voice coil resistance

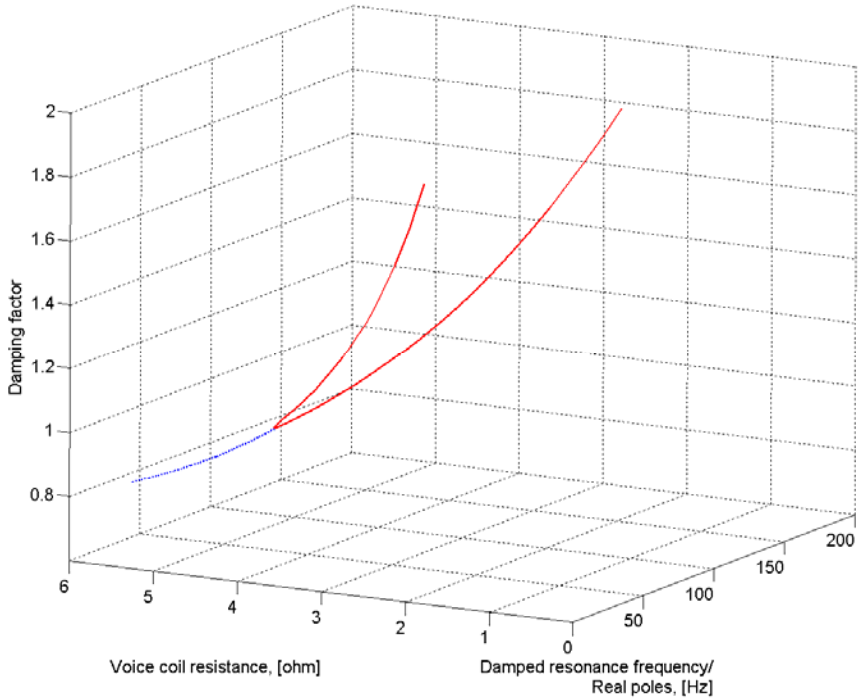

Figure 4.9: Resonance frequency, blue; real poles, red; and damping factor as function of voice coil resistance R_e, modelled by equation 1.8. Default R_e= 4.5Ω.

Decreasing the voice coil resistance increases the damping and has a similar effect as increasing the force factor or decreasing the moving mass; however, the efficiency is merely proportional to the reduction of the voice coil resistance, in that it is proportional to the square of the force factor increase and the square of the moving mass decrease.

Summary and Continuities of Loudspeaker Unit Designs

All parameters that can improve electrodynamic loudspeakers efficiency increase the damping factor, and after a given point, they turn the complex pole pair into two real poles. Either way results in efficiency improvements in a non-flat-frequency response whereby equalization is needed.

Until now, the loudspeaker has been seen as a linear system, but if a short light voice coil is used, the force factor has a strong decade by large displacements due to the voice coil being driven out of the magnetic gap making the linear relation no longer valid. A non-linear investigation is needed, and the relation between power loss and sound pressure levels also needs to be found.

4.3. Electrical Power Consumption

The electrical power consumption as a function of sound pressure/diaphragm acceleration does not have a linear relationship. The relation will be derived by finding the power consumption defined by Equation 4.11.

$$W_e(s) = i(s) \cdot e(s) = \frac{1}{Z(s)} \cdot e(s)^2 \qquad \textit{Equation 4.11}$$

The acceleration and the sound pressure in the far field are proportional to the input voltage, and the power consumption is proportional to the input voltage squared. Most of the power used by the loudspeaker is converted to heat in the voice coil [B1]. This can lead to breakdown of the loudspeaker due to overheating when playing loud.

Around the mechanical resonance frequency the impedance is dominated by the mechanical resonance, and the power loss is small. In this range, the previous assumption that the electrical loss is resistive loss in the voice coil is false. In the case of Figure 4.4, it is also demonstrated that the assumption is invalid near the resonance frequency.

Instead of using the voice coil resistance the loudspeaker impedance is used. Equation 1.11 is rewritten to the admittance expression in Equation 4.12, i.e., the transfers the function from the voltage to the current *i(s)* i.e.,

$$\frac{1}{Z(s)} = \frac{i(s)}{e(s)} = \frac{\frac{1}{\mathrm{R_e} + sL_\mathrm{e}} \cdot \left(s^2 + \frac{r_m}{m_m} \cdot s + \frac{1}{c_m \cdot m_m} \right)}{s^2 + \frac{Bl^2 + R_e \cdot r_m}{m_m \cdot (R_e + sL_\mathrm{e})} \cdot s + \frac{1}{c_m \cdot m_m}} \qquad \textit{Equation 4.12}$$

The electrical power W_e (s) driving the loudspeaker will be:

$$W_e(s) = i(s) \cdot e(s) = \frac{1}{Z(s)} \cdot e(s)^2 = \frac{\frac{1}{\mathrm{R_e} + sL_\mathrm{e}} \cdot \left(s^2 + \frac{r_m}{m_m} \cdot s + \frac{1}{c_m \cdot m_m} \right)}{s^2 + \frac{Bl^2 + R_e \cdot r_m}{m_m \cdot (R_e + sL_\mathrm{e})} \cdot s + \frac{1}{c_m \cdot m_m}} \cdot e(s)^2$$

Equation 4.13

The non-linear electrical power consumption versus sound pressure level result in the question: How does the nonlinear power loss influences the loudspeaker design?

4.4. Nonlinear Loudspeaker Efficiency

Based on the linear efficiency analysis, it can be concluded that, to achieve high efficiency, a light moving mass should be implemented with a strong magnetic system; this results in a short voice coil. The idea of increasing efficiency by shortening the voice coil has previously been presented by Bright [B13], who showed how the sensitivity of mobile phone micro loudspeakers could be increased by reducing the length of the voice coil.

The drawback of the short voice coil is that it moves out of the magnetic field by moderate displacements and the force factor decreases. Thus, more power has to be sent to the loudspeaker to regain the lost force. This correction can be implemented by a compensator that linearises the loudspeaker. However, linearising the loudspeaker has two disadvantages: the need for a larger power amplifier, and extra heat dissipation in the loudspeaker. An analysis of the influence of the nonlinear force factor regarding efficiency is needed.

An important parameter in loudspeaker unit design is the maximum power loss in the loudspeaker. The lost power determines the maximum voice coil resistance and sets the diameter of the used voice coil wire. The maximum loss depends on the worst case input signal and also the design parameters of the loudspeaker. Around the resonance frequency, the losses are determined mainly by the damping of the loudspeaker; otherwise, the losses are in the voice coil.

The input signal is very difficult to define, due to it typically being music. Both distribution in level and frequency are interesting for analysing the efficiency performance of a loudspeaker. To look at the influence of those parameters in loudspeaker design, a case study is presented of the nonlinear efficiency characteristic. Different test signals and approaches are tested.

4.5. Nonlinear Efficiency Design

With the background knowledge of efficiency and the loss in efficiency caused by increasing diaphragm displacement, a set of case study examples are discussed. For the case study, a 6½ inch driver was constructed for the simulation based on a redesign of an exiting driver, Table 4.1 page 76.

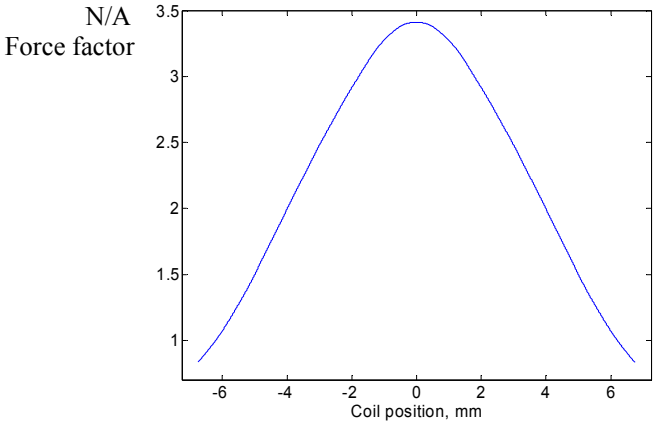

Figure 4.10: Electromechanical conversion current to force.
The Bl force factor of a simulated loudspeaker unit. 2 layers, 48 windings.

Given that a large input voltage has a relatively large power dissipation and that linearising the loudspeaker requires an increase in voltage gain, it is important to have a high efficiency for large displacement levels. Reversing the electro-mechanical conversion nonlinearity (Figure 4.10), can achieve this effect. This can be accomplished by placing the voice coil differently. The nonlinear efficiency design is achieved by moving the voice coil to the edges as shown in Figure 4.11.

The investigation in this section will review the efficiency of the nonlinear loudspeaker in a case study and test the design concept of an open voice coil. This efficiency review will test the benefits and disadvantages of this strategy by moving the optimum efficiency from small displacements to higher displacement levels. The short voice coil layout will be compared with a long voice coil to verify the efficiency improvement of a short voice coil.

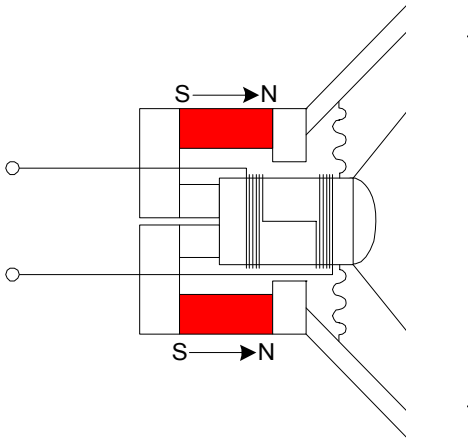

Figure 4.11: The basic idea of the efficiency layout is to split the voice coil up into two parts and leave the central position empty.

In the simulation, a linear model of the loudspeaker was extended with a force factor dependent on the diaphragm position (Figure 4.12). The magnetic data used is based on measurement data from the magnetic system of the loudspeaker unit.

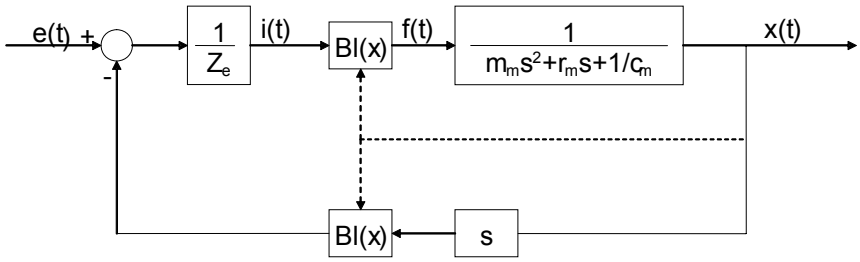

Figure 4.12: Linear loudspeaker model with a nonlinear force factor block, Bl(x).

The force factor data was produced by measuring the magnetic system with a test voice coil, a two layer, six windings coil. The loudspeaker magnet and the test voice coil can be seen in Figure 4.13. The test setup and more details can be found in Appendix 4.

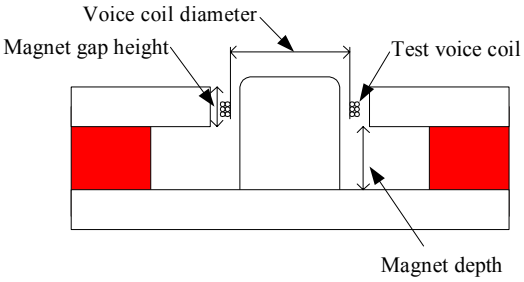

Figure 4.13: Cross-section of the used magnet with the test voice coil from the measuring setup.

Magnet gap height	4mm
Magnet depth	14mm
Magnet opening	1.5mm
Wire diameter	0.27mm
Voice coil diameter	25mm
Voice coil height	13.5mm

Table 4.3: Magnet specifications.

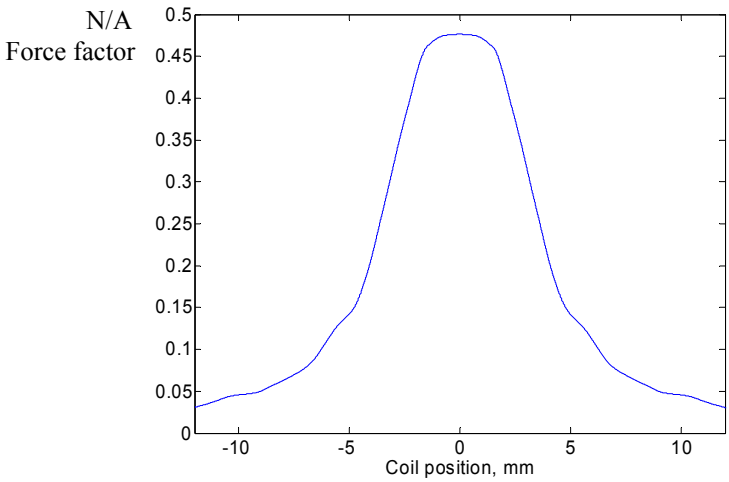

Figure 4.14: The electromechanical conversion for a magnetic system with overhang. Measured and simulated with the test voice coil, six windings in two layers.

From the result of the test voice coil measurement, the nonlinear force factor was constructed using a simulation program. The simulation program calculates the force factor function from a placement description of the winding on the voice coil.

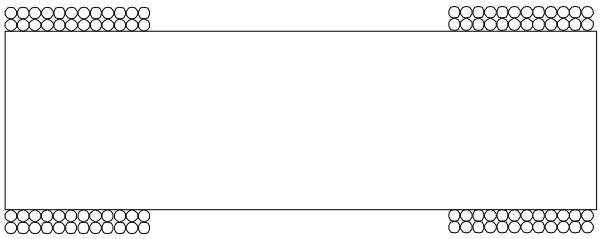

Figure 4.15: Cross- section of the voice coil layout used in the simulation, 2 layers, 48 windings, open space in the middle; 7.0 mm.

The number of windings were chosen to fill 48% of the maximum space of the voice coil, leading to R_e=2.3Ω. Three voice coil layouts were chosen for further investigation. One layout with the winding centrally placed, as a normal loudspeaker unit, "0mm open"; the second leaving the central position open, windings were placed as far apart as possible, with the corresponding voice coil layout shown in Figure 4.15, "7.0mm open". The third was in between, "3.5mm open". The results of the simulations of the force factor are shown in Figure 4.16.

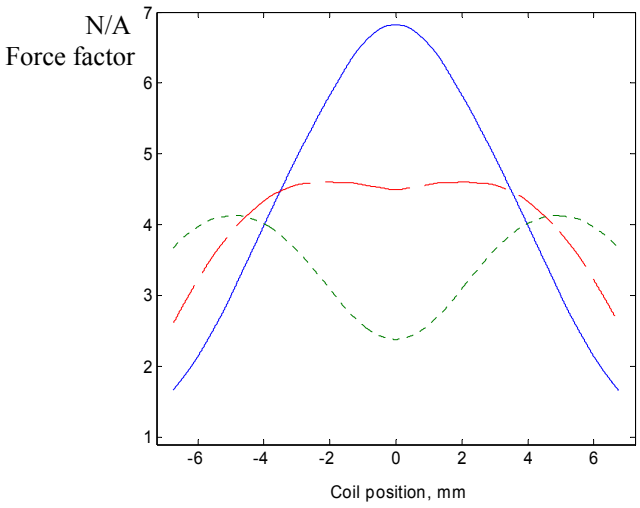

Figure 4.16: The electro mechanical conversion for: —Blue; 0mm open, ---Red; 3.5mm open, ...Green 7.0mm open. The results are multiplied by two to obtain a better damping factor.

Figure 4.16 shows the force factor of the three voice coil layouts. The maximum distance of the diaphragm from equilibrium is +/-6.75 mm. One interesting point is that the force factor was larger on the normal layout for displacements smaller than 3.5mm for the design with 3.5mm open space, and smaller than 4mm for the design with 7mm open. Both values were greater than 50% of the maximum displacement.

Comparing the two most different voice coil layouts, 0mm and 7mm opening with the same amount of windings and magnet system, there is a 125% force factor increase at the maximum

distance from rest position. This leads to a decrease in force factor of 62% near the rest position.

4.5.1. Power Consumption

The main objective is to find reduction in the power loss in loudspeakers, or at the system level, the power amplifier and loudspeakers power consumption in order to improve efficiency. The problem, when determining power loss is in finding a representative signal. The intention of this simulation study was to design a loudspeaker that has high efficiency at large displacements. This limits the test to low frequencies and/or to music playing at the maximum volume.

The power consumption is calculated in a loudspeaker model corresponding to Figure 4.12, implemented in Matlab Simulink (W=e·I); simulation model details can be found in Appendix 1. Figure 4.17 shows power consumption at maximum displacement using sinusoidal, +/-6.75 mm versus frequency from 30 to 120Hz.

In nonlinear systems, such as that produced when a nonlinear force factor is introduced to a loudspeaker, instability can occur [F1]. For a loudspeaker, this instability will, at some frequencies, change the rest position of the diaphragm; a DC-shift. For one frequency there will be two stable rest positions; one with a positive offset and one with the same negative offset. The offset is dependent on frequency as well as displacement level. This effect can be reduced by linearising or flatting the force factor; one solution is to make an opening in the middle of the voice coil, as designed here. The simulation shown in Figure 4.17 leads the DC shift to increase power consumption for 0mm open space from 70Hz and upwards and for the voice coil design with 3.5mm open space from 80Hz and upwards. The maximum opening has no DC shift.

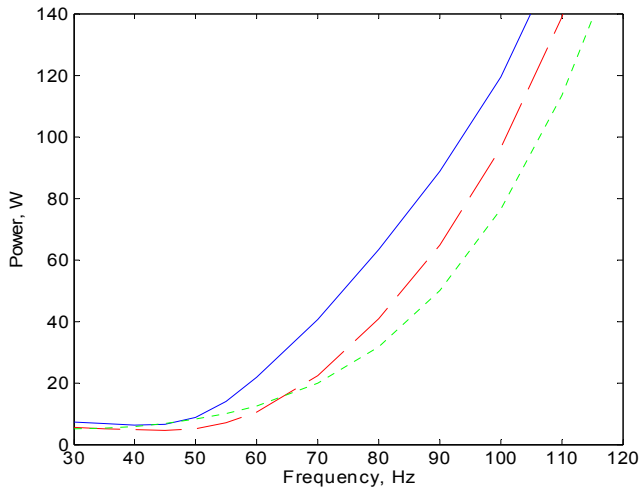

Figure 4.17: Power consumption versus frequency, diaphragm displacement; 6.75mm at all frequencies. ...Green=7mm, --Red=3,5mm and —Blue=0mm open space.

Figure 4.17 shows a clear improvement using the alternative designs, but the signal is not representative as the sound pressure level increases at higher frequencies with constant displacement. In the next data set, the displacements at the different frequencies are set equal to the levels achieved with the constant voltage of a linear loudspeaker, achieving a constant acceleration over the resonance frequency 50Hz. The displacement at 60Hz for Figure 4.18 is 2.0mm, for Figure 4.19 is 4.0mm, for Figure 4.20 is 5.0mm, and for Figure 4.21 is 6.75mm.

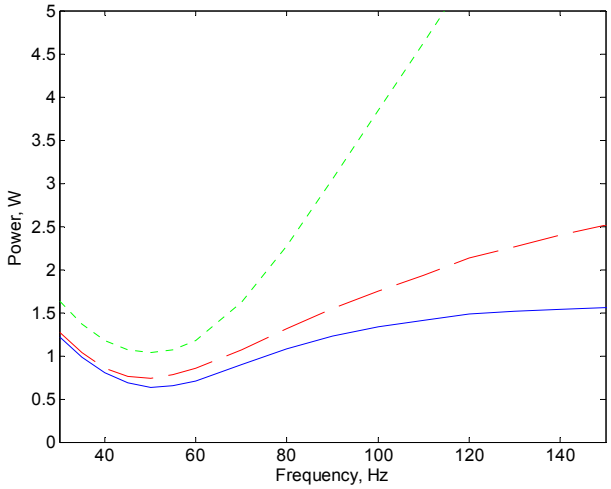

Figure 4.18: Power consumption versus frequency, diaphragm displacement; 2.0mm @60Hz. Constant diaphragm acceleration over the resonance frequency, 50Hz...Green=7mm, --Red=3,5mm and —Blue=0mm open space.

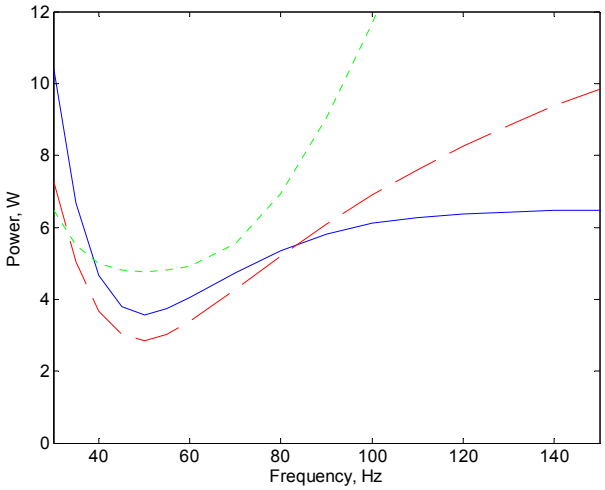

Figure 4.19: Power consumption versus frequency, diaphragm displacement; 4.0mm @60Hz. Constant diaphragm acceleration over the resonance frequency, 50Hz...Green=7mm, --Red=3,5mm and —Blue=0mm open space.

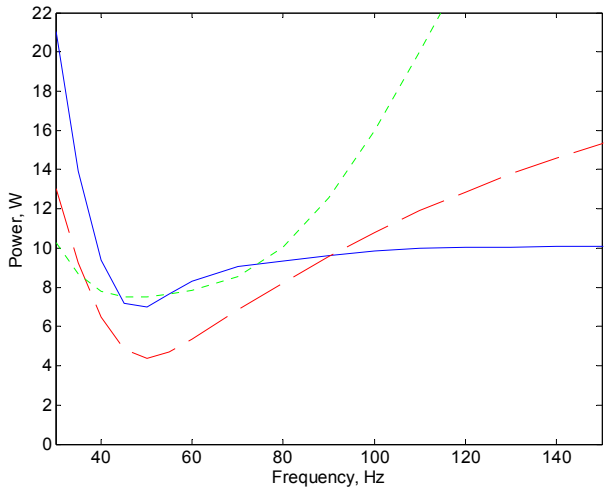

Figure 4.20: Power consumption versus frequency, diaphragm displacement; 5.0mm @60Hz. Constant diaphragm acceleration over the resonance frequency, 50Hz...Green=7mm, --Red=3,5mm and —Blue=0mm open space.

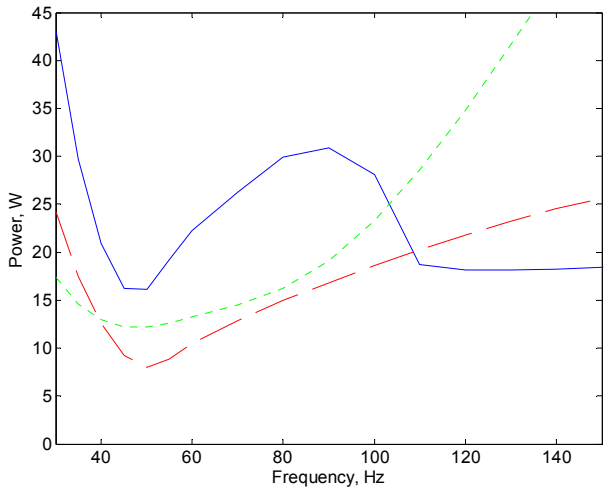

Figure 4.21: Power consumption versus frequency, diaphragm displacement; 6.75mm @60Hz. Constant diaphragm acceleration over the resonance frequency, 50Hz...Green=7mm, --Red=3,5mm and —Blue=0mm open space.

In general, this principle only demonstrates relevance for large displacements. In the cases shown, the voice coil design with 3.5mm open space only has relevance for frequencies below 100 Hz. Larger displacements levels will increase the frequency range.

Figure 4.21 shows that from 60Hz to 110Hz there is an unexpected high power consumption on the normal wound voice coil. This is caused by the DC-shift, which is equal to the voice coil being at the edge of the magnetic field and the voltage gain having been increased to obtain constant diaphragm acceleration.

4.5.2. Efficiency Analyses of Voice Coil Designs

To obtain a better background for comparing the efficiency of the different voice coil designs, the short voice coil designs are compared with a long voice coil. Longer voice coil designs are frequently used today. A long voice coil has a better linearity and less need for compensation. The voice coil resistance was held constant and a fully wound voice coil designed. Table 4.4 shows the data from the short light voice coils, and the coil design for the fully wound voice coil.

	Short voice coil designs	Long voice coil
Resistance	2.34Ω	2.34Ω
Voice coil length	6.5mm	13.5mm
Number of windings	48	78
Wire diameter	0.27mm	0.35mm
Wire length	8.0m	13.1m
Voice coil weight	4.1g	11.0g
Diaphragm diameter	124mm	124mm
Diaphragm mass	7.9g	7.9g
Moving mass (m_m)	12.0g	18.9g

Table 4.4: Voice coil designs, specifications. Repetition of table 2.1.

The force factor from the three short voice coil designs and the long voice coil are presented in Figure 4.22.

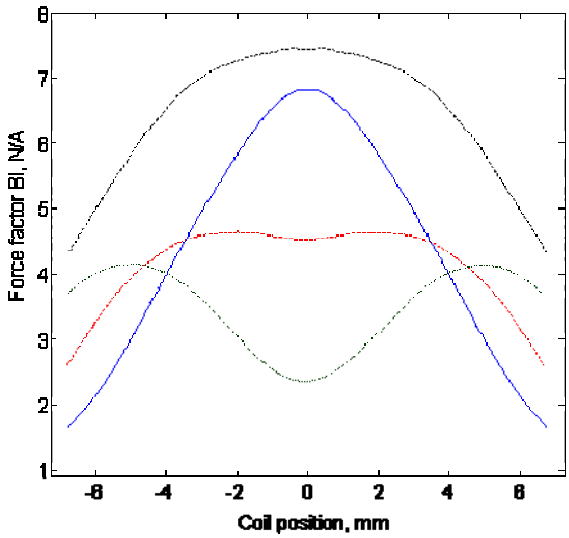

Figure 4.22: Fully wound voice coil (.-.-.).
Short voice coil; 0mm open voice coil (___), 3.5mm open (---), 7.0mm open (....).

The force factor of the larger voice coil is stronger, but it is also heavier and thicker. In Table 4.4 the efficiency loss for the extra mass was calculated using Equation 4.5. The magnet gap was 1.5mm and the extra wire thickness led to the need for an 11% greater air gap, less B field, in the terms of efficiency, resulting in a loss of 0.9dB, calculated from Equation 4.5 and magnet circuit analysis.

In Tables 4.5 to 4.7, the efficiency was normalized to 0dB for the long voice coil and the losses for different parameters were calculated. Negative numbers are losses compared to the long voice coil.

Efficiency loss	Short voice coil designs	Long voice coil
Weight	3.9dB	0dB
Magnet gap	0.9dB	0dB
Voice coil thickness	0.54mm	0.7mm
Voice coil weight	4.1g	11.0g

Table 4.5: Loudspeaker efficiency. Efficiency change due to magnet and voice coil change.

The disadvantages of the thicker and heavier voice coil add up to a loss of 4.8dB efficiency. The gain from the larger force factor is more difficult to calculate because it is highly non-linear. The efficiency of the voice coil designs relate to the amplitude of the used signal, the frequency of the signal and also, the mechanical design of the loudspeaker unit where the voice coil is mounted. Therefore, the efficiency of the voice coils is found from two different methods. First, a simulation at a fixed frequency with the case loudspeaker unit and second, the efficiency is calculated with the linear efficiency equation, Equation 4.5. The linear equation is used on the nonlinear loudspeaker based on the fact that the diaphragm is making small movements around a fixed position.

Table 4.5 gives the calculation and simulation results of the efficiency change due to the force factor difference shown in Figure 4.22. The short voice coil designs are compared with the long voice coil. The simulation case was made with a 70Hz sine wave with the amplitude of 2, 4 or 6.75mm (Nonlinear model 70Hz). At the resonance frequency, the efficiency is highly dependent on the damping factor. The damping factor changes with the change of force factor; thus, it influences the results. To eliminate this dependency, the linear efficiency from Equation 4.5, has been used, with the limitation that the diaphragm only makes small displacements around x. The efficiency calculation is made with the force factor from the used voice coil design at the displacement position of x.

Force factor efficiency change	Short voice coil designs (nonlinear model 70Hz)	Short voice coil designs (linear equation 4.5)	Long voice coil
Voice coil design 0mm open	x_{peak}=2; -0.2dB x_{peak}=4; -1.7dB x_{peak}=6.75; -3.9dB	x=0; -0.8dB x=3; -3.0dB x=6; -7.4dB	0dB 0dB 0dB
Voice coil design 3.5mm open	x_{peak}=2; -0.8dB x_{peak}=4; -1.6dB x_{peak}=6.75; -1.4dB	x=0; -4.4dB x=3; -3.7dB x=6; -3.9dB	0dB 0dB 0dB
Voice coil design 7mm open	x_{peak}=2; -2.5dB x_{peak}=4; -1.9dB x_{peak}=6.75; -0.8dB	x=0; -9.9dB x=3; -5.7dB x=6; -2.0dB	0dB 0dB 0dB

Table 4.6: Efficiency of voice coils, force factor. Second column; nonlinear model 70Hz with displacement, with the peak amplitude of x_{peak}. Third column; small displacements around x, linear model, Equation 4.5.

The efficiency number changes in Table 4.6 are only related to the change in force factor. Comparing the short voice coil with the long, all numbers were negative which is not

surprising since the long voice coil has a stronger force at all positions (Figure 4.22). The low frequency 70Hz simulation result of efficiency obtained better results generally for the short voice coil than that calculated due to the damping factors influence on the power consumption by small force factors. In the high frequency range, the displacement level was relatively small, but modulated with the low frequency components. This leads to the assumption that small movements are made with different displacement offsets.

The overall efficiency calculation/simulation is shown in Table 4.7. The force factor efficiency results (Table 4.6) are added to the efficiency loss caused by the weight and magnet gap, 4.8dB. The linear addition is an estimate due to the mass and force factor changing both the resonance frequency and the damping of the loudspeaker. However, this is a minor error and will not cause a major difference.

Total efficiency change	Short voice coil designs (non-linear model 70Hz)	Short voice coil designs (linear equation 4.5)	Long voice coil
Voice coil design 0mm open	x=2; 4.6dB x=4; 3.1dB x=6.75; 0.9dB	x=0; 4.0dB x=3; 1.8dB x=6; -2.6dB	0dB 0dB 0dB
Voice coil design 3.5mm open	x=2; 4.0dB x=4; 3.2dB x=6.75; 3.4dB	x=0; 0.4dB x=3; 1.1dB x=6; 0.9dB	0dB 0dB 0dB
Voice coil design 7mm open	x=2; 2.3dB x=4; 2.9dB x=6.75; 4.0dB	x=0; -5.1dB x=3; 0.9dB x=6; 2.8dB	0dB 0dB 0dB

Table 4.7: Overall efficiency of voice coils. Second column; nonlinear model 70Hz with displacement with the peak amplitude of x_{peak}. Third column; small displacements around x, linear model, Equation 4.5.

The results show that the voice coil with 3.5mm open space has improved in all cases. The 0mm open space losses by large displacements and the 7mm open space losses by small displacements, linear calculation in comparison to the long voice coil. The 3.5mm and 7mm open space designs show the nonlinear simulation generally provides better results due to the damping being small; therefore, the efficiency is high near the resonance frequency.

Overall the design with 3.5mm open space shows good results in the efficiency tests. The result emphasizes the importance of low mass. Based on the linear calculation and the fact that the loudspeaker is used mostly at small displacements, the normal short voice coil is therefore very interesting. Table 4.7 confirms Bright's [B13] results showing that short voice coils are more efficient. There are two reasons for this. Firstly, the mass is reduced and secondly, the thinner wire allows more wire in the strongest part of the magnetic field, as previously discussed.

4.5.3. Application with Music

For the efficiency simulation of the short voice coil designs with music, a home audio subwoofer was designed. This choice was made, because the simulated loudspeaker unit is a home audio device and has matching parameters to a home audio subwoofer. With regards to the technology, open voice coil designs have relevance in applications where high displacement levels often occurs, as in subwoofers and P.A. systems.

The musical power tests were made using two simple samples of music. The first is one beat from a bass drum, and the other is a melody played on a bass guitar. The music samples were sent through the loudspeaker model and filtered with a first-order low pass filter, f_c=125Hz. The power consumption was calculated using the three different force factor functions. The first-order filter was chosen because the used loudspeaker unit targets home audio equipment as a subwoofer. In Figures 4.23 and 4.24, the displacement distributions in intervals of 10% are shown for the music samples.

Bass drum

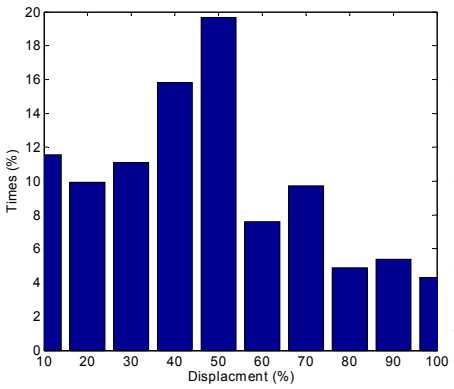

Power use:
0mm open
2.2W

3.5mm open
2.1W

7.0mm open
2.7W

X_{max} = 6.5mm
X_{rms} = 3.3mm

Figure 4.23: Displacement levels in 10% decades. Bass drum, one beat.

Bass guitar

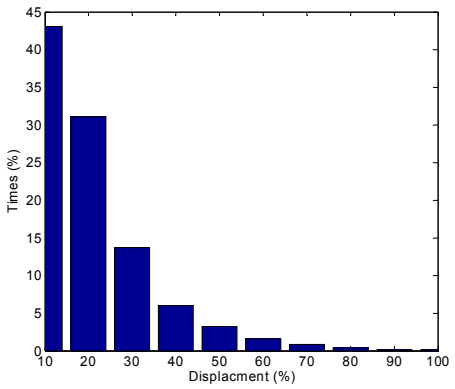

Power use:
0mm open
1.8W

3.5mm open
1.6W

7.0mm open
1.9W

X_{max}=6.8mm
X_{rms}=1.4mm

Figure 4.24: Displacement levels in 10% decades. Bass guitar.

The power used by the three different voice coil layouts playing the music samples with the same displacement level is shown beside Figures 4.23 and 4.24. X_{max} is the maximum peak displacement and X_{rms} is the rms displacement level.

Figure 4.25 can be used to compare the displacement distribution with the power consumption of the three different voice coil layouts. Figure 4.25 was produced with a 100Hz sine input signal with a DC offset in a nonlinear simulation model. One simulation is as an example kept between 90 to 100% of the displacement level. After the test, the data were interpolated.

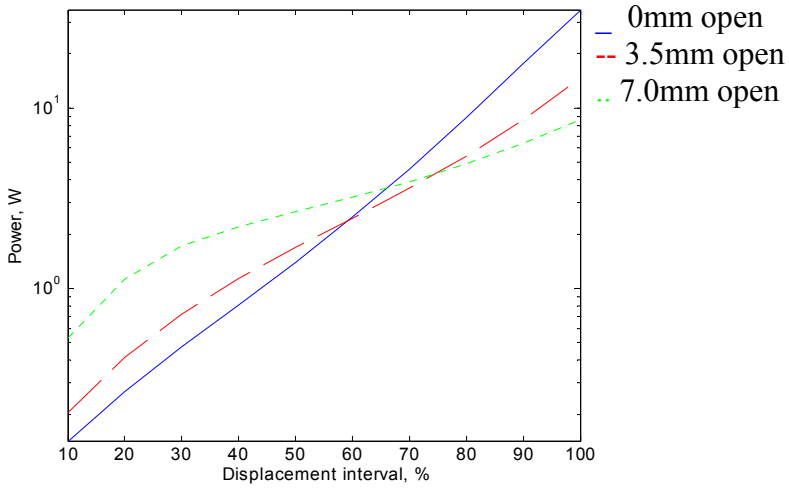

Figure 4.25: Power use versus displacement in intervals of 10%. Power consumption is scaled logarithmically.

The power consumption shown in Figure 4.25 is scaled logarithmically. The short voice coil without an opening has, in this case, approximately logarithmic power consumption in regards to its displacement level. The consumption level of the three voice coil layouts intersect at around 60% displacement level. Under normal conditions, a loudspeaker is driven at small displacements and only seldom over 60%. The difference in power consumptions between the layouts has a large difference at large displacements; however, this does compensate for the music distribution. The examples in Figures 4.23 and 4.24 were played at maximum volume and the power consumption of the non-open layout and the 3.5mm opening were very close. The 3.5mm opening showed 5-11% less power consumption. The relevance of the open design will be greater in application under other conditions. A list of important conditions and considerations with regard to designing a loudspeaker system are given below:

Clipping:	Typically, when a music system is played at a high volume there will be a level of clipping. The level of clipping is typically large as it is expected to be a noisy party environment with individuals not engaged in focused listening. The rms displacement is increased.
Compression:	A high level of compression will change the placement distribution function such that, more power is “moved” to large displacements. This could have relevance in applications with small transducers relative to the wanted output, e.g., mobile phones.
Power Amplifier:	A limited voltage range and power capability of the power amplifier is other aspects than power loss in the loudspeaker unit. The solution provides the maximum displacement of the diaphragm with a smaller amplifier.

4.5.4. Power Amplifier Considerations

An interesting system consideration is the combination of power amplifier and the loudspeaker as one system. From a system perspective, the total power consumption is minimized. An example with the three voice coil layouts, together with a class D power amplifier is given. In Table 4.8, a simulation example is shown comparing the three voice coil layouts.

	dB spl	0mm open	3.5mm open/ difference	7mm open/ difference
Needed amplifier		42W (4Ohm)	31W -26%	24W -43%
Idle power loss		346mW	297mW -49mW	262mW -84mW
Back ground music, I	76dB	50mW	65mW 15mW	109mW 59mW
Background music, II	80dB	100mW	135mW 35mW	203mW 103mW

Table 4.8: Comparing power consumption of the amplifier when using the three voice coil designs.

The first row "Needed amplifier" is the power required for obtaining the same maximum sound pressure for the three coil layouts. The second row is the "Idle power loss" in a class D amplifier corresponding to the required size. The third and fourth rows are two background levels, one fairly low 76dB in the listening position, 1 kHz, on a typical two-way loudspeaker construction, and the other is a high, 80dB, background listening level.

The calculations in Table 4.8 are based on the simulation model which was also used for the power consumption tests. In the case of background music I and II a 60Hz sinusoidal signal was used and the displacement levels were respectively x=±0,24mm and x=±0,33mm.

Table 4.8 focuses on the area where the open voice coil designs have their drawback. However, in relation to home audio products this is very important because the sound pressure level presented is used more than 98% of the time. In these cases, which are of more interest from an environmental aspect than from a loudspeaker engineering perspective, the idle power consumption of the power amplifier is very important. For the low listening, normal levels, the power loss is larger in the power amplifier than the loudspeaker, and from this perspective the amplifier design is more important.

The 7mm open design be useful with the limited voltage range of a power amplifier. One example is a typical 5.1 channel system where the satellite speaker has a 24W power amplifier and the same size amplifier can be used for the subwoofer with an open voice coil design. The rms level of the subwoofer will be larger than the satellites.

4.6. Discussion of Loudspeaker Efficiency

Efficiency and small loudspeakers are very important parameters in many applications today. There are the requirements of reducing size in flat panel TVs and obtaining the same performance as that obtained from picture tube TVs where more room was available for the loudspeaker enclosure and the heat dissipation from the loudspeaker and amplifier was not a problem [B30]. Today's powerful portable devices have high quality audio stream performance, but, for example, the loudspeakers in mobile phones have a very limited audio performance due to their small size and limited power handling. Many other applications are limited by the loudspeaker. An important step forward is to improve the efficiency. For very small devices, it is not only power loss that is a problem but also the piston size, which is too small to produce a useful sound pressure level at low frequencies.

The efficiency can be improved by increasing the force factor and re-establishing a flat frequency response. The frequency response is flattened with pre-filtering of the loudspeaker signal [V2]. It has been shown that this approach achieves significant improvements in efficiency. The draw back is the increased cost of the stronger magnet, but the overall improvement can reduce the costs of the power amplifier and power supply unit. In regard to the power amplifier, it is important to state that a class A or B can not be used due to the high back EMF [V2].

Efficiency can also be achieved by reducing weight, which can be done by shortening the voice coil [B10]. The drawback to this is decreased linearity of the force factor (see Chapter 2.2.2). The linearity can be regained by applying a feed forward controller that includes pre-filtering if the frequency response is non-flat.

All efficiency improvements in regard to optimising the linear loudspeaker parameters towards higher efficiency result in a higher damping factor and the loudspeaker can thus not achieve a flat frequency response. In addition to the loudspeaker unit parameters, there are also acoustic design options which have not been investigated. Today, many loudspeaker constructions include a Helmhols resonator ventilated box, which also has to be taken into account when optimising the efficiency.

The design of a high efficiency loudspeaker system requires consideration of the power consumption of the loudspeaker and the power amplifier. Adjusting the nonlinearities, for example, by placing the voice coil winding differently the relationship between the amplifier and loudspeaker losses could be optimised. The proposed open voice coil design could also be a good approach, together with a higher force factor where very high peak voltage requirements can occur.

4.7. Conclusion of Loudspeaker Efficiency

Digital signal processing allows improvement in the efficiency of electrodynamic loudspeakers. Digital signal processing is important because the loudspeaker unit design does not require a flat frequency response or a linear transducer. The efficiency improvements can be made by enlarging the force factor, which leads to the option of a thinner and lighter voice coil. The voice coil can then be shortened. This leads to loss of linearity, but improvement in efficiency. The linearity can be regained by nonlinear compensation. The maximum power loss in the loudspeaker is an important parameter for obtaining a high efficiency and can, to some extent, be changed by a different voice coil layout.

Chapter 5

5. Distortion Correction of Loudspeakers

To enable an extra dimension of freedom in loudspeaker unit designs, both linear and nonlinear distortion correction are important. Feedback structures and a feed forward controller are reviewed.

A feed forward controller is constructed for a simulation case of loudspeaker parameter drift.

5.1. Different Methods for Distortion Correction

5.1.1. Feedback Structure

Distortion correction has been known for many years in audio engineering because of power amplifiers. With great success, feedback has been applied to power amplifiers, so that today they have very low distortion, often less than 0.1%. With power amplifiers, is it easy to apply feedback because the output is a voltage or a current that can be measured and compared with the input. Since feedback today is well known and shows good results in power amplifiers, this may be a good starting point for distortion cancellation in loudspeakers. The output of the loudspeaker is sound, which implies that a microphone for measuring the sound could be used and fed back to the input as shown in Figure 5.1.

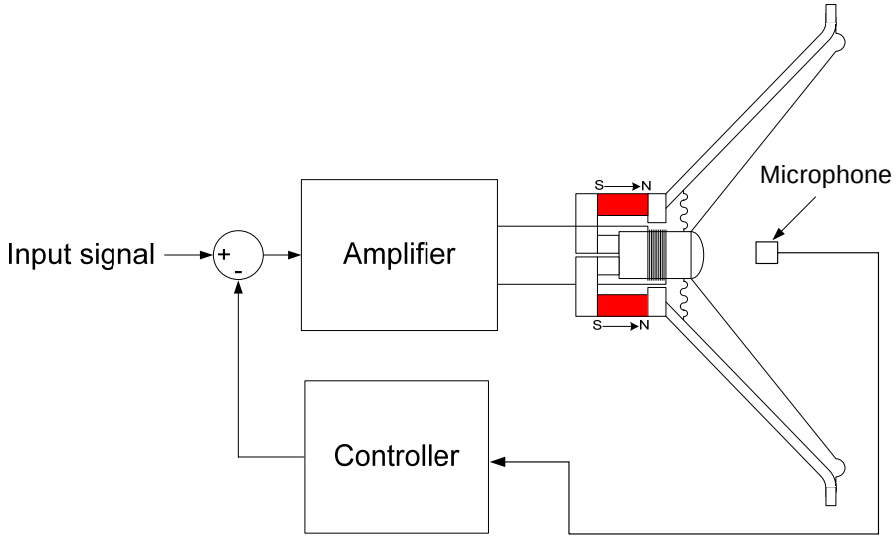

Figure 5.1: Feedback system with microphone.

Unfortunately there are many difficulties obtaining the output, the sound from the loudspeaker:

- Time delay of the measurement.
- External noise from other sources.
- Placement of the microphone.
- Errors from the microphone will not be cancelled
- Cost of the microphone

The acoustic path introduces a time delay, or the phase shift limits the feedback system to operate only at low frequencies. The placement problem of the microphone can, to some extent, be solved by placing the microphone inside the loudspeaker enclosure. The sound pressure inside the loudspeaker enclosure can be very large and it can be a problem to find a microphone that is sufficient for the application, e.g. a subwoofer. The conclusion, because of the limited frequency range, the microphone placement problem and the cost of the microphone, is that this application has a limited range for loudspeaker systems.

Many of the problems related to the microphone feedback system are due to the microphone itself. Instead of feeding the sound pressure back, the diaphragm acceleration can be fed back. An accelerometer can be attached to the diaphragm, as shown on Figure 5.2.

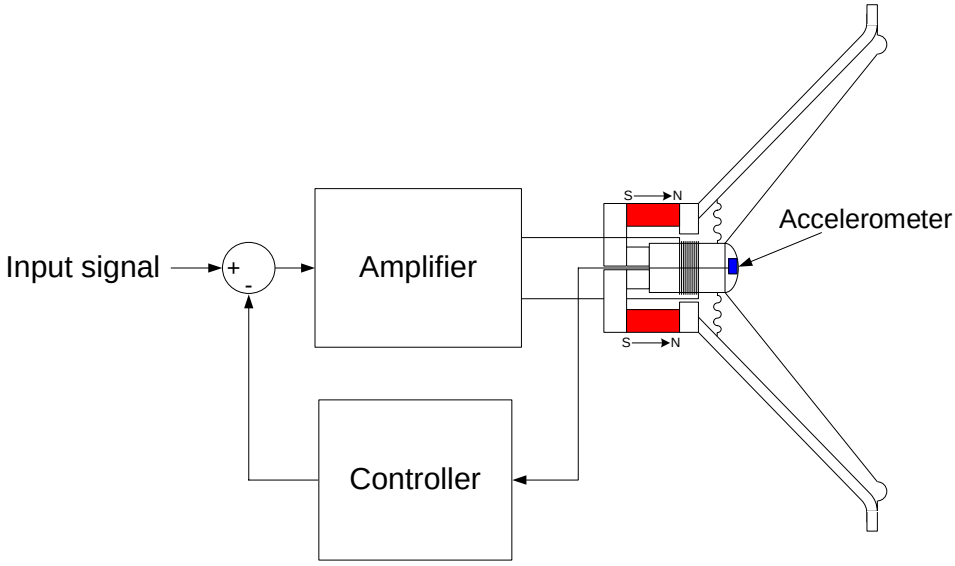

Figure 5.2: Feedback system with accelerometer.

The accelerometer application has not been analysed or tested in any detail. Obvious disadvantages can be listed as follows:

- Added extra mass to the diaphragm decreases efficiency
- Errors from the accelerometer will not be cancelled
- The additional cost of the accelerometer

A known problem that has not been investigated is the interference of the magnetic field of the loudspeaker with the accelerometer. This setup is also limited to relatively large loudspeaker units, due to the need to apply extra mass to the diaphragm. Also, the extra cost limits the usability of the motional feedback with an accelerometer. Even now there are applications that can benefit from feedback with sensing the acceleration, as was shown by Hall [H40], who has used it with success. Many of the problems caused by motional

feedback can be resolved by an optical sensor, but these are very expensive, and are only used primarily in measuring devices today.

Using the loudspeaker current is the next step backwards, since feeding back using the sound pressure or making motional feedback are not feasible. Current feedback is generally known from its use in current controlled power amplifiers, and its benefit is that the nonlinearities of the voice coil are suppressed [M20]. The other nonlinearities are not compensated and this makes it a less useful solution. Another structure must therefore be considered.

5.1.2. The Feed Forward Structure

The intention of a feed forward controller is to predistort the input signal, such that errors in the loudspeaker are cancelled. A feed forward structure is shown in Figure 5.3.

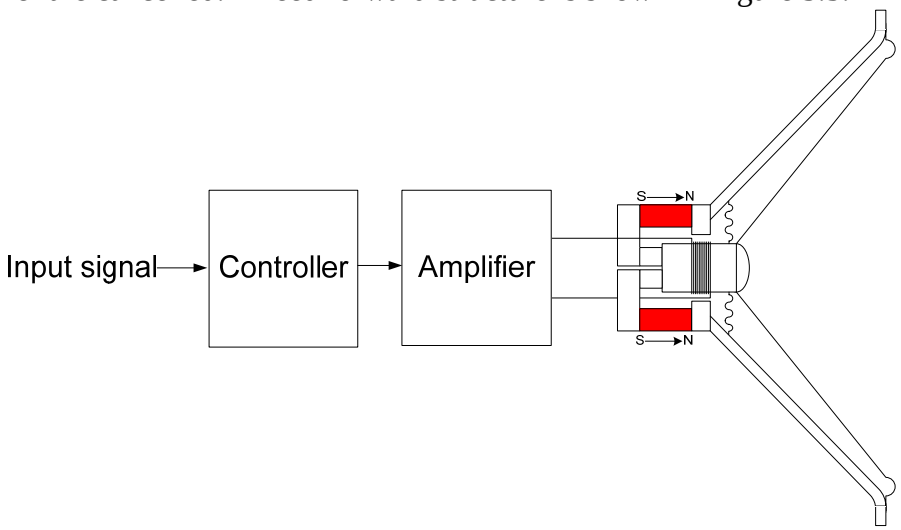

Figure 5.3: Feed forward system.

The feed forward controller is based on a model of the loudspeaker. The model and its parameters have to be a precise match in order to eliminate all distortion. By underestimating the distortion level, the distortion to some extent will be reduced, but this might not be significant. The distortion level can increase by an overestimation of distortion. The positive benefit of a feed forward controller is that no extra sensor has to be added. The drawback is that parameter drift of the loudspeaker is not taken into account, and model errors limit the cancellation. A small controller is constructed in the next section and tested with parameter drift, as a simulation study.

5.2. Feed Forward Controller for Loudspeakers

5.2.1. History of Feed forward Controllers for Loudspeakers

A feed forward controller is based on feedback linearization theory. Feedback linearization was applied to loudspeakers in the early 90's to cancel distortion caused by nonlinearities. A paper in 1995 by Suykens [S10] described an example of applying feedback linearization to a loudspeaker, ending up with a controller, but the improvements in distortion were not tested. Schurer [S1], in 1997, demonstrated a feed forward controller that improved the distortion of a loudspeaker. Klippel [K2] has several times since demonstrated feed forward controllers, but no nonlinear error cancellation has been shown to have been implemented in any product.

5.2.2. Basic Implementation of Feed Forward Controller

Basically, a feed forward controller is the inverse dynamics of a loudspeaker, and the signal is predistorted through this inverse system, before it is sent to the loudspeaker. This approach cancels the unwanted distortion caused by the nonlinearities in the loudspeaker, but also cancels the wanted linear dynamics (2^{nd} order high-pass filter). Therefore, the linear dynamics are reintroduced as a filter, before the controller. The "inverse dynamics" implemented by the compensator (controller) requires the displacement and the diaphragm velocity as inputs. This is implemented by a loudspeaker model, the observer, which calculates the displacement and velocity. Optimization methods for the observer, as well as further details, are described in Klippels paper [K2].

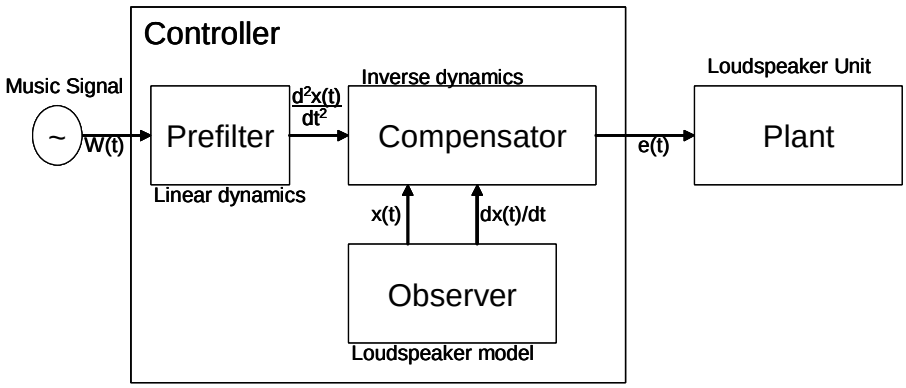

Figure 5.4: Block diagram of loudspeaker with feed forward controller based on feedback linearization.

In this project, solutions for minimizing the number of calculations in the controller implementation are not considered, but a simple implementation that is easy to use for research shall be derived. The solution chosen is to implement the controller in the analogue domain. It was implemented in the Matlab/Simulink environment, which will solve the

analogue equations. The discretization was made by a numerical differential equation solver in Simulink. General methods for discretization of controllers are presented in [B10] and [S10].

5.2.3. Analogue Implementation of Feed Forward Controller

A linear model, i.e. the linear lumped loudspeaker model, can be extended to a nonlinear model. It is possible to add/exchange nonlinear elements into a linear system; an example is the force factor given as a nonlinear function of the displacement, [K10]. The suspension compliance and force factor position nonlinearity can be directly implemented, by exchanging the linear parameter in the equations with the position dependent nonlinear function. The voice coil induction cannot directly be exchanged, as the physical behaviour is changed when the induction not is constant (see section 2.3.1).

For designing the controller, the nonlinear loudspeaker equations will be rewritten, to separate the equation in the linear dynamic system and the nonlinear system. The nonlinear inverse dynamic system can be derived, and prefiltering of the signal through this system will compensate the nonlinearities in the loudspeaker model.

The linear loudspeaker model is given by equation 5.1 and 5.2, repeated from chapter 1, and the loudspeaker is simplified to a second order system with L_e=0 for simplicity. This simplification reduces the equations significantly and makes them easier to understand for this documentation, but there is no difference in the method.

Electrical:

$$e(t) = \mathrm{R_e} \cdot i(t) + Bl \cdot \frac{dx(t)}{dt} \qquad \textit{Equation 5.1}$$

Mechanical

$$Bl(x) \cdot i(t) = m_m \cdot \frac{d^2x(t)}{dt} + R_m \cdot \frac{dx(t)}{dt} + k_m \cdot x(t) \qquad \textit{Equation 5.2}$$

Combined equation

$$Bl(x) \cdot \frac{e(t)}{\mathrm{R_e}} - \frac{Bl(x)^2 \cdot \frac{dx(t)}{dt}}{\mathrm{R_e}} = m_m \cdot \frac{d^2x(t)}{dt^2} + r_m \frac{dx(t)}{dt} + K_m \cdot x(t) \qquad \textit{Equation 5.3}$$

It has been shown by Small [S30] that the acceleration of the diaphragm is equal to the sound pressure in the far field. The diaphragm acceleration in equation 5.3 is therefore equal to the sound pressure. The objective is to implement the reverse dynamics, and the output of the loudspeaker is set equal to the input voltage of the controller, instead of the sound pressure. By rewriting equation 5.3, and replacing the diaphragm acceleration with the compensator input, the compensator equation 5.4 appears. This equation is similar to Bright's result [B1, eq. 3.15].

$$e(t)\cdot\frac{Bl(x(t))}{\mathrm{R_e}} = K(x(t))\cdot x(t) + (R_m + \frac{Bl(x)^2}{\mathrm{R_e}})\cdot\frac{dx(t)}{dt} + m_m\cdot\frac{d^2x(t)}{dt^2} \qquad \textit{Equation 5.4}$$

Equation 5.4 is shown graphically in Figure 5.5 as the controller is implemented in the simulation.

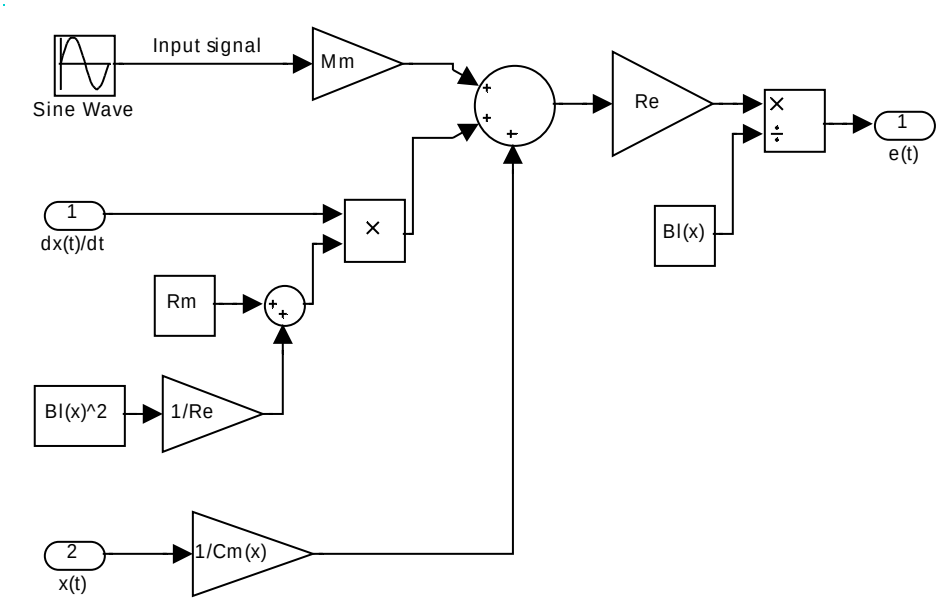

Figure 5.5: Block diagram of compensator as implemented in Simulink.
Some of the loudspeaker parameters are written with capital letters in the simulation model.

The nonlinear functions in the controller are implemented with an 8th order polynomial fit to the data. The observer is implemented as the simulation model shown in Appendix 1, Figure 10.1.

5.3. Feed Forward Controller Simulation

5.3.1. Simulation Implementation

The analogue controller is implemented in Simulink/Matlab as the simulation model described in Appendix 1. Figure 5.5 illustrates the implementation made in Simulink, followed by a loudspeaker model.

5.3.2. Test of Controller

The data used for the controller and the simulation model are the same and, therefore, the controller should be able to cancel all distortion. This is, of course, only a result that has theoretical interest, and as for testing, the implementation of the controller operates sufficiently.

A THD+N simulation are for the frequency range 50-500Hz produced with maximum displacement at 50Hz and equal sound pressure level by the different frequencies. Figure 5.6 shows the distortion without the controller. The distortion level with the controller, Figure 5.7, was calculated to $8 \cdot 10^{-12}$% THD+N, which shows that the controller is working as expected and that the accuracy of the simulation is satisfactory.

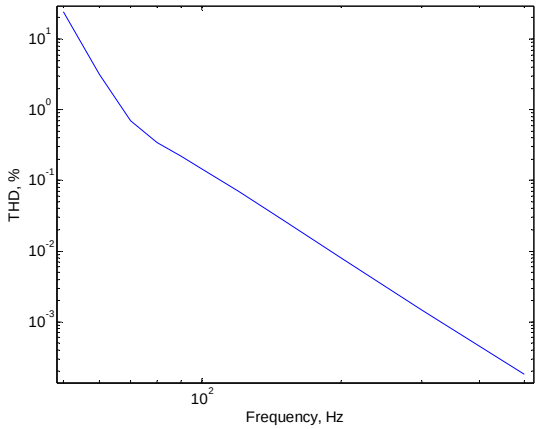

Figure 5.6: THD for the frequency range 50-500Hz. Loudspeaker with nonlinear force factor and suspension compliance from appendix 2.

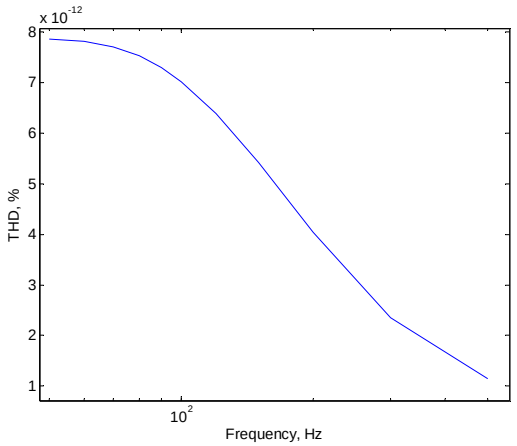

Figure 5.7: THD for the frequency range 50-500Hz. Compensated loudspeaker with nonlinear force factor and suspension compliance from appendix 2.

5.4. Temperature Drift of Parameters

After looking at the simulation results of the idealized feed forward controller, a case study was made for analysing the sensitivity to the difference of loudspeaker parameters in the controller and the loudspeaker. The simplest test is probably to include the drift of the linear parameters, due to temperature change. The linear data are easy to measure and can easily be implemented in the simulation, by changing the parameter values in the loudspeaker model. The test were based on the results made by Krumps [K20], shown in Table 5.1, and applied to the loudspeaker used in this project. The change found by Krump, in the temperature range from 20°C to 80°C, is applied to the loudspeaker model in the simulated system. All data used correspond to the nonlinear functions, e.g. the force factor is scaled by -13% according to Table 5.1. The simulations are repeated, changing the linear parameters in the loudspeaker model (Plant), one by one. Results are shown in Figures 5.8 to 5.12. In Figure 5.13 all parameters are changed to 80°C and in Figure 5.14 is the controller disabled.

Parameter	Change 20°C to 80°C
Voice coil resistance, R_e	20%
Force factor, Bl	-13%
Moving mass, m_m	-10%
Suspension compliance, c_m	9%
Mechanical resistance, r_m	-42%

Table 5.1: Temperature drifts of linear parameters according to Krump [K20]

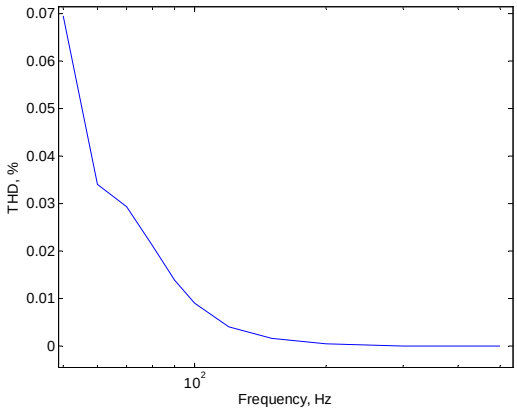

Figure 5.8: THD for the frequency range 50-500Hz. Voice coil resistance, R_e 20% increased with feed forward system.

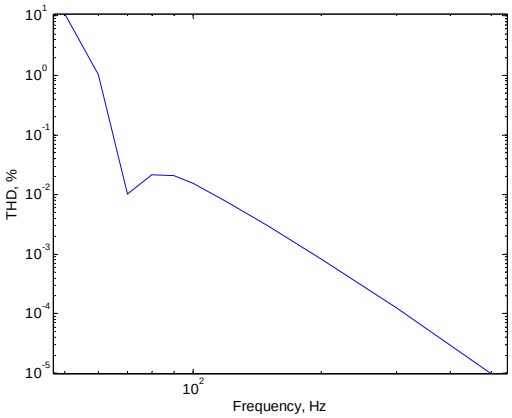

Figure 5.9: THD for the frequency range 50-500Hz. Force factor, Bl 13% decreased with feed forward system.

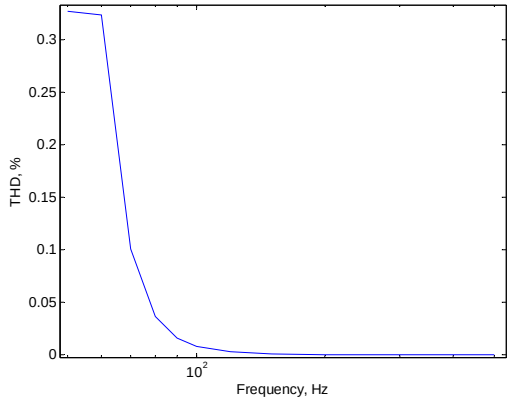

Figure 5.10: THD for the frequency range 50-500Hz. Moving mass m_m 10% decreased with feed forward system.

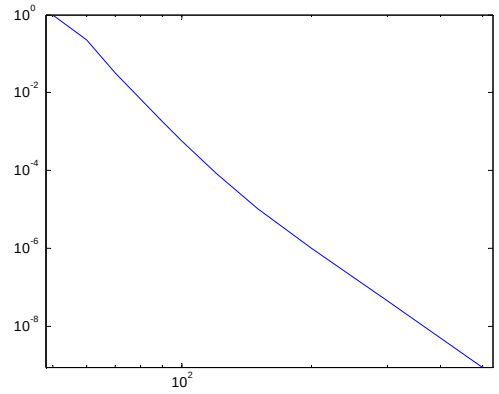

Figure 5.11: THD for the frequency range 50-500Hz. Suspension compliance C_m 9% decreased with feed forward system.

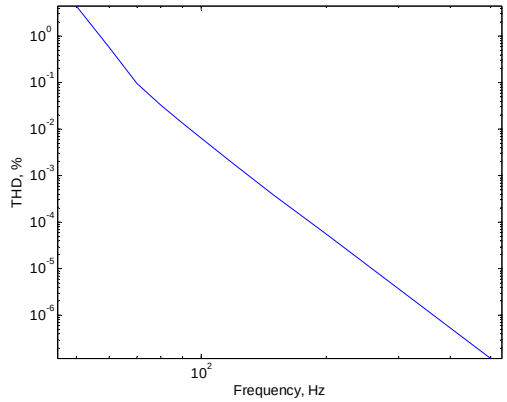

Figure 5.12: THD for the frequency range 50-500Hz. Mechanical resistance R_m 42% decreased with feed forward system.

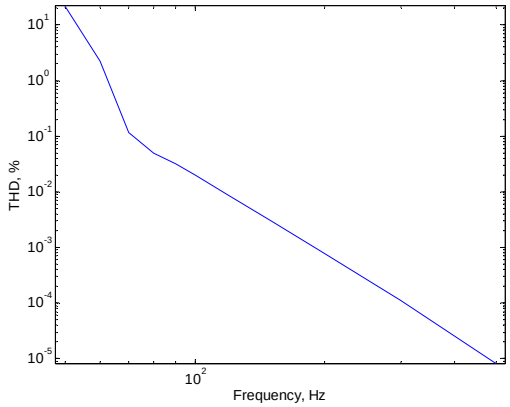

Figure 5.13: THD for the frequency range 50-500Hz. Drift in all parameters according to table 5.1, 80°C, with feed forward system.

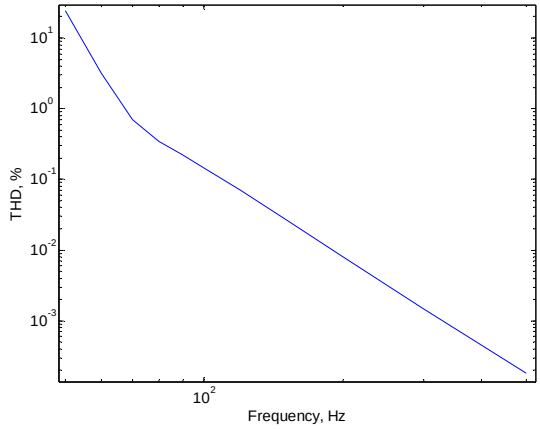

Figure 5.14: THD for the frequency range 50-500Hz. Drift in all parameters according to table 5.1, 80°C, only loudspeaker, non compensator.

Generally, the distortion is only large at large displacement, corresponding to the lowest frequencies on the graphs. The drift of the force factor is the single parameter that introduces the largest distortion (11%). The drift of mechanical loss (as a single parameter) gives 4.5% distortion; but this parameter is simulated with the maximum drift of 42%. If all parameters have the changes according to Table 5.1, the distortion goes up to 22% (Figure 5.13), which is almost the same distortion level (24%) as the loudspeaker driven without a controller (Figure 5.14). In chapter 3, a set of loudspeaker units were investigated and several other causes for drift of the loudspeaker parameters were found, including aging, production spread and other external parameters. Based only on the simulation result of the drift due to temperature, the feed forward controller is inefficient. If it is possible to estimate the parameters with an accuracy of 5% (mainly the force factor), distortion less than 1% can be obtained, [P22].

Uncertainties of the model, as shown in chapter 2, have limited the test of the compensator of a physical loudspeaker. It is also not possible to follow all parameter changes of the loudspeaker on a running test. Achieving a better loudspeaker model is needed to enable the controller to cancel distortion sufficiently. Tests of the nonlinearities from this study have, except for the suspension compliance, been shown to be relatively stable (see further details in chapter 2). According to Bright, [B1] drift of the nonlinear parameters are small, but the drift

of the linear parameters are of importance. To overcome the drift of the linear loudspeaker parameters, Bright investigated a system identification method for his micro loudspeakers that finds and feeds back the linear loudspeaker parameters. These facts lead to the decision to investigate a system identification method for the loudspeaker types used in this project (see next chapter).

5.5. Discussion of Distortion Correction of Loudspeaker

For feedback strategies a sensor is needed to obtaining the feedback signal. The sensors available today limit the use of feedback system to low frequencies. Optical laser displacement measurement sensors with a useful frequency range are very expensive and considered to expensive also in the coming years.

A very inexpensive solution is implementing a feed forward controller. A model based controller has in other projects shown useful results, Schur and Klippel. The model tested in this project is not sufficient and a better model has to be fount, see more details in chapter 2. Model error will limited the distortion cancellation. The simulation has shown that at least the linear loudspeaker parameters have to be updated continuously, also shown by Bright [B10]. The sensitivity is high to the voice coil resistance and the force factor due to the current and force at the diaphragm is changed [S1].

The controller designed in this section is an analogue version which is easy understandable and easy to make changes in and read physical signals as the loudspeaker current, displacement etc. This design is made for research and in end applications can the result be transformed to the digital version. The analogue controller is implemented in Simulink and loudspeaker tests can be made with an offline controller.

5.6. Conclusion of Distortion Correction of Loudspeaker

Feedback compensation has today a very limit target application group due to sensing problems of the feedback signal. This problem might in the future be resolve by better and cheaper sensors.

Feed forward compensation is very cost efficient but it needs at least a procedure that on the flight can track the linear loudspeaker parameter drift. For making a sufficient feed forward controller is a better loudspeaker model needed, even know that the model can estimate the 3rd harmonic in of a few decibels. A feed forward controller will thereby be able to reduce the distortion due to the 3rd harmonic. Further investigations and research has to be made on the model before the controller can make major distortion improvements. The results of the loudspeaker modelling indicate possibilities of obtaining more then half the distortion at high displacement levels at low frequencies.

Chapter 6

6. System Identification

System identification is a well-known topic and several textbooks discuss it both in terms of adaptive filters and system identification. The topic is highly interesting in the context of loudspeaker protection and for estimating the parameters for a feed forward compensation. As shown in the previous chapter, a nonlinear feed forward compensator can not be implemented without compensation of parameter drift during operation.

This chapter begins with a short introduction to the existing system identification of loudspeakers. This is followed by a digital model of the loudspeakers that the presented system identification models are based on. A linear system identification of the loudspeaker is then presented and the system identification signal is discussed in the context of music. The general system identification methods of the FIR and IIR model structures are reviewed, including a discussion of their benefits and extra requirements. Selected simulation results of the system identification systems are given and the FIR based system is tested with music.

6.1. Literature on Loudspeaker System Identification

System identification in the context of loudspeakers has been used to estimate loudspeaker parameters, for example, as presented in 1988 by Knudsen [K12]. A major step forward in this respect has been the implementation of a measuring system; the Klippel analyzer [K4] that includes the major non-linearities.

Further work is needed to integrate the system identification of loudspeakers into end products. In end products, the parameters can be used for protection, fault analysis and compensation to improve sound quality. The products have to find the parameters from the sound that is usually produced by this end product. In measuring devices, the test signal can be optimized and good measurement conditions can be achieved. In end products the signal is typically music or speech. Bright [B10] has investigated system identification of the micro loudspeakers used in mobile phones.

Products are available on the market today that can estimate the resistance at DC [C10] i.e. the voice coil resistance. From the voice coil resistance, the voice coil temperature can be found and used for protection.

6.2. System Identification of a Loudspeaker

The linear lumped loudspeaker parameter can be found by measuring the impedance and the movements of the diaphragm. This can be implemented by a current measurement and optic displacement sensor, as demonstrated by Knudsen [K12].

Further system identification is based on a voltage and current measurement. Usually the voltage from the power amplifier is known and the current is measured. The transfer function from voltage to current is shown in Equation 6.1, the admittance.

$$H(s)=\frac{i(s)}{u(s)}=\frac{\frac{1}{\mathrm{R_e}+sL_\mathrm{e}}\cdot\left(s^2+\frac{r_m}{m_m}\cdot s+\frac{1}{c_m\cdot m_m}\right)}{s^2+\frac{Bl^2+(R_e+sL_\mathrm{e})\cdot r_m}{m_m\cdot(R_e+sL_\mathrm{e})}\cdot s+\frac{1}{c_m\cdot m_m}} \qquad \textit{Equation 6.1}$$

A useful simplification for finding the low frequency parameters is to neglect the voice coil induction, L_e=0, Equation 6.2.

$$H(s)=\frac{i(s)}{u(s)}=\frac{\frac{1}{\mathrm{R_e}}\cdot s^2+\frac{r_m}{R_e\cdot m_m}\cdot s+\frac{1}{c_m\cdot m_m\cdot \mathrm{R_e}}}{s^2+\frac{Bl^2+R_e\cdot r_m}{m_m\cdot R_e}\cdot s+\frac{1}{c_m\cdot m_m}} \qquad \textit{Equation 6.2}$$

Five coefficients can be found from the transfer function in Equation 6.2. The overall gain, in this case the voice coil admittance, the natural frequency and the damping of both denominator and nominator. Unfortunately, when the loudspeaker is a second-order complex system, the denominator and nominator have the same natural frequency. This is resolved in measuring systems by a displacement measurement but this is not considered an option in this work as a displacement sensor is assumed to be too expensive and, in some applications, the space is limited. One parameter has to be assumed constant or fixed so the drift of a parameter can be found. The most stable is the moving mass (see Chapter 3.2).

6.2.1. Digital Model of a Loudspeaker

System identification is usually implemented in the digital domain on a digital signal processor. This requires that a digital model or representation of the loudspeaker is made.
By bilinear transformation of Equation 6.2, the digital version can be found.

$$H(z) = \frac{i(z)}{u(z)} = \frac{b_0 \cdot z^2 + b_1 \cdot z + b_2}{z^2 - a_1 \cdot z - a_2}$$ *Equation 6.3*

a_n	the filer coefficients (IIR)
b_n	the filer coefficients (FIR)

The direct digital implementation of a linear loudspeaker model is a second-order digital transfer function with two poles and two zeros, an auto regressive moving average (ARMA). From the digital coefficients, the linear loudspeaker parameters can be found by pole zero mapping. The resonance frequency and damping factor are found and shown in Equations 6.4 and 6.5. The gain constant can be derived and related to the voice coil resistance by Equations 6.2 and 6.3.

Resonance frequency and damping:

$$\omega_n = Mod\left(\frac{1}{T_s}\ln\left(\frac{-a_1 + \sqrt{a_1^2 - 4 \cdot a_2}}{2}\right)\right)$$ *Equation 6.4*

$$\xi = \frac{2 \cdot \omega_n}{a_1}$$ *Equation 6.5*

R_e voice coil resistance:

$$R_e = \frac{1}{b_0}$$ *Equation 6.6*

The second order pole/zero digital model can also be implemented by an all zero representation. The number of zeros or FIR filter coefficients depends on the impulse response length of the loudspeaker.

An all zero representation, FIR filter structure is given by:

$$H(z) = \frac{i(z)}{u(z)} = b_0 + b_1 z^{-1} + ... + b_m z^{-m}$$ *Equation 6.7*

6.3. Linear Identification of Loudspeaker Unit

6.3.1. Use of the estimated parameters

The estimated loudspeaker parameters can be used in different contexts. For clarity, they will be divided into two groups.

The first group of applications where the linear parameters are sufficient are loudspeakers with equalisation of non-flat frequency response, with protection and/or fault diagnosis.

The second group is nonlinear distortion cancellation. Nonlinear distortion cancellation has its own group because the controller needs all the basic linear lump parameters and the major loudspeaker nonlinearities, Bl(x), $c_m(x)$, and $L_e(x)$, Klippel [K2]. According to Bright [B10], the drift of the linear loudspeaker parameters is relatively large, but the drift of the nonlinear functions such as force factor, compliance, and voice coil induction as a function of the coil position is small. The intention was to perform a system identification on the linear parameters and use the pre-measured nonlinearities. Bright's tests were performed on micro loudspeakers for mobile phones. In this thesis, hi-fi bass mid-range loudspeaker units have been studied. It is shown that the suspension compliance nonlinearity not is stable, as it varies with changes in temperature caused by the diaphragm motion and power loss in the voice coil (see Chapter 2.6 or [P6]). This leads to a need for both the linear parameters and some non-linear functions to be identified to obtain a sufficient compensator. This work focuses on the implementation of a linear identification system and, from this, adjusting/scaling/offsetting the nonlinear functions fitted by the linear parameters.

6.3.2. Linear model structure for a nonlinear plant

System identification consists of three parts. These are, the object that has to be identified, "the plant", in this case the physical loudspeaker unit, a model that behaves in the same way as the plant, and an algorithm that adjusts the model parameters such that the difference in output between the plant and the model is minimized (structure shown in Figure 6.1). The loudspeaker is a nonlinear system, but it is assumed to be fairly linear for small displacements and is estimated with a linear loudspeaker model. When playing music, the loudspeaker is not in the non-linear region very often and it is possible to disable the system identification algorithm when the loudspeaker is working in the nonlinear region. If the loudspeaker parameters are identified as being in the nonlinear region with a linear model then the parameters will be slightly misaligned [K11].

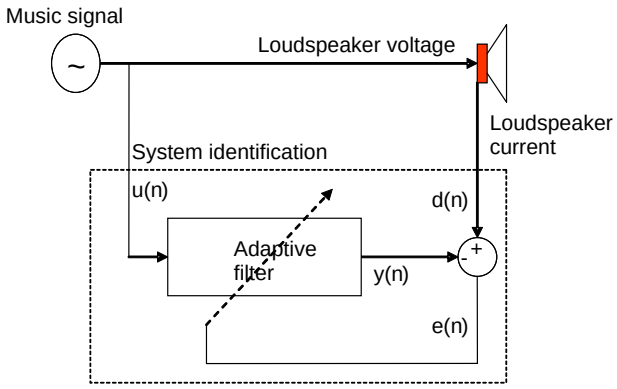

Figure 6.1: Overall system identification structure of loudspeaker from current and voltage.

6.3.3. Estimation of mechanical parameters

The magnitude of the loudspeaker impedance plot (shown in Figure 6.2) can be divided into two parts. Frequencies less than 400Hz are dominated by the bass resonance, and frequencies above 400 Hz are dominated by the voice coil induction. If only the bass resonance is to be identified, then the voice coil induction can be neglected.

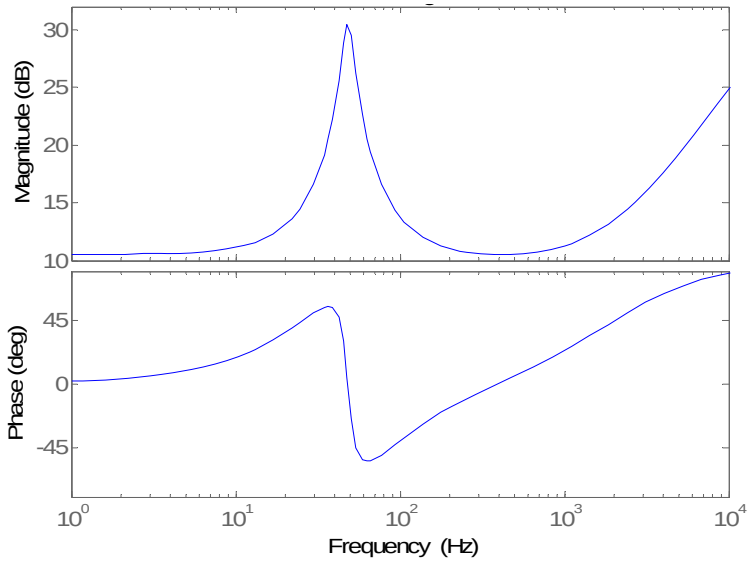

Figure 6.2: Impedance of the loudspeaker used in the system identification tests, modelled by Equation 6.1.

Identifying the voice coil inductance can be done by focusing on the frequency range above 400 Hz. It is important to state that the voice coil modelled by a resistor and a "traditional inductor" is not sufficient. A better solution is to use a function with a slope of 3dB/oct instead of the 6dB/oct of an inductor. The physical reason for this is the loss in the magnet structure of the loudspeaker [T10]. Often the bass mid-range unit is filtered in the loudspeaker application and a sufficient frequency estimation bandwidth cannot be achieved to estimate the voice coil.

6.4. Identification Signal

The purpose of the identification signal is to cover all frequencies in the important frequency range. In the case of identifying the mechanical and electrical parameters of a typical 6½ inch loudspeaker unit, it is approximately the range from 0-200Hz. The lowest frequency range is used for estimating the voice coil resistance, the DC resistance. A good identification signal is white noise that is frequency limited to the important frequency range [H1, K10, K12].

6.4.1. Music for system identification

Music is very difficult to define. It generally contains some instruments and/or voices. There is a frequency range within which musical signals usually fall but there will be cases where sounds within music not have a very broad frequency range. In general it is only voices that are problematic and a few instruments that only have high frequencies. Electronic music has a wide bandwidth and is generally good for identification. The frequency components outside of audible range are usually filtered away in the production stages. This can be a problem for estimating the voice coil resistance but a small DC offset can resolve this problem.

Several types and styles of music have been tested. The music sample chosen for the tests presented here uses acoustic instruments. This type of music showed the largest spread in the simulation and was therefore chosen for presentation. Figure 6.3 shows the frequency content of the music signal.

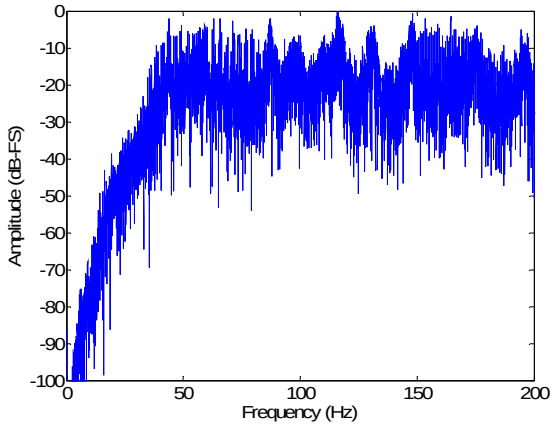

Figure 6.3: Frequency spectra of the first minute of "The Joker" by The Steve Miller Band.

6.5. System Identification Methods

This section offers an introduction to system identification with an adaptive filter and describes the basic principles involved. This knowledge is based on the textbook by Haykin [H1]. In Sections 6.6 and 6.7 two system identification methods are applied to loudspeakers.

6.5.1. Introduction to system identification

System identification using an adaptive filter requires the following steps:

1. Selection of model structure
2. Selection of minimization criteria (cost function)
3. Selection of updating algorithm

Given an unknown dynamic system, the purpose of system identification is to design an adaptive filter that provides an approximation to the system. In the framework of system identification, the loudspeaker is the unknown system (plant), and the target is to determine a set of model parameters describing the plant (loudspeaker).

The first step is the selection of a model structure of the plant. A simple second-order model auto regressive moving average (ARMA) for the loudspeaker was employed to identify the linear mechanical loudspeaker parameters. Application of an IIR structure (recursive/feedback) in adaptive filtering can be troublesome as recursive filters can be unstable. Therefore, in most cases, adaptive filters employ FIR filter structures. A drawback of the FIR filter model is that the coefficients have to be transformed to a parametric model. A FIR and ARMA-based model was investigated and compared for the identification of loudspeakers.

An appropriate broadband input signal u(n) is supplied to the plant and the model. The output of the plant is considered to be the "desired" signal d(n) and the output signal y(n) of the model is the "predicted" signal. The model parameters are adjusted until y(n) is equal to d(n) in the ideal case. The adjusted parameters (after convergence) are the estimated loudspeaker parameters. Normally, the fit will not be exact. The deviation is assessed by defining an "error performance measure" (cost function).
The mean square error is applied as the cost function, defined as:

$$J(\hat{w}) = E\{e^2(n)\} \qquad \textit{Equation 6.8}$$

J()	cost function
e(n)	error signal, defined as: e(n) = d(n) – y(n)
E{}	expected value (mean)
$\hat{w}$	a vector containing the model parameters

The goal is to minimize J($\hat{w}$) using an adaptive updating algorithm, adjusting the model

parameters $\hat{w}$ until the minimum of $J(\hat{w})$ is obtained. The parameter set which corresponds to the minimum of $J(\hat{w})$ is the best possible approximation to the unknown loudspeaker parameters. One approach to finding the minimum of the error-performance surface is through the gradient method.

Application of an adaptive FIR filter and the simple LMS algorithm (stochastic gradient algorithm) would be the most straightforward approach. In this case, the coefficient vector (containing the FIR filter coefficients) is updated sample-by-sample using the updating algorithm given by:

$$\hat{w}(n+1) = \hat{w}(n) + \mu\, \hat{u}(n)\, e(n) \qquad \textit{Equation 6.9}$$

$\hat{w}(n)$	FIR filter coefficients vector
μ	step size parameter
$\hat{u}(n)$	input signal vector,
$e(n)$	error signal

Definition of input signal vector:

$$\hat{u}(n)=[u(n), u(n-1), u(n-2)\ldots u(n-m)]$$

m	the length of the filter, $\hat{w}(n)$.

Generally, the adaptive algorithm consists of two steps; calculation of the error signal and coefficient update. The LMS algorithm was extended to the normalized LMS algorithm to eliminate the influence of the input signal level.

It is necessary to choose between an ARMA-based model or a FIR-based model. Both methods are reviewed and simulated. Section 6.6 reviews the ARMA model and Section 6.7, the FIR model.

6.6. ARMA model (IIR structure)

In the following simulations, the ARMA model is employed to obtain the needed parameters. The specific basic ARMA system identification theory is first explained followed by the necessary extras needed for the implementation.

6.6.1. ARMA system identification theory

According to Haykin [H1], there are two common approaches to the application of adaptive IIR filters for system identification:

1. Output error method
2. Equation error method

6.6.2. Output error method

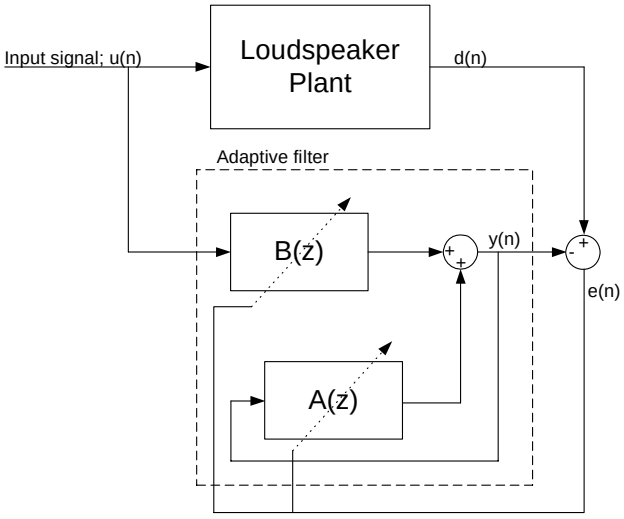

Figure 6.4: Output error method.

In the "output error" method, the "gradient descent algorithm" minimizes the cost function defined in Equation 6.8. The error signal is given by:

$$e(n) = d(n) - y(n) \qquad \textit{Equation 6.10}$$

The predicted signal y(n) (output of the model) is given by:

$$y(n) = \sum_{i=1}^{2} a_i(n)y(n-i) + \sum_{i=0}^{2} b_i(n)u(n-i) \qquad \textit{Equation 6.11}$$

The corresponding transfer function is given by:

$$H(z) = \frac{Y(z)}{U(z)} = \frac{B(z)}{1 - A(z)} \qquad \textit{Equation 6.12}$$

For a second-order system, as presented in Section 6.2:

$$B(n) = b_o(n) + b_1(n)\, z^{-1} + b_2(n) z^{-2} \qquad \textit{Equation 6.13}$$
$$A(n) = a_1(n)\, z^{-1} + a_2(n) z^{-2}$$

z^{-p} represents a delay of p samples.

A major problem with this method is that the minimization process can be trapped at a local minimum, resulting in erroneous values of the model parameters. This problem can be alleviated by constraining the parameter range to the proper vicinity of the nominal values of the loudspeaker parameters (using a priori information about the parameter values). An advantage to this is that the estimated parameters are unbiased (if the global minimum is found).

6.6.3. Equation error method

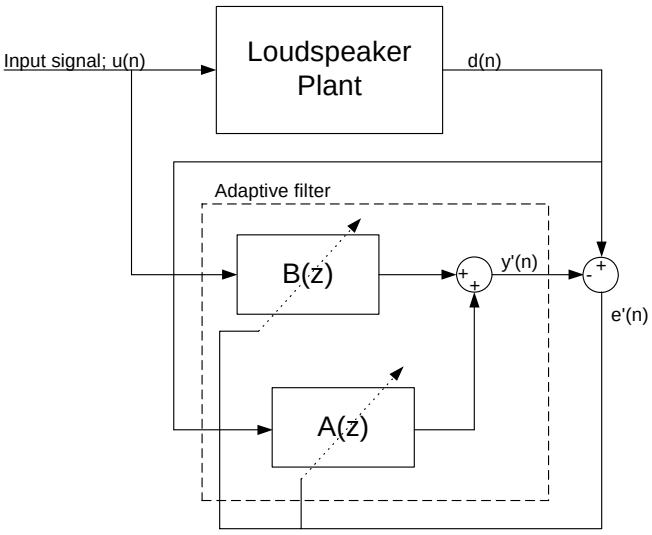

Figure 6.5: Equation error method.

The "equation error" approach has the advantage of having a linear minimization process [H1], which guarantees a global minimum during the minimization process. The "equation error" method is based on a modified predicted output given by:

$$y'(n) = \sum_{i=1}^{2} a_i(n) d(n-i) + \sum_{i=0}^{2} b_i(n) u(n-i) \qquad \textit{Equation 6.14}$$

where the second term on the left side of the equation is modified by "replacing" y(n) with the desired signal d(n), a kind of "supervised leaning". A disadvantage of the method is that the estimated parameters are "biased" or "have an offset", thereby reducing the precision in the system identification.

6.6.4. Stability check

The stability check is necessary for the IIR-based systems. To ensure stability it is made according to Figure 6.6 which shows the parameter room for stable IIR coefficients. The marked area in the figure is the complex pole pairs [H1, page 59]. Stability check, poles inside the unity circle of Equations 6.12 and 6.13:

$$1 \geq a_1 + a_2$$
$$-1 \geq a_1 - a_2$$
$$-1 \leq a_2 \leq 1$$

Equation 6.15

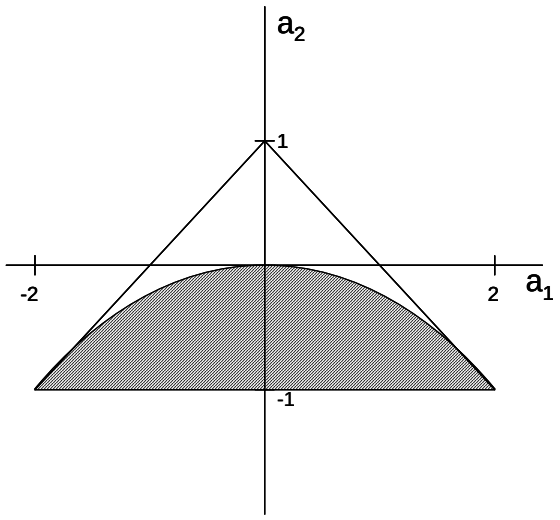

Figure 6.6: Stability region of AR parameters a_1 and a_2.

Two methods for stability handling are investigated. In the first method (the simplest), updating is omitted if a pole is outside of the unit circle. This ensures stability but the coefficients will, in many cases, not converge to the correct values (critical for pole positions close to the unit circle). In the second method, a pole outside of the unit circle is reflected to the reciprocal position (new-radius = 1/ (actual-radius). The second method works much better and convergence is obtained smoothly and without problems.

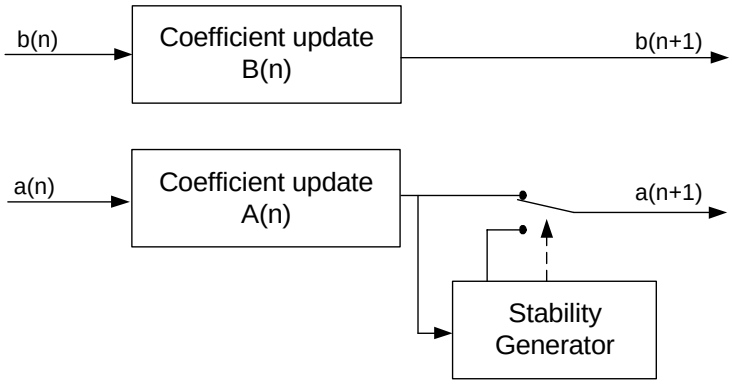

Figure 6.7: Stability check & coefficient updating.

6.6.5. Step size parameter and sampling frequency

Before implementation, the sampling frequency and step size have to be selected. The sampling frequency must be sufficiently high that the high frequency warping occurring in the bilinear transformation does not influence the model. In the present case, the loudspeaker unit has a resonance frequency of 50Hz and, for identification of the linear mechanical loudspeaker parameters, frequencies up to around 200Hz are needed according to Figure 6.2. The textbook "Digital Control of Dynamic Systems" [F1] recommends a 20 to 40 times higher sampling frequency. In the present simulations 5 kHz was employed.

The step size has a trade-off; if too small, the system will converge slowly, if too large, the system will not converge and/or come into the unstable region. The step size depends on the system identification method and pole placement of the physical systems [P21].

6.6.6. Parameter space

In the application of this research, the target is to take care of drift and production spread of loudspeaker units, more detail can be found in [P22] or Chapter 3. Using the information about the spread of the loudspeaker parameters, the parameters of the ARMA model were limited to an area, see Figure 6.8. The figure shows the parameter space of the IIR filter coefficients. The spread is set to +-20% of the resonance frequency and the damping factor.

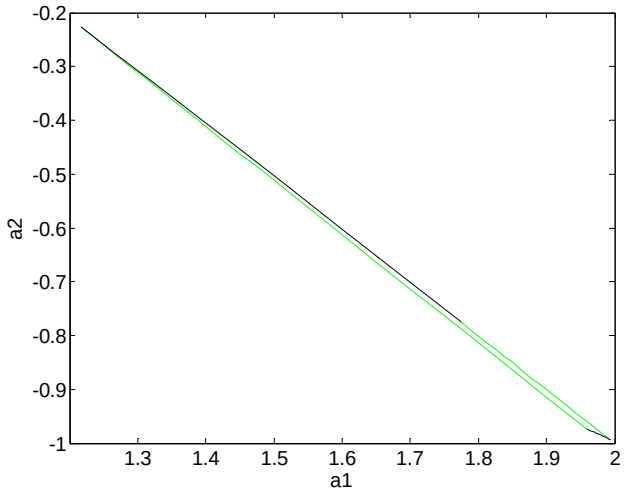

Figure 6.8: The parameter range of the IIR filter in the tested loudspeaker, +-20% of the resonance frequency and damping factor. The sampling frequency is 5 kHz.

The parameter space can be used to minimize the number of local errors by guiding the algorithm in of the parameter space.

6.6.7. Error surface of the ARMA model structure

The error surface structure is very important as it determines the way that the coefficients are adjusted in the target. Bright [B12] found that the coefficients can take a "detour" instead of the direct way. A further problem is that the residual error is small far away from the correct setting and large around the error minimum [B12]. This is problematic because, in order to obtain a fast convergence, the steps must be larger when far away and small when close to the local errors.

However, improvements can be made. Bright proposed and tested several methods [B12]. Threshold on the conversion parameters can be used. Bright found the useful threshold for updating the conversion parameters through the study of the error surface. Bright tested square root mapping for scaling of the gradient and achieved a significant improvement in the conversion speed.

Even though these improvements can probably be made to the error surface, the basic gradient surface structure is still very difficult to overcome and this can be a major reason for using a different technique.

6.6.8. Simulation implementation of ARMA model

The simulation models were implemented in a Simulink/Matlab environment. The plant used was a continuous loudspeaker model with linear loudspeaker parameters and a voice coil induction that had been set to zero. The input signal was white noise.
Used loudspeaker parameters:

Parameter	Size
Voice coil resistance, R_e	2.30 Ω
Voice coil inductor, L_e	0 mH
Force factor, Bl	2.0 N/A
Moving mass, m_m	12.4 g
Suspension compliance, c_m	1.19 mm/N
Mechanical resistance, r_m	1.73 kg/s

Table 6.1: Data of the simulated linear loudspeaker 6½" unit.

This loudspeaker was under damped (ξ=0.52) and the poles were relatively close to the unit circle. The low damping made it more difficult for the ARMA model to converge.

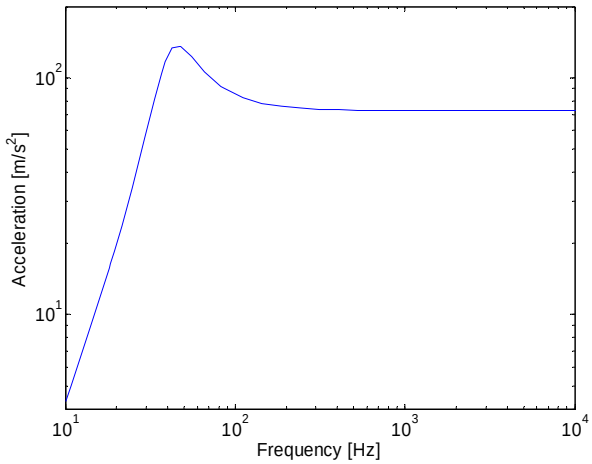

Figure 6.9: The frequency response of the loudspeaker used for the ARMA model. The damping factor is 0.52.

6.6.9. Output error method

When an over-damped system is used, the correct parameters can be found. When the system is less damped and the poles are closer to the unit circuit, the output error method fails; the algorithm becomes trapped in a local minimum. The local minimum can occur within the possible parameter space (Figure 6.8) and therefore may not be corrected using the priori knowledge of the system. According to Haykin [H1], local minima are one of the disadvantages of the output error method. The output error method can be trapped in a local minimum even when starting with the correct parameters.

6.6.10. Equation error method

According to Bright [B10], the equation error method is more reliable than the output error method. The simulation results obtained though this work found the equation error method to be much more advantageous. The under-damped systems, which could not be identified with the output error method, could now be handled. The stability check was only enabled in a few cases. The convergence time was also shorter.

When the simulation was started, the white noise generator was also started; this applies as a step inputs to the loudspeaker. When the system is started with the correct parameters the obtained parameters will become misadjusted at the start of the simulation and then move back to the correct value due to the applied step response. Figures 6.11 and 6.12 show this case. Figure 6.10 shows the error between the plant and the system identification model. Figure 6.11 is the estimated resonance frequency and Figure 6.12 is the estimated damping.

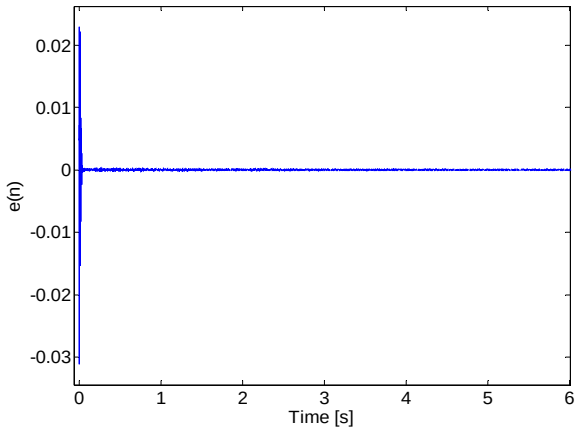

Figure 6.10: Error signal obtained from the equation error method, started with the correct parameters. (F_s=5kHz)

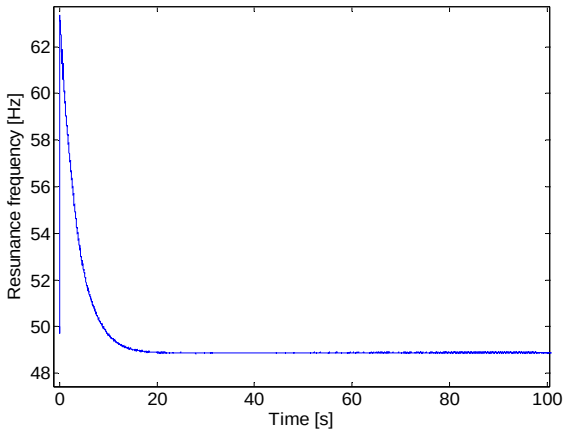

Figure 6.11: Resonance frequency factor estimates using the equation error method, started with the correct parameters. (f_n=50Hz)

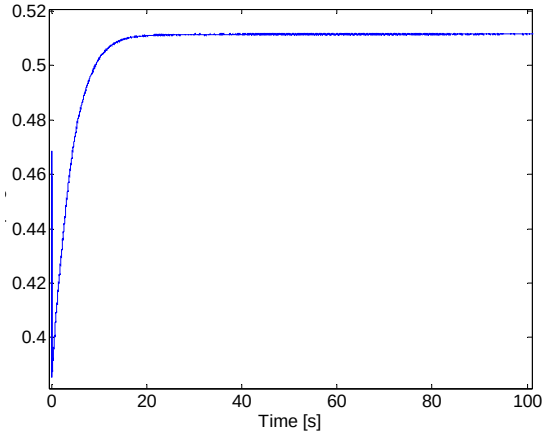

Figure 6.12: Damping factor estimates using the equation error method, started with the correct parameters. (ξ =0.52)

The simulation estimate had an offset of about 2% for the resonance frequency and correspondingly for the damping factor. The convergence to the final value from about 4%

error and lower was very slow and it is believed that better results can be obtained, see Bright [B12].

When the sampling frequency is too low, the error signal will not converge and the estimated parameters will drift. If the step size chosen is too large, the error signal will again fail to converge. By using too small a step size, the convergence time of the parameters can be very long.

6.6.11. Model errors

The ARMA equation error method provides useful results as long as the model used matches the identified plant. When a model difference occurs, for example if the voice coil induction is included, the system does not converge correctly. The voice coil inductance can be filtered away as proposed in Section 6.3.3 however, even if most of the voice coil induction is filtered away, there will still be small differences between the model and the plant and this increases the minimum error signal.

6.6.12. Identification signal for ARMA system identification

When the identification signal is changed from white noise to music signals the conversion speed decreases significant. The ARMA equation error method is sensitive to the distribution of the input signal due to the inconvenient error surface. Bright found that music signals and speech can have long conversion times and that the problem relates to the error surface where the parameters will easily make a long detour from the current setting to the optimal setting [B12]. The parameters will be misadjusted before they approach the optimal setting.

6.7. FIR structure

6.7.1. FIR system identification theory

The FIR filter structure is an approximation to the loudspeaker impulse response with an all zero structure. When the optimal settings are found, the FIR filter coefficients are "equal to" the truncated loudspeakers impulse response.

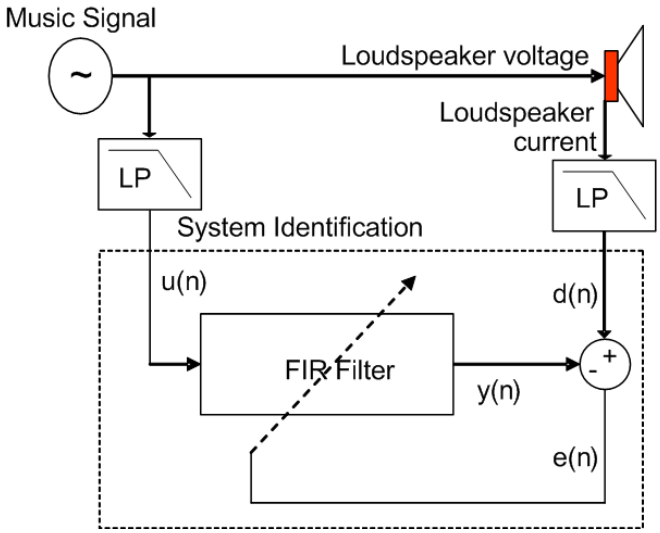

Figure 6.13: Principle of the FIR filter- based normalized LMS identification system.

$$y(n) = \hat{w}(n)\, u(n) \qquad \textit{Equation 6.16}$$

$\hat{w}(n)$ a vector with the FIR filter coefficients

The FIR filter coefficient update is relatively simple and has been shown in Section 6.5. The LMS update algorithm is repeated in Equation 6.17.

$$\hat{w}(n+1) = \hat{w}(n) + \mu\, \hat{u}(n)\, e(n) \qquad \textit{Equation 6.17}$$

6.7.2. Filter length

There are two considerations regarding filter length and sampling frequency; the frequency resolution of the extracted data and the time window of the impulse response.

The length of the FIR filter has to be such that it is able to store the important part of the loudspeaker impulse response. The impulse response of the 6½ inch loudspeaker with a resonance frequency of 50Hz is about 50ms.

The impulse response found can be converted to a frequency response using DFT and the resolution is related to the number of points in the DFT and the sampling frequency, according to Equation 6.18 [P10].

$$F_{\text{resolution}} = \frac{F_s}{M} \qquad \textit{Equation 6.18}$$

$F_{\text{resolution}}$	the frequency resolution
F_s	the sampling frequency
M	length of FIR filter

The basic optimization of the used system identification algorithms was performed with a linear loudspeaker model. A good trade-off for frequency resolution, to avoid the test signal having a high influence at specific frequencies during musical input, was to use a sampling frequency of 4kHz and a filter length of M = 200, giving a frequency resolution of 20Hz; a relative low resolution.

6.7.3. Translating the FIR filter coefficients

The drawback of the FIR filter model is the non-physical representation of the filter coefficients. There are basically two ways of translating the FIR filter coefficients into the linear loudspeaker parameters. One must either recalculate the FIR model into an ARMA model, in time domain, or interpret the FIR filter coefficients in the frequency domain.

In time domain; the FIR filter coefficients are converted into an ARMA model, Equation 6.3. The ARMA model can be converted, as shown in Equations 6.4, 6.5 and 6.6, into the physical parameters. The FIR filter coefficients can be converted into an ARMA model with the "Prony" algorithm. The inputs of the Prony function is the FIR filter coefficients and the order of the transfer function, in this case this was two. The algorithm is based on the Least Mean Square; a detailed description can be found in [P30].

The frequency domain response was obtained by an FFT of the impulse response. The admittance in the frequency domain had a clear dip around the bass resonance that was relatively easy to detect. There are several known methods for estimating the resonance

frequency and the damping factor. Basically, the magnitude of the loudspeaker impedance has to be fitted. In this study only a few points were used. The resonance frequency and the mechanical damping factor can be calculated from Equations 6.19 and 6.20. f_1 and f_2 are the frequencies where the admittance is 6dB up after and before the bass resonance.

$$f_n = \sqrt{f_1 \cdot f_2} \qquad \textit{Equation 6.19}$$

$$\varsigma = \frac{f_1 - f_2}{2 \cdot f_n} \qquad \textit{Equation 6.20}$$

f_n the natural frequency of the loudspeaker
f_1 the frequency where the admittance is 6dB up, after f_n
f_2 the frequency where the admittance is 6dB up, before f_n
ς mechanical damping factor ($1/Q_{ms}$)

6.7.4. Error surface of FIR model structure and step size

The LMS error surface is the major advantage of the FIR structure. The surface is uni-modal and the gradient is large far away from the minimum and becomes smaller closer to it. There is no need to check for local minimums or instability as with the ARMA models. The FIR model is, due to the filter coefficients, not directly translatable and this makes it very difficult to correct the algorithm or bias the coefficients.

The FIR filter itself does not have any feedback, but the adaptive coefficient adjustment has the potential to destabilise the system. The step size had to be chosen in a range where the adaptive system was stable and the convergence time was not too long. There are different methods to find the value of the step size parameter; it was decided to look at the filter coefficients. The end of the filter coefficients, or the tail of the impulse response, begins to oscillate when the step size is getting close to the stability margin.

The step size is adjusted by trial and error as it is relatively easy to find a useful range and the chosen step size is in the centre of this range (0.001).

6.7.5. Simulation implementation of FIR model

The system identification algorithm was implemented in Matlab and the loudspeaker model was implemented in Simulink. The system identification code takes the data from the model or from a measurement of a physical loudspeaker.

The 6½ inch loudspeaker unit that previously has been investigated is used (see Appendix 2). The all zero implementation was not critically sensitive to an under-damped loudspeaker and so a loudspeaker that was physically available was used as an example for testing the performance of the FIR algorithm.

6.7.6. Optimisation of settings

The system identification algorithm was optimised with a linear loudspeaker model. It was then tested with a nonlinear model and finally it was used with the real loudspeaker in a measurement set-up. All stages were investigated with white noise and music as the input signals.

The loudspeaker data for the FIR system identification was filtered with a second-order low-pass filter with a cut-off frequency of 400 Hz and a damping factor of 0.7. The filter cut-off frequency was chosen such that the voice coil induction influence is filtered out (see also Section 6.3.3).

6.7.7. FIR system identification simulation

The algorithm was first tested with a linear loudspeaker model with the voice coil inductance included and then, using a nonlinear simulation model. The FIR filter coefficients were initialized at zero and were fairly well-tuned within 10 seconds; the error signal is shown in Figure 6.14. The identification was run for one minute before the magnitude and phase of the admittance was derived (Figures 6.15 and 6.16). For comparison, the bode plot of the loudspeaker model is also plotted on Figures 6.15 and 6.16.

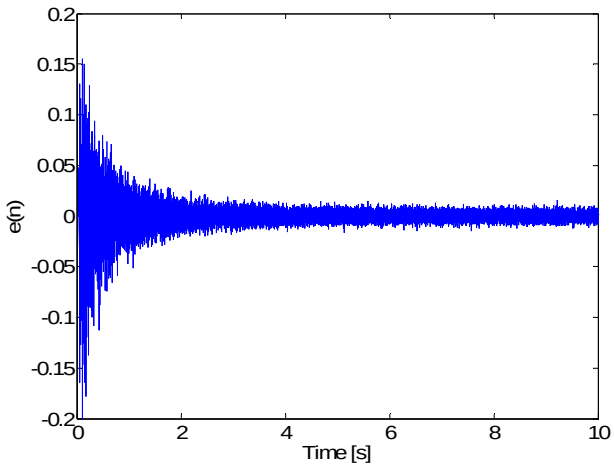

Figure 6.14: The error signal from the MA model.

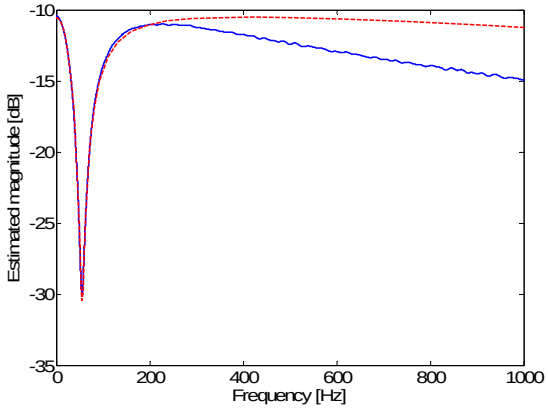

Figure 6.15: Estimated magnitude of the linear loudspeaker model using white noise (___), and bode plot of linear loudspeaker (---). Estimated bass resonance is 55.2 Hz and damping factor ς=0.143. R_e=3.32Ω

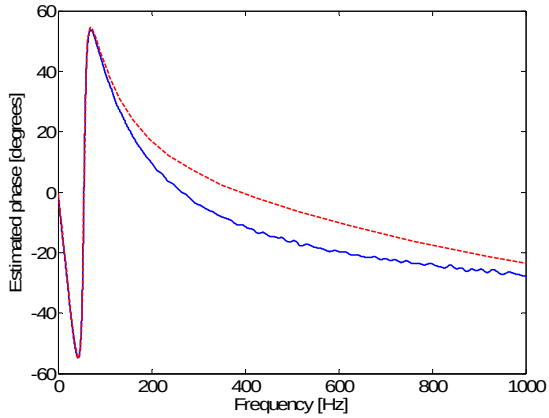

Figure 6.16: Estimated phase of the linear loudspeaker model using white noise (___), and bode plot of linear loudspeaker (---). Estimated bass resonance is 55.2 Hz and a damping factor ς=0.143. R_e=3.32Ω

Parameter	Loudspeaker	Estimated
f_n	55.5 Hz	55.2Hz
ς	0.135	0.143
R_e	3.36Ω	3.32Ω

Table 6.2: System identified data using linear model, first column contains the real data.

Table 6.2 shows the data obtained using system identification and the parameters from the loudspeaker. There was an error of 0.5% of the resonance frequency, 1.2% of the voice coil resistance and 5.9% of the damping. Except for the damping, the accuracy was acceptable. The error of the damping was due to the simplified determination of the damping factor. A better fitting function could be implemented.

The tests with a nonlinear model describe the behaviour of the linear system identification system and its dependency of signal level. According to Knudsen [K11], the identified parameters will have a small offset and the algorithm will not be driven into an unknown state. The test results are summarized in Table 6.3 and the magnitude of admittance for the maximally tested displacement level is shown in Figures 6.17 and 6.18.

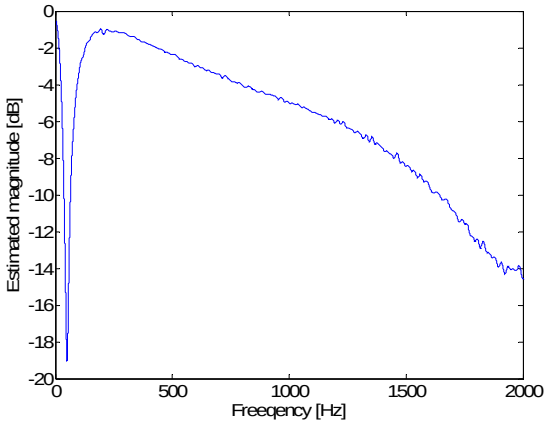

Figure 6.17: Estimated magnitude of the non-linear loudspeaker model using white noise. Estimated bass resonance is 48.0 Hz and damping factor; ς=0.159. R_e=3.35Ω

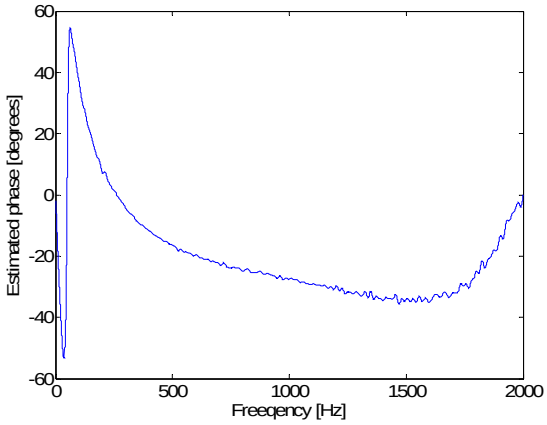

Figure 6.18: Estimated phase of the non-linear loudspeaker model using white noise. Estimated bass resonance is 48.0 Hz and damping factor; ς=0.159. R_e=3.35Ω

Table 6.3 shows three simulations with different input levels, 100mVrms, 1Vrms and 10Vrms. This corresponds to the displacements 23µm, 230µm and 2,3mm by a 100Hz sinusoidal.

Parameter	f_n	ς	R_e
Loudspeaker	55.5Hz	0.135	3.36Ω
Loudspeaker, c_m=c_m(x=0)	48.1Hz	0.156	3.36Ω
Estimated, 23µm@100Hz	48.0Hz	0.158	3.35Ω
Estimated, 230µm@100Hz	48.0Hz	0.159	3.33Ω
Estimated, 2,3mm@100Hz	50.0Hz	0.131	3.34Ω

Table 6.3: System identified parameters of the non-linear mode; first row is the linear lumped data, second row, a linear loudspeaker with the compliance at zero displacement from the non-linear measurement, and the subsequent rows, the non-linear simulations with the maximum displacement level at 100 Hz.

Due to the displacement nonlinearity of the suspension compliance, increasing displacements causes compliance to become stiffer and this leads to an increase in the resonance frequency by increasing displacements, as shown at the maximum level in Table 6.3. The first two rows are the data from the loudspeaker model. The first "loudspeaker" is with the measured parameters based on the linear model and the second, "loudspeaker, c_m=c_m(x=0)", has non-linear functions with a very small displacement. The difference in resonance frequency from 48,1Hz to 55.5Hz is due to the suspension stiffness at the rest position, when the loudspeaker has a large excitation (see Section 2.3.3). The estimated data are close to the model at 48.1Hz. Increasing the displacement level increases the resonance frequency as expected.

6.7.8. System identification applied to loudspeaker unit

The tests were then repeated using measurement data of voltage and current from the 6½ inch loudspeaker unit that had been sampled into the computer with a USB soundcard. The current measurement was made with a 25mΩ resistance in series with the loudspeaker. The current measurement was amplified with an instrumentation amplifier [S50].

The used amplifier in the setup had a DC-filter that dampened the low frequencies in the measurements, influencing the estimate of the voice coil resistance.

Table 6.4 shows three different levels of white noise in the loudspeaker.

Parameter	f_n	ς	R_e
Loudspeaker	55.5 Hz	0.135	3.36 Ω
Estimated, 100mV_{rms}	54.9Hz	0.138	3.31Ω
Estimated, 1V_{rms}	53.6Hz	0.158	3.29Ω
Estimated, 10V_{rms}	51.6Hz	0.228	4.56Ω

Table 6.4: System identified parameters for loudspeaker; first row is the linear data from the Klippel Analyser followed by estimates of the measured data with different input levels.

The measured resonance frequency was lower than that measured previously, but this error was assumed to be caused by parameter drift which would correspond to a 3 to 4°C change (see Table 3.2). In the other two measurements, the displacement was in a range where the assumption of using a linear loudspeaker model is invalid. Here the results could be compared with the estimation of the nonlinear loudspeaker model. The resonance frequency decreased rather than increasing as expected. Heating of the loudspeaker suspension makes it softer and this could have been the cause [P24]. The heating of the loudspeaker suspension was not included in the simulation model of the nonlinear system identification estimation test. The resonance frequency had decreased 6% (Table 6.4); this was reflected in a 12% change of suspension compliance. In Section 2.3.3, a change of 25% in suspension compliance was seen for this loudspeaker unit. This would mask the effect of the nonlinear suspension compliance behaviour in this test.

6.7.9. Music for identification

The linear loudspeaker model was tested with the chosen music signal and then this was applied to the loudspeaker.

The effect of the musical input on the magnitude and phase of the linear loudspeaker model is shown in Figure 6.19 and 6.20, and in Table 6.5.

Parameter	f_n	ς	R_e
Loudspeaker	55.5Hz	0.135	3.36Ω
Steve Miller Band	55.4Hz	0.130	3.37Ω

Table 6.5: System identified parameters of linear model with music.

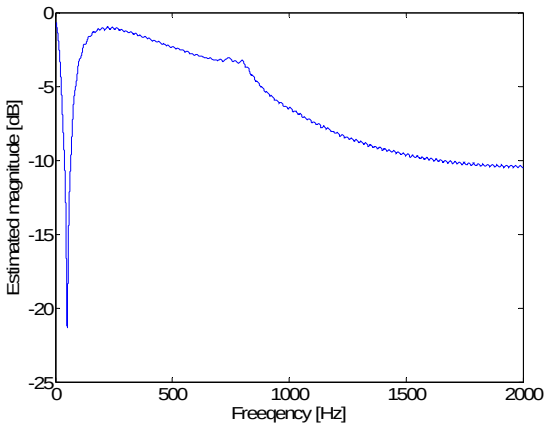

Figure 6.19: Estimated magnitude of the loudspeaker with "Steve Miller Band" "The Joker" after the first minute.

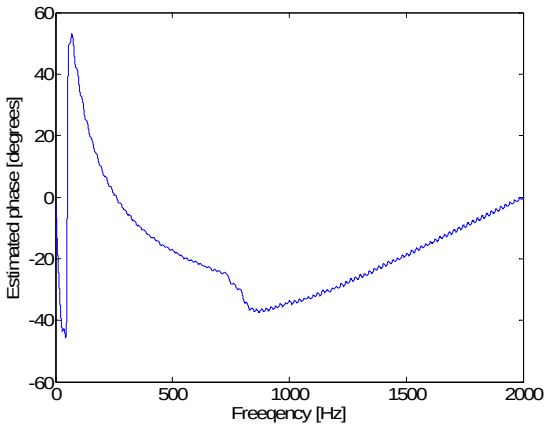

Figure 6.20: Estimated phase of the loudspeaker with "Steve Miller Band" "The Joker" after the first minute.

The estimated parameters were close to the actual loudspeaker parameters. On the magnitude and phase plot, there was an unknown discontinuity at 700Hz. It can be assumed that a part of the musical signal influences this area.

The same music sample was applied to the loudspeaker unit and identified according to Table 6.6.

Parameter	f_n	ς	R_e
Loudspeaker	55.5 Hz	0.135	3.36 Ω
Estimated, 100mV_{rms}	54.6Hz	0.153	4.30Ω
Estimated, 1V_{rms}	53.7Hz	0.163	4.50Ω
Estimated, 10V_{rms}	49.7Hz	0.234	4.78Ω

Table 6.6: Loudspeaker unit parameters system identified using Steve Miller Band; 'The Joker'.

The tested music provided good results similar to the estimated resonance frequency obtained using white noise. The damping factor results had a higher spread, but it is uncertain whether this was due to an estimation error or to the actual behaviour of the loudspeaker with this test signal. The voice coil resistance was more difficult to estimate with music as it does not usually contain frequencies less than 20Hz. The unknown discontinuity from the simulated result is not present in the estimated data from the physical setup, which is shown for the 10V setting only in Figure 6.21. The low frequency error that caused the wrong voice coil resistance estimate is clearly shown. This may have been caused by a low signal-to-noise ratio caused by the small low frequency content and the DC filter in the amplifier.

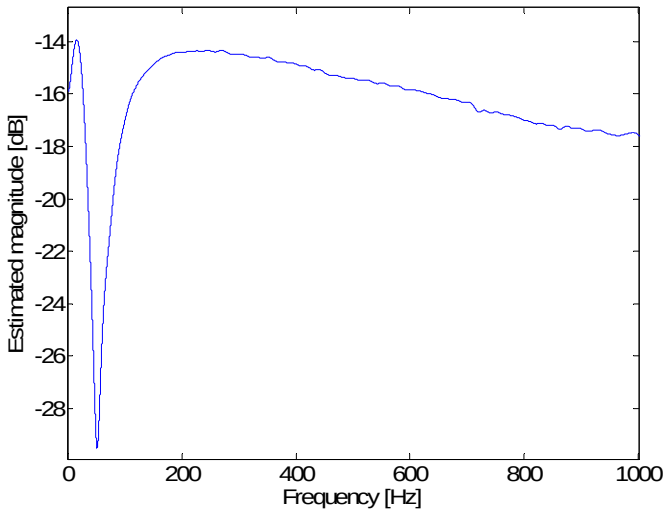

Figure 6.21: Estimated magnitude of the loudspeaker with "Steve Miller Band" "The Joker" after the first minute. 10V loudspeaker measurement.

Different music samples have been used to test the estimated values. The performance is very similar with a relatively small spread and the music result shown is among the most problematic that has been tested. When identifying the linear loudspeaker parameters, there is an uncertainty caused by the signal dependency of the loudspeaker parameters, and the parameters generally drift. This led to the decision not to present more music data or make a spread analysis.

6.8. Discussion of System Identification

The investigation of system identification in this project was performed in order to track the linear parameter drift in the context of implementing a nonlinear distortion cancellation. The intention was to use the estimated linear loudspeaker parameters, together with the pre-measured non-linear functions, $Bl(x)$, $c_m(x)$ and $L_e(x)$. In the investigation of the suspension compliance presented in Section 2.3.3, it was unfortunately found that the nonlinear suspensions function is unstable, $c_m(x)$. A nonlinear estimation needs to be investigated. The suspension has its primary influence around and under the resonance frequency and therefore simple adjustments may be sufficient to resolve this problem.

The outcome of the investigation of online system identification of linear loudspeaker parameters has shown that a relatively simple FIR-based NLMS system identification algorithm achieves good results. The important benefits of the FIR-based system identification compared with an IIR based, ARMA model, is the more beneficial error surface (quadratic) for the FIR-based model, which is less sensitive to the identification signal and model errors and has a faster convergence time. The objective of this research was to find the linear loudspeaker parameters using a music signal and this was achieved successfully.

It is important to use a sufficient frequency resolution to estimate the impedance of the loudspeaker. As a compromise the frequency resolution was chosen to 20 Hz, not in a range where characteristics of the music signal can be estimated, and the resonance frequency can still be found with an accuracy of approximately 0.5 Hz.

Before the algorithm can be used in a product, several extra functions need to be developed, such as a system that limits the range in which the identification algorithm is used. The functions shall determine when a music signal is useful for identification and when the loudspeaker is operating in a “linear” range.

The system requires a better current measurement than is usually available in a power amplifier, where it usually is used for short circuit protection. Identifying the linear parameters will, through the voice coil resistance change, be able to estimate the voice coil temperature [C10]. This can be utilised in active loudspeaker protection to avoid overheating. Protecting the loudspeaker from overheating allows the design margin for the maximum power handling to be reduced, giving an opportunity to improve efficiency with a thinner and lighter voice coil (see Chapter 4).

6.9. Conclusion of System Identification

The linear loudspeaker parameters can be found using musical signal with a FIR-based NLMS system identification algorithm, using the loudspeaker current and voltage. Some add-on's in relation to signal detection and the conversion of the FIR filter coefficients to physical parameters need to be improved (especially an improved algorithm to determination of the damping factor). The tests were performed on a 6½ inch loudspeaker unit with a resonance frequency of 50Hz and with an impulse response, with significant data within approximately 50ms. The used FIR filter was 200 taps long and operated with a sampling frequency of 4 kHz (25mS length), providing 20Hz frequency resolution. The step size shall be around 0.001. It was important to apply a pre-filter to eliminate the loudspeakers high frequency response and thereby focus the algorithm on the mechanical resonance. In this case, the influence of the voice coil inductance was suppressed by filtering frequencies of about 400 Hz with a second-order filter.

The ARMA, IIR-based system identification, is a solution with which the conversion to physical loudspeaker parameters can easily be made. This method is sensitive to the identification signal and model errors, making it very difficult to use for this online application.

Error Correction of Loudspeakers,

Chapter 7

7. Digital Loudspeaker Array

This thesis research is based on the analysis of one dimensional errors in loudspeaker units and signal processing for compensating one dimensional distortion sources. DLA (Digital loudspeaker arrays) have multiple inputs, which do not limit the signal processing to one dimension. Previous studies of DLA have reviewed audio performance; therefore, in connection with this project, the efficiency of DLA analysed is based on an existing DLA setup.

The study of digital loudspeaker arrays was made during a visiting period to the Audio Group led by John Mourjopoulos, at the University of Patras, Greece. The total study is presented in the paper "Performance analysis of digital loudspeaker arrays" [P25]. In this thesis, the focus is on the driver properties of DLA, and physical limitations that are introduced by the transducers. The chapter begins with a basic introduction to DLAs and future loudspeaker possibilities.

7.1. Future Loudspeaker Possibilities

The concept of loudspeakers has not changed significantly for many years [B2]. This thesis work has reviewed and investigated benefits that can be obtained by applying digital signal processing and redesigning the loudspeaker unit. The author believes that these techniques, and improved versions of it, together with acoustical design, will find major impact in the coming decades. Most of this thesis work has focused on options that, today, can be implemented with applying signal processing; however, which options and needs will the next generation of loudspeakers have?

Smaller size, high quality loudspeaker are already needed today. This will include a benefit if there is no need for a high power amplifier.

On a single sound device, is it useful to have multi signal processing for sound effects as spatial placement.

One solution that might have possibilities for resolving these needs is a loudspeaker array with many small transducers. If the transducers are driven with a digital signal, then the implementation of the drivers for the transducers is very simple and efficient to implement.

Digital loudspeakers have previously been investigated in relation to acoustic properties, but have not been reviewed in terms of efficiency and loudspeaker/transducers conditions, which have importance for investigating the possibilities for digital loudspeaker arrays (DLA).

The work on digital loudspeaker arrays investigates the efficiency of the digital loudspeaker and the transducer properties with tools previously used in this work. This will try to answer the question: Should loudspeakers be made digital?

This chapter starts with a short introduction to the basic theory and some techniques of DLA. It is followed by a small signal analysis of the signals that the loudspeakers in the array have to conduct. Finally, the driver condition and power consumption are investigated.

7.2. Direct Acoustic Emission of Digital Signals

The concept of DLA is that a digital signal is emitted directly as pulses and then it reconstructs the analog signal in air. Alternatively, DLA acts as an acoustic Digital-to-Analogue Converter (DAC) on a digital input signal consisting of N bits. In practice, this *N* bit stream may be generated from over sampling and requantisation of a multibit signal. As it is known, the m^{th} sample instantaneous output of any such DAC would be:

$$A_m = b_{1,m} \cdot 2^0 + b_{2,m} \cdot 2^1 + \ldots + b_{N,m} \cdot 2^{N-1} \qquad \textit{Equation 7.1}$$

Assuming that the maximum value of $b_{n,m}$ is 1, then A_m expresses the number of activated elements.

Digital loudspeaker arrays currently are based on small moving-coil speakers to reconstruct acoustic signals out of binary audio streams. Two methods for transforming the digital PCM sound signal to a digital signal for the DLA are reviewed in the following section; Bit Assignments.

7.2.1. Bit Assignments

The bit assignment is a different representation of the digital signal for driving the DLA. Two methods are presented here, the bit grouped assignment used in previous studies [M10, T20], and an alternative version tested in the simulation doing the research: the bit summed [K30].

The conversion from a PCM word to the bit group assignment is shown in Figure 7.1. The individual bits of the PCM word are sent directly to the DLA where there are N groups corresponding to the number of bits in the PCM word. The significance of the bits are represented by the number of transducers in each group, group one has 1 transducer, group two has 2 transducers, and group three has 4 transducers, etc.

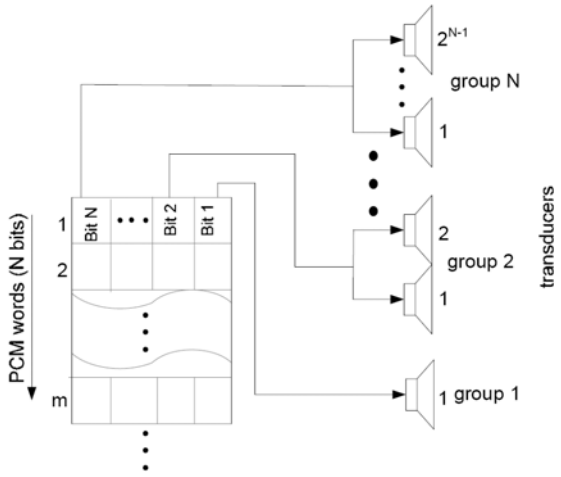

Figure 7.1: Bit grouped PCM word mapping on the bit-grouped array

An example of a 3 bit signed is constructed with a 100Hz sinusoidal signal. In Figure 7.3 a sample of the 3 bit loudspeaker array is shown, where the 100Hz signal uses 4 digital levels.

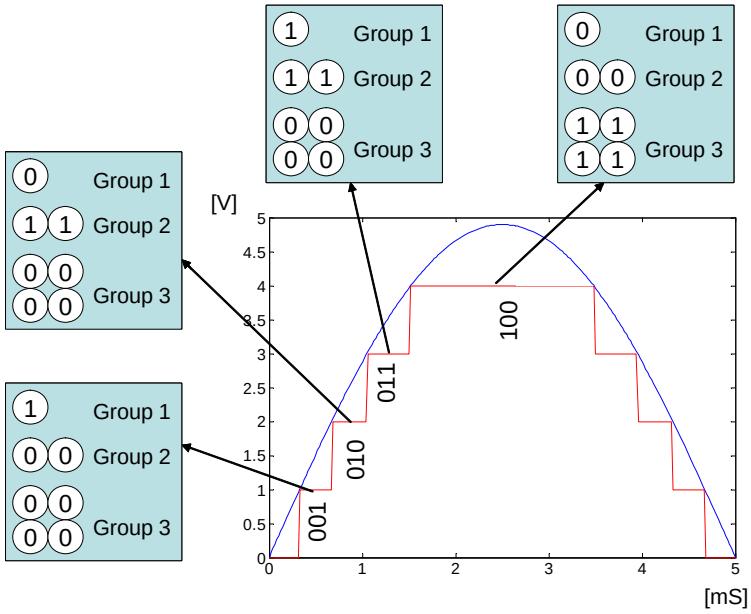

Figure 7.2: Example for N=3-bit sinusoidal binary input signal mapping to DLA bit-grouped assignment.

The bit summed assignment turns the transducers on one by one by an increasing level, Figure 7.3. The number of used transducers with a word length of N bit is the same for the bit grouped and the bit summed assignment. In the case of the bit summed, an increment of one step is equal to one transducer being turned on, see Figure 7.4. In the bit grouped assignment there are different scenarios; an example from digital level 3 to 4 shows that at level 3, group 1 and 2 are on and the others off, see Figure 7.2. At level 4, the 4 transducers in bit group 3 are on and all others off, equivalent to 3 transducers switched off and 4 on in the digital level change from 3 to 4.

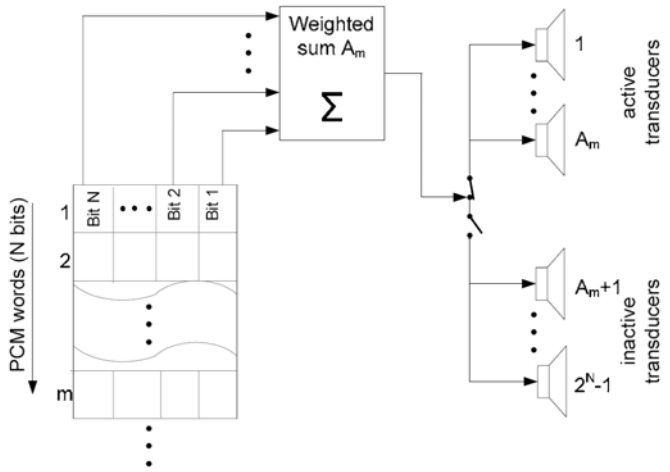

Figure 7.3: Schematic analogy of the bit summed PCM word mapping on the array

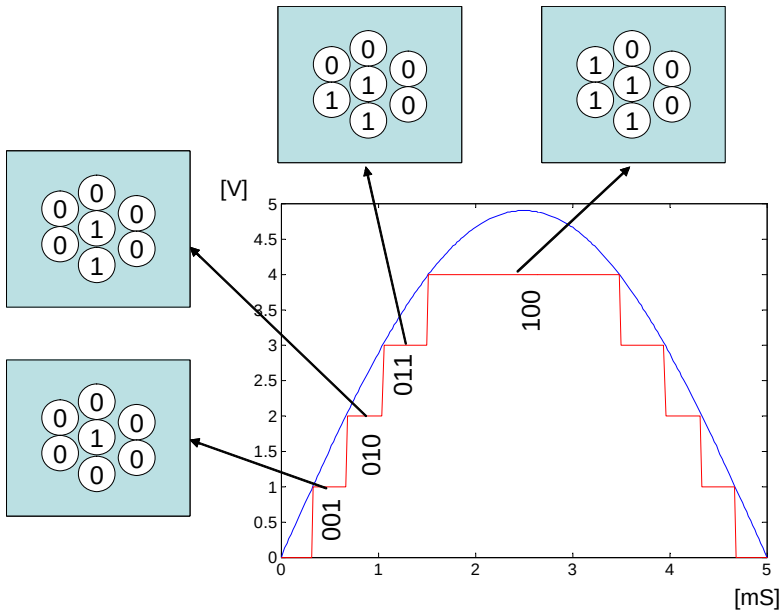

Figure 7.4: example for N=3-bit sinusoidal binary input signal mapping to DLA bit-summed assignment.

7.3. Transducer Signal Analyzes

For the further analysis of the transducer properties of DLA, the signals of the bit grouped and bit summed assignment are analysed in this section.

7.3.1. Bit Grouped

A full scaled, 0dBFs, 100Hz signal is applied and the time signal for the three groups are shown in Figure 7.4 to 7.6, and the corresponding frequency plots are shown in Figure 7.7 to

7.9. The time plots show that the bit group assignment generates many switches of the transducers by the less significant bits. All transducers or bit groups carry the fundamental frequency as well as a broad banded frequency spectrum with many harmonics.

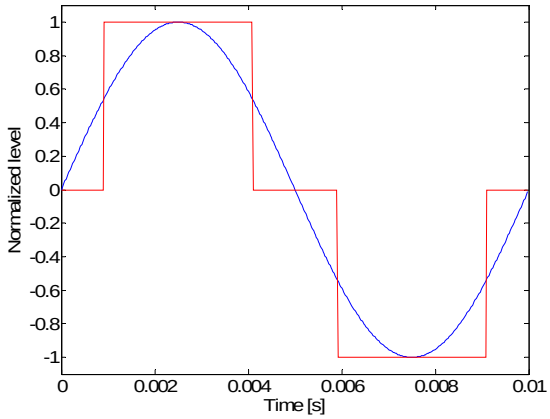

Figure 7.4: Time plot of MSB in a bit group assignment and the input signal. Sinusoidal 100Hz, 0dBFs.

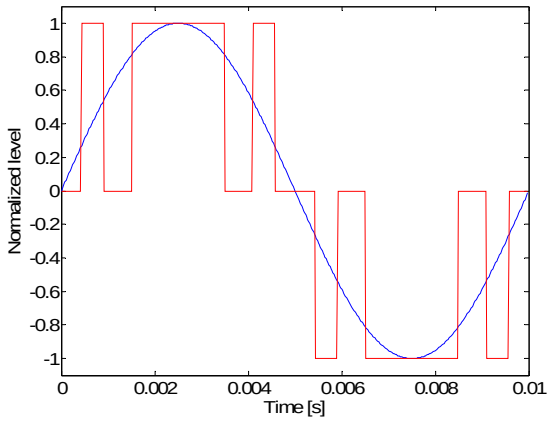

Figure 7.5: Time plot of the second MSB in a bit group assignment and the input signal. Sinusoidal 100Hz, 0dBFs.

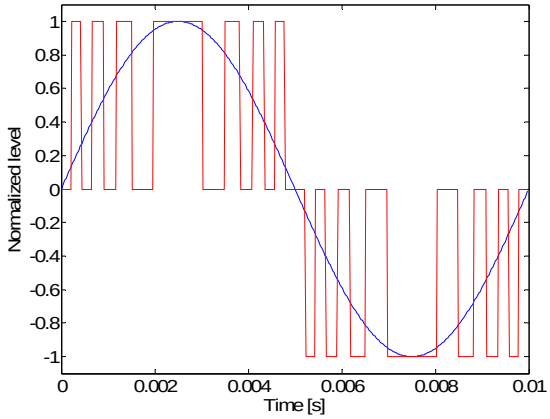

Figure 7.6: Time plot of LSB in a bit group assignment and the input signal. Sinusoidal 100Hz, 0dBFs.

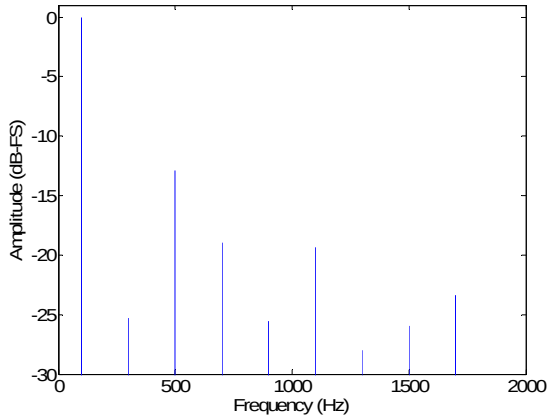

Figure 7.7: Frequency spectra of MSB in a bit group assignment. Sinusoidal 100Hz, 0dBFs.

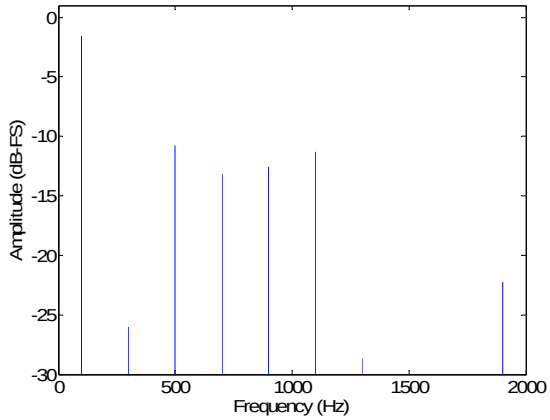

Figure 7.8: Frequency spectra of the second MSB in a bit group assignment. Sinusoidal 100Hz, 0dBFs.

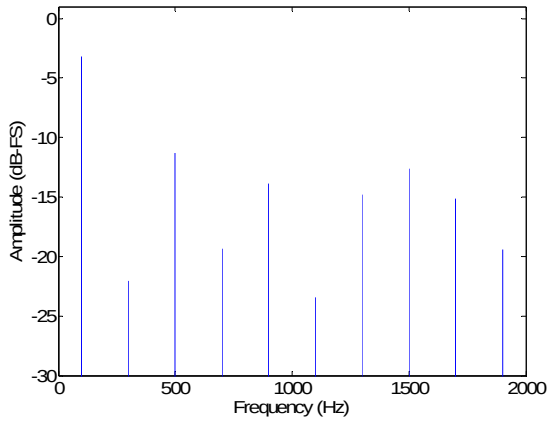

Figure 7.9: Frequency spectra of LSB in a bit group assignment. Sinusoidal 100Hz, 0dBFs.

7.3.2. Bit Summed

The same scenario shown for the bit grouped assignment is shown for the bit summed assignment.

In the 3 bit DLA shown, there are 7 transducers and in the bit summed assignment 7 different signals that are in contrast to 3 signals for the bit grouped assignment. Only the signal for the 1st and the 7th transducer are shown. It can be noticed that each channel only switches on one time in the positive direction and once in the negative direction. This behaviour saves energy for switching losses. A more detailed study on the switching behaviour is found in the results of the simulation study [P25].

All channels also have the fundamental when the bit summed assignment is used, but the level of the fundamental is more than 7 dB down by the 7th channel compared to the 1st channel, Figure 7.13 and 7.14. For the bit grouped assignment, the difference is only 3 dB, and the transducers share the signal more evenly. This difference is very important in relation to the efficiency of the loudspeaker array.

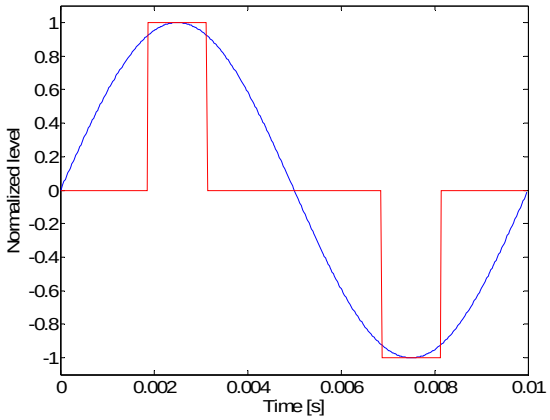

Figure 7.11: Time plot of the 7th channel in a 3 bit one by one assignment and the input signal. Sinusoidal 100Hz, 0dBFs.

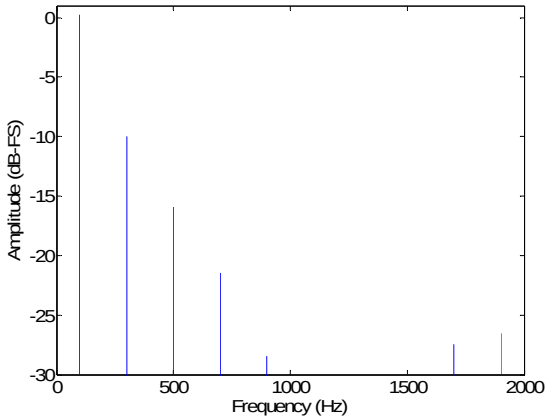

Figure 7.13: Frequency plot of the 7th channel in a 3 bit one by one assignment. Sinusoidal 100Hz, 0dBFs.

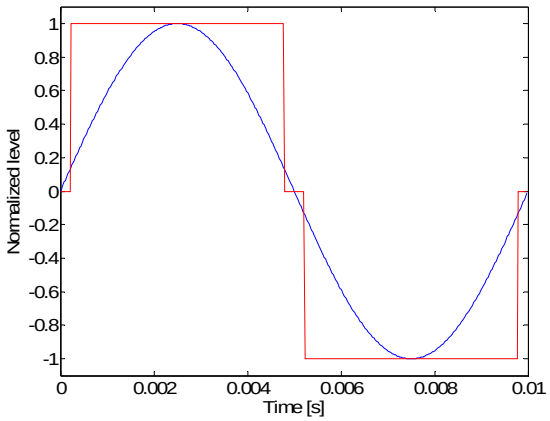

Figure 7.12: Time plot of the 1st channel in a 3 bit one by one assignment and the input signal. Sinusoidal 100Hz, 0dBFs.

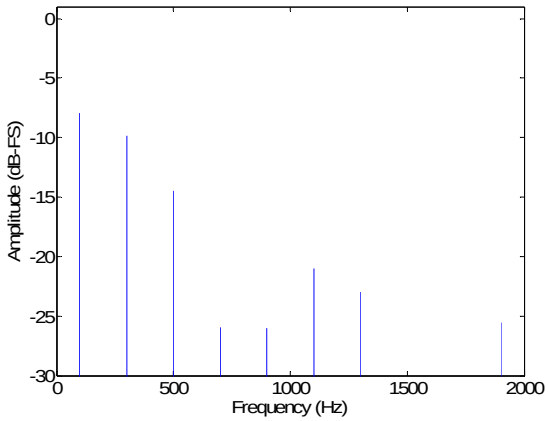

Figure 7.14: Frequency plot of the 1st channel in a 3 bit one by one assignment. Sinusoidal 100Hz, 0dBFs.

It is significant to note that the signal analysis of the individual transducer signals in DLA are broadband due to the requirement for the reconstruction of infinite series of harmonics, which is in contrast to transducers reproducing analogue signals [P25]. Furthermore, the signal assigned to each transducer requires reproduction of all audio frequencies.

7.4. Acoustic Properties of Loudspeaker Arrays

The loudspeakers in the array are seen as many individual point sources emitting sound. Due to all the loudspeakers not being at the same point, off-axis distortion is introduced. Distortion has been one of the main topics in the previous studies of DLA[H20, T20, M10]. Off-axis DLA response will be largely dominated by the out-of-phase summation of individual element contributions, which is due to the different acoustic paths between the receiver and the DLA elements. This emphasizes the need for small transducers for reducing the paths length distortion.

7.5. Today's DLA Implementation

Current state-of-the-art digital loudspeaker research focuses on using conventional moving-coil transducers arranged in arrays [M10]. In the technology of DLA, the limitations are connected to the transducer, which has to carry the full audio frequency and be very small to minimize the out-of-axis acoustic path effect. In the constructed DLA, the frequency range is limited from low frequencies due to the size of the transducers, less than 200Hz. The DLA is implemented with 32 elements of a small loudspeaker unit, the Odyssey 2 from Harman multimedia, specification shown in Table 7.2. This loudspeaker can be tuned to emit sound from 200Hz, which is very low for a transducer of this size; the drawback is low sensitivity.

Moving mass, m_m	0.13g
Suspension compliance, c_m	1.2 mm/N
Mechanical loss, r_m	0.14 kg/s
Voice coil resistance, R_e	3.2 Ω
Voice coil inductions, L_e	38mH
Force factor, Bl	0.9 N/A
Diaphragm Area, S	1.76 cm^2

Table 7.1: Linear loudspeaker parameters of Harman multimedia odyssey 2.

7.6. Sensitivity of Loudspeaker Array

The bit-grouped and bit-summed assignment methods are simulated and compared to an equivalent analogue system. The systems consisted of 32 small multimedia loudspeaker units, Table 7.1. The simulation is implemented from the linear parametric loudspeaker model and driven by a 1 KHz sinusoidal input signal. The same system was used in a DLA form, driven by a PCM sinusoidal signal.

Sensitivity here is defined as the sound pressure calculated at 1m distance for a total DLA using the electrical power of $1W_{rms}$. The sensitivity in a digital transducer array will appear as a function of active elements. Because of the standard 1 Watt driving power it is possible to either activate few DLA elements supplied with a high amplitude signal or equally divide the power to all DLA elements and drive them with lower amplitude signals. In Table 7.2 the system gains are adjusted until the consumption of 1W with all elements active is achieved. The sound pressure is than calculated.

System	Sensitivity (dB SPL/W/m)
1 transducer for analog input signal	76.4
32 transducers for analog input signal	91.3
32 transducers in a DLA for digital input signal, bit summed assignment.	90,4
32 transducers in a DLA for digital input signal, bit grouped assignment.	90.6

Table 7.2: Sensitivity of alternative loudspeaker and array implementations. In all cases is the input signal 1KHz sinus.

The analogue loudspeaker array implementation is the most efficient. The main cause for this is that the power is equally shared between the transducers. The power consumption rises with the square of the input voltage, see chapter 4.3. Secondly, the analogue loudspeaker does not have to produce the digital harmonic. The simulation does not take the power amplifier need for the analogue implementation into account where DLA only needs a switch.

Between the two bit assignments there is also a difference in power consumption: in this situation, it is the power distribution between the transducers that dominates the power consumption. At a full scale signal level the bit group assignment has an advantage due to the signal distribution between the transducers. Hence, by the sensitivity measure, the number of activated transducers has to take into account the digital level, the sensitivity has to be investigated as a function of the digital level. Figure 7.15 shows DLA sensitivity as a function of active transducers for the two bit-assignment strategy.

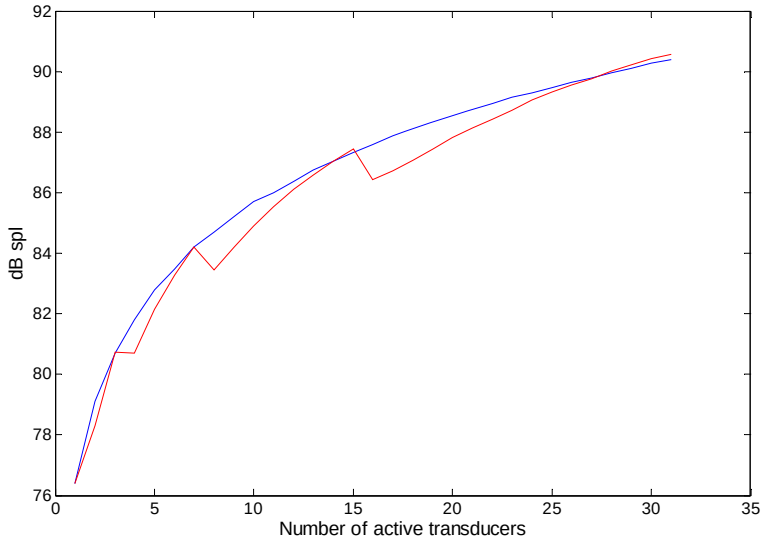

Figure 7.15: DLA sensitivity at 1 m (on-axis) as a function of number of active transducers for driving the system with a 1kHz sinusoidal signal of 1Watt rms. (—) bit-grouped assignment, (---) bit-summed assignment.

By reviewing the sensitivity at different levels and the numbers of active transducers, the drawbacks of the extra switching of the elements in the bit group assignment can be found. For a few levels the bit group assignment has a better efficiency than the bit summed assignment, which is due to better power distribution between the transducers, but overall the extra switching of the bit group assignment consumes extra energy.

7.7. Alternative Loudspeaker Design

As previously mentioned, DLA is limited in its frequency range by the small loudspeakers that are needed. The trade off is that the loudspeakers have to be very small to minimize out-of-axis acoustic path effect; on the other hand, the loudspeakers have to carry the full frequency range. At low audio frequencies, there are two problems; the mechanical resonance frequency of the loudspeakers and the piston volume, maximum sound pressure level, the same problem that occurs when designing an analogue loudspeaker.

7.7.1. Piston Volume

The maximum sound pressure produced by the DLA is given by the total piston volume of air V that the transducers can move, i.e. the maximum displacement x_{max} times the diaphragm area S, equation 7.2. It should be noted that reproduction of low frequencies requires the largest piston volumes.

$$V = S \cdot x \qquad \textit{Equation 7.2}$$

A well known similar relationship also applies to any traditional loudspeaker driven by an analogue signal. It is now useful to obtain comparative results between the analogue and the digital case. For the analogue case, a larger single loudspeaker unit can be used. The comparison is made with a small loudspeaker box application which typically could be a surround sound loudspeaker, which will be a good application for a DLA.

	Traditional loudspeaker	DLA
Loudspeaker type (the transducer)	low-mid speaker	multimedia speaker
Diameter (inches)	3½	2/3
Diaphragm area (cm^2)	49 cm^2	1.76 cm^2
Max displacement, X_{max} (mm)	2.5	1.4
Total piston volume (cm^3)	12.3	0.25
Number of elements	1	49

Table 9.3: Comparing the piston volume of a 3½'' analogue speaker unit with transducers that can be used in a DLA implementation.

The last row in Table 9.3 indicates that approx. 49 small multimedia loudspeakers would be needed to produce the same sound pressure (in terms of the piston volume activated), as the mid-high range loudspeaker of comparable dimension to that of the DLA.

7.7.2. Mechanical Resonance Frequency

Small loudspeaker units have a high mechanical resonance frequency due to the low moving mass. This physical limitation is difficult to overcome and is probably one of the major drawbacks of DLA.

A possible solution is to use another transducer making low frequencies; an implementation could be a typical subwoofer. In this way the benefit of directivity control can still be used from the DLA since the DLA reproduces the frequency where the spatial information is located.

Another open, and not yet investigated, solution is to connect all small loudspeaker units together and thereby obtain the low resonance frequency. By increasing frequency the transducer will be split up into individual transducers. The drawback is that a more complex amplifier has to be used; however, further investigation of the bit assignment method for alternative transducers has to be made.

Finally, a connection to the efficiency study can be made as a non-flat frequency response with large magnets and low mass can also be an alternative for overcoming the mechanical resonance frequency.

7.8. Discussion of Digital Loudspeaker Array

DLA opens new opportunities for audio reproduction. The multi input system offers enhanced spatial control. Surround sound would be a good application for DLA, where it is possible to make special control with one loudspeaker.

There are clearly physical limitations set by the transducers for DLA, i.e., the resonance frequency of the small loudspeakers and the need for many small loudspeaker units for obtaining high sound pressure.

A trade-off in the construction of DLA can be to use an ineffective transducer that has a relative low resonance frequency. Even with the inefficient multimedia loudspeaker units used in the example from the previous work, the DLA efficiency is comparable to analogue systems.

The author believes that DLA may have a future in some applications but the physical limitations are delaying the breakthrough of practical DLA applications.

7.9. Conclusion of Digital Loudspeaker Array

Digital loudspeaker arrays offer multi inputs, which make it possible to include digital signal processing for other purposes, i.e., 3D audio by a single input analogue loudspeaker. The efficiency is comparable or better than an analogue loudspeaker, but the size and frequency range requirements of the loudspeakers used in the array are unrealistic for a full range module. Alternative transducers are needed for expanding the frequency range, or the DLA should only be used in a frequency range of, let us say about 200Hz.

The loudspeaker should not go completely digital in the near future as new transducer technology is needed for enabling higher sound pressure levels and low frequencies.

Chapter 8

8. Discussion and Conclusion

8.1. Discussion

Meeting today's demand for high sound quality mini loudspeakers is impossible in many applications. The request for smaller loudspeaker enclosures relates to matching the size of the general audio equipment. 30 years ago the major audio source was the turntable, which was followed by the compact disc player, and today is it a memory stick integrated into a mobile phone. On TVs, the size requirements have taken a single step from tube TVs to the flat screen TVs. In contrast, the development of loudspeakers has brought small improvements with regards to size. This is primarily due to:

- The loudspeaker's mechanical resonance frequency in the enclosure
- Power loss in the loudspeaker unit
- Maximum displacement level of the bass loudspeaker unit
- Obtaining flat frequency response
- Achieving low distortion

The research made in this project assumes that the last two points can be corrected by digital signal processing. The investigation began with observations of the efficiency of a bass-mid range loudspeaker unit. From previous studies, interesting results have been found by increasing the force factor, which not only increases the efficiency, but can also change the loudspeaker from being a complex second order system to a second order system with two real poles [V2, V3]. This partially helps to solve the problem of the mechanical resonance frequency, because the limitation of playing frequencies below the resonance frequency is partly removed. It has been shown, in this thesis, that other efficiency improvements generate the same changes of the dynamic behaviour of the loudspeaker unit, towards two real poles. An important efficiency improvement is the decrease in the moving mass by reducing the amount of windings on the voice coil [B13]. It is worth noting that the short voice coil not only introduces a more nonlinear force factor but also decreases efficiency by large displacements. After shortening the voice coil, the mass can be decreased as well by making the voice coil thinner, to some extent, which increases the voice coil resistance. When the overall efficiency is increased, the need for the maximum power handling is reduced and the voice coil resistance can be increased. The maximum power handling is often chosen very high by the manufacturers in order to avoid breakdown due to overheating. Instead of this passive protection, it is recommended that the change in voice coil resistance be measured, thereby obtaining the voice coil temperature [C10], which can be a part of the signal processing required. In the study of efficiency and short voice coils, ways of distributing the voice coil differently, and thereby obtaining different efficiency as function of displacement level, have also been studied [P20]. This parameter can be used for changing the maximum power loss, the peak voltage requirements, rms power consumption and linearization of the loudspeaker unit. The voice coil layout design options can also be used for optimizing or emerging system requirements on the power amplifier in a loudspeaker system or the total power consumption of the musical system.

Feedback compensation provides good results in power amplifiers where distortion is reduced significantly. For loudspeaker feedback solutions, a sensor is required for obtaining a feedback signal of either the sound pressure or the diaphragm movements. The sensors available on the market today limit feedback systems for loudspeakers to large loudspeaker units for low frequencies. This led to this study excluding feedback structures as a solution, but it can be a very useful solution in the future, when better sensors are available.

Feed forward compensation is a model based error correction that requires a precise model of the loudspeaker to provide sufficient distortion reduction. This project's modelling has shown that major improvements are needed. The addition of time varying suspension behaviour has improved the loudspeaker model and can also be related to the Christensen and Olsen [C1] study. They adjusted the suspension compliance and this improved their simulation results significantly. The manual adjustment that Christensen and Olsen made in their study can be related to time varying suspension behaviour. There are known improvements that have not been implemented in this project's simulation model. Even with these improvements, the model is not expected to enable the feed forward controller to make significant improvements of sound quality. A major study should be made of loudspeaker modelling. The author believes that a feed forward control in the near future can cancel the distortion introduced by efficient loudspeaker design.

When a sufficient model is obtained, it will be necessary to track the loudspeaker parameter changes [S2, P21, B10]. Through the project, a simple adaptive algorithm has been developed that can find the linear loudspeaker parameters with music as input signal through measurements of loudspeaker current and voltage. Even though some of the nonlinearities have changed due to production spread and temperature change, the author believes that a feed forward compensator can reduce the distortion level with a set of premeasured nonlinearities. The feed forward controller can be tested with the parameter tracking algorithm, when a useful model of the loudspeaker has been found. The parameter tracking can also be used for thermal protection, as previously mentioned, and this can in itself compensate for the drawback of the required current measurement.

The thesis has focused on the study of one dimensional signal processing for cancelling distortion source in the electro-mechanical part of the loudspeaker unit. With digital loudspeaker arrays (DLA) is it possible to control directivity which can be useful for 3D audio and advanced signal processing of the sound field. The DLA has drawbacks in connection to the loudspeaker requirements, which makes it impossible to achieve a full range DLA with techniques as they are known today. The author believes that DLA will have a useful future in some applications as surround sound.

8.2 Conclusion

The initial objective of this project was to design a loudspeaker unit that benefited from the possibilities of digital signal processing. This led to a study of loudspeaker efficiency improvement possibilities, where there is not the constraint of flat frequency response and linear behaviour of the loudspeaker unit. Increasing the force factor and making the voice coil lighter are two good options. It is possible to cut the power consumption down to 1/3 or less. When making the voice coil shorter and lighter, more distortion is introduced, which must then be cancelled. The maximum resistance of the voice coil is set by the maximum power dissipation. A voice coil layout method is proposed that can reduce the maximum power loss, the drawback is that the efficiency at small displacements is reduced. An alternative option is an active control of maximum power dissipation in the loudspeaker. This can be achieved by measuring the voice coil temperature through the change in voice coil resistance and reducing the power sent to the loudspeaker in case of overheating.

A model based feed forward controller has been designed to cancel the errors introduced by the efficient loudspeaker unit design. A very precise loudspeaker model is needed for the feed forward controller. The loudspeaker model used includes the major nonlinearities, Bl(x), $c_m(x)$, and $L_e(x)$. In this project, the model is improved by the addition of the time varying behaviour of the suspension compliance. A signal dependency of the suspension compliance is found, which relates to heating of the suspension. A thermal model is constructed and included in the simulation. This improves the simulation results under and around the loudspeaker resonance frequency. The model should be valid at low frequencies but it is only able to model the distortion by large displacements within 2-10 dB. The even harmonics are under-modelled approximately 10dB. The 3rd harmonic is modelled within 2 dB. A disagreement of the diaphragm rest position in the measured nonlinearities and the measurement setup can be an error source. At small displacement levels, the coherence decreases, and the model fit for small displacements is very weak. It is proposed and shown by others that the inclusion of flux modulation improves the simulation of the distortion level. The author recommends that further research should focus loudspeaker modelling both at small and large displacement levels and relate this to sound quality.

The model errors led to only a simulation study of the feed forward controller being made. An offline controller was constructed in Matlab/Simulink, which provided good results. A study of 13 loudspeaker units' production spread and temperature drift found that the linear parameters easily drift 5-20%. The nonlinear force factor, Bl(x), and voice coil inductions, $L_e(x)$, proved to be fairly stable, but the suspension nonlinearity changed its behaviour. The feed forward controller was once more simulated with the mismatch of the linear loudspeaker parameters due to temperature change. The feed forward compensator became inefficient and in order to obtain a significant distortion reduction, the linear parameters must be within approximately 5% for targeting maximum 1% THD.

A system for tracking the linear loudspeaker parameters online with a music signal was investigated. A good result was obtained by using a NLMS FIR based system identification based on the loudspeaker current and voltage. The system was tested with a 6½ inch loudspeaker unit where the resonance frequency and damping factor was found. The system could approximately find the parameters in 30 seconds with no initial information and track small changes faster. The frequency resolution of the estimated response is important for

obtaining useful loudspeaker data from music signals. The frequency resolution was 20Hz, which was a good compromise for modelling the low frequency behaviour of the loudspeaker and handle the impact of the music signals. A useful step size was around 0.001 and it is important to focus the algorithm around the resonance frequency where the target data is. This could be obtained by filtering frequencies above 400 Hz away. If the NMLS FIR algorithm is to be used in a product further work is needed for implementing a signal selector that can determine if a signal can be used for identification. Secondly, improvements of the parameter conversion of the FIR filter coefficients to loudspeaker parameters need to be made. With these extras, the system identification method presented should be able to find the linear loudspeaker parameters within 5% and thereby enable the feed forward controller to cancel the distortion introduced by the efficiency loudspeaker design proposed in this thesis.

The last chapter looks into digital loudspeaker arrays as an alternative solution to the original focus of redesigning an analogue loudspeaker unit. The advantage of the loudspeaker array lies in the multiple inputs that can enable advanced 3D signal processing. The drawback is the limitation of the small loudspeaker units needed for the array. This limits the DLA from producing low frequencies, if an alternative transducer is not constructed. As loudspeakers are known today there are limit target applications. The efficiency is compatible to analogue loudspeakers but the full frequency range need for the small transducers is a major drawback. The next development step for loudspeakers is not to make them digital, but a limit range of application can benefit from digital loudspeaker arrays.

9. References

9.1 Literature List

[A1]	Agerkvist, Finn T. Conference,	Modelling loudspeaker non-linearities". 32nd AES Hillerød Denmark, 2007.
[A10]	Aldoshina, Irina, Voishvillo, Alexander Mazin, Victor	Modeling of Flux Distortion in Moving Coil Loudspeakers by the Finite Element Method. 98th AES Convention, Paris 1995.
[B1]	Borwick, John	Loudspeaker and Headphone Handbook, ISBN 0-408-011387-7
[B10]	Bright, Andrew	Active Control of Loudspeakers: An Investigation of Practical Applications, Ph.D. thesis Ørsted DTU (2002)
[B11]	Bright, Andrew	Simplified Loudspeaker Distortion Compensation by DSP AES 23rd International Conference, Copenhagen, Denmark (2003)
[B12]	Bright, Andrew	Adaptive IIR Filters fof Loudspeakers Parameter Tracking. AES 32nd International Conference, Hillerød, Denmark (2007)
[B13]	Bright, Andrew	Compensation Non-Linear Distortion in an 'Equale-Hung' Voice Coil . 111th AES Convention, New York 2001.
[B20]	Birt, David	Nonlinearities on Moving Coil Loudspeakers with Overhung Voice Coil. 88th AES Convention, Montreux 1990.
[B30]	Behrends, Herwig Bradinal, Werner, and Heinsberger, Christoph	Loudspeaker Systems for Flat Television Sets 123rd AES Convention, New York 2007.
[B40]	Bell, Alexander Graham	United States Patent No. 174,465. 1876.
[C1]	Christensen, Knud Bank Olsen, Erling Sandermann	Nonlinear Modelling of Low Frequency Loudspeakers- A More Complete Model, 100th AES, 1996

[C10]	Chapman, Peter John	Thermal Simulation of Loudspeakers, AES 104th Amsterdam. (1998)
[C20]	Castor-Perry, Kendall, Lars, and Bell, Kenneth M.	A Low-cost, All-SMD Chip Set for High- Risbo, Performance, True-Digital Audio Power Amplification, Silicon for Audio-AES 16th UK Conference 2001.
[D1]	Dodd, Mark	The Transient Magnetic behavioue of Loudspeaker Motors. 111th AES Convention, New York 2001.
[D10]	Delta, Danish Electronics, Light and Acoustics	Termisk Rigtig Apparatkonstruktion, Delta 2002.
[F1]	Franklin, Gene F., Powell, J. David and Workman, Michael	Digital Control of Dynamic Systems. 1998. ISBN: 0131499300
[H1]	Haykin, Simon	Adaptive Filter Theory (Fourth Edition). Prentice Hall, 2002, ISBN 0-13-090126-1
[H10]	Hansen, Lasse S., Pedersen, Anders R. Søndergård, Martin.	Efficiency Optimization of Loudspeakers. Bachelor project at Aalborg Unerversity Esbjerg 2007.
[H20]	Huang, Y. S. C. Busbridge, D. S. Gill	Distortion and Directivity in a Digital Transducer Array Loudspeaker, J. Audio Eng. Soc., Vol. 49, No. 5, 2 May 2001.
[H30]	Hawksford, M.O.J.	Smart Digital Loudspeaker Arrays, J. Audio Eng. Soc., Vol. 51, No. 12, 2003 December.
[H40]	Hall, David S. Hall	Design Consideration for an Accelrometer-Based Dynamic Loudspeaker Motional Feedback Systems. AES 87th Convention New York, 1989
[K1]	Klippel, Wolfgang	Nonlinear Adaptive Controller for Loudspeakers with Current Sensor, Klippel Gmbh
[K2]	Klippel, Wolfgang	The Mirror Filter- A New Basis for Reducing Nonlinear Distortion and Equalizing Response in Woofer Systems. University of Technology, 1992.

[K3]	Klippel, Wolfgang	Non-linear large signal behaviour of electrdnamic loudspeakers at low frequencies" J. Audio Eng. Soc., Vol 40, 1992, 483-496.
[K4]	Klippel, W. & Seidel, U.	Fast and Accurate Measurement of Linear Transducer Parameters, 110th AES Convention, 2001.
[K5]	Klippel, Wolfgang	Dynamic Measurement of Loudspeaker Suspension Parts. J. Audio Eng. Soc., Vol 52, 2007, 443-458.
[K6]	Klippel, Wolfgang	Loudspeaker Nonlinarities, Causes and Symptoms, Klippel GmbH
[K10]	Knudsen, Morten:	Experimental modelling of dynamic systems, Aalborg University 2003.
[K11]	Knudsen, Morten:	Direct Estimation of Physical Parameters in Nonlinear Loudspeaker Models, Aalborg University.
[K12]	Knudsen, Morten:	Loudspeaker modelling and parameter estimation, 100th AES, 1996.
[K13]	Knudsen, Morten, Jensen, J., Julskjær, V. Rubak, Per	Determination of Loudspeaker driver parameters using system identification technique, Journal of the Audio Engineering Society 37(9) (1989)
[K14]	Knudsen, Morten: P. Hansen, J. Grue Jensen	The Significance of Viscoelastic Effects in Loudspeaker Parameter Measurements, 88th AES, 1990.
[K15]	Knudsen, M. & Grue Jensen, J.	Low frequency loudspeaker models that include suspension creep, Journal of the AES, Vol 41, No 1/2 , 1993.
[K20]	Krump, G.	Zur Temperaturabhängigkeit von Lautsprecherparametern, presented at DAGA-97, (1997). ISBN 3-9804568-2-X
[K30]	Keele, Jr. D. B. (Don)	Comparison of Direct-Radiator Loudspeaker System Nominal Power Efficiency vs. True Efficiency with High-Bl Drivers, 115th AES convention 2003.

[L1]	Lodge, Oliver Joseph	British patent No. 9712, April 27, 1898.
[M1]	Mazin, Victor	Modelling of Magnetic Hysteresis and its Influence on Harmonic Distortion in Eletrodynamic Loudspeakers, AES 106th Munich, May 1999
[M10]	Mendoza-López, J. S. C. Busbridge and P. A. Fryer.	Direct acoustic Digital-to-Analog conversion with Digital Tranducer Array Loudspeakers, J. Audio Eng. Soc. , Vol. 55, No. 6, 2007 June.
[M20]	Mills, P. G. L. and Hawksford, M. O. J.	Transconductance Power Amplifier Systems for Current-Driven Loudspeaker, J. Audio Eng. Soc. , Vol. 37, No. 10, 1989 October.
[M30]	McCrum, Buckley, and Bucknell	Principles of Polymer Engineering, 2003 Page 117-176
[N1]	NSW	Electrical Fitters and Mechanics Trades Course, Applied Electricity Stage 2, Department of Technical Education, NSW (1964)
[N10]	Neumann, J. J. and Kaigham, G. J.	CMOS-MEMS Membrane for Audio-Frequency Acoustic Actuation, Sensors Actuators A, vol. 95, pp.175–182 (2002).
[O1]	Olsen, Erling Sandermann	Nonlinear Modelling of Low Frequency Loudspeakers, 98th AES, 1995
[O2]	Olsen, Erling Sandermann	Measurement of Mechanical Parameters of Electrodynamic Loudspeakers, 98th AES, 1995
[O3]	Olsen, Erling Sandermann Thorborg, Knud	Diaphragm Area and Mass Nonlinearities of Cone Loudspeakers, 99th AES, New York, 1995
[P1]	Poulsen, Torben	Ear, Hearing and Speech, Technical University of Denmark (Ørsted) 2001.
[P10]	Proakis, John G. Manolakis, Dimitris G.	Digital Signal Processing, Third edition 1996. ISBN: 0-13-394289-9
[P20]	Pedersen, Bo R., Agerkvist, Finn T.	Efficient Non-Linear Loudspeakers AES 120th conversion Paris (2006)
[P21]	Pedersen, Bo R., Rubak, Per.	Linearization of Nonlinear Loudspeakers AES 121th conversion San Francisco (2006)

[P22]	Pedersen, Bo R., Rubak, Per	Online Identification of Linear Loudspeaker Parameters, AES 122nd Convention, Vienna, 2007.
[P23]	Pedersen, Bo R., Rubak, Per.	Musical Transducer-less Identification of Linear Loudspeaker Parameters", 32nd AES Conference, Hillerød Denmark, 2007.
[P24]	Pedersen, Bo R., Agerkvist, Finn T.	Time Varying Behaviour of the Loudspeaker Suspension. AES 123rd conversion New York (2007)
[P25]	Pedersen, Bo R., Fotios Kontnmichos, John Mourjopoulos	Performance analysis of digital loudspeaker Arrays. Submitted to J. Audio Eng. Soc..
[P30]	Parks, T.W., and C.S. Burrus	Digital Filter Design, John Wiley & Sons, 1987, pp.226-228.
[R1]	Rasmussen, Knud:	Højttaler, Technical university of Denmark Ørsted, 1996.
[R10]	Rice, C. W. Kellog, E. W.	Notes on the development of a new hornless Loudspeaker. JAIEE 12, page 461-480, 1925.
[R20]	M. Rausch, R. Lerch, M. Kaltenbacher, H. Landes	Optimization of electrodynamic loudspeaker-design parameters by using a numerical alculation scheme.
[S1]	Schurer, Hans Slump ,Cornelis H. and Herrmann , Otto E.	Theoretical and Experimental Comparison of Three Methods for Compensation of Electrodynamic Transducer Nonlinearity. J. Audio Eng. Soc. Vol. 46, No. 9 1998 September
[S2]	Schurer, Hans	Linerization Of Electroacoustic Transducers, University of Twente Enschede, 1997
[S10]	Suykens , Joahan, Vandewalle , Joos, Ginderdeuren , Johan Van	Feedback Linearization of Nonlinear Distortion in Electrodynamic. Loudspeakers. J. Audio Eng. Soc. Vol. 43, No. 9 1995 September
[S20]	Suzuki , Kiyoaki and Nomoto, Isami	Computerized Analysisand Observation of the Vibration Modes of a Loudspeaker Cone. J. Audio Eng. Soc. Vol. 30, No. 3 1982 March

[S30] Small, R.H. — Direct-Radiator Loudspeaker System Analysis, J Audio Eng. Soc. Vol. 20, pp.383-395, June 1972.

[S40] Siemens, Ernst W. — Moving-coil transducer, with a circular coil of wire in a magnetic field. U.S. patent 1874 (No. 149,797)

[S50] Sedra, Adel S. and Smith, Kenneth C. — Microelectronic Circuits, Fifth edition ISBN: 0-19-514252-7

[T1] Thiele, A. N — Loudspeakers in Vented Boxes, J. Audio Eng. Soc., Vol. 19. pp. 382-392. May 1971

[T10] Thorborg, Knud — An Improved Electrical Equivalent Circuit Model for Dynamic Moving Coil Transducers, AES 122nd Vienna May 2007.

[T20] Tatlas, N.A. J. Mourjopoulos — Digital Loudspeaker Arrays driven by 1-bit signals Audio Eng. Soc. 116th Convention, May 2004.

[V1] Vanderkooy, John — A Model of Loudspeaker Impedance Incorporating eddy currents in the pole structure, 84th AES, 1988

[V2] Vanderkooy, John Boers, Paul — High-Efficiency Direct-Radiator Loudspeaker Systems, 113th AES, 2002

[V3] Vanderkooy, John, Boers, Paul, Aarts, Ronald — Direct-Radiator Loudspeaker Systems with High Bl, 114th AES 2003

[V10] Voishvillo, A, Terekhov, Alex, Czerwinski, Gene Alexandrov, Sergei — Graphing, Interpretation and Comparison of Results of Loudspeaker Nonlinearity Measurment 113th AES 2002

[V11] A. Voishvillo and M. Olyshin. — Computer modeling of air distortion in Compression chamber of horn drivers with centrally supported diaphragm, J. Audio Eng. Soc. vol. 43, no. 12, December 1995.

[W10] Wiik, T.H. — Transient Distortion caused by Non-Linearities in driving force and suspension of a loudspeaker, 56th AES Paris 1977.

Appendix 1

10.1. Loudspeaker Simulation Model

The nonlinear simulation models used in the simulation of the distortion level and power consumption are described here.

10.1.1. Simulink

Simulink is an integrated part of Matlab. Simulink is a graphical representation of signal processing or modelling. In the simulation, it was used as an analogue simulation where the differential equations of the loudspeaker were directly implemented (for example Figure 1.6). Simulink solves the differential equation numerically with the differential equations solver from Matlab. In this project's simulations the ODE45 solver was used. The data from Simulink was transferred to Matlab for the data to be sampled for it's a fixed sampling frequency for further processing.

10.1.2. Processing of results from Simulink

From the loudspeaker model implemented in Simulink, time signals were outputted as the diaphragm velocity, loudspeaker current, loudspeaker power consumption etc. This data was transferred to Matlab where they were processed. Functions were then made that could plot data, make an FFT plot, calculate THD+N and an RMS function.

For some of the simulation, a small controller was also implemented that could cause constant diaphragm acceleration by adjusting the gain.

10.1.3. Non-linear force factor power consumption

The power consumption simulation in Chapter 4 used a linear loudspeaker model that included a non-linear force factor. The force factor was implemented with a look-up table where the magnetic data was inputted. A vector with the power consumption, product of voltage and current, was sent to Matlab.

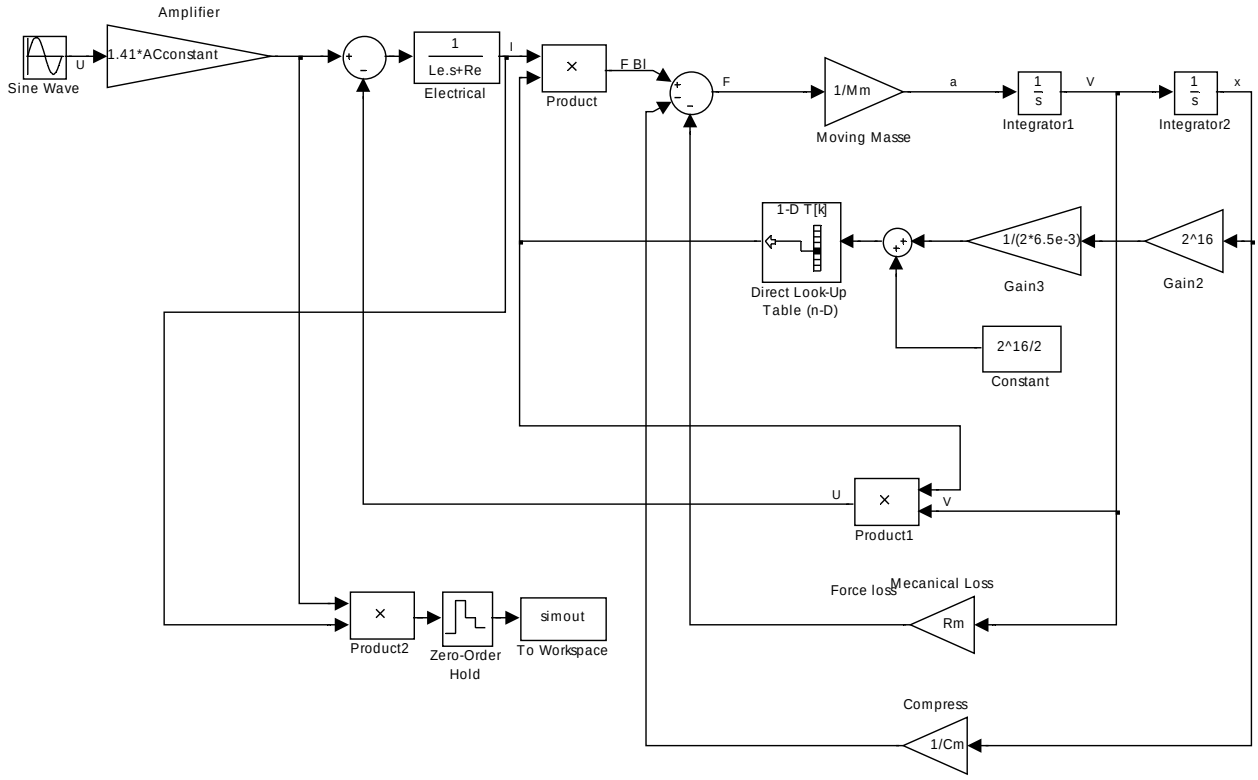

Figure 10.1: Simulink model of the power consumption model used in Chapter 4.

10.1.4. Velocity simulation with major non-linearities

The distortion simulation included the displacement non-linearities of the force factor Bl(x), the suspension compliance $c_m(x)$, and the voice coil resistance. These were implemented with an eighth-order polynomial fit obtained with the Klippel analyser. The time varying suspension behaviour was included. The model was implemented in sub-sections and the main sheet is shown in Figure 10.2, and the loudspeaker sub-sheet in Figure 10.3. This loudspeaker model was also used for the parameter drift simulation in Chapter 5 and therefore, it has offset parameters included.

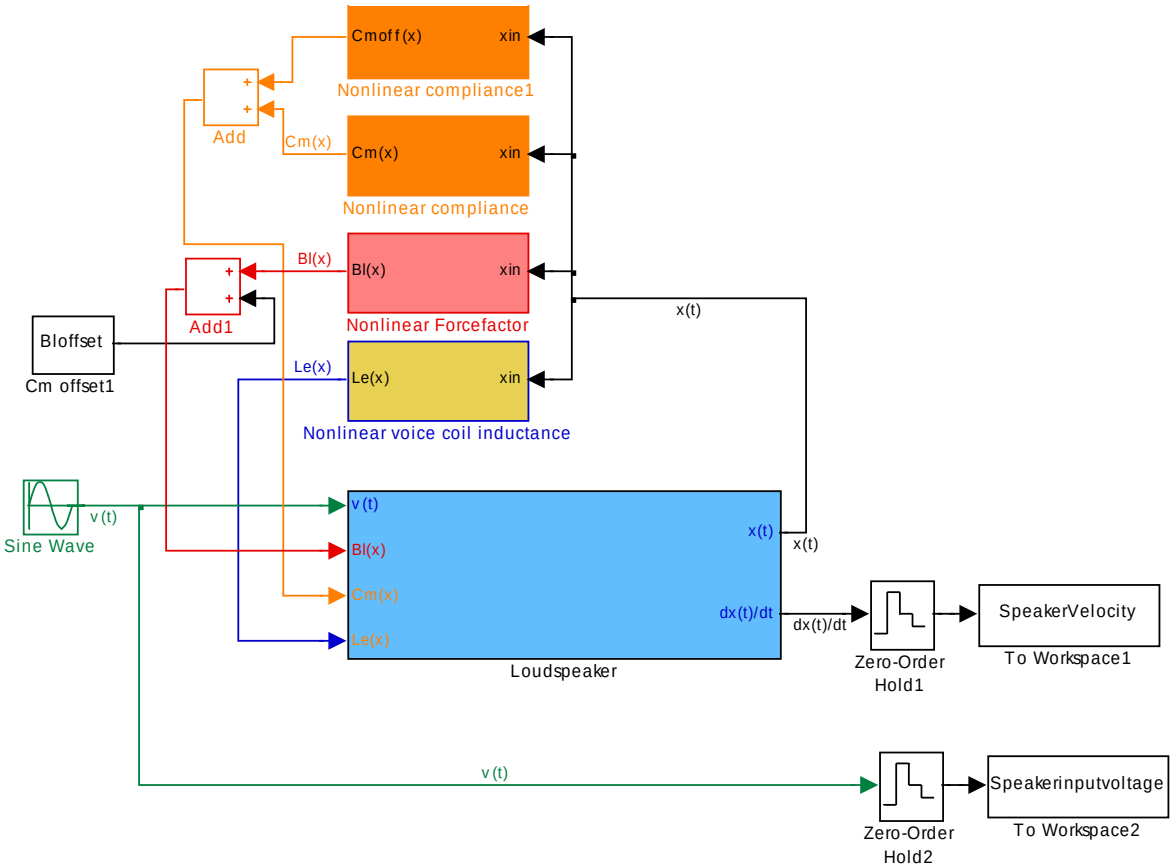

Figure 10.2: Simulink model of the non-linear loudspeaker model used in distortion simulations, main sheet.

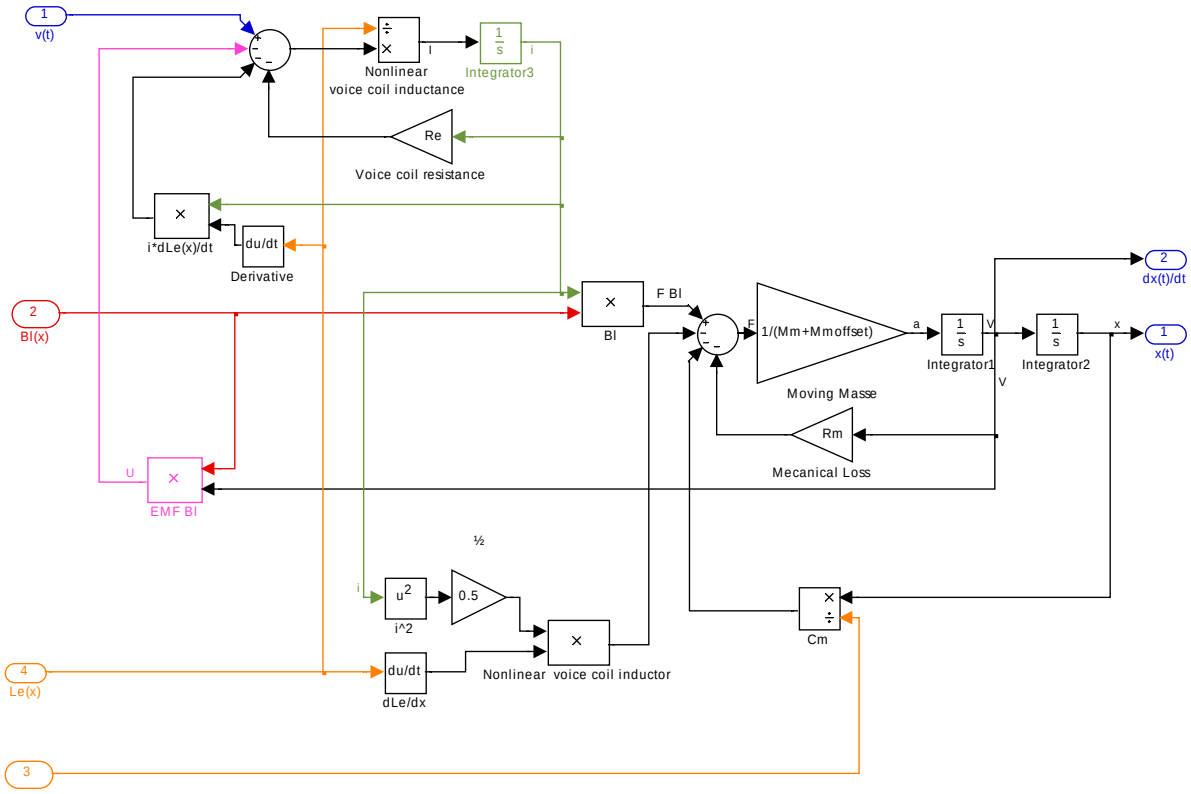

Figure 10.3: Simulink model of the non-linear loudspeaker model used in the distortion simulations, sub-sheet loudspeaker. Inputs: loudspeaker voltage, force factor, suspension compliance and voice coil inductance.

Appendix 2

10.Loudspeaker Unit Data

In the examples given throughout this thesis, most used the same loudspeaker unit which will be described here. Information has been presented on its specific used, it's at the time varying suspension behaviour, the loudspeaker distortion measurements in Chapter 2 and Appendix 3, the loudspeaker parameter drift and the practical test of the FIR-based system identification. Other samples of the same loudspeaker unit have also been used.

10.1. Loudspeaker Unit

The loudspeaker unit is a bass mid-range unit from a DALI two-way loudspeaker (Figure 10.4).

Figure 10.4: Picture of the Dali Blue 2002 loudspeaker where the case loudspeaker unit is used.

The loudspeaker unit is a 6½ inch bass mid-range loudspeaker unit. The linear data were measured with the Klippel measurement system (shown in table 10.1). The loudspeaker was used for the time varying suspension behaviour and the distortion measurement and for the FIR based system identification test was it an other sample (Table 10.2).

Parameter	Size
Voice coil resistance, R_e	3.36 Ω
Voice coil inductor, L_e	0.274 mH
Voice coil inductor LR circuit, L2	0.396 mH
Voice coil inductor LR circuit, R2	1.27 Ω
Force factor, Bl	4.90 N/A
Moving mass, m_m	14.7 g
Suspension compliance, c_m	0.56 mm/N
Mechanical resistance, r_m	0.784 kg/s

Table 10.1: Linear data of the DALI 311541 6½" unit.
Used for the time varying suspension behaviour and distortion measurements.

Parameter	Size
Voice coil resistance, R_e	3.30 Ω
Voice coil inductor, L_e	0.266 mH
Voice coil inductor LR circuit, L2	0.394 mH
Voice coil inductor LR circuit, R2	1.92 Ω
Force factor, Bl	4.95 N/A
Moving mass, M_m	14.35 g
Suspension compliance, C_m	0.54 mm/N
Mechanical resistance, R_m	0.786 kg/s

Table 10.2: Linear data of the DALI 311541 6½" unit.
Used for the FIR based system identification test.

Dali has supported this project by supplying 13 samples of the used loudspeaker unit used for the production spread analysis (see more in Chapter 3). In Table 10.3 is the production year and lot; in Table 10.4 are the linear data of all units.

Year	Lot	Quant
2002	2T92A	3
2003	3TD4A	2
2005	5H1132A	4
2006	6H734B	4

Table 10.3: Used loudspeaker unit DALI 311541.

Lot	Number unit	Force factor	Suspension compliance	Moving mass	Mechanical losses	Voice coil resistance	Voice coil inductance
2T92A	1	5.16N/A	0.5N/m	15.02g	0.93kg/s	3.26Ω	0.265mH
2T92A	2	5 N/A	0.56 N/m	14.35g	0.89 kg/s	3.33 Ω	0.27mH
2T92A	3	4.94 N/A	0.54 N/m	14.02g	0.857 kg/s	3.28 Ω	0.27mH
3TD4A	4	5.06 N/A	0.55 N/m	14.58g	0.82 kg/s	3.29 Ω	0.263mH
3TD4A	5	4.98 N/A	0.57 N/m	13.78g	0.832 kg/s	3.28 Ω	0.263mH
6H734B	6	4.9 N/A	0.56 N/m	14.69g	0.78 kg/s	3.36 Ω	0.27mH
6H734B	7	4.97 N/A	0.55 N/m	14.96g	0.8 kg/s	3.37 Ω	0.275mH
6H734B	8	4.91 N/A	0.54 N/m	14.85g	0.8 kg/s	3.38 Ω	0.27mH
6H734B	9	4.8 N/A	0.56 N/m	14.43g	0.76 kg/s	3.24 Ω	0.26mH
5H1132A	10	4.83 N/A	0.55 N/m	13.9g	0.76 kg/s	3.25 Ω	0.26mH
5H1132A	11	4.95 N/A	0.54 N/m	14.35g	0.786 kg/s	3.3 Ω	0.27mH
5H1132A	12	5.09 N/A	0.5 N/m	15.04g	0.78 kg/s	3.4 Ω	0.274mH
5H1132A	13	5.01 N/A	0.52 N/m	14.24g	0.78 kg/s	3.32 Ω	0.27mH

Table 10.4: Linear data for all DALI 311541 units.

The data shown in Table 10.4 are shown graphically one parameter at the time for comparison in Figures 10.5 to 10.10.

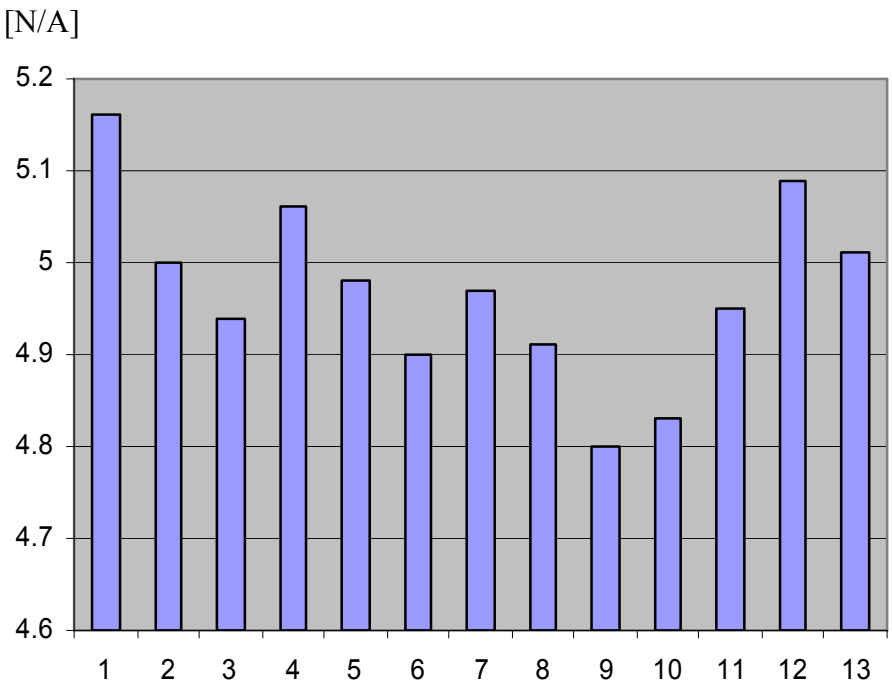

Figure 10.5: The force factor of the 13 loudspeaker units.

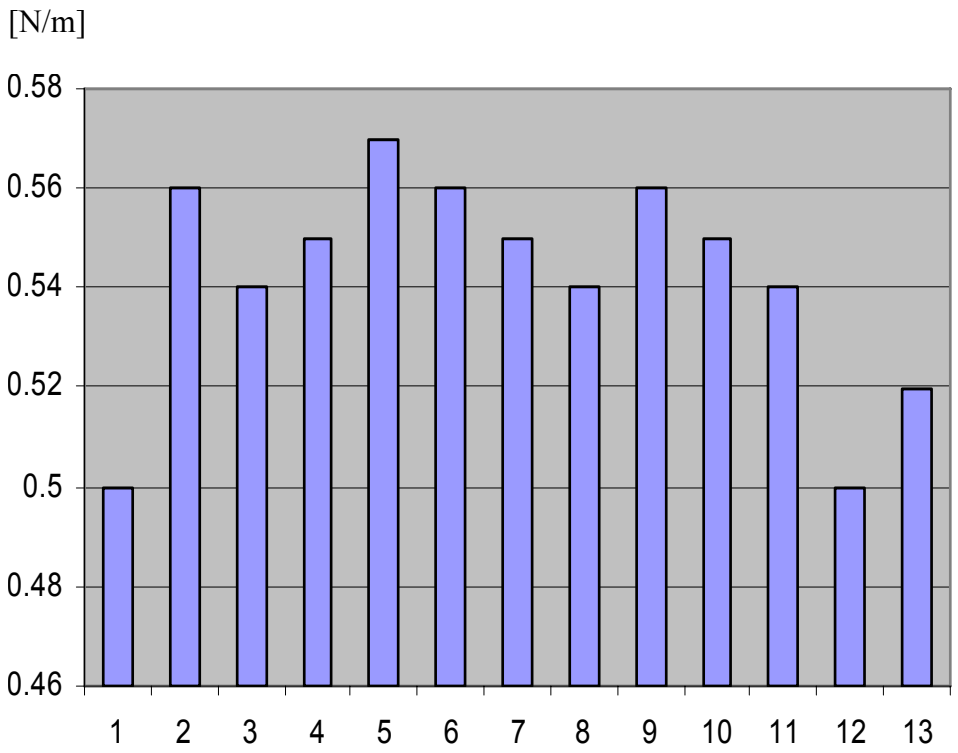

Figure 10.6: The suspension compliance of the 13 loudspeaker units.

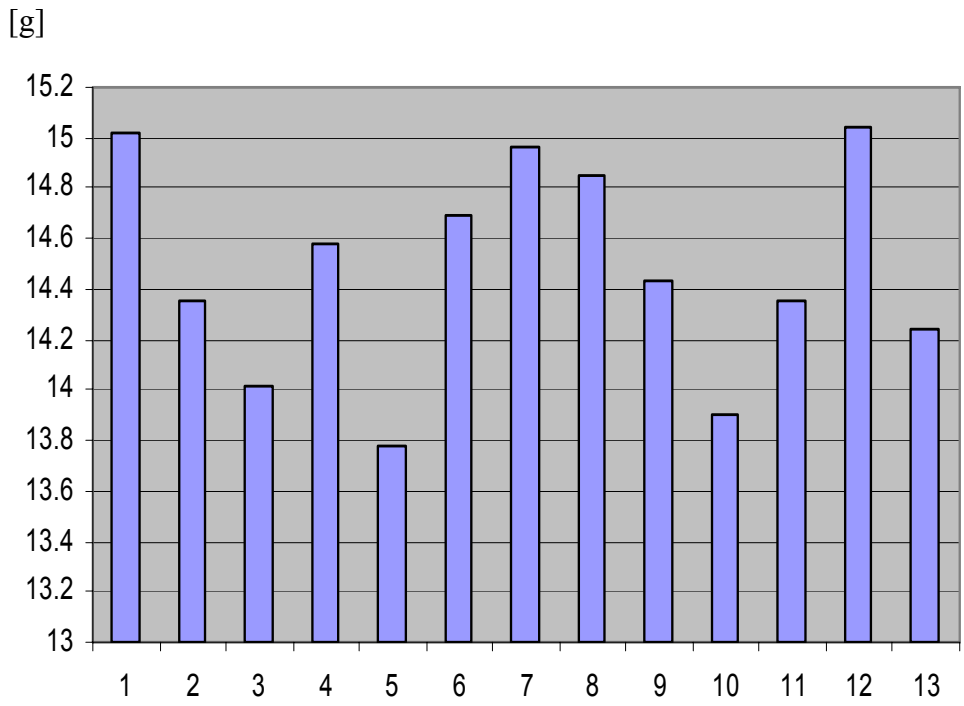

Figure 10.7: The moving mass of the 13 loudspeaker units.

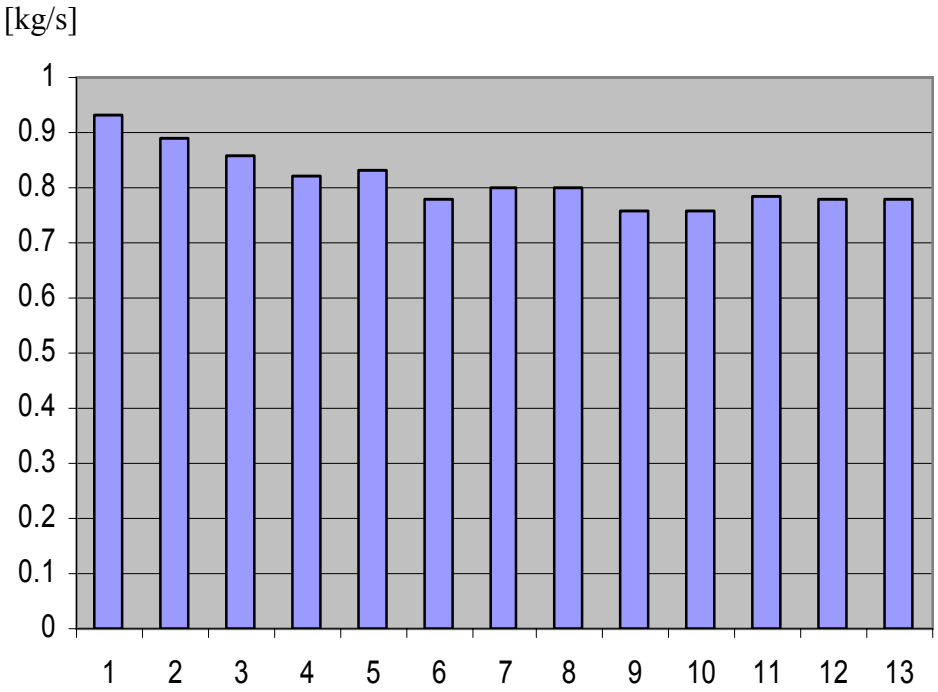

Figure 10.8: The mechanical losses of the 13 loudspeaker units.

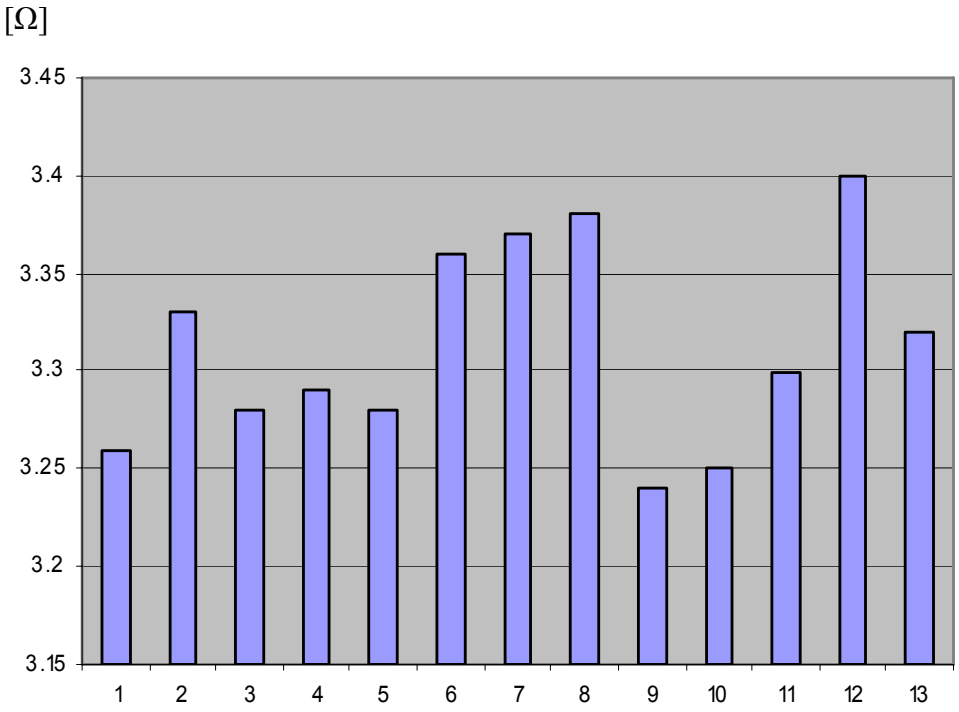

Figure 10.9: The voice coil resistance of the 13 loudspeaker units.

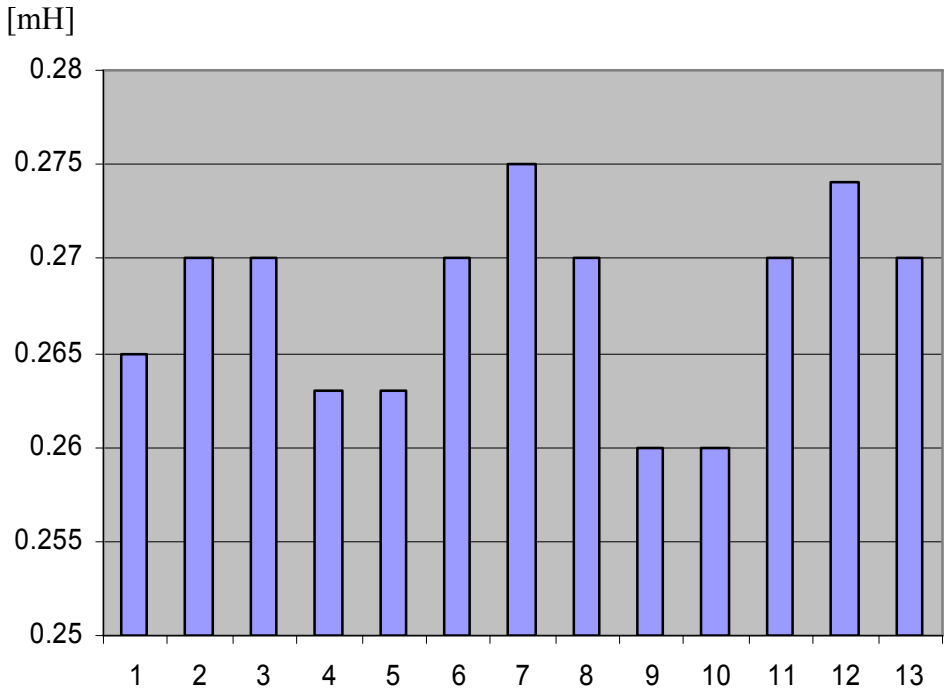

Figure 10.10: The voice coil inductance of the 13 loudspeaker units.

Appendix 3

10.3. Loudspeaker Measurement and Simulation

The total simulation/measuring series presented in Section 2.7 are presented in this appendix.

The loudspeaker velocity was measured and compared with the results obtained from the simulation model shown in Appendix 1. The loudspeaker used is described in Appendix 2

10.3.1. Loudspeaker Measurement Series

The measurement series was performed by measuring the diaphragm velocity with a douppeled precision laser (see Appendix 5). The tests were performed with a sine signal at half the resonance frequency, at the resonance frequency, and at double the resonance frequency. All frequencies were measured at four different levels 1, 2, 5 and $10V_{peak}$ input signal.

10.3.2. Results

The results are shown together with the corresponding simulation in the order listed in Table 10.5.

Figure number	*Input frequency*	*Input level*
Figure 10.11	*28 Hz*	*1 V_{peak}*
Figure 10.12	*28 Hz*	*2 V_{peak}*
Figure 10.13	*28 Hz*	*5 V_{peak}*
Figure 10.14	*28 Hz*	*10 V_{peak}*
Figure 10.15	*55 Hz*	*1 V_{peak}*
Figure 10.16	*55 Hz*	*2 V_{peak}*
Figure 10.17	*55 Hz*	*5 V_{peak}*
Figure 10.18	*55 Hz*	*10 V_{peak}*
Figure 10.19	*110 Hz*	*1 V_{peak}*
Figure 10.20	*110 Hz*	*2 V_{peak}*
Figure 10.21	*110 Hz*	*5 V_{peak}*
Figure 10.22	*110 Hz*	*10 V_{peak}*

Table 10.5. Overview of the measurement series.

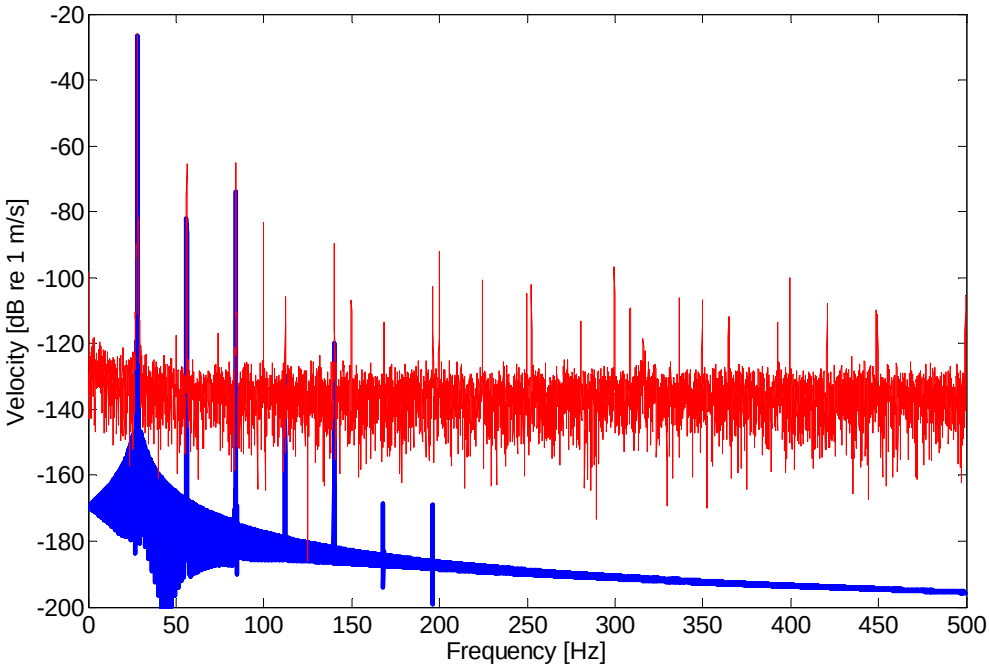

Figure 10.11: One V_{peak} sinus signal at ½ the resonance frequency. Red is measured and blue is simulated.

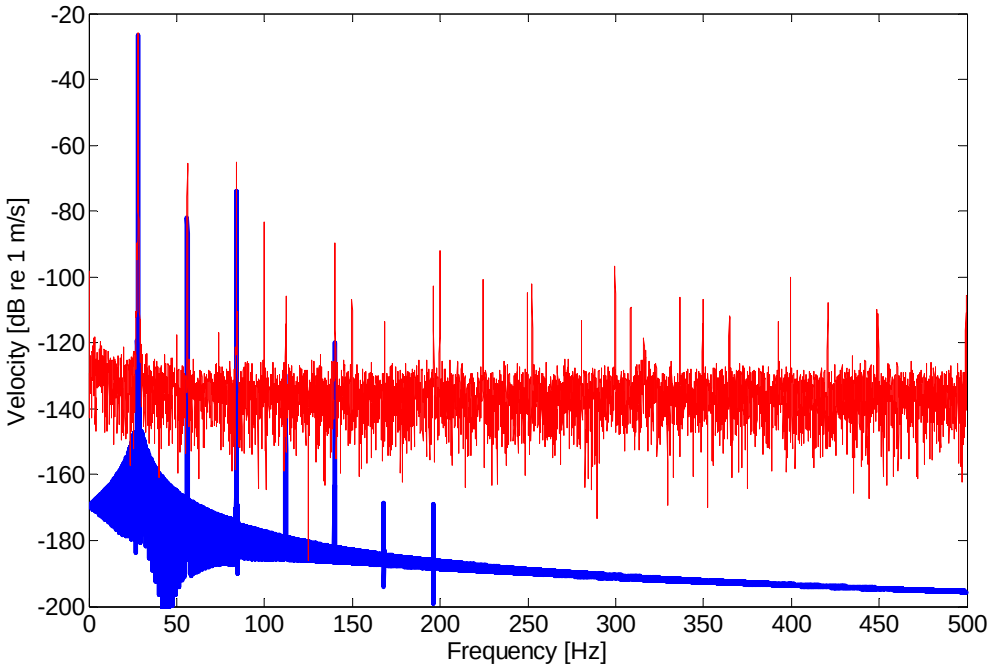

Figure 10.12: Two V_{peak} sinus signals at½ the resonance frequency. Red is measured and blue is simulated.

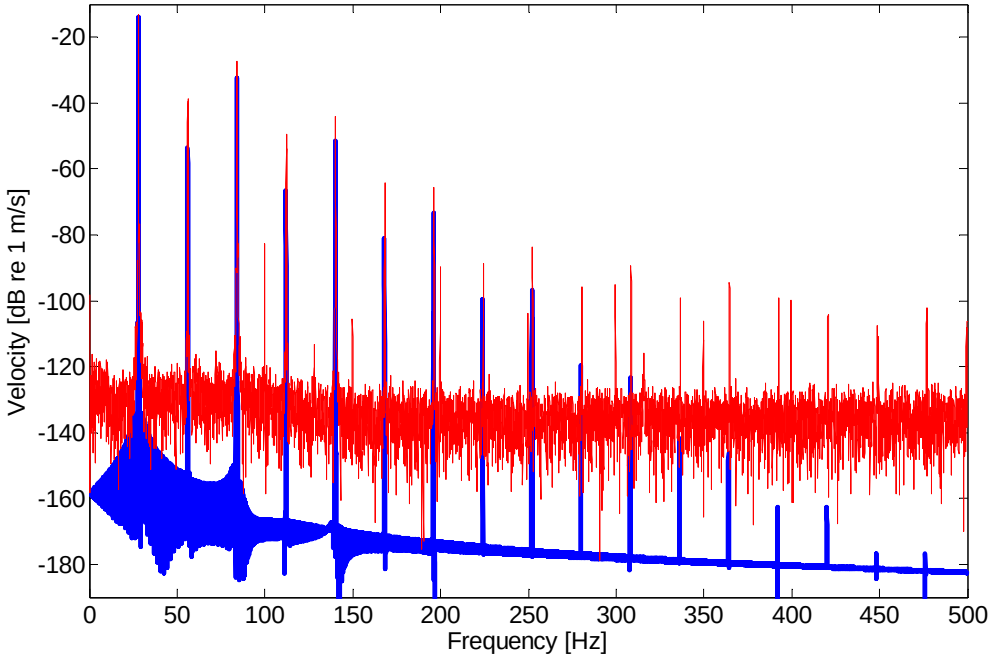

Figure 10.13: Five V_{peak}, sinus signals at ½ the resonance frequency. Red is measured and blue is simulated.

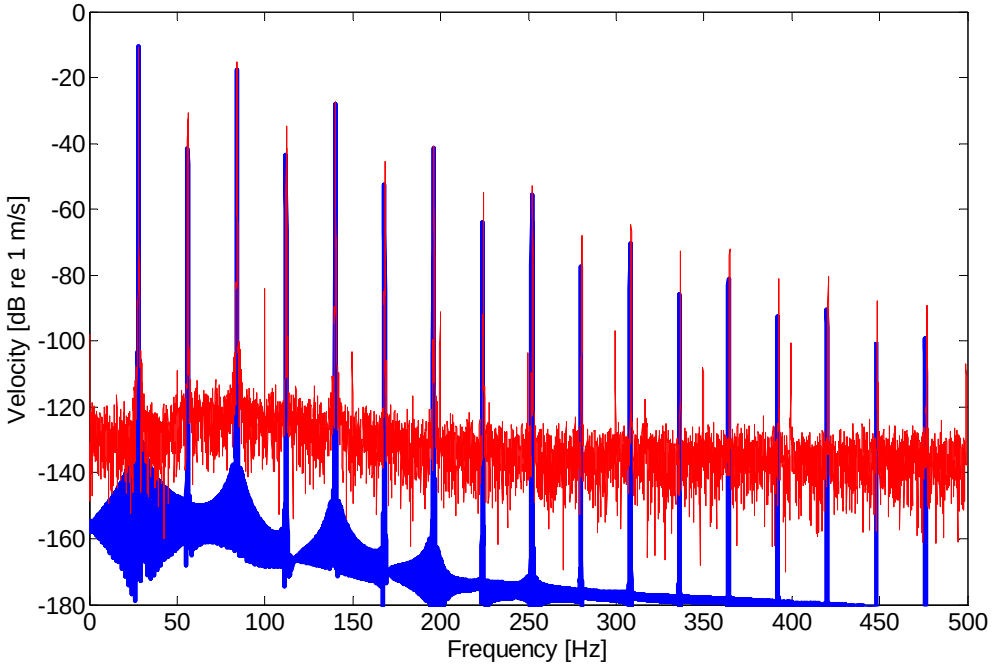

Figure 10.14: Ten V_{peak}, sinus signals at ½ the resonance frequency. Red is measured and blue is simulated.

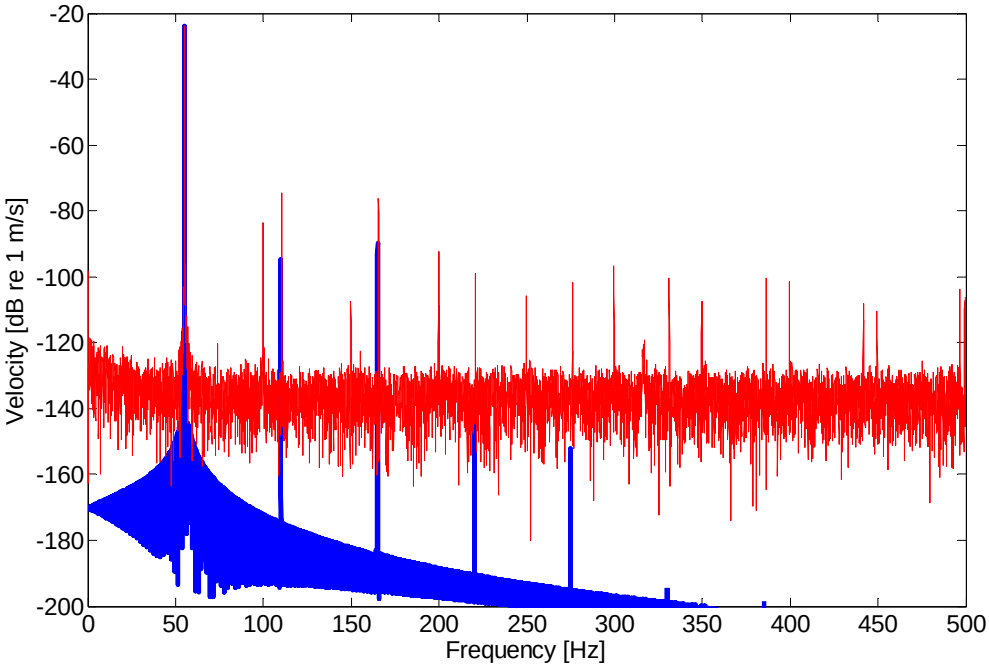

Figure 10.15: One V_{peak} sinus signal at the resonance frequency. Red is measured and blue is simulated.

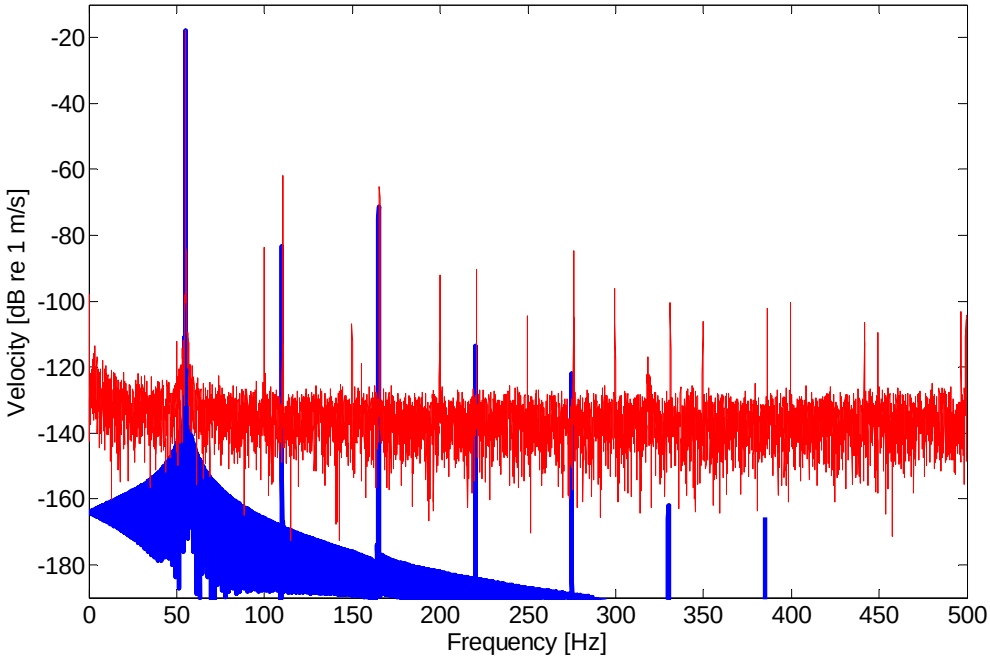

Figure 10.16: Two V_{peak}, sinus signals at the resonance frequency. Red is measured and blue is simulated.

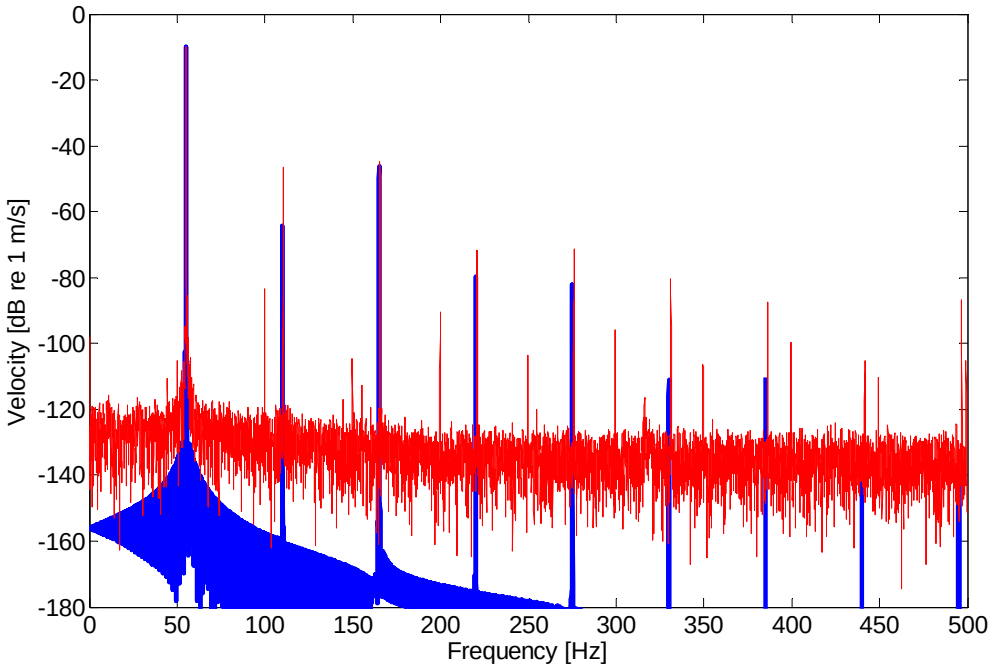

Figure 10.17: Five V_{peak}, sinus signals at the resonance frequency. Red is measured and blue is simulated.

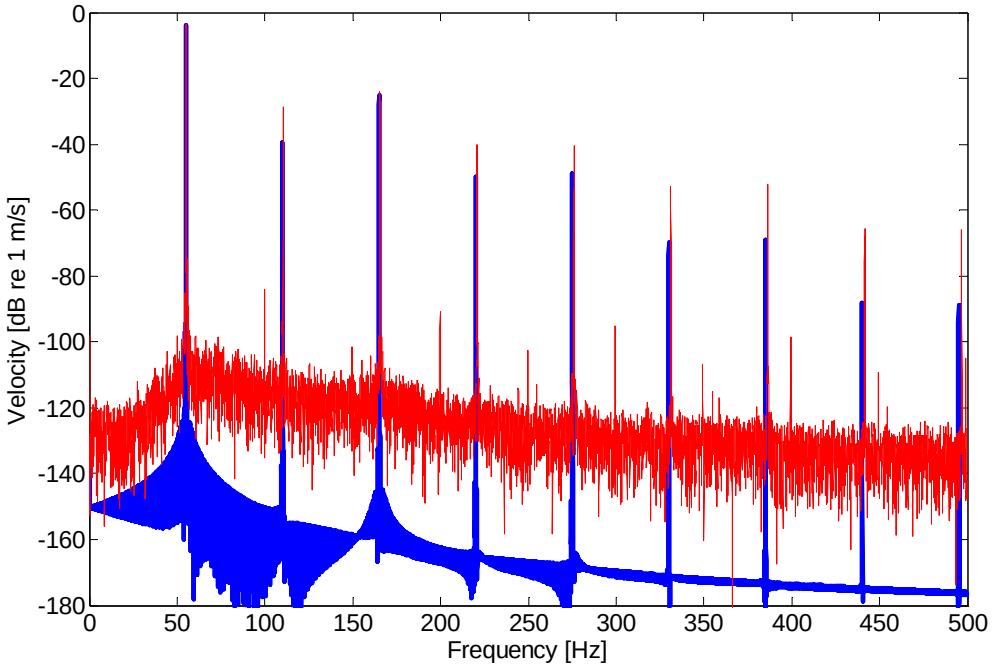

Figure 10.18: Ten V_{peak} sinus signals at ½ the resonance frequency. Red is measured and blue is simulated.

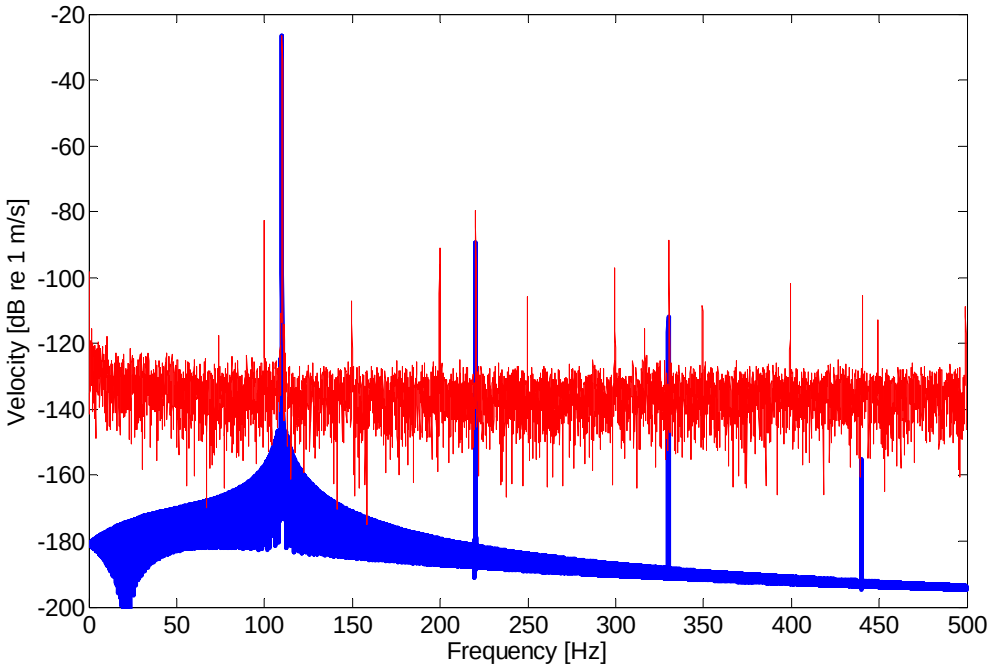

Figure 10.19: One V_{peak} sinus signal at twice the resonance frequency. Red is measured and blue is simulated.

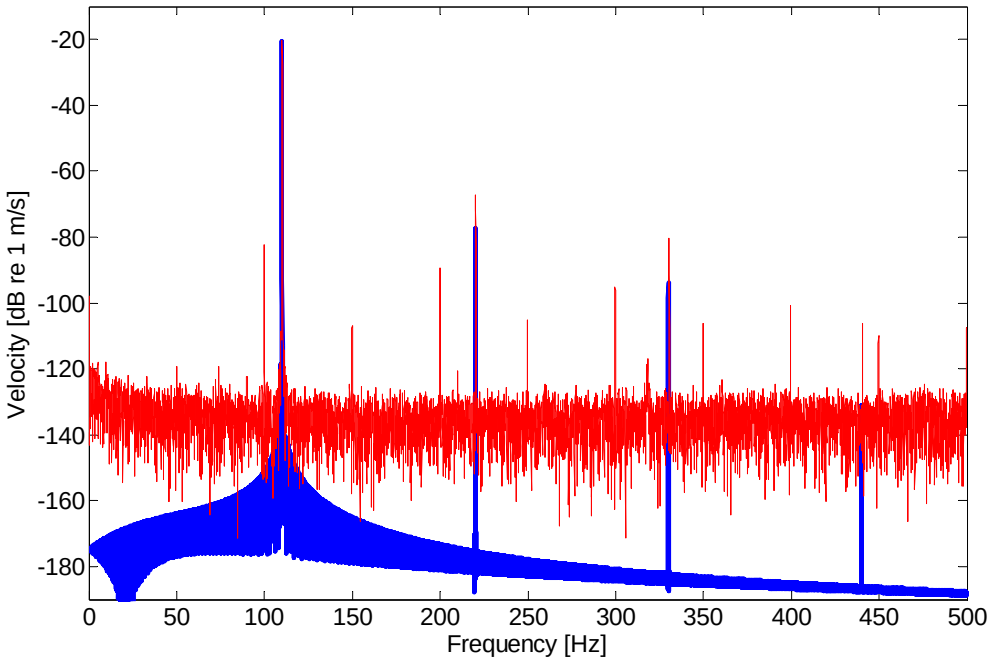

Figure 10.20: Two V_{peak} sinus signals at twice the resonance frequency. Red is measured and blue is simulated.

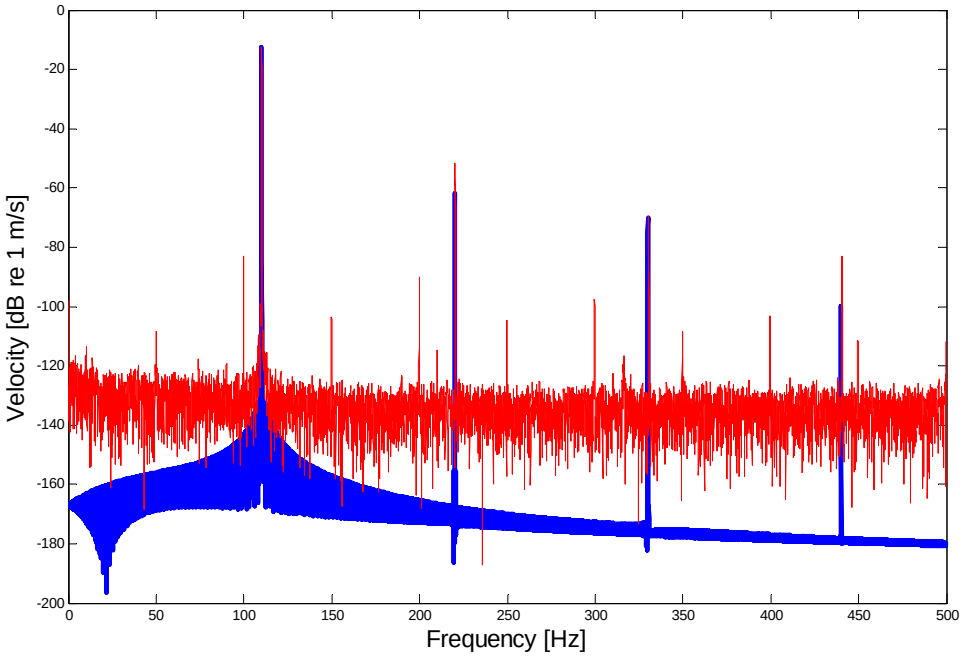

Figure 10.21: One V_{peak} sinus signal at ½ the resonance frequency. Red is measured and blue is simulated.

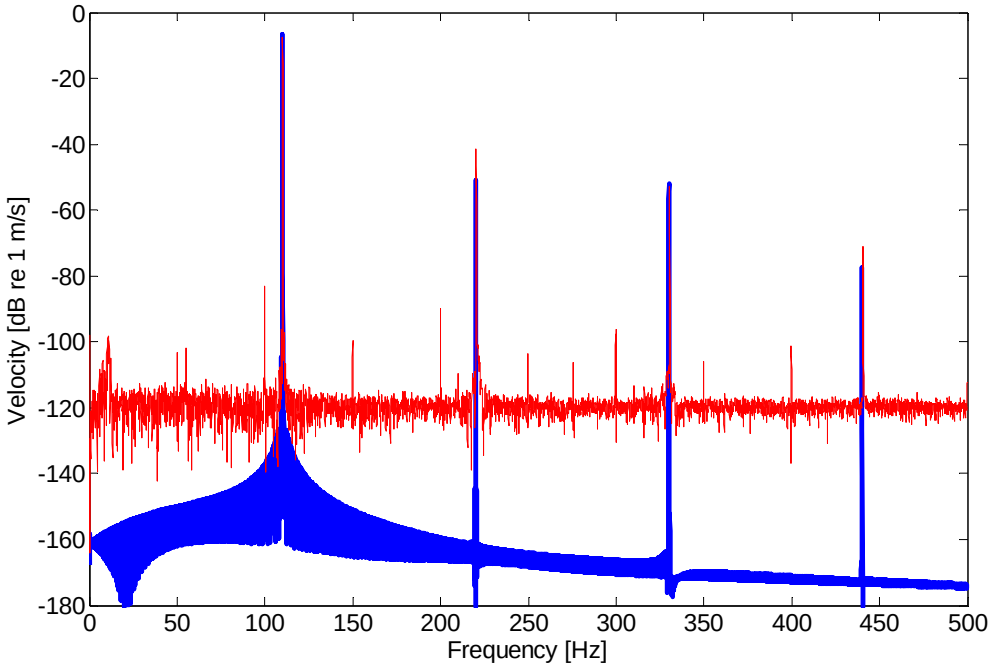

Figure 10.22: Ten V_{peak} sinus signals at twice the resonance frequency. Red is measured and blue is simulated.

Appendix 4

10.4. Force Factor Measurement and Simulation

The magnetic data shown in Chapter 2 and the nonlinear efficiency simulation from Chapter 4 are based on the magnetic data measurements presented in this appendix. The different force factors were obtained from a simulation program based on the measured magnetic data. The principles of the simulation are also shown in this appendix.

10.4.1. Nonlinear force factor from voice coil design

A simulation program was developed that could produce a graph of the electromechanical conversion with different ways of placing the voice coil. This was based on the magnetic data of a one winding voice coil; the test voice coil. The program made it possible to place the windings as decided on the voice coil. The Matlab program produced the electromechanical conversion graph from the design parameters and the test voice coil measurements. This was done according to Equation 10.1.

$$Bl(x) = \sum_{w_n=1}^{n} \sum_{x=-x_{\max}}^{x_{\max}} Bl_{test}(x - \mathrm{W}_{\mathrm{position}}(\mathrm{w}_{\mathrm{n}})) \qquad \textit{Equation 10.1}$$

x	position of the diaphragm,
Bl(x)	force factor function
x_{max}	maximum displacement of the diaphragm
w_n	winding number
n	numbers of windings on the voice coil
$Bl_{test}(x)$	data set from the test voice coil
$W_{position}(w_n)$	position of the windings

A physical setup was made to obtain the correct electromechanical conversion of the test voice coil, the one winding voice coil. This formed the foundation for the simulation program.
The principle in the physical setup was the reverse of what a loudspeaker does. In a loudspeaker, the voice coil produces a movement when electrical current is sent through it. In the test setup, the test voice coil was moved and the voltage was measured. The

test voice coil was driven by the vibrations provided by another speaker. By moving the position of the loudspeaker, the position of the test voice coil was also moved.

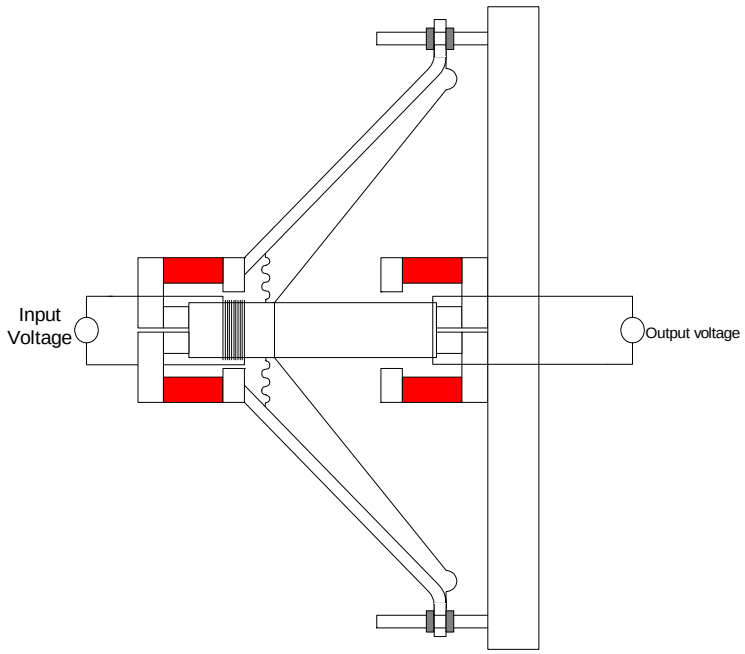

Figure 10.23: Principal drawing of the measurement setup.

Due to the low signal-to-noise ratio in the test setup, the test voice coil was extended to six windings, as shown in Figure 10.23, which shows the cross-section of the magnet. Specific details about the magnetic system are listed in Table 10.5.

Magnet gap height	4mm
Magnet depth	14mm
Magnet opening	1.5mm
Wire diameter	0.27mm
Voice coil diameter	25mm
Voice coil height	13.5mm

Table 10.5: Magnet specifications.

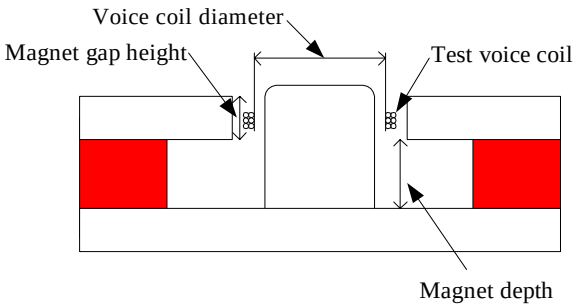

Figure 10.24: Cross-section of the magnet used with the test voice coil, from the measuring setup.

10.4.2. Result of magnetic measurement

First, a test voice coil was positioned in the loudspeaker magnet system (the test voice coil is shown in Figure 10.24). This measurement was then used in the simulation program to find the distribution of the wires on the voice coil.
Figure 10.25 shows the results of the measurements obtained with the test voice coil.

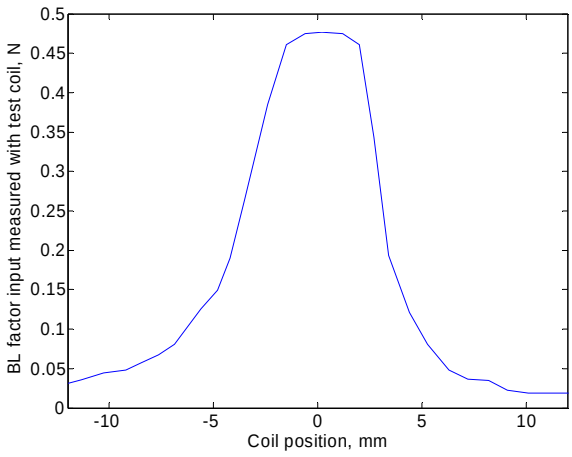

Figure 10.25: The electro mechanical conversion, the Bl factor, for the test voice coil, six winding in two layers.

The measured flux in the chosen magnet is shown in Figure 10.26. The flux was not symmetrical as the magnet system was not symmetrical (Figure 10.24). In Figure 10.25, the negative x-axis corresponds to the voice coil moving into the magnet. The flux inwards compared to the flux outwards of the magnet corresponds to the principal flux flow in Figure 10.26; pay attention to the flux lines. It can be seen that the flux is spread out inwards as there is metal inside. As the metal is not extended over the magnetic gap, the flux is creeping to the top of the central pole piece.

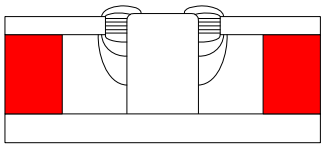

Figure 10.26: Illustration of the magnetic flux in the used magnet, asymmetrical flux.

For further simulation, a symmetrical magnetic design was used. The magnet was extended with a central pole piece (Figure 10.27). The corresponding force factor graph is based on the measurements of the non-symmetric system. The force factor function of the symmetric magnet design was made by using one half of the non-symmetric design and mirroring this on the other side. This approach may not give the exact result, but it is acceptable, since the symmetrical system showed the flux close to a half of the measured magnetic system (Figure 10.27). The inside flux data was used for the force factor shown in Figure 10.28.

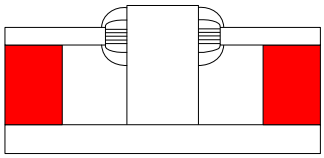

Figure 10.27: Magnetic design with symmetry flux; magnetic system with overhang.

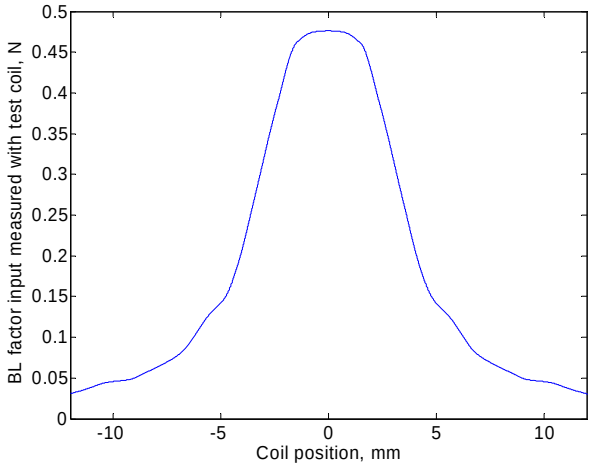

Figure 10.28: The electromechanical conversion for a magnetic system with overhang. Measured and simulated with the test voice coil, six windings in two layers.

The simulations in Chapter 4 are based on the data from Figure 10.28, the results of the test voice coil. From the result of the test voice coil, the electromechanical conversion graph was constructed using the simulation program.

Appendix 5

10.5. Velocity Measurement of Diaphragm

The measuring setup for the series presented in Section 2.7 and Appendix are shown and explained in this appendix.

10.5.1. Measurement Setup

The Measurement series was performed by measuring the diaphragm velocity with a douppeled precision laser. The measurement point of the laser was in between the diaphragm and the dustcap, as shown in Figure 10.31.

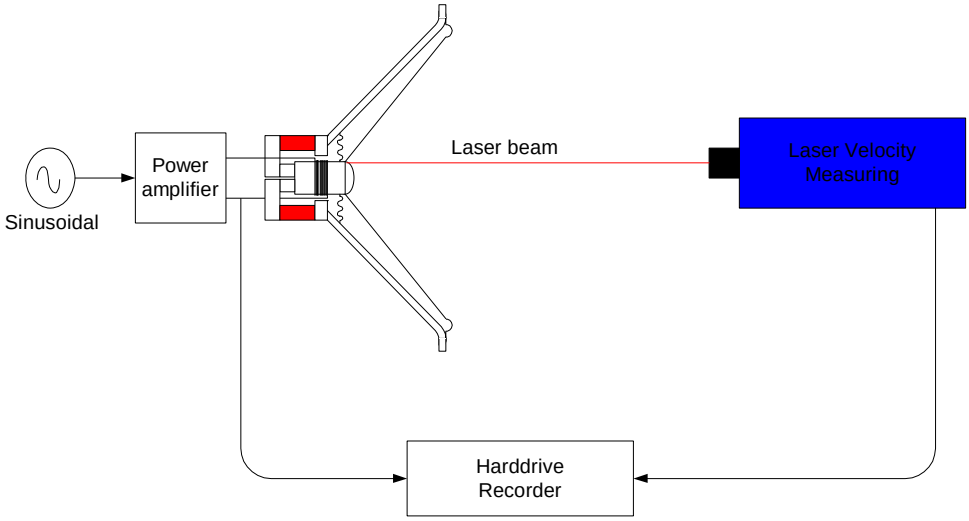

Figure 10.31: Diaphragm velocity measurement setup

Calibration: The recorded level of the loudspeaker input voltage on the hard drive recorder was calibrated according to a fixed voltage level. The laser measurement was calibrated with a pistophone measurement.

Equipment used:

Power Amplifier	NAD 218
Sinusoidal	CD player with Sinusoidal CD: Sony ESD202
Laser Velocity Measurement	Polytec OFV-5000+OFV-505
Hard drive recorder	Sound devices 744T
Calibrator	Brüel and Kjær pistophone

Table 10.6: Equipment used in the test.

ISBN: 987-87-7606-024-4